PACIFIC EARTHQUAKE ENGINEERING RESEARCH CENTER

Large-Component Seismic Testing for Existing and Retrofitted Single-Family Wood-Frame Dwellings

A Report for the “Quantifying the Performance of Retrofit of Cripple Walls and Sill Anchorage in Single-Family Wood-Frame Buildings” Project

Kelly Cobeen
Wiss, Janney, Elstner, Associates, Inc.

Vahid Mahdavifar
University of California, Berkeley

Tara Hutchinson

Brandon Schiller
University of California, San Diego

David P. Welch
Stanford University

Grace S. Kang
Pacific Earthquake Engineering Research Center

Yousef Bozorgnia
University of California, Los Angeles

PEER Report 2020/20
Pacific Earthquake Engineering Research Center
Headquarters, University of California at Berkeley

November 2020

PEER 2020/20
November 2020

Disclaimer

The opinions, findings, and conclusions or recommendations expressed in this publication are those of the author(s) and do not necessarily reflect the views of the study sponsor(s), the Pacific Earthquake Engineering Research Center, or the Regents of the University of California.

Large-Component Seismic Testing for Existing and Retrofitted Single-Family Wood-Frame Dwellings

A Report for the "Quantifying the Performance of Retrofit of Cripple Walls and Sill Anchorage in Single-Family Wood-Frame Buildings" Project

Kelly Cobeen
Wiss, Janney, Elstner, Associates, Inc.

Vahid Mahdavifar
University of California, Berkeley

Tara Hutchinson
University of California, San Diego

Brandon Schiller
University of California, San Diego

David P. Welch
Stanford University

Grace S. Kang
Pacific Earthquake Engineering Research Center

Yousef Bozorgnia
University of California, Los Angeles

PEER Report 2020/20
Pacific Earthquake Engineering Research Center
Headquarters at the University of California, Berkeley

November 2020

ABSTRACT

This report is one of a series of reports documenting the methods and findings of a multi-year, multi-disciplinary project coordinated by the Pacific Earthquake Engineering Research Center (PEER and funded by the California Earthquake Authority (CEA). The overall project is titled "*Quantifying the Performance of Retrofit of Cripple Walls and Sill Anchorage in Single-Family Wood-Frame Buildings*," henceforth referred to as the "PEER–CEA Project."

The overall objective of the PEER–CEA Project is to provide scientifically based information (e.g., testing, analysis, and resulting loss models) that measure and assess the effectiveness of seismic retrofit to reduce the risk of damage and associated losses (repair costs) of wood-frame houses with cripple wall and sill anchorage deficiencies as well as retrofitted conditions that address those deficiencies. Tasks that support and inform the loss-modeling effort are: (1) collecting and summarizing existing information and results of previous research on the performance of wood-frame houses; (2) identifying construction features to characterize alternative variants of wood-frame houses; (3) characterizing earthquake hazard and ground motions at representative sites in California; (4) developing cyclic loading protocols and conducting laboratory tests of cripple wall panels, wood-frame wall subassemblies, and sill anchorages to measure and document their response (strength and stiffness) under cyclic loading; and (5) the computer modeling, simulations, and the development of loss models as informed by a workshop with claims adjustors.

Quantifying the difference of seismic performance of un-retrofitted and retrofitted single-family wood-frame houses has become increasingly important in California due to the high seismicity of the state. Inadequate lateral bracing of cripple walls and inadequate sill bolting are the primary reasons for damage to residential homes, even in the event of moderate earthquakes.

Physical testing tasks were conducted by Working Group 4 (WG4), with testing carried out at the University of California San Diego (UCSD) and University of California Berkeley (UCB). The primary objectives of the testing were as follows: (1) development of descriptions of load-deflection behavior of components and connections for use by Working Group 5 in development of numerical modeling; and (2) collection of descriptions of damage at varying levels of peak transient drift for use by Working Group 6 in development of fragility functions. Both UCSD and UCB testing included companion specimens tested with and without retrofit. This report documents the portions of the WG4 testing conducted at UCB: two large-component cripple wall tests (Tests AL-1 and AL-2), one test of cripple wall load-path connections (Test B-1), and two tests of dwelling superstructure construction (Tests C-1 and C-2). Included in this report are details of specimen design and construction, instrumentation, loading protocols, test data, testing observations, discussion, and conclusions.

ACKNOWLEDGMENT AND DISCLAIMER

ACKNOWLEDGMENT

This research project benefited from the interaction of many researchers and practitioners We would like to express our sincere appreciation to the following individuals and organizations for their support of this project.

The testing group (Working Group 4) was supported by the PEER–CEA Project Team (Jack Baker, Henry Burton, Greg Deierlein, Seb Ficcadenti, Bret Lizundia, Curt Haselton, Charlie Kircher, Thor Matteson, Frank McKenna, Vahid Mahdavifar, Silvia Mazzoni, Gilberto Mosqueda, Sharyl Rabinovici, Evan Reis, Chia-Ming Uang, John van de Lindt, and Farzin Zareian) and the Project Review Panel participants (Colin Blaney, Doug Hohbach, John Hooper, and Charlie Scawthorn). Support from the CEA Team (Janiele Maffei, Shawna Ackerman, Badie Roshandel, and Erin Rogers) and their Advisory Committee (John Osteraas, Brian McDonald, Keith Porter, and Tom Heaton) is also gratefully acknowledged.

The testing discussed in this report was conducted at the Structures Laboratory of the University of California, Berkeley (UCB), Department of Civil and Environmental Engineering, located in Davis Hall on the UCB campus. We would like to acknowledge and thank the structures laboratory team (Shakhzod Takhirov, Phillip W. Wong, Llyr Griffith, Cruz Carlos, and Matthew Cataleta) for providing professional services at different stages of the project testing including construction, instrumentation, testing, and demolition. We would like to also acknowledge and thank Saarman Construction and GreenWall Tech for providing installation of stucco and plaster on wood lath.

This research study was funded by the California Earthquake Authority (CEA). The support of CEA is gratefully acknowledged.

The PEER–CEA Project UCB testing team at the start of Specimen AL-1 testing.

DISCLAIMER

This research study was funded by the California Earthquake Authority (CEA). The support of the CEA is gratefully acknowledged. The opinions, findings, conclusions, and recommendations

expressed in this publication are those of the author and do not necessarily reflect the views of the CEA, the Pacific Earthquake Engineering Research Center (PEER), members of the Project Team, or the Regents of the University of California.

TABLE OF CONTENTS

LIST OF TABLES

LIST OF FIGURES

1 Introduction and Literature Review

1.1 INTRODUCTION

This report is one of a series of reports documenting the methods and findings of a multi-year, multi-disciplinary project coordinated by the Pacific Earthquake Engineering Research Center (PEER) and funded by the California Earthquake Authority (CEA). The overall project is titled "*Quantifying the Performance of Retrofit of Cripple Walls and Sill Anchorage in Single-Family Wood-Frame Buildings*," henceforth referred to as the "PEER–CEA Project."

The overall objective of the PEER–CEA Project is to provide scientifically based information (e.g., testing, analysis, and resulting loss models) that measure and assess the effectiveness of seismic retrofit to reduce the risk of damage and associated losses (repair costs) of wood-frame houses with cripple wall and sill anchorage deficiencies as well as retrofitted conditions that address those deficiencies. Tasks that support and inform the loss-modeling effort are: (1) collecting and summarizing existing information and results of previous research on the performance of wood-frame houses; (2) identifying construction features to characterize alternative variants of wood-frame houses; (3) characterizing earthquake hazard and ground motions at representative sites in California; (4) developing cyclic loading protocols and conducting laboratory tests of cripple wall panels, wood-frame wall subassemblies, and sill anchorages to measure and document their response (strength and stiffness) under cyclic loading; and (5) the computer modeling, simulations, and the development of loss models as informed by a workshop with claims adjustors.

Within the PEER–CEA Project, detailed work was conducted by seven Working Groups, each addressing a particular area of study and expertise, and collaborating with the other Working Groups. The seven Working Groups are as follows:

Working Group 1: Resources Review

Working Group 2: Index Buildings

Working Group 3: Ground-Motion Selection and Loading Protocol

Working Group 4: Testing

Working Group 5: Analytical Modeling

Working Group 6: Interaction with Claims Adjustors and Catastrophe Modelers

Working Group 7: Reporting

This report is a product of the Working Group denoted in bolded text above.

This report is a product of the Working Group 4 (WG4) denoted in bolded text above. Physical testing was carried out at the University of California San Diego (UCSD) and University of California, Berkeley (UCB). Leadership for WG4 was provided by Dr. Tara Hutchinson and Brandon Schiller of UCSD, Dr. Vahid Mahdavifar of UCB, and Kelly Cobeen.

The primary objectives of the testing were identified by the project to be: (1) development of descriptions of load-deflection behavior of components and connections for use by Working Group 5 (WG5) in development of numerical modeling; and (2) collection of descriptions of damage at varying levels of peak transient drift for use by Working Group 6 in development of fragility functions. Both the UCSD and the UCB testing included companion specimens tested with and without retrofit.

To this end, WG4 developed an overall testing plan; see Appendix A of this report. This report documents the portions of the WG4 testing conducted at UCB: two tests of large-component cripple walls (Tests AL-1 and AL-2), one test of cripple wall–load path connections (Test B-1), and two tests of dwelling superstructure construction (Tests C-1 and C-2).

Additional reports addressing WG4 work include: (a) a series of reports addressing the UCSD small-component tests; and (2) a report addressing the relationship between UCSD small-component and UCB large-component testing written jointly by WG4 and members of WG5.

Discussion of the ultimate use of the data generated can be found in Working Group 5 and 6 Reports. Discussion of the displacement-based loading protocols developed by the project for use in testing can be found in the Working Group 3 report.

The focus of this report is the large-component testing conducted at UCB. Included in this report are details of specimen design and construction, instrumentation, loading protocol, test data, testing observations, discussion, and conclusions. In addition to the documentation provided in this report, the test data in its entirety has been archived and is available on the PEER website.

Note that the terms “existing” and “retrofitted” are used interchangeably in this report.

1.2 REPORT ORGANIZATION

This report is organized into the following chapters:

- Chapter 1: Introduction and Literature Review. This chapter provides a brief introduction, how the report is organized, and a literature review;
- Chapter 2: Overview of UCB Testing. This chapter provides an overview of testing at UCB. Testing aspects common to all tests are described including: the loading protocol, data collection, test setup, the test foundation, and supplemental gravity load;
- Chapter 3: Group A Large-component Testing. This chapter provides detailed discussion of the two large-component cripple wall tests, noted as Tests AL-1 and AL-2. Included are: specimens design and construction, loading protocol, instrumentation, gravity loading, test results, discussion, and conclusions:
- Chapter 4: Group B Load Path Connection Testing. This chapter provides detailed discussion of the large-component cripple wall–load path connection

test, noted as Test B-1. Included are: specimens design and construction, loading protocol, instrumentation, gravity loading, test results, discussion, and conclusions;

- Group C: Combined Materials in Occupied Stories Testing. This chapter provides detailed discussion of two large-component tests of dwelling superstructure walls braced with finish materials commonly found in California dwellings, noted as Tests C-1 and C-2. Included are: specimens design and construction, loading protocol, instrumentation, gravity loading, test results, discussion, and conclusions;
- References. Provides references cited in the report;
- Appendix A: Working Group 4 Testing Plan. The testing plan originally developed by WG4 to guide the testing efforts, with updates during the course of project work;
- Appendix B: Specimen Drawings. Drawings sets of test specimen configurations, and instrumentation are provided, including details of framing and fasteners used in specimen construction. Also included are details of instrumentation for each specimen;
- Appendix C: Damage Observations during Testing. Detailed observations were made during testing. This section provides details of those observations organized by drift ratio; and
- Appendix D: Post-Test Finish Removal Observations. Following completion of testing, finish materials were selectively removed to observe underlying conditions. This section documents observations made.

1.3 LITERATURE REVIEW

The scope of testing addressed by this report includes a wide range of component and connection types. The literature review below summarizes the existing body of knowledge thought to be most relevant to the types of components and connections that were tested. The literature survey is broken into four groups: cripple walls and their load path connections, dwelling superstructure wall components, testing of full-scale buildings, and other literature of interest. Also available is a literature-review document developed jointly by and spanning the work of all of the PEER–CEA Project working groups; see the PEER website for further information.

1.3.1 Cripple Walls and Their Load Path Connections

Included in this section is literature relevant to testing of cripple walls and their load path connections. The load path connections include the anchorage of walls to foundations and shear clips that transfer load from the floor framing above into the top plates of cripple walls. Overall, there was limited information available on these topics, making this a high priority for PEER–CEA Project testing.

Shepherd and Delos-Santos (1991). An experimental program investigated the capacity of two- and four-foot-tall cripple walls (16 ft in length) under existing and retrofitted designs. No finishes were considered in this program. The loading protocol was cyclic load controlled.

Chai et al. (2002). An experimental program evaluated the capacity of 2×4 cripple walls (12 ft in length) under existing and retrofitted designs both in level and stepped configurations. Stucco exterior finish was considered in some of the tests. Retrofitted tests included the addition of wood structural panel sheathing, extending either two-thirds of the wall length (in two 4-ft-long sections) or for the full wall length. Monotonic, normal, and near-fault loading histories were used in testing based on CUREE quasi-static lateral displacement history recommendations [Krawinkler et. al. 2001].

Fennel et al. (2009). An experimental program evaluated wood sill plate to concrete connections to determine capacity and failure modes. The testing was conducted in response to significant reductions in anchor bolt capacity introduced in Appendix D of ACI 318-08 [ACI 2008]. As a result of testing, it was recommended that anchor bolt capacities for the design of wood sill plate attachment to concrete foundations be assigned using the higher values associated with National Design Specification for Wood (NDS) [AWC 2015] based on the wood portion of the connection rather than the smaller capacity assigned by ACI-318. Test specimens included only foundation sill plates and no wall above. This study serves as one available source of test data for wood connections to concrete foundations.

Mahaney and Kehoe [2002]. An experimental test program evaluated anchorage of wood-frame shear walls to concrete foundations. The testing was undertaken in response to observed splitting of wood foundation sill plates in the 1994 Northridge, California, earthquake. The testing was run using walls that were strengthened to move the failure into the wall anchorage. Walls were tested with a wide range of conditions, including with and without nuts, with cut washers, and with steel plate washers. The testing resulted in recommendations for use of steel plate washers in new construction and retrofits. This report serves as one source of information on performance of anchor bolt connections at the bottom of cripple walls.

Ficcadenti et al. [2004]. An experimental test program evaluated shear transfer connections between the top of wood light-frame shear walls and floor framing systems above. The testing evaluated both conventional construction connections (representing a common pre-retrofit condition in residential construction) and a series of configurations adding proprietary clip angles and other connection types representative of retrofit conditions. This report serves as one available source of information on performance of load path connections at the top of cripple walls, as well as connections between rim joists and stem walls where no cripple wall is present.

1.3.2 Dwelling Superstructure Wall Components

A topic of considerable interest for the PEER–CEA Project was the seismic performance of walls in the superstructure of dwellings (the occupied stories that include interior finish materials). This is of particular interest because for most dwellings the finish materials (stucco, siding, plaster, gypsum wallboard, etc.) also serve as the seismic bracing system. Component test data that includes these materials, alone or in combination is key to developing analytical models of structural response. Included in this section is literature most relevant to wall components common in dwellings.

Arnold et al. [2003; 2007]. *CUREE EDA-03* and *EDA-07*. Experimental test programs evaluated occupied story walls braced with stucco exterior and gypsum wallboard interior finishes, with construction typical of the 1970s. The first phase (*EDA-03*) introduced gravity loading and stucco boundary conditions that were representative of the first story of a two-story dwelling; the second phase (*EDA-07*) was representative of a dwelling with a second story. The boundary conditions included wrapping of stucco around corners and an enhanced stucco connection at the top. Walls were 16 ft long and 8 ft high and included door and window openings. This testing illustrated significantly higher capacities and lower drifts at peak shear capacity than other testing of stucco and gypsum board where representative boundary conditions were not used.

Forest Products Laboratory [1951]. *Results of Racking Tests of a Few Types of House-Wall Construction*, by E. W. Kuenzi, USDA Forest Products Laboratory, in cooperation with Housing and Home Finance Agency, filed 16 October 1951. This report describes testing of various wall-bracing materials, including horizontal and diagonal lumber sheathing alone and in combination with let-in bracing and plaster on wood lath. Walls tested were fully sheathed and 8 ft-0 in. high × 8 ft-0 in. long. Walls were tested using single-direction monotonic loading. The test setup included stiff overturning restraint of the panels; therefore, the test results were comparable to the American Society for Testing and Materials (ASTM) E72 [ASTM 2015] test methods.

Forest Products Laboratory [1956]. *The Rigidity and Strength of Frame Walls, Information Reviewed and Reaffirmed Report*, No. 896 by G. W. Trayer, U.S. Department of Agriculture (USDA) Forest Products Laboratory, March 1956. This test report describes testing that was originally conducted circa 1930. The purpose of the testing was to assess the strength and stiffness of wall-bracing materials for light-frame construction, including horizontal lumber sheathing, diagonal sheathing, and plaster on wood lath. Walls tested included 9 ft-0 in. high × 14 ft-0 in. long and 7 ft-4 in. high × 12 ft- 5 in. long assemblies. Both solid walls and walls with door and window openings were included. Most were tested using single-direction monotonic loading, and several wall assemblies were loaded with a large number of vibration cycles. The test setup included stiff overturning restraint of the panels; therefore, the test results were comparable to the ASTM E72 test methods.

Forest Products Laboratory (1958). *Adequacy of Light Frame-Wall Construction Report*, No. 2137 by R. F. Luxford, and W. E. Bosner, USDA Forest Products Laboratory, November 1958. The purpose of the testing was to assess methods to reduce costs through reduction of labor or materials. Control tests used horizontal lumber sheathing of southern yellow pine. These results were compared to horizontal southern yellow pine sheathing with let-in braces and 1/4-in. Douglas-fir plywood sheathing with and without let-in braces. Walls tested were fully sheathed and 8 ft-0 in. high × 12 ft-0 in. long. Testing used single-direction monotonic loading. The test setup included stiff overturning restraint of the panels; therefore, the test results were comparable to ASTM E72 test methods.

Schmid (1984). *Shear Test of Existing Wood Lath and Plaster Walls Relative to Division 88*, by Ben Schmid (1984). Schmid tested two interior plaster and wood lath walls in an unreinforced masonry building in the City of Los Angeles. The walls had initial dimensions 10 ft high × 11-to-14 ft long and were cut down to 8 ft × 8 ft in. to allow attachment of the testing jacks. Both faces of the test walls had plaster and wood lath finishes. The bottom edges of the panel remained per original construction. The plaster and wood lath were cut vertically and left free to slide at the vertical edges. At the top edge, blocking was installed to restrain upward movement of the plaster and wood lath. The dead load of the floor above was used to resist overturning; however, during peak loads, uplift displacements of almost 1 in. were recorded. Testing was force-controlled and involved loading in one direction, release of the load, and loading in the opposite direction. The Test 1 panel withstood four excursions and failed on the fifth. The Test 2 panel withstood six excursions and failed on the seventh. Load histories, load-deflection plots and low-resolution photos of the testing are available.

McMullin and Merrick [2002]. An experimental test program evaluated residential interior gypsum wallboard (partition) walls. Test variables included: fastener type and spacing, loading protocol, top-of-wall boundary conditions, methods of attaching the gypsum wallboard to the top sill, wall-opening layout, innovative construction methods, influence of door and floor trim, and repair strategies. Findings included a distinct change in strength for walls built with various fastener types and wall penetration layouts. Damage patterns began with the initiation of cracks at the wall penetrations and cracking of the paint over a few fastener heads. One of two failure modes were observed after reaching the maximum loads: (1) loosening of the wallboard from the framing by pulling fastener heads through the wallboard; or (2) failure of the taped wall joints and racking movement of the individual gypsum wallboard panels. The overall behavior and levels of damage appears to be related to the rigidity and geometry of the boundary elements of the wall.

Gatto and Uang [2002]. An experimental test program evaluated 8 ft × 8 ft (2.4 m × 2.4 m) wood-frame shear walls, tested under different loading protocols to study the influence of the loading protocol on the response of each specimen. Protocols with large number of cycles at each displacement amplitude produced fatigue fractures in the nails, which caused a reduced ultimate strength and deformation capacity due to the large energy demand. This study provided direct comparison of the performance effects of varying loading protocols, which justified the use of the CUREE Ordinary Protocol [Krawinkler 2001] for the majority of the component testing during the CUREE-Caltech Project. Sheathing materials used in the component testing included wood structural panels, gypsum wallboard, and stucco.

Pardoen et al. [2003]. An experimental test program evaluated the capacity of one and two-story shear walls. Walls were 16-ft long and 8-ft high for the one-story configuration and 17-in. high for the two-story configuration. Walls were fully sheathed or included door, window, and garage door openings; the configurations of the wall and openings matched the dwelling tested on the shake table by Fischer et al. [2001]. Sheathing materials tested included wood structural panel, gypsum wallboard, stucco, and fiber-cement siding. The stucco wall testing did not consider the influence of boundary conditions, which resulted in deflection at peak shear capacity that was significantly larger than those findings by Arnold et al. and were inconsistent with observed earthquake behavior.

Carroll [2006]. The project objective in this study was to establish a basis for probabilistic assessment of the seismic performance of older construction by examining the performance of shear walls, connections, and wood materials from older light-frame buildings Nineteen structures built between 1900 and 1970 scheduled for demolition were sampled for material and connection tests as well as full-sized shear wall tests. Two exterior finish types, horizontal wood siding, and plywood panel siding were tested. The characteristic interior wall covering in buildings of this era was wood lath and plaster. Because of concerns regarding potential for asbestos in the plaster, the plaster was removed before transporting the walls to the testing lab. Plaster was subsequently installed new in the laboratory. Because non-typical materials and attachment methods were used, the relevance of the resulting data is not known.

Ni and Karacabeyli [2007]. An experimental test program with 16 full-scale tests was carried out on shear walls with diagonal and horizontal lumber sheathing. It compared the in-plane shear strength, and investigated the effects of hold-downs, vertical load, and width of sheathing on the in-plane shear wall capacity. Finally, the tests examined whether the shear resistance is cumulative using lumber sheathing on one side and gypsum wallboard panels on the other side.

Bahmani and van de Lindt [2016]. An experimental test program set out to quantify the behavior of wall sheathing and finish materials in combination, a configuration that commonly provides wind and seismic bracing in dwellings. Materials tested alone and in combination include stucco, gypsum wallboard, and wood structural panel sheathing. Because no specific consideration was given to wall boundary conditions and issues regarding the loading protocol, the relevance of this resulting data is not known.

1.3.3 Testing of Full Buildings

The following are the results of full-scale shake-table tests of wood light-frame residential construction.

Fischer et al. (2001). An experimental shake table test of a two-story 1980s era wood light-frame single family dwelling. Tests were conducted for a series of configurations, including bare structure, and the structure with interior and exterior finishes added, at a range of ground-motion levels. Detailed reports provided the location and nature of damage. The dwelling included a very typical structural system common to North America, incorporating several characteristics of modern residential construction. Objectives included study of seismic response of a complete dwelling and evaluation of the effects of wall finish materials, both interior (gypsum wallboard) and exterior (stucco). Final results showed an increase of lateral stiffness and ample evidence supporting the concept that wall finish materials contribute significantly to the strength and stiffness of wood light-frame dwellings.

Mosalam et al. [2002]. An experimental shake table test of a three-story, multi-family, wood light-frame residential building with a soft- and weak-story configuration was performed. The testing incorporated features representative of construction techniques used in California during the 1960s and 1970s. Lateral resistance to earthquake loading was provided by plywood walls located on the perimeter of the building. One side of the ground story was left completely open to allow access for parking cars; this is representative of one common soft- and weak-story residential building configuration. Retrofit consisted of a welded steel moment-resisting frame installed at the garage opening. The shake table experiments of the three-story test building were performed in three main phases: phase I considered an as-built structure without finish materials or retrofit; phase

II considered a retrofitted structure with finish materials installed; and phase III considered an as-built structure with finish materials installed. The finish materials used included stucco on the exterior and gypsum wallboard on the interior of both the ground (garage) level and the upper-story dwelling unit levels. In addition to the dynamic testing, quasi-static component tests were conducted to investigate the performance of an alternate steel moment-resisting frame as well as some of the load path connections.

Mosalam et al. [2008]. An experimental shake table test was performed to evaluate the seismic response of a two-story 1940s-era wood light-frame single-family dwelling of a configuration typical for San Francisco, with the house over garage. Tests were conducted at a range of ground-motion levels and for a series of configurations. Detailed reports provide the global seismic response along with some information of the location and nature of damage. There are additional technical papers available on these tests.

Christovasilis et al. [2009]. An experimental shake table test was performed to evaluate the seismic response of a two-story 1980s era wood light-frame townhouse with an attached garage (configuration per *CUREE Publication No. W-29*) was performed; the test results used in loss estimation studies per *CUREE Publication No. W-18*. Tests were conducted at a range of ground-motion levels for a series of configurations, including bare structure, exterior finishes added, and interior and exterior finishes added. Detailed reports provide the location and nature of damage.

1.3.4 Other Literature of Interest

This section summarizes other available literature.

CUREE [2007, updated 2010]. *CUREE EDA-02* provides guidance for insurance claims adjusters, contractors, and homeowners regarding assessment and repair of earthquake-damaged homes. The report covers both structural and geotechnical components within single-family dwellings. Currently, this document is understood to be widely used by insurance adjustors to assess earthquake damage. It associates observable damage with a range of repair methods and describes the differences in the observed damage level that may lead to an increased scope in the repairs.

FEMA [2012a]. *FEMA P-50* presents a method for assessment of the seismic hazard and vulnerability of wood-frame dwellings. The methodology is based largely on vulnerabilities observed in past earthquakes. Included in Appendix C is a discussion of observed past performance that guides the assessment process. This is one source of collected information on seismic vulnerabilities experienced to date.

FEMA [2012b]. This *FEMA P-50-1 Guidelines* document includes specific guidance for retrofitting a dwelling's seismic vulnerabilities and potentially improving its Seismic Performance Grade. The *Guidelines* provides readers with practical information on retrofit measures to improve the earthquake resistance of a home. In addition, the *Guidelines* are comprehensive, beginning with illustrations of specific retrofit details, with a focus on those retrofits that have the greatest impact on building seismic performance, addressing well-known vulnerable elements such as cripple walls, porch roofs, water heaters, masonry veneer, and chimneys.

FEMA [2015]. *FEMA P-1024* documents the damage to various building types and nonstructural components following the 2014 South Napa event. Although most single-family residential houses were reported to be largely undamaged, homes with known structural deficiencies such as unbraced cripple walls and chimneys were shown to be heavily damaged in a number of cases. Failure occurred in both short and tall cripple walls. The report noted that those homes where the cripple walls had been retrofit to improve seismic performance suffered less damage than that those with unretrofitted cripple walls. Also noted is the lack of guidelines or prescriptive measures to provide seismic retrofit for taller cripple walls, which is a common structural detail for housing located in a flood plain. Unbraced cripple walls were found to have completely collapsed or exhibited large residual drift. Cripple wall damage found to be most common occurred in homes with wood siding and predominantly of pre-1930s construction. Post-earthquake recovery advisories issued with this report address how to repair to earthquake-damaged chimneys, retrofit crawlspace cripple walls, and anchor the dwelling to the foundation.

FEMA [2018]. *FEMA P-1100* is a pre-standard providing a stand-alone resource for assessment and retrofit of common seismic vulnerabilities in wood light-frame dwellings. Vulnerabilities included are cripple wall bracing and anchorage to the dwelling foundation, living-space-over-garage dwellings, hillside dwellings, and brick masonry chimneys. Both simplified engineering and prescriptive methods are provided for retrofit. This document was used to determine retrofit configurations used in the PEER–CEA Project UCB testing.

2 Overview of Testing at UCB

This chapter provides an overview of the PEER–CEA Project tests conducted at University of California, Berkeley (UCB), and introduces characteristics of the testing common to all UCB tests. Included are loading protocol, instrumentation, test setup, foundation, and gravity load. Details specific to each test will be provided in Chapters 3, 4, and 5. Note: the terms "existing" and "unretrofitted" are used interchangeably in this report.

2.1 OVERVIEW

As discussed in Section 1.1, the primary objectives of the PEER–CEA Project testing were to document load-deflection behavior to contribute to WG5 numerical modeling and collect descriptions of damage to contribute to WG6 fragility functions. Prior to the start of testing, a broad look was taken at data available from previous testing and gaps in the available data. Based on this effort, three areas of testing were identified as priorities and included in the project testing plan. These were:

- Group A - testing of cripple walls with various existing finish and sheathing materials, with and without retrofit;
- Group B - testing of cripple wall retrofit load path connections, and
- Group C - testing of selected superstructure finish and bracing materials.

Group A testing was divided between the University of California, San Diego (UCSD) and UCB; UCSD conducted a large number of small-component cripple wall tests, allowing a wide range of variables to be considered, while UCB conducted two Group A large-component cripple wall tests. Groups B and C testing were also conducted at UCB. Details of the UCSD testing can be found in four PEER–CEA Project reports by Schiller and Hutchinson. PEER reports are posted at the PEER website (*https://www.peer.berkeley.edu*) under "Publications and Products" (*https://peer.berkeley.edu/publications-products*).

A brief description of the UCB tests is provided in Table 2.1. The primary objective of UCB Group A tests was to study the behavior of cripple walls with boundary conditions as close as possible to those occurring in representative dwellings for use as a basis to judge how closely the UCSD small-component tests replicated the response of the cripple wall in a complete dwelling. The primary objective of UCB Group B tests was to study the performance of commonly used retrofit load path connectors for which load deflection and performance information was not publicly available. The primary purpose of the UCB Group C tests was to fill prominent gaps in testing information available for occupied story finish and sheathing materials commonly found in the California housing stock. For further information, see the testing plan in Appendix A.

Table 2.1 UCB Text Matrix

Test group	Specimen	Existing (E) or retrofit (R)	Exterior finish	Interior finish (in superstructure only)
A (cripple walls)	AL-1	E	Stucco over horizontal wood sheathing	Gypsum wallboard
	AL-2	R	Stucco over horizontal wood sheathing	Gypsum wallboard
B (load path connections)	B-1	R	Horizontal wood siding (shiplap)	N.A.
C (occupied story walls)	C-1	E	Horizontal wood siding (shiplap)	Plaster on wood lath
	C-2	E	T1-11 sheathing with typical non-shear wall installation	1/2-in. gypsum wallboard installed per conventional construction

2.2 LOADING PROTOCOL

A quasi-static lateral displacement history loading protocol was developed by Working Group 3 for use in this testing. The loading protocol was developed using analytical studies of model dwellings, and, in particular, took into consideration: (1) the response over a broad range of ground motion levels, consistent with the objective of developing fragility functions; and (2) the wide range of materials to be tested. For more details, the reader is referred to the PEER–CEA Project WG3 Task 3.1 report. PEER reports are posted at the PEER website [*https://www.peer.berkeley.edu*] under "Publications and Products" [*https://peer.berkeley.edu/publications-products*].

The displacement history was specified by drift ratio (i.e., displacement as a percentage of loaded specimen height, h. For Specimens AL-1, AL-2 and B-1, the displacement was imposed at the top of the cripple wall, with “h” taken as the clear height of the cripple wall, from the top of the foundation to the underside of the floor framing. For Specimens B-1 and B-2, the displacement was being applied at the top of the full-story-height walls, with “h” taken as the story clear height from the top of the foundation to the underside of the roof framing. The height of the floor or diaphragm was not included in h because the displacement occurring over this height was thought to be negligible.

The imposed lateral displacement history is presented in Table 2.2. A portion of this history up to a 3% drift ratio is illustrated in Figure 2.1. The tests were first subjected to seven very small displacement initiation cycles, with an amplitude of 0.002h (0.2% drift level). The displacement amplitude and number of cycles then proceeded as shown in Table 2.2. This loading protocol continued until the specimen had been loaded past peak strength, and the post-peak load in each cycle had dropped to 60% of the specimen peak strength. After this, each drift cycle amplitude was increased by 0.020h (at 2% drift-level increments).

This loading cycle increment continued until the post-peak load in each cycle had dropped to 20% of the specimen peak strength. At this point, a monotonic push was performed. If it was judged that the 20% residual strength strength was not feasible, judgment was relied on to determine when to start the monotonic push. The focus was to continue with the cyclic protocol to as high a drift ratio as possible, given test set-up limitations and safety concerns.

A constant loading rate for all the cycles was targeted to minimize the occurrence of inertia and strain-rate effects. Rate of loading guidance was taken from ISO [1999] and CUREE [2001], which recommend a displacement rate between 0.1 mm/sec and 10 mm/sec based on the geometry of the specimen and the limitations of the hydraulic system. The loading rates of 0.0787 in/sec (2 mm/sec) for the AL-1, AL-2, and B-1 and 0.1575 in/sec (4 mm/sec) for the C-1 and C-2 tests were selected. These rates met the rate of loading recommendations, while also providing a reasonable time of loading.

Table 2.2 Loading protocol.

Cycle level**	No. cycles	Drift level*	Drift ratio
1	7	0.002h	0.2%
2	4	0.004h	0.4%
3	4	0.006h	0.6%
4	3	0.008h	0.8
5	3	0.014h	1.4%
6	3	0.02h	2%
7	3	0.03h	3%
8	2	0.04h	4%
9	2	0.05h	5%
10	2	0.07h	7%
11	2	0.09h	9%
12	2	0.011h	11%

* h is the clear height of the cripple or shear wall.

** Once the peak load occurred, the subsequent drift levels were monitored to see when a 40% drop in peak load occurred. After this, each drift cycle was increase by 2% instead of the normal 1%. Once an 80% drop in peak load occurred, the monotonic push was performed.

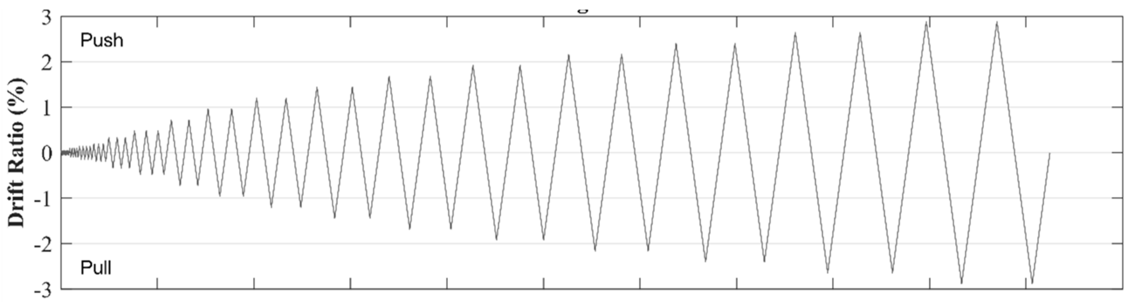

Figure 2.1 General lateral displacement history for testing of all specimens.

2.3 DATA COLLECTION

This section provides a general description of data collected during testing. A large amount of data was collected over the course of each test. Included were visual information (crack mapping, visual examination, photo documentation, video documentation, and laser scanning) and numerical data, which continuously captured using a large number of load and displacement transducers. While most of the data collection methods were applicable to all specimens tested, the exact detail of instrumentation varied depending on the varying specimen configuration; see Chapters 3, 4, and 5. All of the data collected has been archived by PEER.

2.3.1 Visual Data Collection

The visual data described above was primarily captured at set pause points in the loading protocol. At each given drift level, the loading was paused at the first peak pushing (displacement to the west), at the first peak pulling (displacement to the east), and at the subsequent return to zero displacement at the end of the first full displacement cycle. In addition, a pause occurred at the zero displacement at the finish of last cycle for each displacement level. Each of these pauses was used to rigorously inspect the specimen, mark cracks, document damage, and record observations. After reaching a post-peak drop to 60% of the specimen's peak shear capacity, inspection was reduced by skipping the zero displacement stop. Small differences occurred between the target drift and the drift actually achieved by the actuator due to the practicalities of actuator control. Photos included in this report were primarily taken at the peak displacement for the noted drift ratio. Additional photos at zero displacement are included in archived data.

During pauses in testing, laser scans were made of the overall specimen to capture overall geometry, including capturing the drift levels exhibited by the superstructure and the cripple walls. Several video and still cameras were used both outside and within the specimens to track specific behaviors. Some of the cameras recorded photos through the entire duration of the test, while others were stopped during the test for various reasons. Hand-held cameras were used to obtain photographs of the specimen through the course of the test; see Figure 2.2 for the plan showing the locations of the stationary cameras relative to Specimens AL-1 and AL-2. A similar layout was used for the other test specimens.

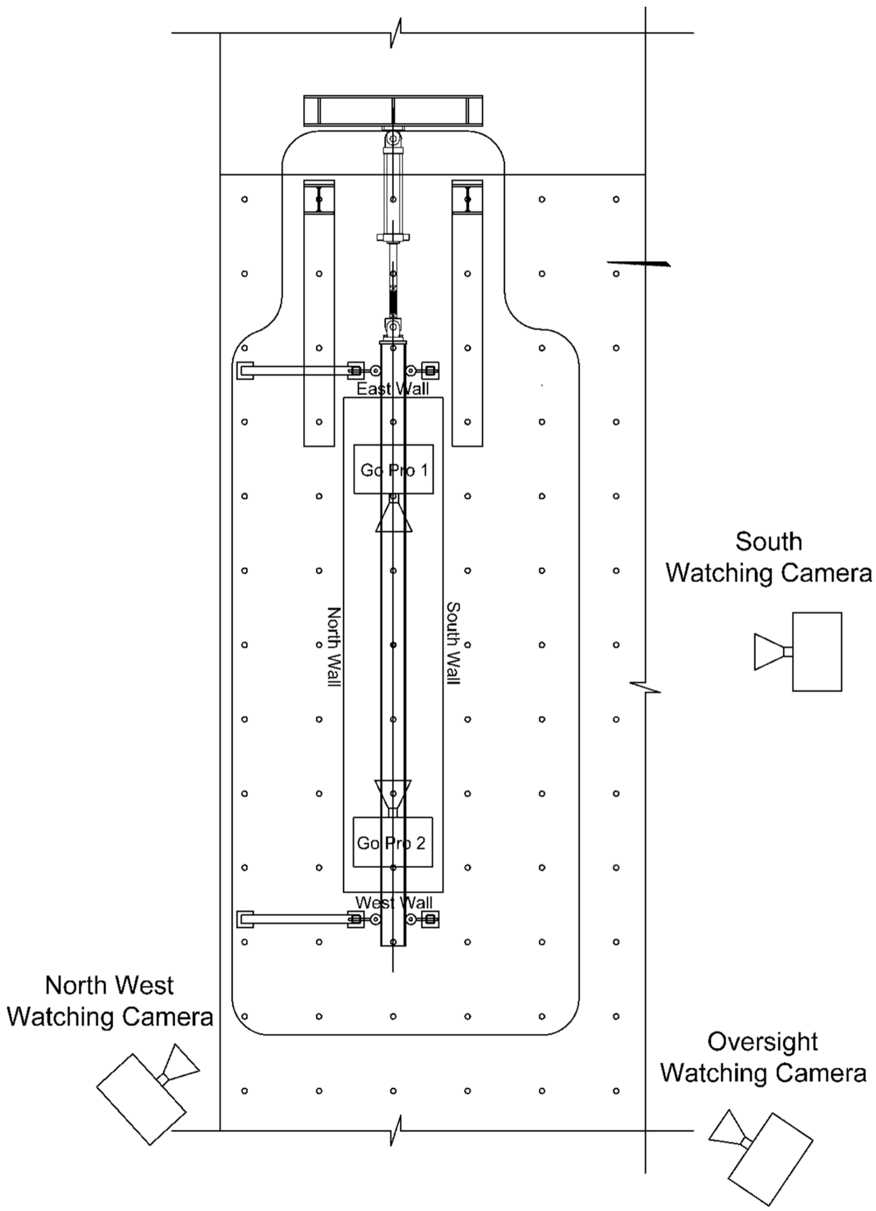

Figure 2.2 Locations of the stationary cameras used for Specimens AL-1 and AL-2.

2.3.2 Instrumentation

While the visual data described above was captured primarily at set pause points in the loading protocol, the instrumentation recorded data continuously during the testing. The instrumentation recorded the following data: applied lateral loads, anchor bolt forces, global and local displacements, and displacements at the test boundaries (i.e., specimen interface with foundation and loading beam). The types of instrumentation used are shown in Figure 2.3. Details of instrumentation for each test specimen will be addressed in Chapters 3, 4, and 5.

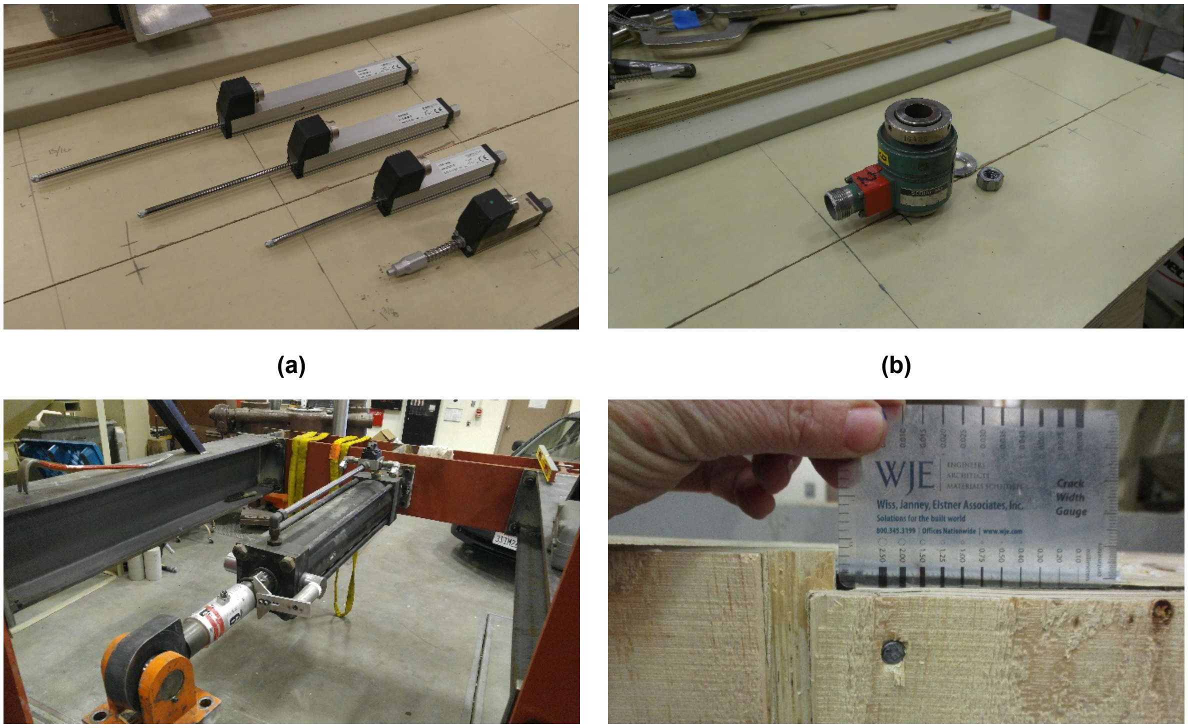

(a) (b)

(c) (d)

Figure 2.3 **Instrumentation tools and transducers: (a) LVDTs; (b) a string potentiometer; (c) actuator with embedded load cell and position sensor; and (d) crack gauge meters for visual inspection.**

2.4 TEST SETUP

Figures 2.4, 2.5, and 2.6 provide schematic diagrams of the test setup for Specimens AL-1 and AL-2, Specimen B-1, and Specimens C-1 and C-2, respectively. Included in these figures are the relative positions of the actuator, the loading beam, and the test specimen.

The lateral load from the actuator was transferred to the floor or roof diaphragm using a W12 × 40 steel loading beam welded to a 20-in.-wide × 0.5-in.-thick steel plate. The steel plate was fastened through the diaphragm sheathing into blocking placed below using SDS screws (SDS25300). Two rows of screws were installed on each side of the loading beam (four rows total), with screws spaced at 6 in. on center in each row and were staggered between adjacent rows. The steel-to-diaphragm fastening screw and diaphragm were designed such that they neither controlled the capacity of the test nor contributed significantly to deformation of the specimens. The loading beam and fastening are shown in Figure 2.7.

In designing the test setup, out-of-plane stability of the specimen during testing was identified to be a potential concern. As shown in Figure 2.8, a guiding system incorporating restraining frames was used to restrain transverse displacement of the specimen by restraining transverse displacement of the loading beam. A restraining frame was installed at each end of the loading beam. The frames were constructed of HSS sections that were anchored to the strong floor., and which contained internal diagonal braces. Roller sets were provided at each of the two loading beam heights (30 in. and 8 ft-6 in. above the foundation).

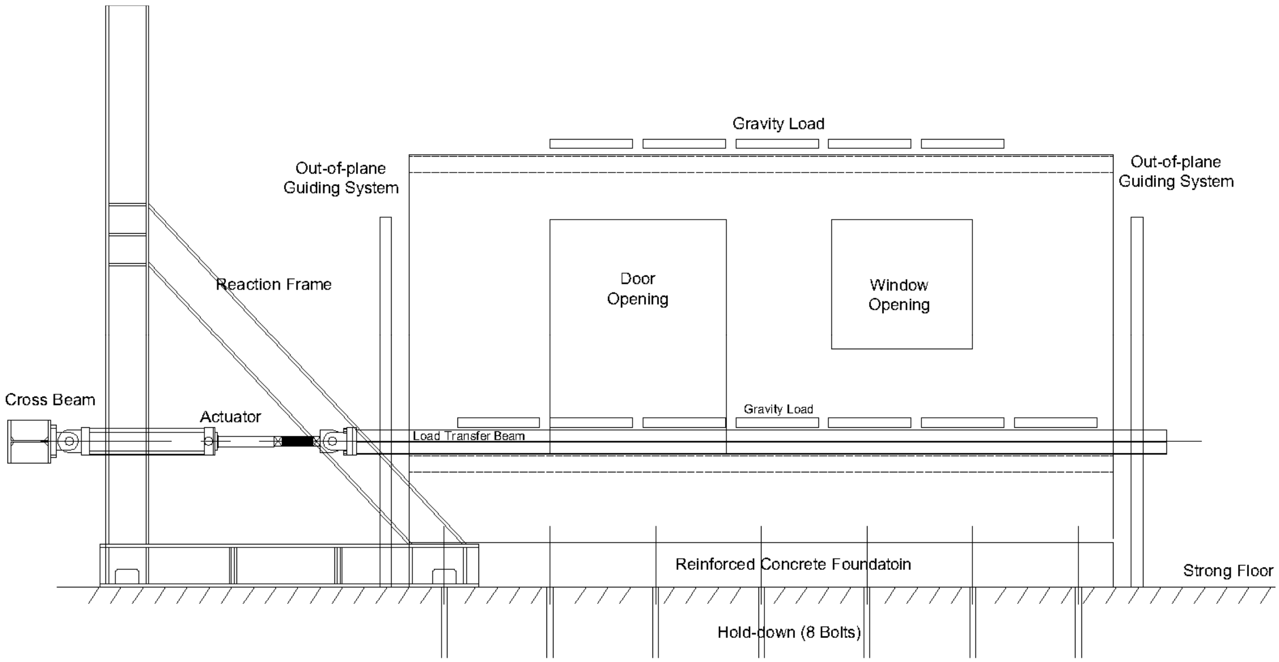

Figure 2.4 Schematic of loading fixture for Specimens AL-1 and AL-2.

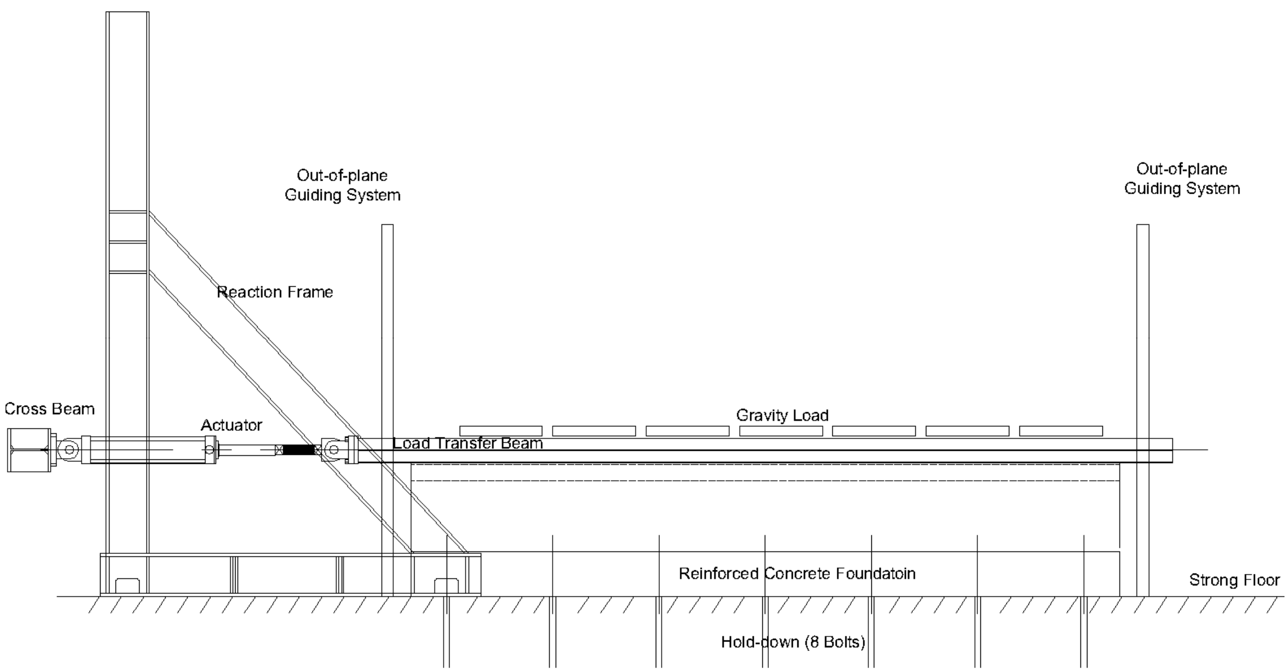

Figure 2.5 Schematic of loading fixture for Specimen B-1.

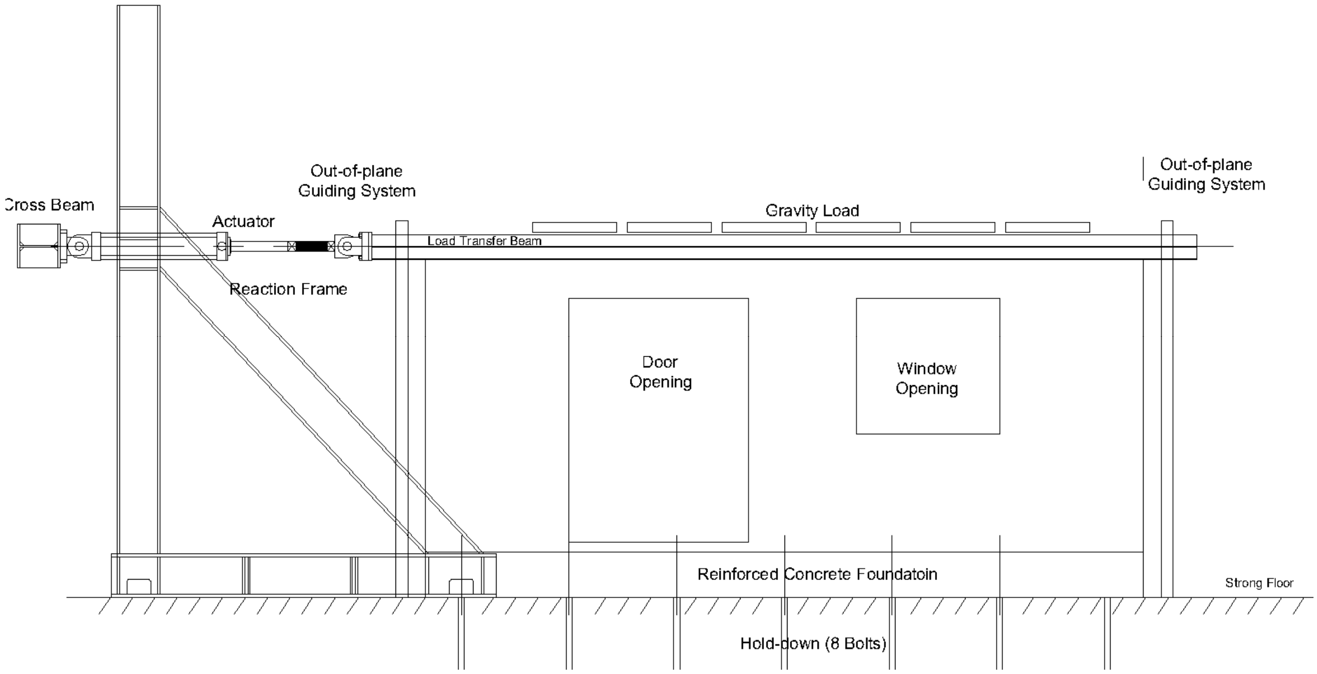

Figure 2.6 Schematic of loading fixture for Specimens C-1 and C-2.

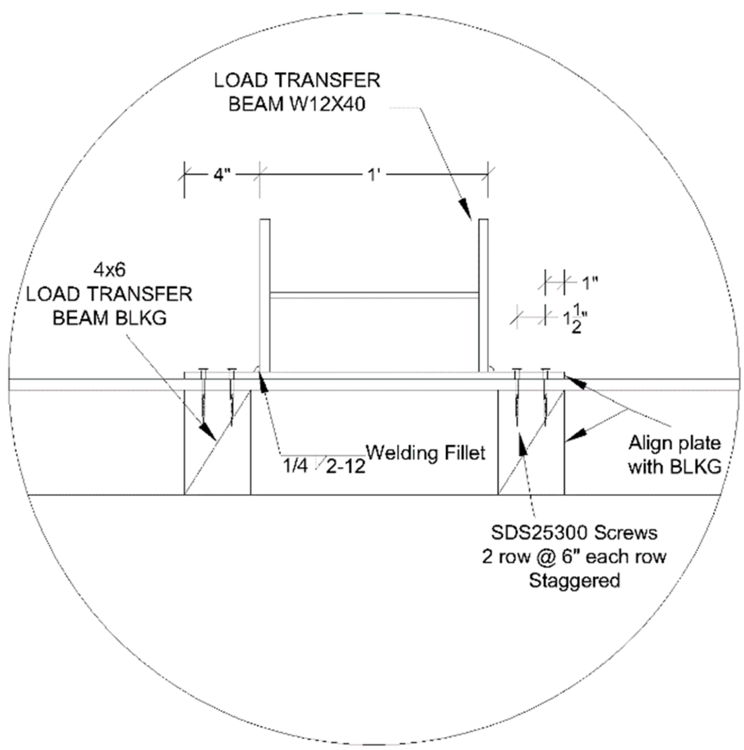

Figure 2.7 Detail of loading beam connection to diaphragm.

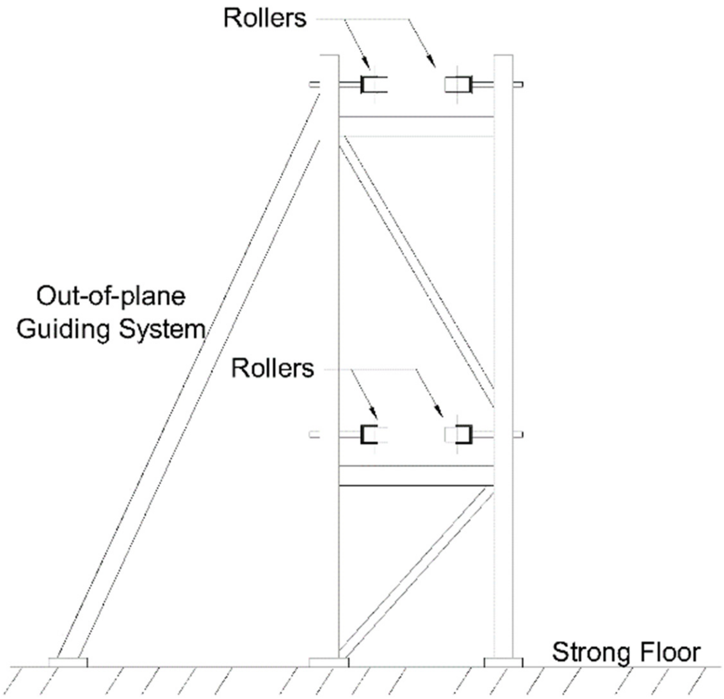

Figure 2.8 **Schematic of restraining frame. The two roller positions accommodate two different loading beam heights.**

2.5 FOUNDATION

The specimens were constructed on a reinforced concrete foundation 4 ft wide, 20 ft long, and approximately 15 in. high. The foundation was cast in place and rigidly anchored to the laboratory strong floor using tensioned tie-down rods. The foundation was constructed specifically for this testing program; the same foundation was used for all five tests. The concrete mix design used a specified design strength of 2500 psi, with the intent of being as representative as possible of the quality of concrete found in existing dwelling foundations. Suitable sleeves for bolts to connect the foundation to the strong floor and for connection of the specimen to the foundation were installed prior to placement of concrete, which were chosen to provide a tight fit for the threaded rods later installed as anchor bolts to best represent cast-in bolts. The layout of the foundation used for all the specimens is shown in Figure 2.9. Further information regarding geometry and steel reinforcement is provided in Appendix B. Note: some limited spalling occurred at the edge of the foundation during testing; as a result, requiring minor patching of the concrete during construction of some test specimens.

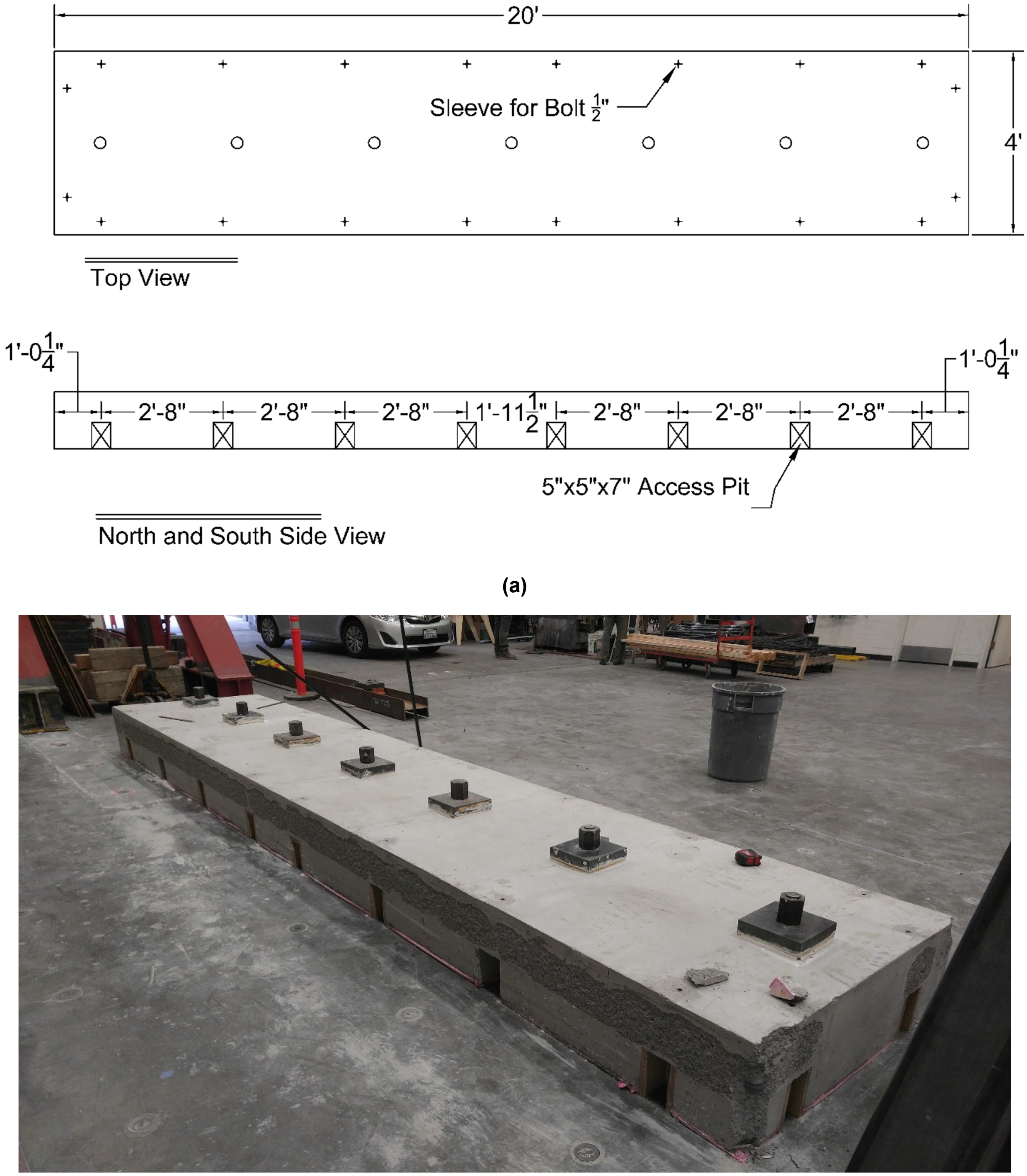

(a)

(b)

Figure 2.9 Foundation layout used for all the specimens.

2.6 GRAVITY LOAD

The test gravity load of each specimen was specified to match a representative dwelling configuration. The gravity load was provided by a combination of the test specimen self-weight, the loading beam self-weight, and lead blocks. The additional lead block weight for Specimens

AL-1 and AL-2 was distributed at both the floor and roof level, at the floor for Specimen B-1, and at the upper (roof) level for Specimens C-1 and C-2. These are illustrated schematically in Figures 2.4, 2.5 and 2.6. The gravity load introduced in Specimen C-1 is shown in Figure 2.10. Further details regarding amount and placement of supplemental gravity load is provided in Chapters 3, 4, and 5.

(a)

(b)

Figure 2.10 Supplemental gravity load provided by lead blocks: (a) lead blocks placed over the loading beam on the Specimen C-1 roof; and (b) racks of lead blocks on the lab floor prior to placement on the specimen.

3 Group A Large-Component Tests

This chapter discusses Group A Large-Component Specimens AL-1 and AL-2. The primary objectives of Specimen AL-1 and AL-2 testing were to help inform WG5 select parameters for numerical studies, and to collect damage information to help WG6 populate fragility functions. In addition, objectives included comparison of cripple wall performance—with and without retrofit—and providing large-component test data that could be compared to the PEER–CEA Project small-component tests conducted at UCSD. The primary goal in designing the specimens' test cripple wall components was to have boundary conditions as close as possible to those occurring in dwellings. Earlier tests [CUREE-EDA 2003] had identified realistic boundary conditions as significantly affecting both the peak shear capacity and drift at peak shear capacity of full-story-height walls with stucco exterior finishes. While representative boundary conditions are likely to have some influence for all finish materials, the inherent strength and continuity of stucco means that it likely represents (across the range of common exterior finish materials) an upper bound of the influence of continuity and, therefore, the influence of boundary conditions.

This chapter provides details of construction for Specimens AL-1 and AL-2, presents test results, and provides discussion and conclusions. Note: the terms "existing" and "unretrofitted" are used interchangeably in this report.

3.1 INTRODUCTION

As discussed, the continuity of the cripple wall stucco was believed to be of importance for these cripple wall tests, including stucco continuity from the top of the cripple wall into the story above, stucco continuity around corners, and stucco continuity down the face of the foundation (a common stucco installation detail in older homes). Therefore, Specimens AL-1 and AL-2 were constructed as three-dimensional (3D) components, 20 ft × 4 ft in plan, which included the cripple wall and a single-story superstructure above and a foundation below; see Figure 3.1.

As reflected in the materials and details of construction, the test specimens were targeted to be representative of construction circa 1940, one of the eras of construction of significant interest to the PEER–CEA Project efforts. The 1943 Uniform Building Code [Pacific Coast Building Officials 1943] and stucco industry documents from this time frame were used to replicate construction details.

The configuration of the test specimen was based on a hypothetical model dwelling with a 30- × 40-ft footprint, with a stucco exterior finish applied over building paper and horizontal lumber sheathing. A dwelling typical of this era would have applied plaster on wood lath interior finish for the occupied stories; because of cost and time required to replicate this finish, the test specimen was constructed with a gypsum wallboard interior instead. Based on the lack of observed drift and damage in the superstructure, the use of gypsum wallboard in place of plaster on wood lath is not believed to have influenced the testing results. Consistent with typical construction practice, no interior finish material was installed on the cripple walls.

The test specimen included 2-ft-high cripple walls seated on the concrete foundation, a framed floor, and 8-ft-tall superstructure walls, covered by a roof. Each of these walls was chosen to have one door (sliding glass or French door) and one window, with the layout of each wall being a mirror image of the other, as shown in the wall elevations in Figure 3.2. The goal was to have the wall configurations be consistent with what might be seen in housing stock of this era, including representative opening and wall-pier dimensions. The loading of the test specimen was parallel to the 20-ft walls. Specimen AL-1 was representative of an existing structure prior to retrofit, while Specimen AL-2 included a retrofit designed in accordance with *FEMA P-1100* [FEMA 2018]. A summary of key characteristics of the two test specimens is provided in Table 3.1. Further information on details of construction follows. Construction drawings for Specimens AL-1 and AL-2 are provided in Appendix B.

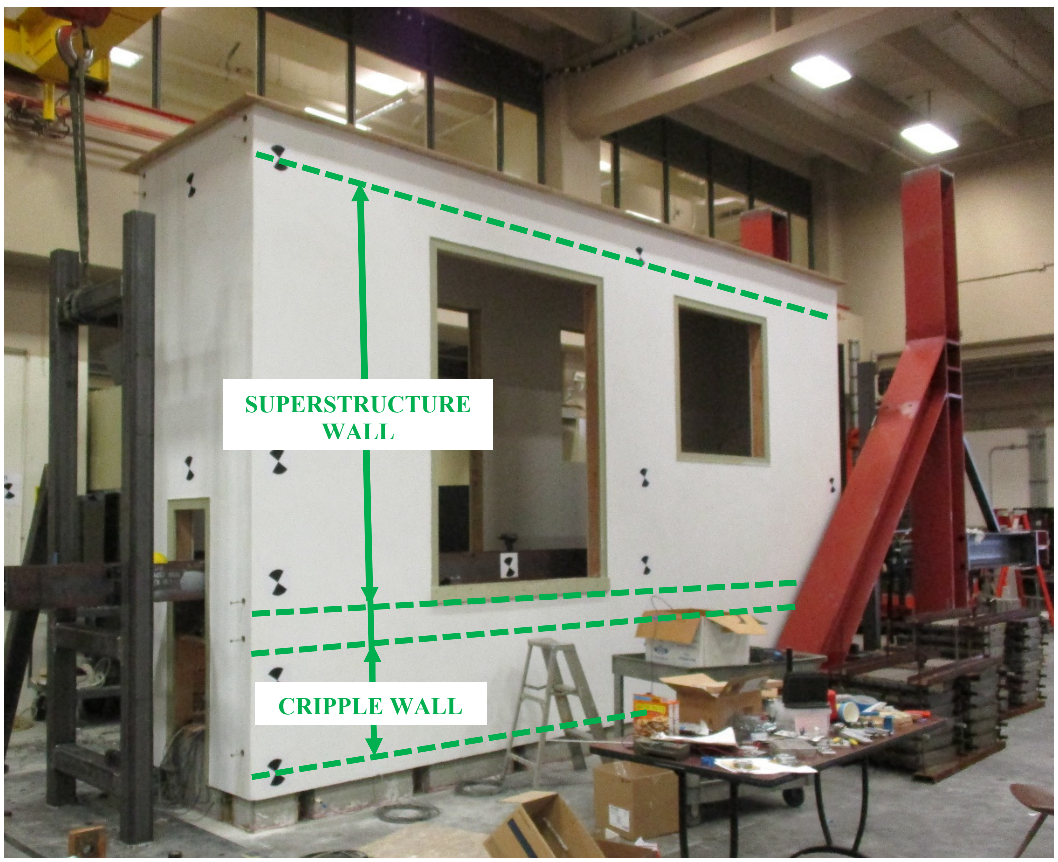

Figure 3.1 Specimen AL-1 prior to start of testing. Figure shows superstructure wall above and cripple wall below.

Table 3.1 Test matrix for Specimens AL-1 and AL-2.

	Existing (E) or retrofit (R)	Exterior finish	Interior finish	Retrofit detail in cripple wall level	Cripple wall height (ft)	Super-structure height (ft)
AL-1	E	Stucco over horizontal lumber sheathing.	Gypsum wallboard	N.A.	2	8
AL-2	R	Stucco over horizontal lumber sheathing.	Gypsum wallboard	Plywood sheathing, extra bolts, and A35 shear clips	2	8

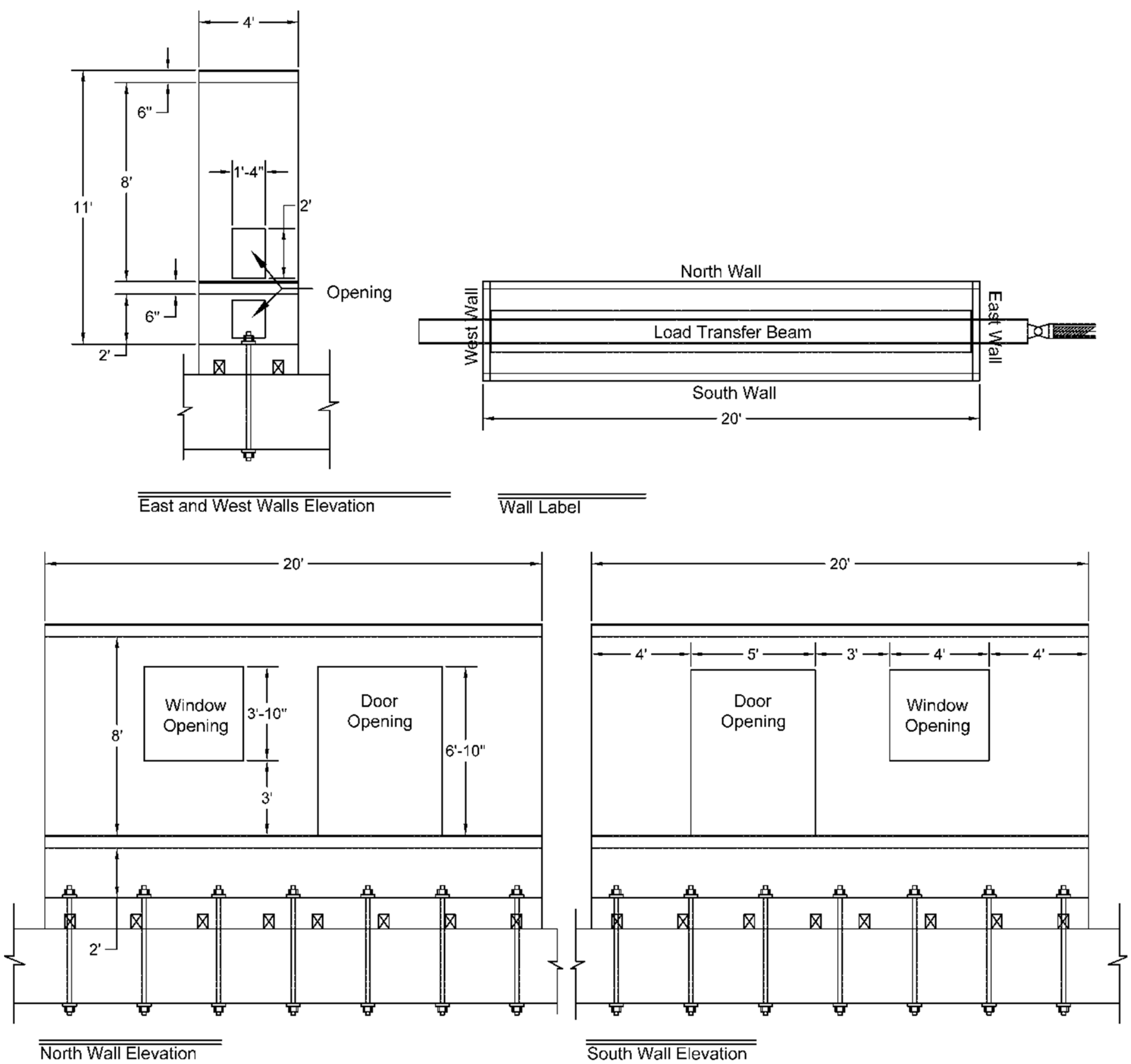

Figure 3.2 Elevation and section figures for Specimens AL-1 and AL-2.

3.2 FRAMING DETAILS

Specimens AL-1 and AL-2 were designed to represent either a single-story dwelling or the bottom story of a two-story dwelling. Each specimen has 2-ft-tall wood-framed cripple walls, with the 2 ft corresponding to the distance between the top of foundation and top of the double top plate. On top of the cripple walls, an approximately 6-in.-tall high-load floor diaphragm was constructed, consisting of 4 × 6 joists at 16 in. on center and 19/32-in. Structural I-plywood floor sheathing. The objective of the high-load diaphragm design was to ensure that the diaphragm would be capable of developing the peak shear capacity of the cripple walls. Because the diaphragm was being used to load the cripple walls (but was not the focus of the project), a more modern high-capacity diaphragm was built.

The superstructure used an 8-ft-tall wall; with the 8 ft corresponding to the distance between the top of the floor diaphragm to the top of the double top plate. A roof diaphragm with a height of approximately 6 in. was constructed above.

The exterior face of the building was covered with Portland-cement stucco, installed over building paper and 1 × 6 horizontal lumber sheathing. Gypsum wallboard, installed in 4 ft × 8 ft sheets, was installed on the interior face of the superstructure walls.

The test specimen was anchored to the foundation using 1/2-in. all-threaded anchor bolts distributed along both the long and short sides of the building. Specimen AL-1 used four bolts on each of the 20-ft-long sides and two bolts on each of the 4-ft ends. Additional bolts were added for the Specimen AL-2 retrofit, which will be discussed in the retrofit design section. The all-thread anchor bolts were inserted into sleeves that had been cast into the foundation to allow for modifications to anchorage for the different component tests. The sleeves were of thin-walled electrical conduit and provided a very tight fit to the threaded rods, limiting displacement between the threaded rod and sleeve to a negligible amount. As shown in Figure 3.3, during testing load cells, were used to measure the tensile forces in a portion of the anchor bolts. The same framing details, interior sheathing, and stucco were used for both specimens. Specimen AL-2 included additional sheathing and connectors, which is consistent with seismic retrofit of cripple walls.

Elevations of the framing of the walls are shown in Figure 3.4. A cross section of the test specimen is shown in Figure 3.5. Framing plans for the floor and roof diaphragms are shown in Figure 3.6. All framing was of Douglas-fir, grade No. 2 or better. Minimum fastening tables from 1940s-era building codes were used in construction of the specimens, which when necessary were supplemented by more recent fastening schedules.

The foundation sill plates were of 2 × 6 nominal Douglas-fir lumber. The 2 × 6 was selected to best replicate 1940s-era construction, where the foundation sill plate was commonly wider than the supporting cripple wall framing. Framing members for the cripple wall studs and top plates were 2 × 6 nominal Douglas-fir lumber ripped to 4 in. deep. The studs were spaced 16 in. on center and were end-nailed to the foundation sill plate and lower top plate using two 16d common nails per stud. The upper top plate was face-nailed to lower top plate using 16d common nails at 12 in. on center two 16d common nails were provided at the corner laps in the top plates, To provide access for placement of instrumentation and to allow observation of performance, the cripple walls had 16 in. wide × 24 in.-high crawl space access openings in each of the 4-ft end walls.

Figure 3.3 Load cell installation within the foundation access pockets.

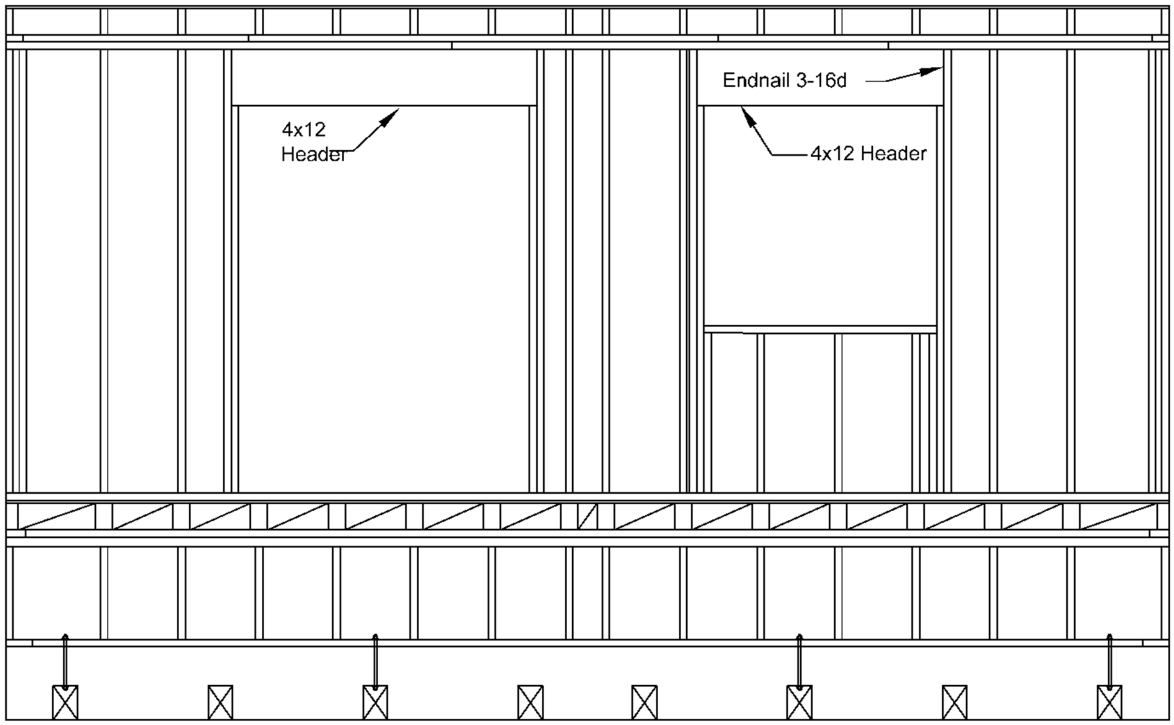

(a)

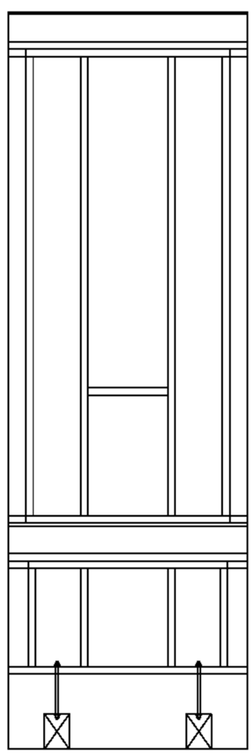

(b)

Figure 3.4 Wall framing details for Specimens AL-1 and AL-2: (a) south-wall framing; and (b) east- and west-wall framing.

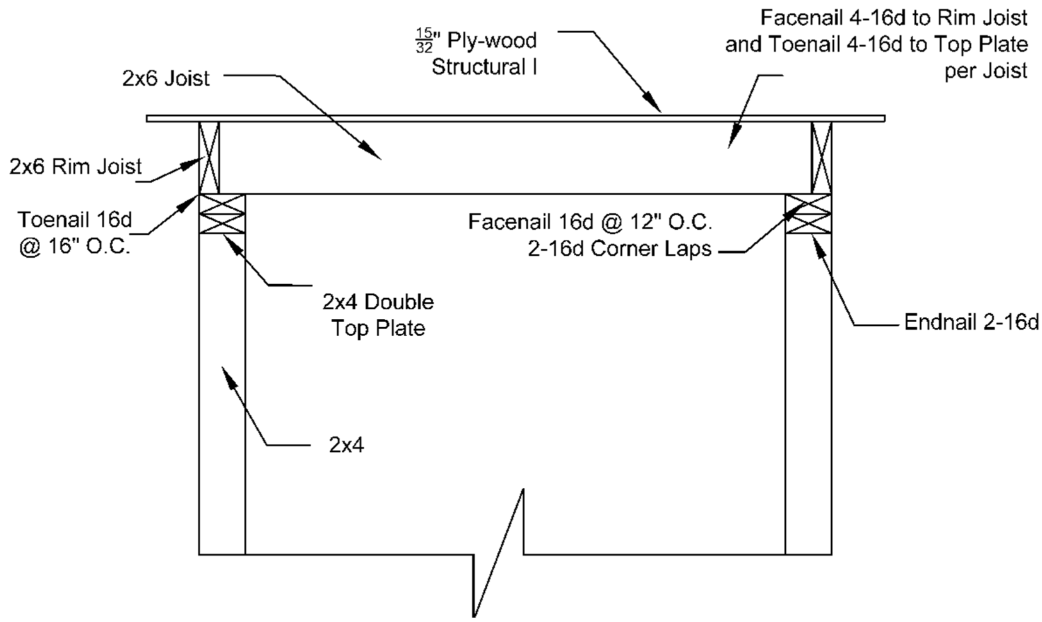

(a)

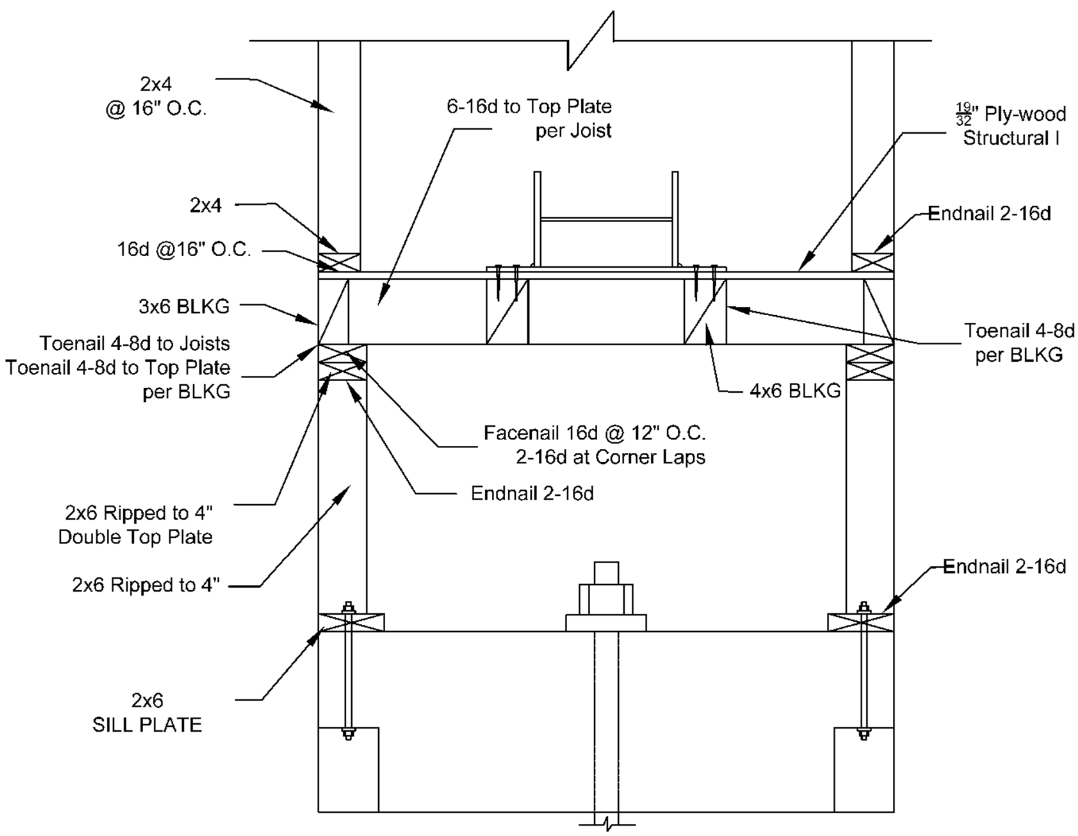

(b)

Figure 3.5 Elevation and section figures for Specimens AL-1 and AL-2.

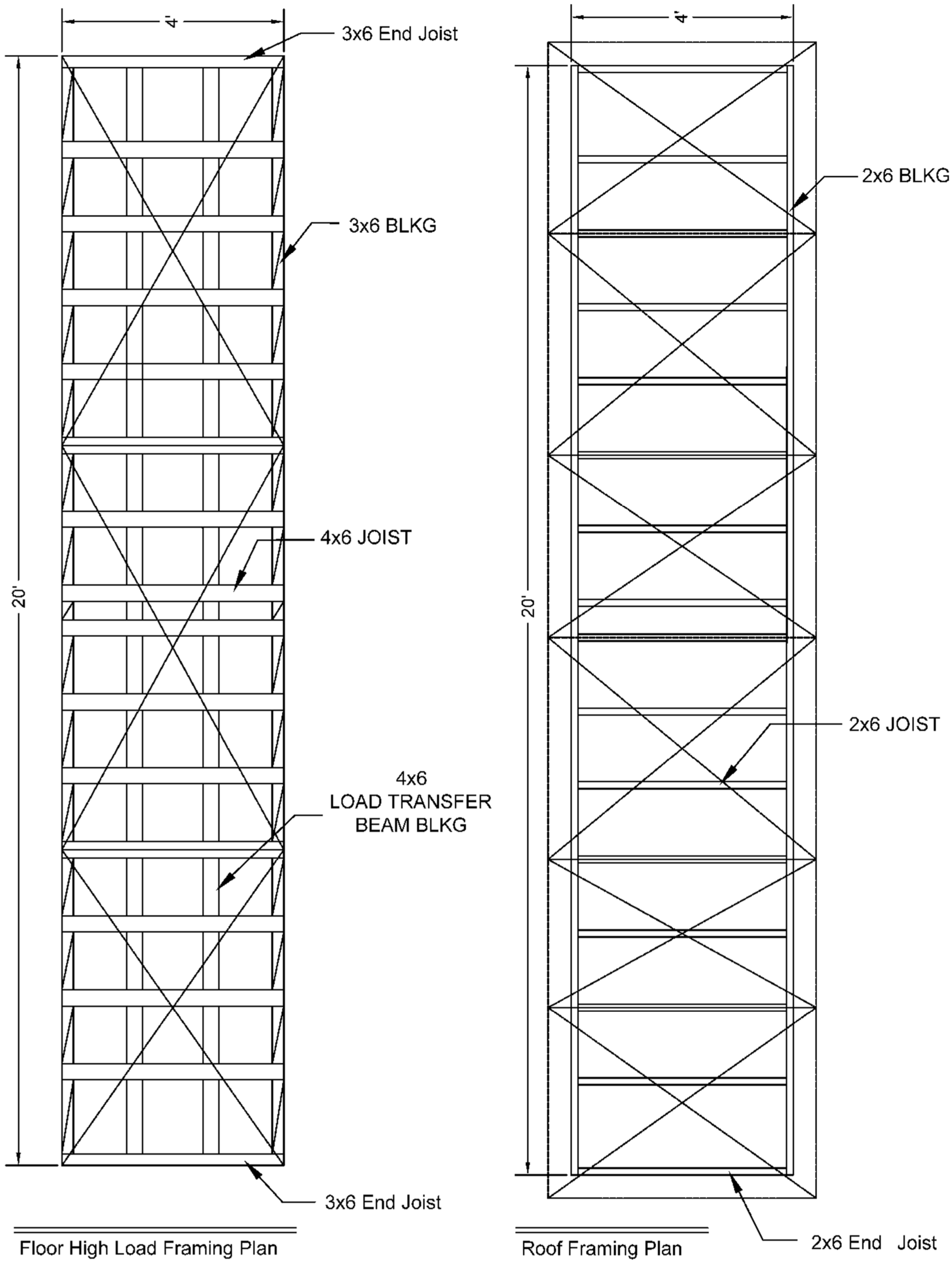

Figure 3.6 Diaphragm framing details for Specimens AL-1 and AL-2.

The high-load floor diaphragm was constructed on top of the cripple walls. To accommodate multiple rows of diaphragm edge nailing as specified for high-load diaphragms by the Special Design Provisions for Wind and Seismic (SDPWS) Standard [AWC 2015], 4 × 6 and 3 × 6 floor framing members were used. The 4 × 6 nominal Douglas-fir lumber joists were spaced 16 in. on center. Rim joists were composed of 3 × 6 nominal Douglas-fir lumber on all four edges of the diaphragm. Six 8d common nails were used to toe-nail joists to the upper top plate (three at each end of the joist). The blocking on top of the cripple wall top plate was toe-nailed to the joists using four 8d common nails (two each end of blocking) and four 8d common nails to the top plate per block. Also, two rows of blocking were provided near the center of the 4-ft diaphragm to provide a substrate for connecting the loading beam to the floor diaphragm. Structural I plywood sheathing of 19/32-in. thickness was used for the floor diaphragm, with four staggered rows of 10d common nails at 2-1/2 in. on center for each row at the diaphragm interior panel edges and boundaries. Field nailing used one row of 10d common nails spaced at 3 in. on center. As discussed previously, the main objective of the diaphragm design was to provide enough strength and stiffness so that the diaphragm would adequately transfer loading beam displacements to the cripple wall without acting as a weak link or contributing significant deformation.

Framing members for the superstructure walls were 2 × 4 nominal Douglas-fir lumber. The studs were spaced 16 in. on center. The sill (sole) plates were 2 × 4 nominal Douglas-fir framing members. The studs were end-nailed to the sill plate using two 16d common nails. The studs also were end-nailed to the lower top plate using two 16d common end nails. The upper top plate was face-nailed to lower top plate using 16d common nails at 12 in. on center; an extra two 16d common face nails were added at the corner laps.

On top of the superstructure walls, the roof was framed with 2 × 6 nominal Douglas-fir joists spaced at 16 in. on center. Four 16d common nails (two each end) were used to toe-nail joists to the upper top plate, and four 16d common nails were used to face-nail the joist to the continuous rim joist. Rim joists were 2 × 6 nominal 20-ft-long Douglas-fir framing members; 16d common nails were used to toe-nail the rim joists to upper top plate. Structural I plywood of 15/32-in. thickness was used for the roof sheathing, with 10d common nails spaced 3 in. on center in the field and 2 in. on center for the interior panel edges and boundary. At all edges of the roof, a 5-in.-plywood overhang was constructed to provide the stucco installers a surface for the top termination of the stucco. In older houses, this surface would commonly be composed of lumber roof sheathing at the roof overhang. For this test program, it was decided to use the roof plywood sheathing in place of lumber sheathing.

Consistent with common dwelling construction in the 1930s and 1940s, horizontal lumber sheathing was installed on the exterior walls prior to installing building paper and stucco. Douglas-fir 1 × 6 lumber sheathing was installed using two 8d common nails at each stud, which was consistent with applicable building codes. The lumber sheathing was installed with gaps of approximately 1/8-in. between boards, which is believed to be consistent with gaps typically found in installed lumber sheathing. Details of lumber sheathing installation can be found in Appendix B. Photographs of the framing and lumber sheathing are shown in Figure 3.7.

Framing and sheathing fasteners were installed with a nail gun. While this created the potential for over-driven nails and subsequent reductions in capacity, little or no overdriving was observed. Therefore, the use of a nail gun is not believed to have affected the testing results. It is noted that finished lumber dimensions have varied over time with "full dimension" (i.e., 2 in. × 4 in.) lumber having been common to the 1920s, an intermediate size (i.e., 1-5/8 in. × 3-5/8 in.) used until the 1960s, and modern sizing (i.e., 1-1/2 in. × 3-1/2 in.) used since. The changing size of framing is not believed to have affected the testing results.

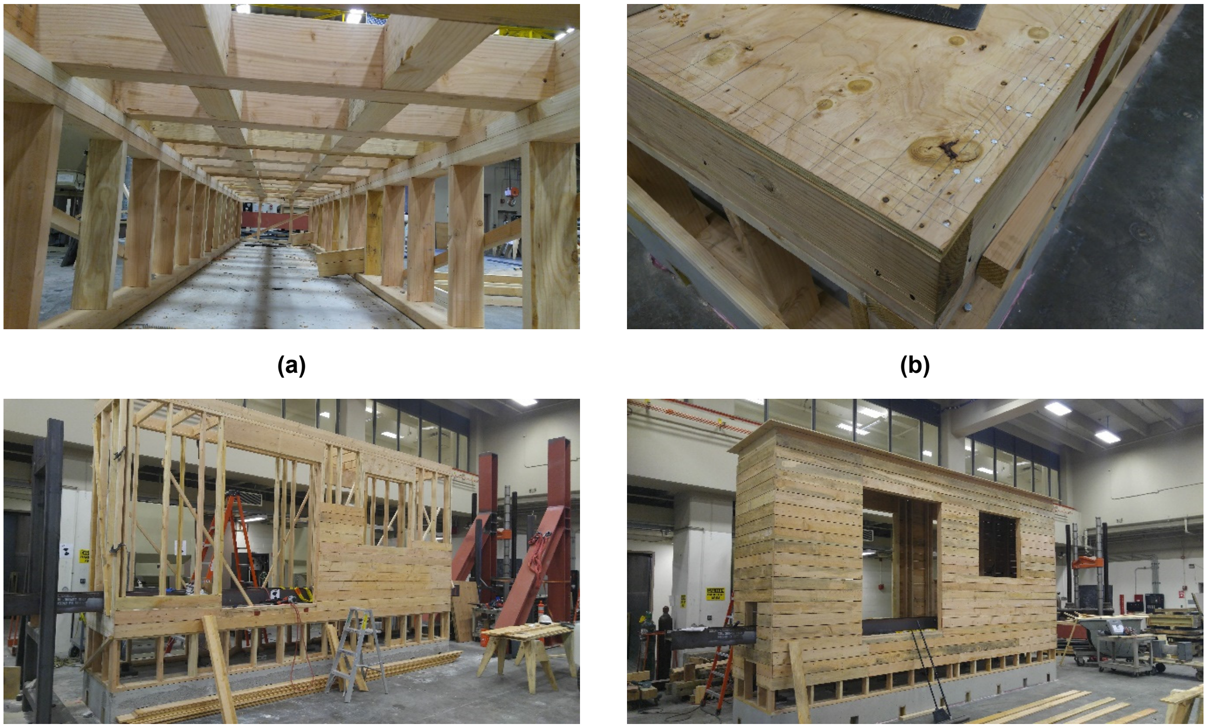

(a) (b) (c) (d)

Figure 3.7 Framing details for Specimens AL-1 and AL-2: (a) crawlspace framing; (b) preparation for floor plywood nailing; (c) wall framing; and (d) side sheathing.

3.3 Installation of Stucco

Stucco materials and installation for specimens AL-1 and AL-2 were provided by general contractor Saarman Construction and their sub-contractor GreenWall Tech. Primary references for the stucco and fasteners were the 1937 and 1943 editions of the Uniform Building Code [Pacific coast Building Officials' Conference 1937; 1943]. The stucco was installed using three coats: a scratch coat (3/8 in. thick), a brown coat (3/8 in. thick), and a finish coat (1/8 in. thick). Figure 3.8 shows the different steps in the installation of the stucco wall finish. Even though photographs are for Specimen AL-1, similar procedures were followed for Specimen AL-2.

(a)

(b)

Figure 3.8 Steps for installation of stucco for Specimens AL-1 and AL-2: (a) installation of building paper and wire lath; and (b) application of scratch coast (3/8 in. thick); (c) application of brown coat (3/8 in. thick); and (d) application of finish coat (1/8 in. thick).

(c)

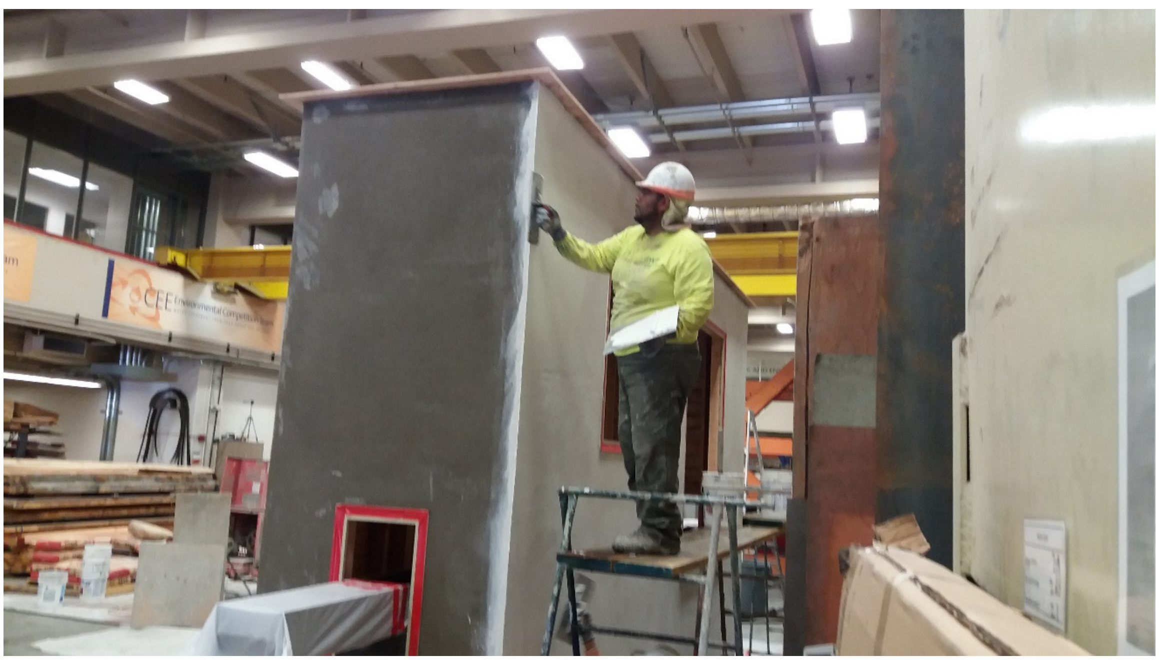

(d)

Figure 3.8 (continued)

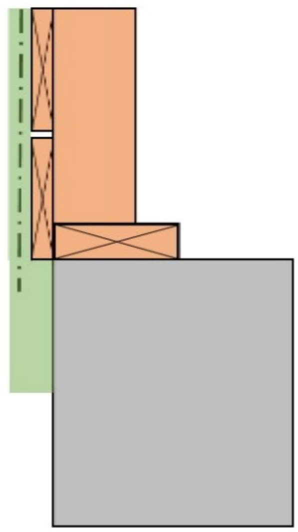

(a) (b)

Figure 3.9 Stucco extension down the face of the foundation; (a) schematic of stucco extension; and (b) stucco extension at end wall.

One significant detailing point was the boundary condition at the bottom of the stucco. Based on a commonly observed condition in older dwellings, the stucco was extended 8 in below the bottom of the foundation sill plate. This was intended to mimic older dwellings where stucco runs down the face of the foundation to below adjacent grade. The building paper and wire were extended down the face of the foundation approximately 2 in. below the bottom of the foundation sill plate and then discontinued. The surface roughness of the concrete foundation was increased slightly by using a hammer to lightly chip the concrete surface prior to installation of the stucco. Figure 3.9 shows the boundary condition of the stucco at the bottom of the stucco.

Prior to installing stucco, a single layer of building paper (Grade D–60 Minute) was installed and attached directly to the lumber sheathing using a standard hammer stapler with 3/8-in.-long leg-collated staples. The building paper covered the entire outer surface of the specimen plus an extra 2-in. overhang that lapped the concrete foundation. Reinforcement for the stucco was provided using chicken wire lath, consisting of hexagonal shaped galvanized 1-1/2-in., 17-gauge wire mesh. The wire lath was attached to the framing using #11 ×1 ½ in. furring nails with 1/4-in. wads, hand hammered, and spaced at 6 in. on center on studs, the foundation sill plate, and the roof rim joist; because the wire lath mesh was 36 in. wide, the pieces had 3 in. of overlap. See Figure 3.10 for photographs showing installation details of the building paper and wire lath.

(a)

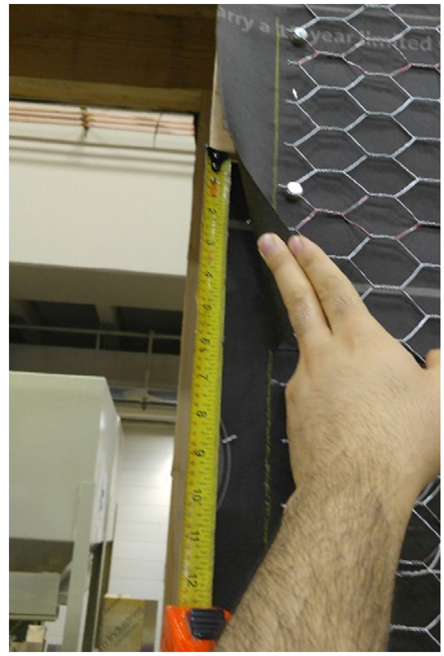

(b)

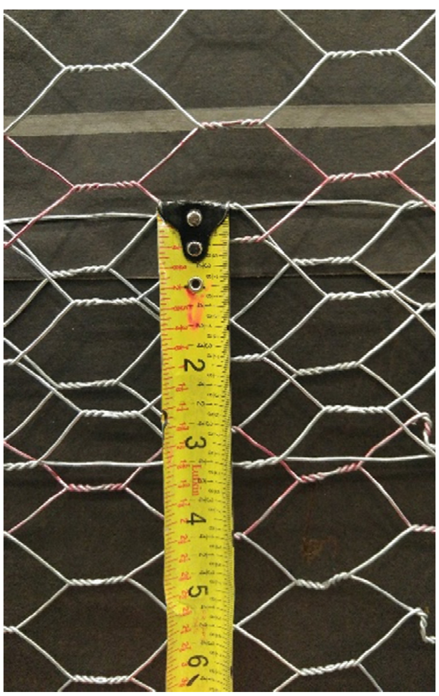

(c)

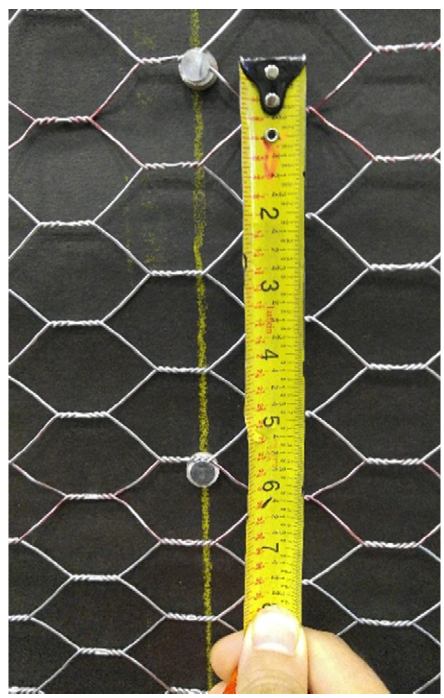

(d)

Figure 3.10 Details for installation of wire lath for stucco: (a) east-end wall; (b) overlap between different rows of building paper; (c) overlap between different rows of wire lath; and (d) space of furring nails at 6 in. on center.

The scratch coat was installed first and kept moist for 48 hours using a visqueen cover and periodic spraying with a water bottle. One week after scratch coat installation, the brown coat was installed and kept moist for 48 hours in the same manner. A mixture of Type II-V Portland Cement, clean graded kiln-dried plaster sand, and Type S lime was used for both scratch and brown coat. Three days after brown coat installation, the finish coat was installed and similarly kept moist for 48 hours. A mixture of White Portland Cement, clean graded kiln-dried plaster sand, and Type S lime was used for the stucco finish coat. At the time of stucco installation, test cubes for each of the three coats were collected for strength testing.

3.4 INSTALLATION OF GYPSUM WALLBOARD

The superstructure interior finish was vertically oriented gypsum wallboard, 1/2-in.-thick, installed in 4- × 8-ft sheets. The gypsum wallboard was fastened using 0.086-in. by 1-5/8-in. drywall nails (roughly equivalent to code specified 5d cooler nails), spaced 7 in. on center over the full height of uniformly spaced studs (16 in. on center) and at wall ends and openings. Extra studs, i.e., king studs at door and window openings, did not have gypsum board nailing, which is consistent installation practices of the era; see Figure 3.11. Specimens AL-1 and AL-2 had neither tape nor joint compound installed at gypsum wallboard joints. No ceiling finish was provided.

(a) (b)

(c) (d)

Figure 3.11 Installation of gypsum board: (a) cupped dry head nails; (b) gypsum wallboard installation; (c) top corner beneath roof diaphragm; and (d) installation at window opening.

3.5 SEISMIC RETROFIT

Test Specimen AL-2 was identical to Specimen AL-1 except that it included a cripple wall seismic retrofit designed in accordance with the *FEMA P-1100* prescriptive design provisions for crawlspace dwellings. Similar to other aspects of the test specimens, the design of the cripple wall retrofit was determined based on a model dwelling, assuming plan dimensions of 30 × 40 ft. For purposes of the retrofit design, the model building was assumed to be two stories over a cripple wall. The short-period design spectral response acceleration, S_{DS}, as determined in accordance with ASCE 7 [ASCE 2010], was taken to be 1.0. This represents dwellings located in high seismic hazard areas but not subjected to near-fault conditions.

The model dwelling was assumed to have a stucco exterior wall finish, plaster on wood lath interior walls and ceiling finishes, and a composition (asphalt) shingle roof. Using this information, the dwelling weight classification was determined to be heavy in accordance with Figure 4.4-1 of *FEMA P-1100*, as shown in Figure 3.12.

Next, the required sheathing, anchor bolts and shear clips were determined from Figure 4.4-9 of *FEMA P-1100*, applicable for $S_{DS} = 1.0$ and two-story dwellings; see Figure 3.13.

In Figure 3.13, the row representing two-story heavy construction and a total area of 2400 ft^2 (two stories at 1200 ft^2 each) was used. For shear wall sheathing, where the table called for 12 ft of wood structural panel nailed at 2 in. on center, the test substituted 19 ft nailed at 3 in. on center; this was calculated to have the same capacity, while resulting in the plywood extending for the full length of the cripple walls. This was chosen in part to better mirror similar tests at UCSD whereby the retrofit sheathing was applied across the full length of the cripple wall. In addition, it was assumed that the stiffness of the W12 loading beam used in the testing apparatus would greatly limit the ability to draw any conclusions regarding use of cripple wall retrofit sheathing if it did not extend the full length of cripple wall; the stiffness of the loading beam would limit the ability of the sheathing to uplift locally at sheathing panel ends.

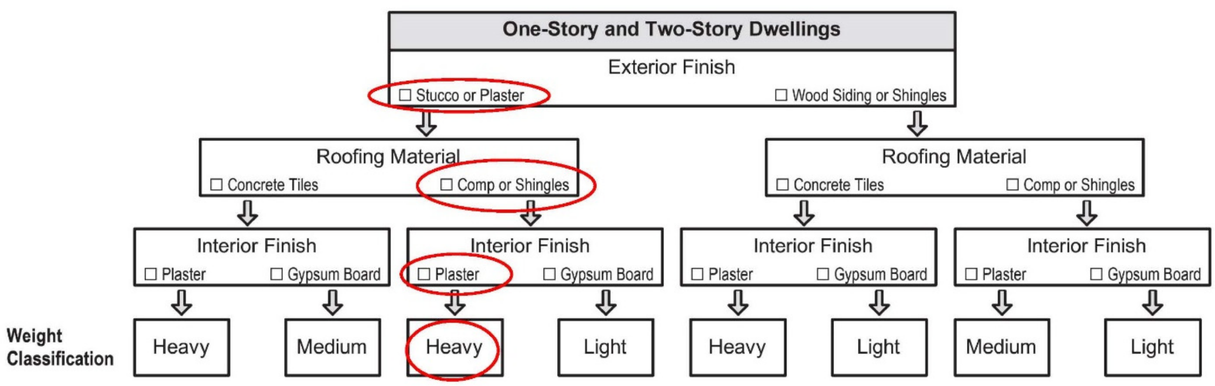

Weight Classification:
This flowchart is used to determine the general weight classification of your home's construction.

1. Check the box of the material that most closely matches your home's finishes.
2. Note the Weight Classification result for use in the Earthquake Retrofit Schedules.

Specific notes for exterior, interior and roof coverings

1. The "wood siding or shingles" exterior finish category also includes finishes of similar weight, including but not limited to fiber-cement and aluminum siding.
2. The "comp or shingles" roofing material category also includes roofing materials of similar weight, including but not limited to roll roofing, built-up felt roofing, single-ply membrane roofing, and metal roofing.
3. The "gypsum board" interior finish category also includes wall finish materials of similar weight, including but not limited to wood board or panel siding.
4. The exterior finish, roofing material and interior finish categories are intended to be identified based on the predominant materials used in construction.

Figure 3.12 Dwelling weight classification from *FEMA P-1100*.

EARTHQUAKE RETROFIT SCHEDULE (S_{DS}= 1.0 Seismic) TWO-STORY																		
Weight Category	Total Area in Square Feet	☒ Mark row that applies	Length Each of Two Braced Wall Sections Required Along Each Perimeter Wall Line									Number of Foundation Connectors or Anchors at Each Perimeter Wall Line Assume Distributed Along Length							
			Plywood Bracing Panels									Foundation Sill Anchors					Floor to Cripple Wall or Floor to Foundation Sill		
			Cripple Wall Height								Plywood Edge Nailing								
			up to 1'	1'-1" to 2'	2'-1" to 4'-0"		4'-1" to 6'-0"		6'-1" to 7'-0"										
			Without Tie-downs	Without Tie-downs	Without Tie-downs	With Tie-downs	Without Tie-downs	With Tie-downs	Without Tie-downs	With Tie-downs		Type "A"	Type "B"	Type "C"	1/2"ø Bolt	5/8"ø Bolt	Type "D"	Type "E" or "F"	Type "G"
2-Story Light Construction	up to 1600		8.0'	8.0'	10.7'	8.0'	12.0'	9.3'	13.3'	9.3'	4"	7	10	11	11	8	17	17	22
	1601 to 2000		9.3'	9.3'	12.0'	9.3'	13.3'	10.7'	14.7'	10.7'	4"	8	12	13	13	9	20	19	26
	2001 to 2400		10.7'	10.7'	13.3'	10.7'	14.7'	10.7'	16.0'	12.0'	4"	9	14	15	15	10	23	22	29
	2401 to 3000		12.0'	12.0'	14.7'	12.0'	17.3'	13.3'	18.7'	13.3'	4"	10	16	18	18	12	27	26	34
	3001 to 4000		14.7'	14.7'	17.3'	16.0'	20.0'	16.0'	21.3'	16.0'	4"	13	20	22	22	15	34	32	43
2-Story Medium Construction	up to 1600		8.0'	9.3'	10.7'	8.0'	13.3'	9.3'	13.3'	10.7'	3"	7	11	12	12	9	19	18	24
	1601 to 2000		9.3'	10.7'	12.0'	9.3'	14.7'	10.7'	14.7'	12.0'	3"	9	13	15	15	10	22	22	28
	2001 to 2400		9.3'	10.7'	13.3'	10.7'	16.0'	12.0'	16.0'	13.3'	3"	10	15	17	17	11	26	25	32
	2401 to 3000		10.7'	12.0'	14.7'	12.0'	17.3'	13.3'	18.7'	14.7'	3"	12	18	20	20	14	30	29	39
	3001 to 4000		13.3'	14.7'	17.3'	13.3'	20.0'	16.0'	21.3'	17.3'	3"	14	23	25	25	17	38	36	48
2-Story Heavy Construction	up to 1600		9.3'	9.3'	12.0'	9.3'	13.3'	10.7'	14.7'	12.0'	2"	9	14	16	16	11	24	23	30
	1601 to 2000		9.3'	10.7'	13.3'	10.7'	14.7'	12.0'	16.0'	13.3'	2"	11	17	18	18	13	28	27	35
	2001 to 2400		10.7'	12.0'	14.7'	10.7'	16.0'	13.3'	17.3'	14.7'	2"	12	19	21	21	14	32	31	41
	2401 to 3000		12.0'	13.3'	16.0'	13.3'	18.7'	14.7'	18.7'	16.0'	2"	14	23	25	25	17	38	37	48
	3001 to 4000		13.3'	16.0'	18.7'	14.7'	21.3'	17.3'	22.7'	18.7'	2"	18	28	31	31	21	48	46	60

Figure 3.13 Selection of the retrofit schedule per the recommendations of *FEMA P-1100*.

Per the Figure 3.13 table, 21 anchor bolts were required over the 40-ft length of the model dwelling. In the test configuration, 10 anchor bolts were provided over the length of each 20-ft wall; see Figure 3.14(a). The test setup allowed for seven anchor bolts each side. An additional three epoxy bolts were added to each side, along with one extra bolt at each end of each wall as required; see Figure 3.14(b). This resulted in a total of twelve bolts on each of the specimen's 20-ft walls. The extra bolts were added using all-thread and Simpson SET-XP epoxy anchors. Steel plate washers were provided on each anchor bolt as required by *FEMA P-1100*.

Per *FEMA P-1100*, 32 Type D shear clips were required over the 40-ft length of the model dwelling, suggesting 16 shear clips over the length of each 20-ft wall. The test setup allowed for installation of 14 of the 16 shear clips on each wall. The shear clip type is shown in Figure 3.15. Simpson A-35 clips were used. These are a commonly used alternative to L70 clips and have roughly equivalent capacity.

At abutting panel edges, stitch nailing of studs was provided as shown in Figure 4.4-16 from *FEMA P-1100*; see Figure 3.16.

Blocking was provided on top of the foundation sill plate to permit edge nailing of the bottom edge of the retrofit plywood, as shown in Figure 3.14(a). A single piece of 2 × 6 nominal Douglas-fir blocking, ripped to 4 in. wide, was used in each stud bay, regardless of presence of anchor bolts. Four 10d common nails were used to face-nail each piece of blocking to the foundation sill plate. The face nails were staggered with 1-1/2-in. minimum spacing. The anchor bolts extended through the blocking, with the steel plate washer and nut located on top of the blocking; see Figure 3.17.

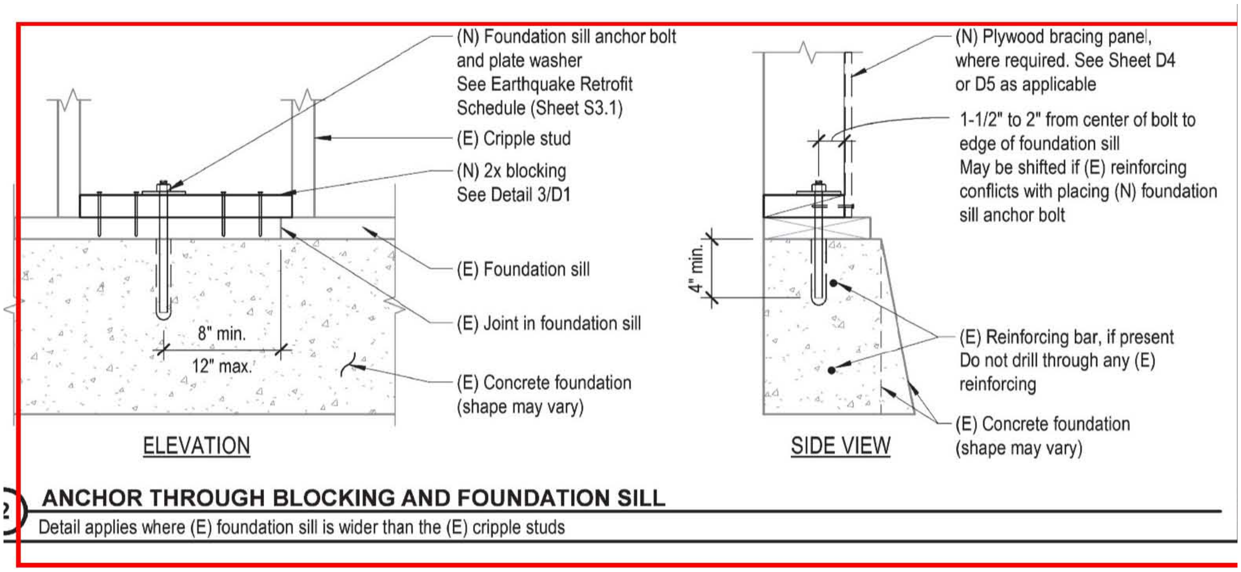

(a)

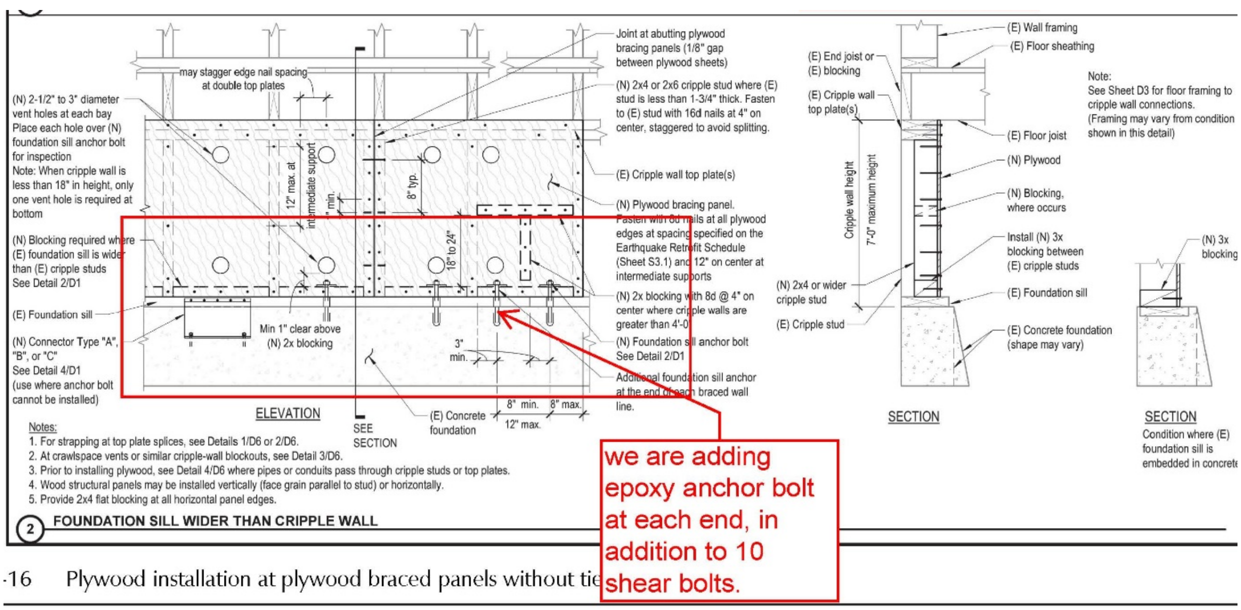

(b)

Figure 3.14 Required sheathing, anchor bolts, and shear clips in accordance with *FEMA P-1100* (draft figure shown, see *FEMA P-1100* for final published figure).

	D	Floor to Cripple Wall or Floor to Foundation Sill	SHEETS D2, D3 & D3.1	565
	E			740
	F			590
	G			445
	H			725

Figure 3.15 Floor to cripple wall sill connector selection per the recommendations of *FEMA P-1100*.

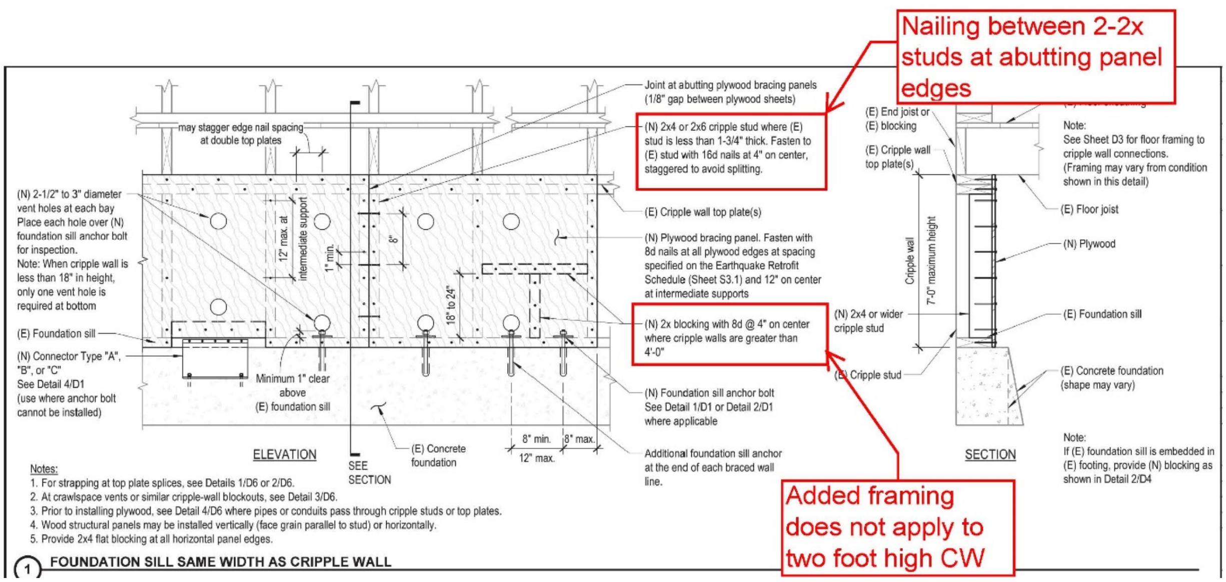

Figure 3.16 Stitch nailing of studs in accordance with *FEMA P-1100* (draft figure shown, see *FEMA P-1100* for final published figure).

The full length of the cripple wall was braced using 15/32-in.-rated sheathing grade plywood; 8d common nails were used to fasten the plywood sheathing to the framing, using an edge nail spacing of 3 in. at all panel edges and 12 in. in the field. The sheathing nailing at the top of the plywood was staggered between the upper and lower top plates, with an effective spacing of 6 in. on center on each top plate. This was in accordance with *FEMA P-1100* draft details. Note: the published *FEMA P-1100* details were revised to require full-edge nailing into the upper top plate in response to the Specimen AL-2 testing. Figure 3.16 shows details of the plywood installation, as specified by *FEMA P-1100*. When installing the sheathing, each panel was seated on the foundation sill plate and nailed in place. This typically resulted in a small gap between the top of the sheathing and the floor framing above; see Figure 3.17 for photos of the Specimen AL-2 cripple wall retrofit.

(a) (b)

(c) (d)

(e)

Figure 3.17 Retrofit details for AL-2: (a) extra threaded bolts added using epoxy; (b) slotted square washer; (c) retrofit blocking ripped to 4 in. wide; (d) retrofit A35 clips; and (e) crawlspace retrofit sheathing.

3.6 LOADING PROTOCOL

The quasi-static lateral displacement history was followed for the testing of Specimens AL-1 and AL-2; see Chapter 2. The amplitude and quantity of displacement cycles for each cycle level are described in Table 3.2. As noted earlier, the key parameter for prescribing the displacement history for tests of Specimens AL-1 and AL-2, was the specimen height 'h,' taken as the 24-in. clear height of the cripple wall from the top of the foundation to the underside of the floor framing above. A constant loading rate of 0.2 mm/sec (0.0787 in./sec) was used for both specimens; see Section 2.2. The testing started with a push to the west to reach the first peak and then the loading was reversed to reach the first pull peak to the east. These cycles were repeated based on the number of cycles designated for each cycle level. For each specimen, a final monotonic push was performed. This push was to the west was due to the loading fixture configuration and to maintain better control in the event of significant damage to the specimen.

Table 3.2 General loading protocol adjusted for AL-1 and AL-2 geometry.

Cycle level	Drift %*	Amplitude (in.)	No. Cycles	Loadin Rate (in./sec)	Total time (sec) per cycle level	Inspection type*
1	0.2	0.048	7	0.0787	17.08	Normal inspection
2	0.4	0.096	4	0.0787	19.52	Normal inspection
3	0.6	0.144	4	0.0787	29.28	Normal inspection
4	0.8	0.192	3	0.0787	29.28	Normal inspection
5	1.4	0.336	3	0.0787	51.24	Normal inspection
6	2	0.48	3	0.0787	73.2	Normal inspection
7	3	0.72	2	0.0787	73.18	Normal inspection
8	4	0.96	2	0.0787	97.58	Normal inspection
9	6	1.44	2	0.0787	146.38	Reduced inspection
10	8	1.92	2	0.0787	195.18	Reduced inspection
11	10	2.4	2	0.0787	243.96	Reduced inspection
12	Monotonic push	10	1	Manually	N.A.	End inspection

* Normal Inspection: Test was paused to make detailed observations following the first push, first pull, zero displacement at the end of each cycle; Reduced Inspection: First push, zero displacement at the end of each cycle.

3.7 INSTRUMENTATION PLAN

A large amount of data was collected over the course of the testing of Specimens AL-1 and AL2. This section describes the instrumentation used to collect data for Specimens AL-1 and AL-2; see Section 2.3 for discussion of other types of data collected. The instrumentation recorded applied lateral loads, anchor bolt forces, global and local displacements, and boundary displacements (slip and uplift relative to the foundation and loading beam). the instrumentation plans for both specimens were identical, the following description is applicable to Specimens AL-1 and AL-2.

This section provides an overview of the instrumentation. An instrumentation schedule and detailed instrumentation plans are provided as part of the specimen drawings in Appendix B.

The overall response of the specimen was characterized using the lateral force measured by the load cell in the actuator, and the lateral displacement measured by a transducer referenced to the loading beam. Over the specimen height, several string potentiometers (string pots) were connected at different heights from a stationary frame to the test specimen to capture absolute displacement of the building at each height. These string pots for the south wall are tagged WLFS1 through WLFS5; see Figure 3.18. Identical instrumentation was also used for the north wall.

Local deformations of the specimen's walls were extensively instrumented. Several diagonal pairs of string pots were used to measure the deformation of the cripple walls. The string pots were mounted on the framing members to measure the overall distortion of the cripple wall framing over the length of the building and the distortion in the middle of the wall length. Pairs of string pots were also mounted in the superstructure to measure the overall wall distortion in the superstructure level. Additional displacement transducers were used to monitor and control the other displacements in the specimens. Several Linear Variable Differential Transformer (LVDT) transducers were used to monitor the slip between the specimen and loading beam, and between the specimen and foundation.

Even though the slip between the foundation and the strong floor was not expected, the potential slip was monitored using one LVDT at one end of the foundation. One pair of diagonal string pots was used to measure potential in-plane deformation of the floor diaphragm, which was connected to the loading beam; see Figure 3.19. In addition, a string pot was connected to the upper corner of the building to monitor potential transverse displacement of the building. Because the loading beam was not restrained to withstand rotation in the vertical plane, rotation of the horizontal loading beam was monitored using two LVDTs mounted in the loading beam, one at the end closer to the loading actuator and one at the other end.

The tension in the anchor bolts connecting the specimen to the concrete foundation was recoded using eight washer loads cells. These washer load cells were placed into the access pockets that were cast into the concrete foundation. The anchor bolts were hand tightened to a snug fit, and then turned with a wrench enough to have a preload in the general range of 500 lb per bolt appear in the load cell. There was no intent to specifically pre-load the bolts but to ensure that increases in tension would be captured by the load cell. A foundation plan showing the instrumented anchor bolts is provided in Figure 3.20.

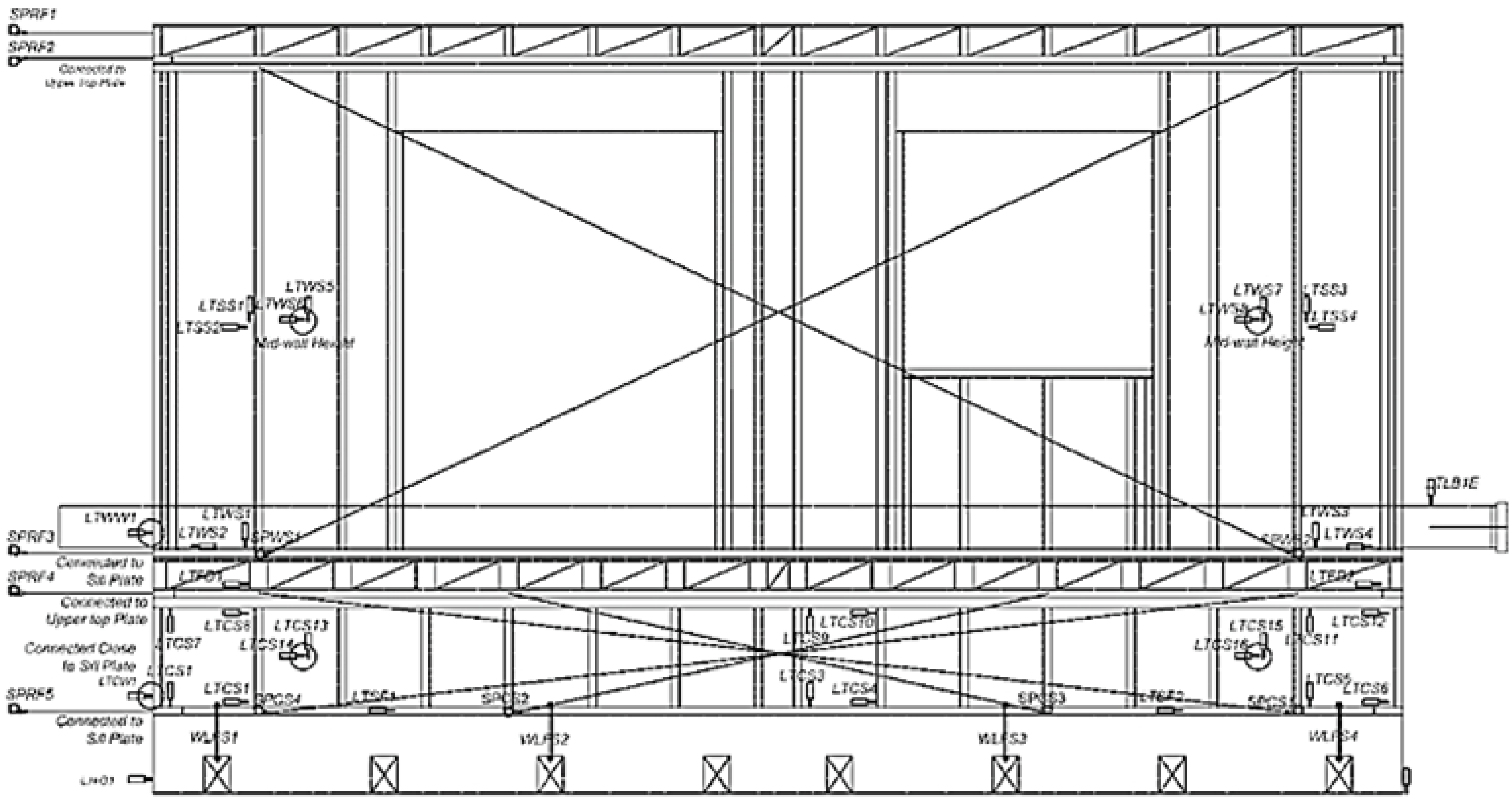

Figure 3.18 Instrumentation layout for south wall, Specimens AL-1 and AL-2.

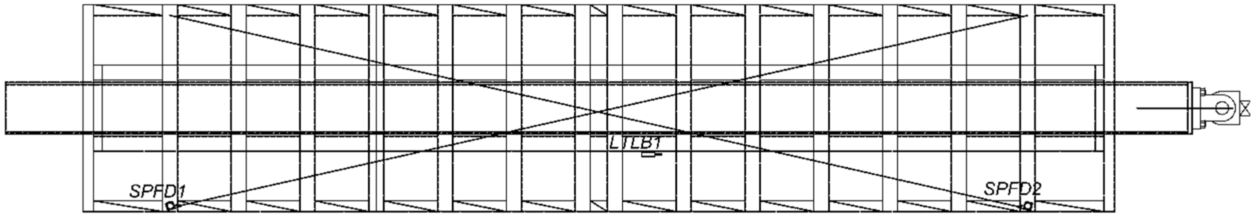

Figure 3.19 Instrumentation layout for floor diaphragm of Specimens AL-1 and AL-2.

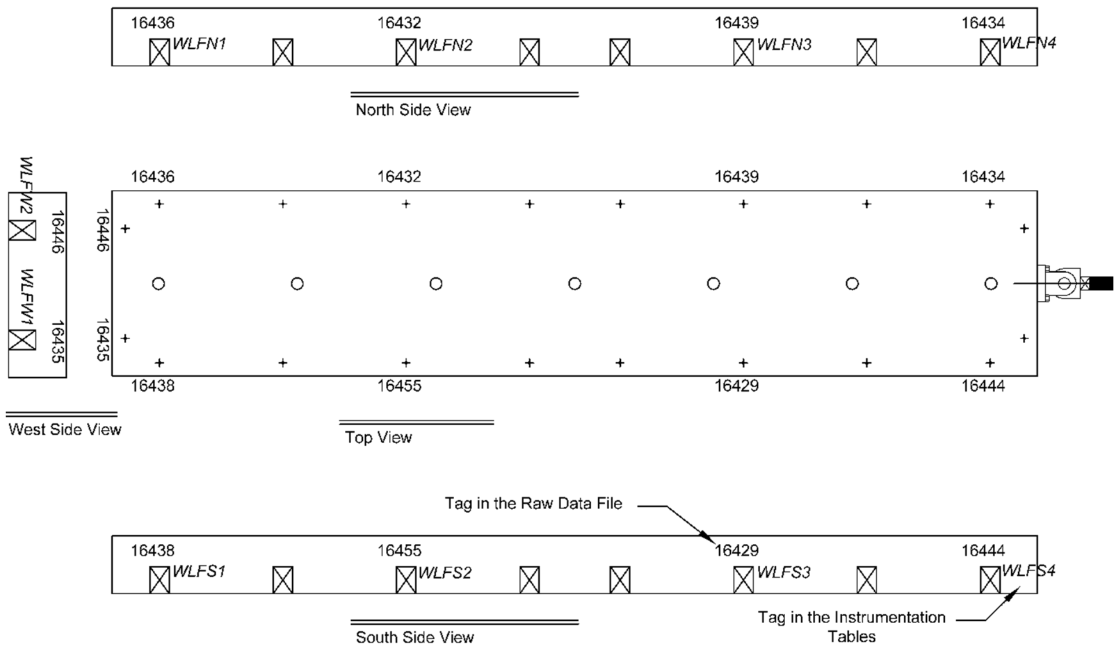

Figure 3.20 Location of load cells to measure the tension in the anchor bolts for Specimens AL-1 and AL-2.

3.8 GRAVITY LOADING

As previously discussed in Section 3.4, the configurations for the test specimens were determined based on an assumed model dwelling with a 30-ft × 40-ft plan dimension. This model dwelling was used to determine the supplemental gravity load to be applied to the specimen during testing. The supplemental gravity load was intended to be representative of the anticipated load being supported by the cripple walls in the model dwelling. This is of significance because this is weight that is available to resist uplift due to overturning during loading.

Gravity loading for Specimens AL-1 and AL-2 were studied based on dwellings having both one and two stories above the cripple wall. The gravity load for a one-story dwelling was chosen because the gravity load for the two-story would not have been practical to place on the structure. The choice to apply gravity loading based on the weight of a one-story dwelling was recognized to represent a lower bound of resisting dead load; as a result, if failure modes were found to be controlled by uplift mechanisms, the choice to use a gravity load based on a one-story model could have resulted in under estimation of the peak strength or peak displacement capacity.

Given that uplift related mechanisms were not observed during testing, the choice of a one-story gravity load is assumed to have little influence over the response.

For testing of Specimens AL-1 and AL-2, the model dwelling was configured to have a stucco exterior wall finish, plaster on wood lath interior wall and ceiling finishes, and a composition shingle roof. The roof, floor, exterior wall, and interior wall unit weights were assigned as 22, 10, 23, and 18 pounds per square foot (psf), respectively. Using these weights, a superstructure weight of 72 kips was calculated, corresponding to an average weight of 60 lbs psf of floor area. Both the unit weights and average weight were checked against data from the *FEMA P-1100* project and were found to correlate well. Of the 72 kips total superstructure weight, 18 kips was assigned to the test specimen based on the 20-ft length being half of the 40-ft dwelling length, and the assumption that 50% of the weight would be supported on interior walls, and the other 50% on the two exterior walls represented by the specimen. The summed self-weight of the specimen and loading beam were determined to be approximately 6 kips. To make up the additional twelve kips required, an additional five kips was added at the roof level using lead blocks; similarly, an additional seven kips were added at the floor level. This same weight was used for Specimens AL-1 and AL-2. Note: The total weight of 18 kips divided by the 40-ft length of the two cripple walls corresponds to 450 lbs plf. This is consistent with the “heavy” superimposed gravity load applied in most of the UCSD small-component tests, which provided a reasonably consistent superimposed weight between the PEER–CEA Project small- and large-component testing.

3.9 SPECIMEN AL-1 TEST RESULTS: CRIPPLE WALL WITHOUT RETROFIT

A large volume of data was collected over the course of the test, including crack mapping, visual observations, photo documentation of the interior and exterior finish materials at the points designated in the loading protocol, and continuous recording by the various instrumentation installed throughout the specimen. Key test results for Specimen AL-1 are described in this section.

The lateral force versus lateral displacement of Specimen AL-1 cripple walls was recorded over the course of testing using instrumentation in the actuator to measure load and displacement. In addition, five pairs of string pots between the specimen and a stationary frame captured the displacement at different heights; because there was no appreciable difference between the displacement measurements from the actuator and the string pots, data from the actuator is reported and used as the basis for discussion. Instrumentation confirmed that slip between the foundation and the foundation sill plate was negligible; with this possible source of slip eliminated, the recorded displacements can be considered drift that was imposed on the cripple walls.

The overall load-displacement response obtained from the actuator is shown in Figure 3.21 and summarized in Table 3.3. The actual drift achieved varied slightly from the targeted drifts shown in Table 3.2 due to the practical limitations of actuator control. The peak unit load listed is the peak load divided by a total cripple wall length of 40 ft (20 ft each on the north and south walls).

The Specimen AL-1 peak shear capacity (54,580 lbs) was seen to occur in the push direction (shown in the negative quadrant), which was also the direction loaded first. This was larger than the peak shear capacity in the subsequent pull direction (49,880 lbs). Based on the total cripple wall length of 40 ft, this resulted in peak unit shears of 1360 and 1250 lbs plf, with an average of 1300 plf. Specimen AL-1 reached peak shear capacity at a drift ratio of approximately 2.9% drift (0.70 in. displacement), corresponding to the de-bonding of the stucco from the concrete foundation.

The drop in load between the first push direction loading and the subsequent pull direction is believed to be mainly due to damaged inflicted in the push direction, which affected the subsequent lateral strength in pull direction. Figure 3.22 shows the envelope curve in the positive and negative quadrants plotted on top of each other. Although there is an approximately 10% drop in peak shear capacity from the negative quadrant push direction to the positive quadrant pull direction, the envelope curves otherwise mirror each other well, with no significant differences.

In the displacement cycle immediately following the cycles at peak shear capacity, a significant drop to approximately 40% of peak shear capacity occurred. This drop was seen in both the push and pull loading directions, and was maintained through drifts to 1.4 in. (6%). This residual strength was thought to rely heavily but not entirely on the strength contribution of the horizontal lumber sheathing underlying the stucco.

The final set of displacement cycles showed a post-peak residual capacity on the order of 20% of peak shear capacity at 1.4 in. or 6% drift, reducing to approximately 12% of peak shear capacity at about 2-1/4 in. (9% drift). Note: testing was able to continue cyclic loading to a drift ratio of 10%, and monotonic loading to a drift ratio of 40%. These are higher displacement levels than commonly attempted in test programs. Data collected in this displacement range is critical for the development of numerical models that describe structural behavior up to and including collapse.

Load deflection information from the final monotonic push is summarized in Table 3.4. This data shows modest retained post-peak capacities to very high drift ratios without collapse. Note: collapse did not occur during the final monotonic push, which extended out to the practical displacement limits of the test setup.

Because of the practical limits of actuator control, the recorded drifts for Specimen AL-1 (Table 3.3) differed somewhat from the drifts targeted by the loading protocol. A similar variation from the targeted drift occurred for Specimen AL-2. To allow direct comparison between these specimens, Specimen AL-1 loads at the targeted drift levels have been interpolated from the envelope curves and are summarized in Table 3.5. This interpolated data is used in Section 3.12 to compare the response of Specimen AL-1 versus Specimen AL-2.

Other important collected data includes the tension in the anchor bolts connecting the specimen to the concrete foundation. Four of the anchor bolts on each 20-ft wall were instrumented using washer load cells. The primary purpose was to determine whether the anchor bolts would be subjected to significant tension loads due to cripple wall lateral loading. Before the start of the test, all the nuts were tightened until the tension in the bolts were measured to be in the range of 500 lbs.

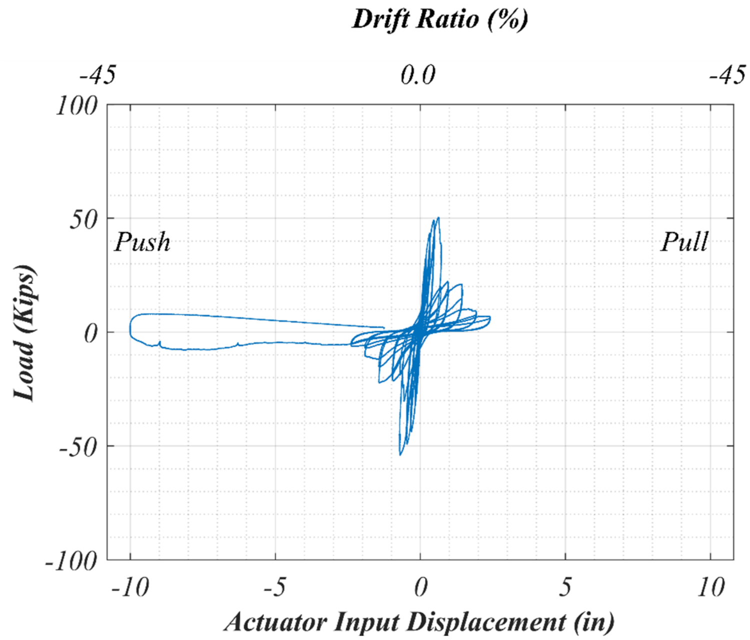

(a)

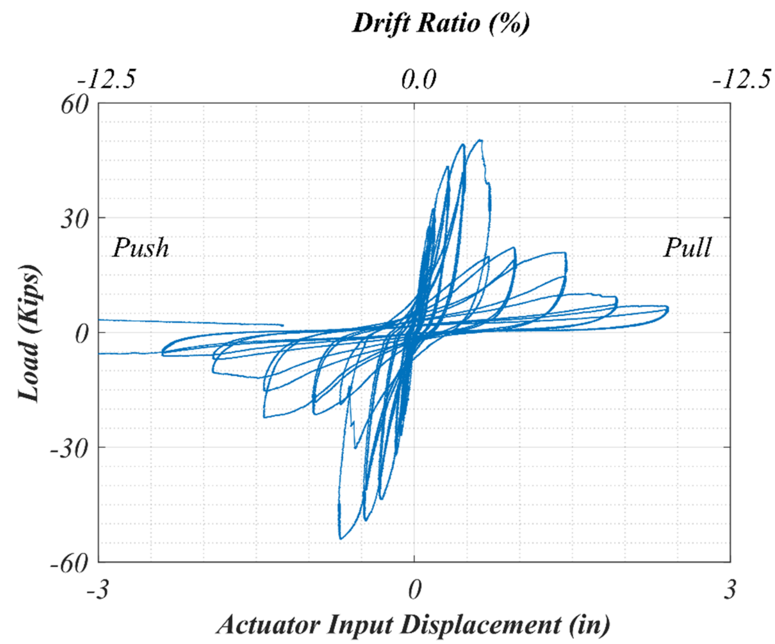

(b)

Figure 3.21 Lateral load versus lateral displacement for Specimen AL-1: (a) full hysteresis plot including monotonic push at the end.; and (b) hysteresis plot excluding monotonic push.

Table 3.3 Summary of test data for Specimen AL-1.

Loading direction	Displacement (in.)	Drift ratio (%)	Peak load (lbs)	Peak unit load (plf)	Cycle peak/ overall peak (%)
First loading direction: push to west	0.0016	0.01	670	20	1
	0.0917	0.40	22,000	550	40
	0.1373	0.57	27,470	690	50
	0.1703	0.71	32,570	810	60
	0.3142	1.3	44,220	1,110	81
	0.4560	1.9	49,770	1,240	91
	0.6960	2.9	54,580	1,360	100
	0.9267	3.9	21,990	550	40
	1.4283	6.0	22,810	570	42
	1.4865	6.0	12,510	310	23
	1.8342	7.6	7,590	190	14
	2.3154	9.6	6,740	170	12
Second loading direction: pull to east	0.0038	0.02	380	10	1
	0.0967	0.40	20,550	510	41
	0.1395	0.58	27,220	680	55
	0.1813	0.76	31,880	800	64
	0.3247	1.4	42,290	1,070	86
	0.4669	1.9	48,700	1,220	98
	0.6175	2.6	49,880	1,250	100
	0.6452	2.7	49,710	1,240	100
	0.9399	3.9	21,790	540	44
	1.4200	5.9	20,460	510	41
	1.6722	7.0	9,690	240	19
	2.2649	9.4	6,580	160	13

Table 3.4 Summary of test data for Specimen AL-1 monotonic push.

Drift	Drift ratio (%)	Loading direction	Peak load (lbs)	Load (plf)	Cycle peak/ overall peak (%)
4 in.	17	Push	5,490	137	10.1
6 in.	25	Push	5,820	146	10.7
8 in.	33	Push	8,220	206	14.0
9 in.	38	Push	7,410	185	13.6
10 in.	42	Push	3,330	83	6.1

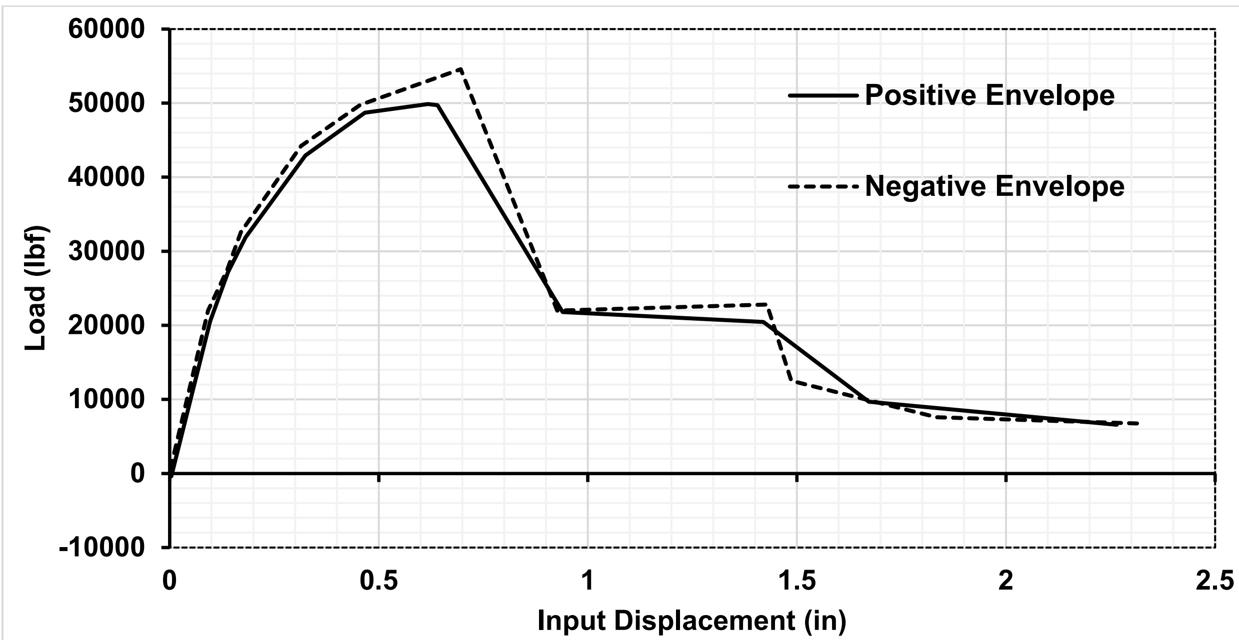

Figure 3.22 **Envelope curves for positive and negative quadrants superimposed. Specimen weight including lead weight and loading beam is approximately 18 kips. Seismic mass tributary to the specimen is anticipated to be approximately 36 kips.**

Table 3.5 Summary of load/ displacement data for Specimen AL-1 interpolated from envelope curve.

Interpolated drift	Loading direction	Interpolated load (lbs)	Interpolated unit load (plf)	Interpolated load/ interpolated peak (%)
0.4% (0.096 in.)	Push	22,510	563	43
	Pull	20,440	511	41
	Average	21,480	537	42
0.6% (0.144 in.)	Push	28,500	712	54
	Pull	27,720	693	56
	Average	28,110	703	55
0.8% (0.192 in.)	Push	34,330	858	65
	Pull	32,700	818	66
	Average	33,520	838	65
1.4% (0.336 in.)	Push	45,070	1,127	86
	Pull	43,380	1,084	87
	Average	44,220	1,106	86
2% (0.48 in.)	Push	50,260	1,256	95
	Pull	48,800	1,220	98
	Average	49,530	1,238	97
2-1/2% (0.60 in.)	Push	52,660	1,317	100
	Pull	49,750	1,224	100
	Average	51,200	1,280	100
3% (0.72 in.)	Push	51,190	1,280	97
	Pull	42,300	1,058	85
	Average	46,750	1,169	91
4% (0.96 in.)	Push	22,050	551	42
	Pull	21,740	543	44
	Average	21,890	547	43
6% (1.44 in.)	Push	20,730	518	39
	Pull	19,600	490	39
	Average	20,170	504	39
8% (1.92 in.)	Push	7,440	186	14
	Pull	8,390	210	17
	Average	7,920	198	15

The plots of the tension that developed in the washer load cells located at the north side are provided in Figure 3.23. The change in anchor bolt load during testing, while observable, is relatively insignificant, with the total range of load being between zero and 400 lbs, which are noted to be minimal loads given the level of lateral loading imposed on the specimen.

Documentation of the condition of the specimen during testing included visual observations and photographs, which occurred at the designated hold points in the loading protocol. The observed behaviors included cracking of stucco, separation of the stucco from the foundation and framing, and many other details documented over a range of drift levels. Observation of the cripple wall horizontal wood sheathing from the crawlspace interior at several points was possible during most phases of testing.

To aid in the tracking and photographing of stucco cracks, the cracks were marked on the stucco finish using colored pens. A line was drawn alongside the length of the crack, and a tick mark was drawn at the observable crack end, along with a numerical indication of the drift ratio at which the crack was first noted. Different colors were used as follows: green to record stucco cracking observed prior to the start of the test (consistent with anticipated stucco shrinkage cracking); black marker was used to chart the crack lines in the first push (towards the west) to each of the drift ratio; and red and blue markers were used for the first pull (to the east) peak and back to zero displacement, respectively. Other noted damage was marked in the same manner.

Except for the cracking of stucco that occurred prior to the start of testing, the great majority of cracking and other behaviors was observed to occur over the height of the cripple wall and at the floor level, with little cracking extending up into the superstructure walls. As shown in Figure 3.24 taken at the end of testing, little in the way of stucco cracking was marked from the floor level up; therefore, the subsequent discussion below focuses on the cripple wall and floor levels. Detailed documentation of observations at each drift level are provided in Appendix C.

Prior to the start of testing, hairline cracking of the stucco occurred due to a combination of common shrinkage cracking and crack progression as the lead weights were set on the structure. These hairline cracks tended to follow a vertical direction and were generally uniformly distributed along the specimen length; see Figure 3.25.

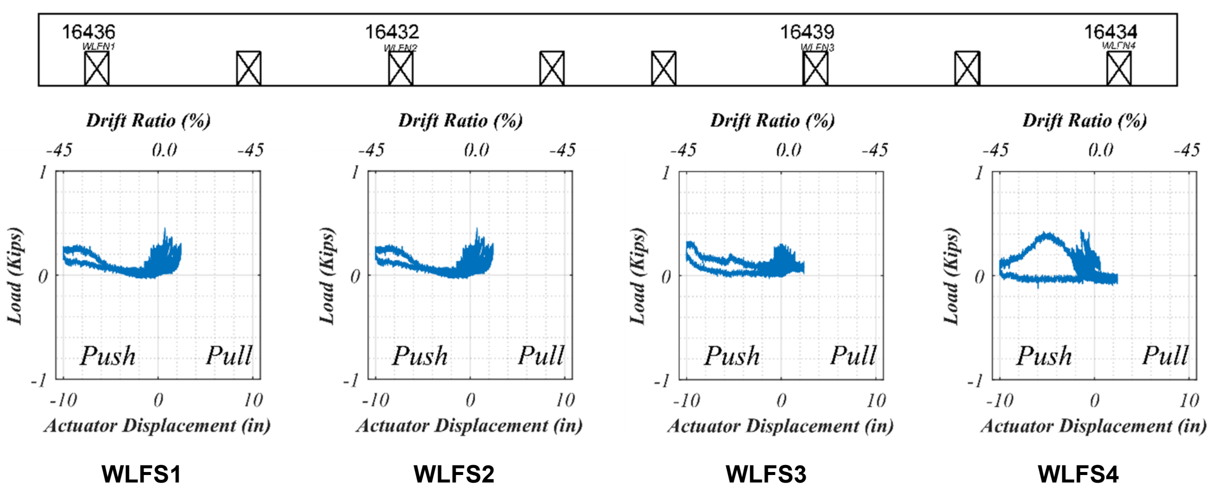

Figure 3.23 Tension developed in bolts in the north wall for Specimen AL-1.

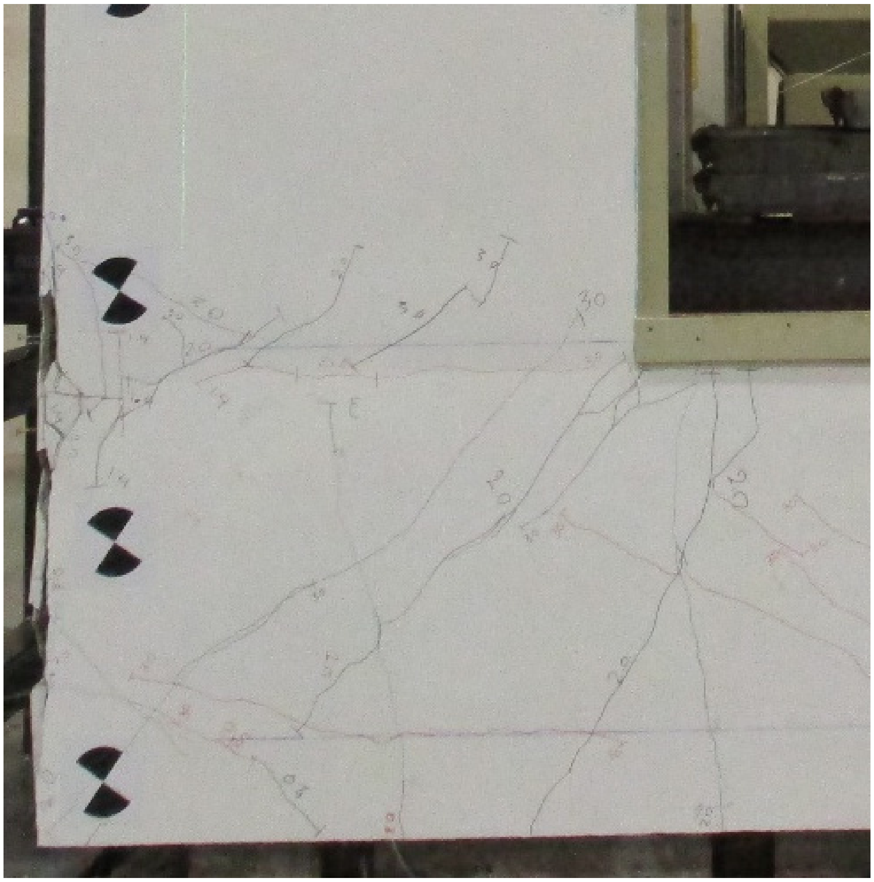

Figure 3.24 Specimen AL-1 at zero displacement near the conclusion of cyclic testing. Note that marked stucco cracking is primarily located at the cripple wall and floor levels.

Figure 3.25 Vertical shrinkage and settling cracks before start of loading.

The main progression of damage during testing involved the stucco cracking on the east and west end walls (perpendicular to the direction of loading), deteriorating, and finally being pushed off of the supporting sheathing and framing. This deterioration was necessary to allow racking of the north and south cripple walls to accommodate the imposed displacements. This progressive deterioration can be seen in Figure 3.26. Cracks widened, stucco wires broke, stucco pieces dislodged and then fell, and finally the end wall stucco was pushed completely free of the sheathing and framing.

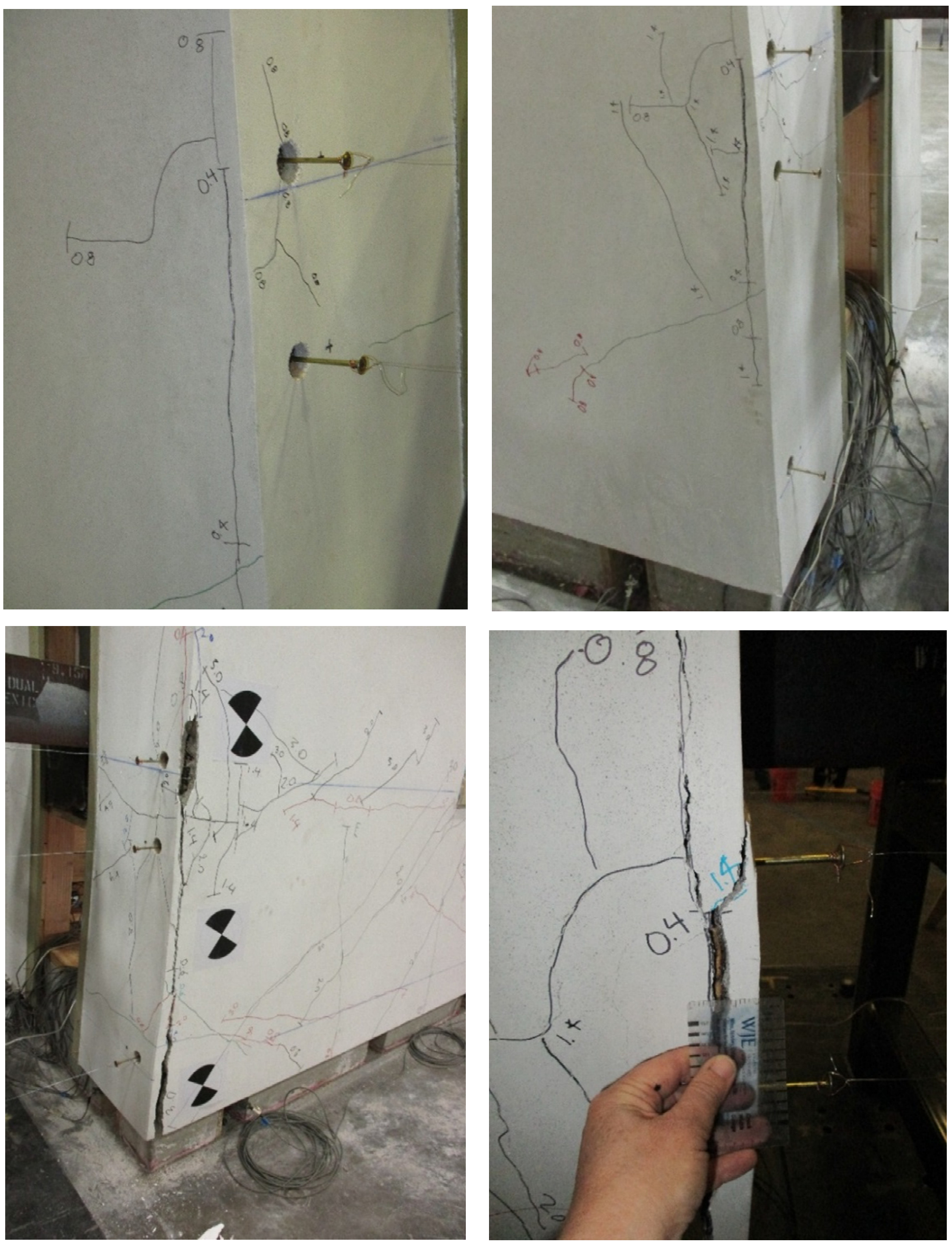

Figure 3.26 Stucco damage observed at end walls. Drift ratios are (clockwise from upper left) 0.8%, 1.4%, 2%, and 6%. Numbers marked on specimen indicate drift ratios at which each segment of crack was first observed.

While the end wall stucco was deteriorating, the stucco on the north and south cripple walls remained substantially planar, with the cracking remaining near hairline. Little or no imposed displacement was accommodated by in-plane distortion of the stucco itself. Global rotation of the stucco did not occur, as the superstructure walls served to restrain the stucco. As shown in Figure 3.27 at loading to a target displacement of 2% drift, the sheathing and framing at the floor level was observed to have slid approximately 1/4-in. relative to the stucco (approximately half of the imposed actuator displacement), indicating that the framing was detaching from and moving relative to the stucco at the floor level. As shown in Figure 3.28, at loading to a target displacement of 3% drift, a popping noise occurred, and the stucco was observed to have broken its bond to the foundation. From this point on, the cripple wall stucco remained substantially planar and detached gradually from the sheathing and framing, with the stucco progressively flaring away from the base of the cripple wall, like a skirt; see Figure 3.29.

As the stucco at the end walls broke open, the lumber sheathing behind the stucco could be seen. The lumber sheathing helped to sustain residual loads through significant levels of displacement. Significant withdrawal of the nails holding the lumber sheathing to the framing was observed, with nails becoming completely withdrawn near the end of testing. The stucco helped to retain the lumber sheathing boards in place despite the nails being completely withdrawn; see Figure 3.30.

The gypsum wallboard did not sustain any notable damage during this test. This is consistent with the lack of drift imposed on the superstructure and the very limited damage of the stucco in the superstructure; see Figure 3.31.

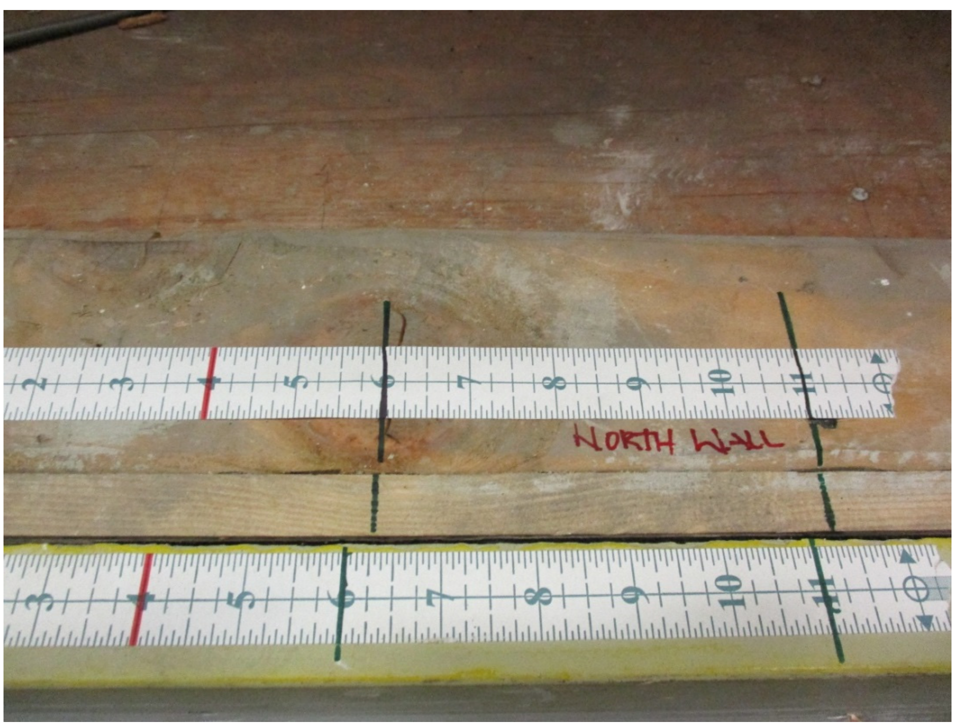

Figure 3.27 Specimen at 2% drift ratio. Stucco has slipped in-plane relative to sheathing and framing; photograph taken at 2% drift ratio.

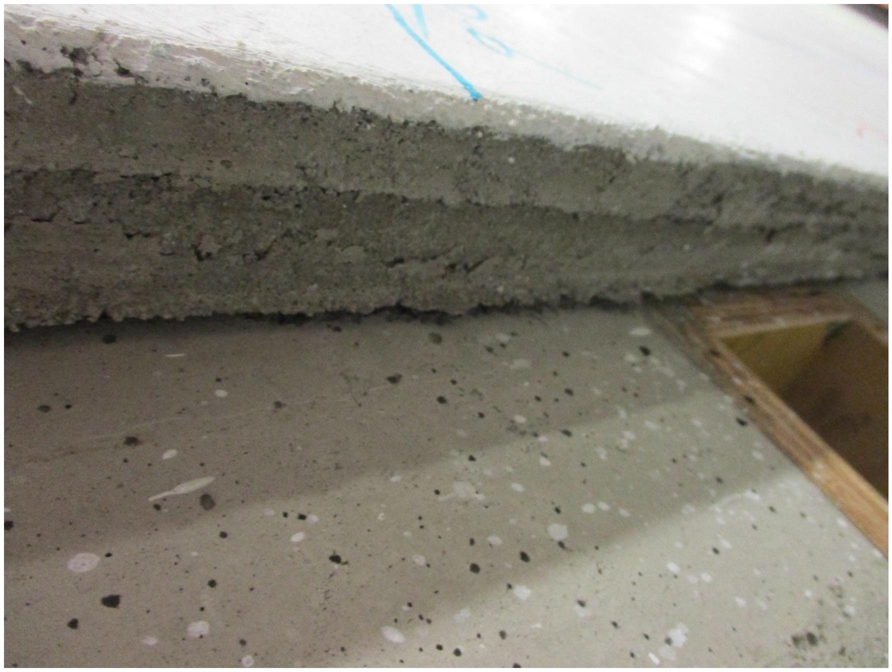

Figure 3.28 **Specimen damage at 3.0% drift ratio. Stucco is debonded from the foundation.**

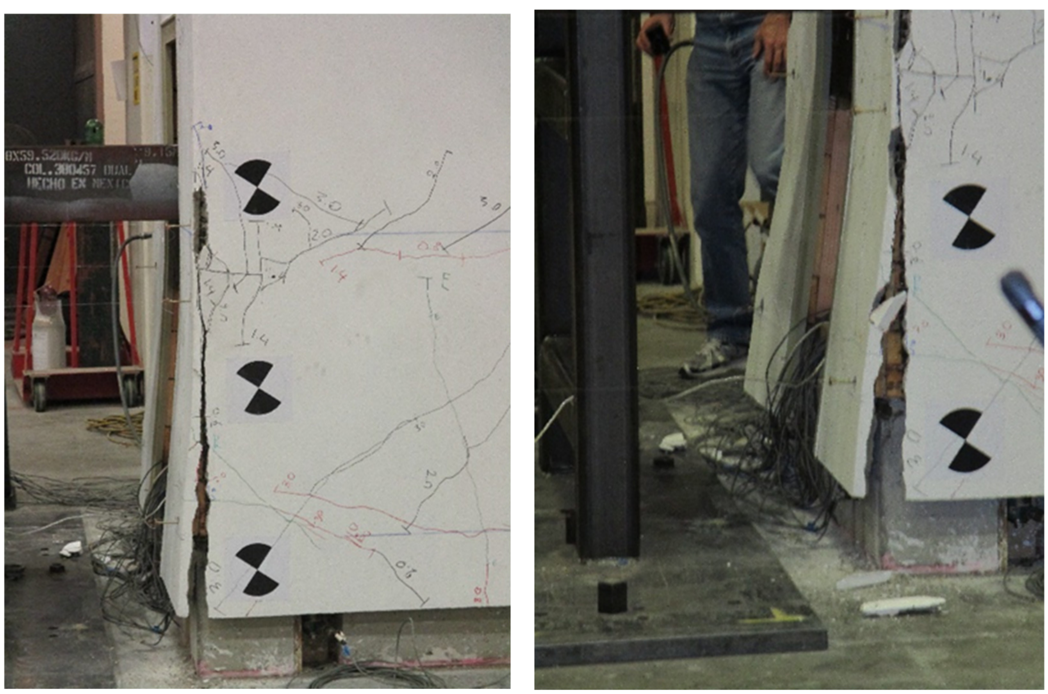

Figure 3.29 **Stucco flaring away from the framing and foundation. This behavior was seen on all four sides.**

Figure 3.30   Lumber sheathing nails withdrawn from supporting frame.

(a)   **(b)**

Figure 3.31   Gypsum wallboard at the door opening at conclusion of testing.

3.10 SPECIMEN AL-2 TEST RESULTS: CRIPPLE WALL WITH RETROFIT

Similar to Specimen AL-1, the lateral force versus lateral displacement of the Specimen AL-2 was recorded using embedded instrumentation in the actuator to measure actuator input displacement. This data is shown in Figure 3.32 and summarized in Table 3.6. The peak lateral load in the push direction was 90,000 lbs and in the pull direction was 82,100 lbs. Both of these occurred at a drift of approximately 0.67 in. (2.8% drift), which is similar to the displacement at peak shear capacity for Specimen AL-1. Divided by the summed cripple wall length of 40 ft., the unit shears are 2250 and 2053 plf, for an average of 2150 plf.

Similar to Specimen AL-1, a drop of approximately 10% was observed between peak shear capacity in the first push loading direction and in the second pull direction. The overall character of the envelope curves in the push and pull directions was very similar compared to Specimen AL-1, as seen in the superimposed curves in Figure 3.33.

There was a drop in peak load in both the positive and negative quadrants in the displacement cycles immediately following the peak shear capacity cycles. Unlike Specimen AL-1, which dropped to approximately 40% of peak shear capacity, Specimen AL-2 dropped to between 80% and 90% of peak shear capacity (a capacity reduction of 10 to 20%). This included an initial drop, followed by a slight increase in load up to a second peak at just under 6% drift; a very gradual decline in peak load for subsequent displacement cycles occurred, with peak loads still above 50% of peak shear capacity at drifts above 10%.

Incremental reductions continued out to more than 25% retained residual capacity at drifts of approximately 13.5% (3.24 in.), beyond which monotonic loading was imposed. The retention of a large portion of the peak shear capacity to significant post-peak displacements were markedly different compared to Specimen AL-1's response.

Following the completion of the cyclic loading, a final monotonic push was conducted. The floor diaphragm was push horizontally off of the supporting cripple walls during this push, causing separation between the upper and lower cripple wall top plates; most of the displacement recorded during this final push was due to slip rather than drift in the cripple walls. As a result, the displacements reported in Table 3.7 are not identified as drift. Note: even with the diaphragm sliding relative to the cripple walls, residual capacities from the monotonic push ranged from 14 to 21% of peak shear capacity, slightly larger than the residual capacities for Specimen AL-1.

As shown in Table 3.6 and similar to Specimen AL-1, the recorded drifts for Specimen AL-2 differ somewhat from the drifts that were targeted by the loading protocol due to the practical limitations of actuator control. To allow direct comparison between these specimens, Specimen AL-2 loads at the targeted drift levels have been interpolated from envelope curves, which are summarized in Table 3.8. This interpolated data is used to compare the response of Specimen AL-1 versus AL-2; see Section 3.12.

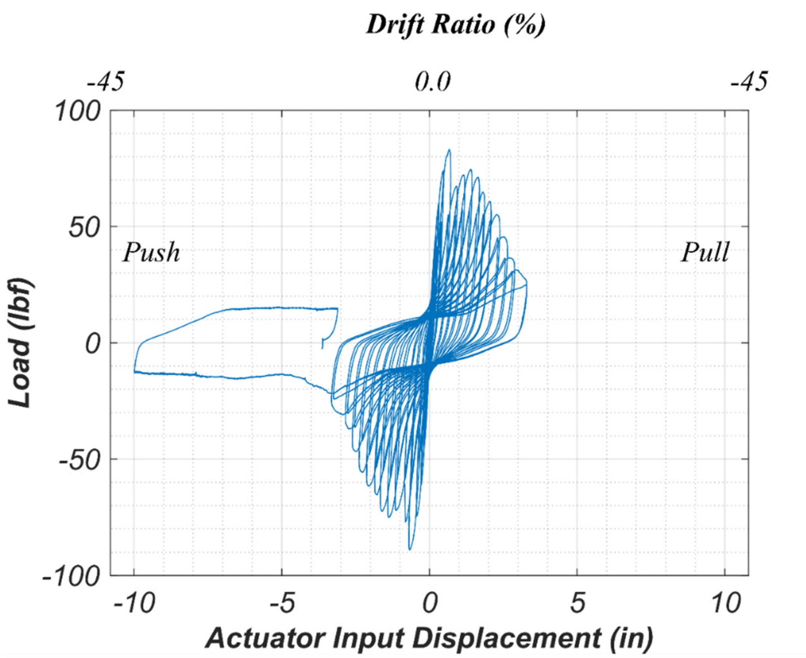

(a)

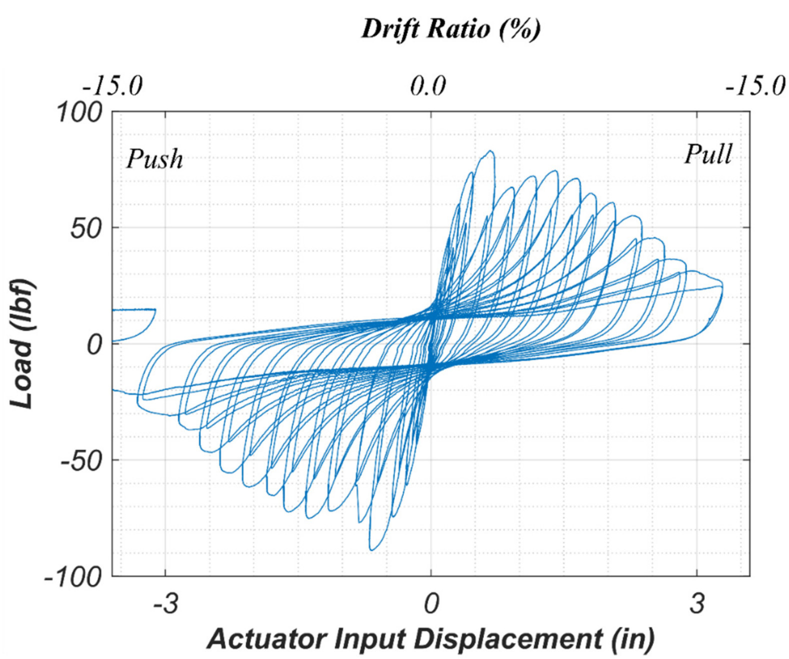

(b)

Figure 3.32 Lateral load versus lateral displacement of specimen AL-2: (a) full hysteresis plot including monotonic push at the end; and (b) close up of full hysteresis plot.

Table 3.6 Summary of test data for Specimen AL-2.

Loading direction	Displacement (in.)	Drift ratio (%)	Peak load (lbs)	Peak unit load (plf)	Cycle peak/ overall peak (%)
First loading direction: push to west	0.0071	0.02	2,440	61	3
	0.0088	0.04	7,070	177	8
	0.0104	0.04	7,450	186	8
	0.0165	0.07	10,360	259	12
	0.0440	0.18	18,260	457	20
	0.1625	0.67	44,120	1,103	49
	0.2784	1.2	54,720	1,368	61
	0.4229	1.8	75,450	1,886	84
	0.6690	2.8	90,000	2,250	100
	0.8135	3.4	77,990	1,950	87
	1.1288	4.7	73,020	1,825	81
	1.3782	5.7	76,150	1,903	85
	1.6062	6.7	73,400	1,835	82
	1.7732	7.4	66,410	1,660	74
	2.0588	8.6	62,660	1,566	70
	2.2527	9.4	56,650	1,416	63
	2.4730	10.3	47,800	1,195	53
	2.7373	11.4	38,040	951	42
	2.9449	12.3	32,020	800	36
	3.2124	13.4	25,180	630	28
	3.2723	13.6	22,910	573	25
Second loading direction: pull to east	0.0198	0.08	1,930	48	2
	0.0236	0.09	2,790	70	3
	0.0247	01.0	2,930	73	4
	0.0500	0.21	12,430	311	15
	0.0555	0.23	14,050	351	17
	0.0714	0.30	18,810	470	23
	0.0758	0.32	19,640	491	24
	0.2050	0.85	44,780	1,120	55
	0.3181	1.3	59,080	1,477	72
	0.4599	1.9	72,800	1,820	89
	0.6719	2.8	82,110	2,053	100
	0.9059	3.8	66,320	1,658	81
	1.1581	4.8	71,140	1,778	87
	1.4020	5.8	73,490	1,837	90
	1.6464	6.9	70,110	1,753	85
	1.8085	7.5	63,740	1,593	78
	2.0568	8.6	59,720	1,493	73
	2.2694	9.5	54,110	1,353	66
	2.5303	10.5	44,590	1,115	54
	2.6995	11.2	35,440	886	43
	2.9401	12.2	30,320	758	37
	3.2598	13.6	23,750	594	29

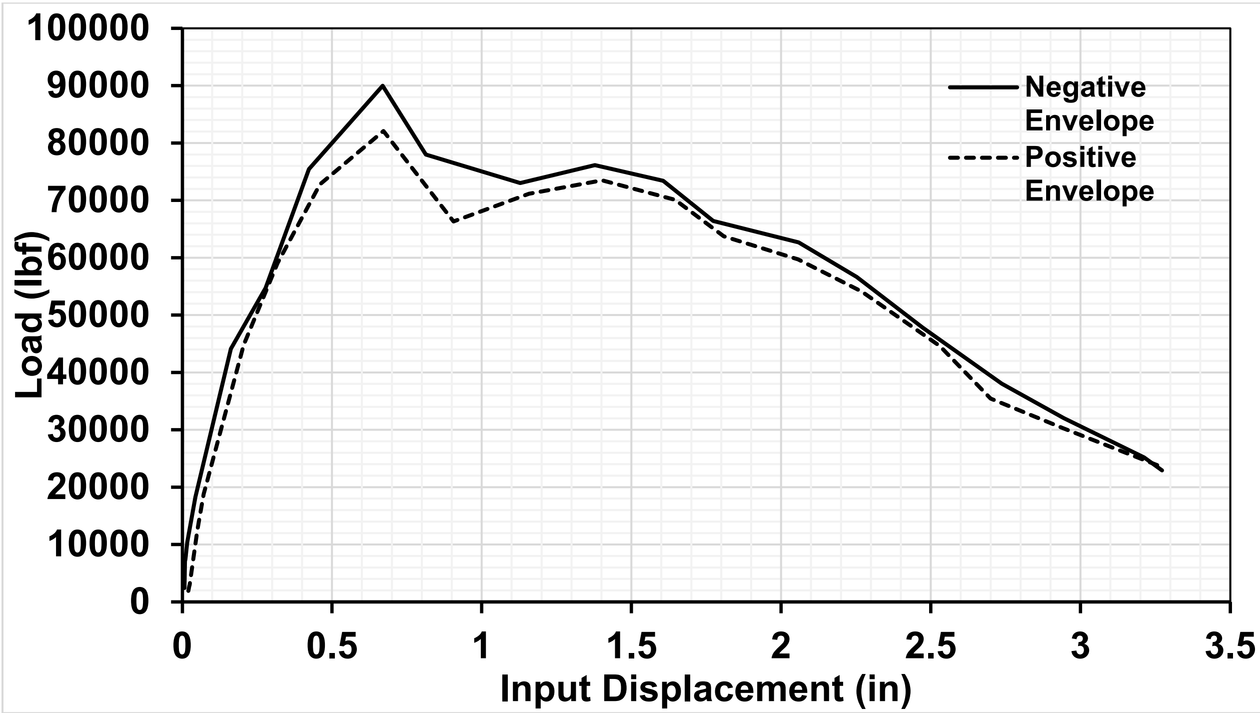

Figure 3.33 Specimen AL-2 envelope curves overlaid. Specimen weight including lead weight and loading beam is approximately 18 kips. Seismic mass tributary to the specimen is anticipated to be approximately 36 kips.

Table 3.7 Summary of test data for Specimen AL-2 monotonic push.

Displacement*	Loading direction	Peak load (lbs)	Peak unit load (plf)	Cycle peak/ overall peak (%)
4 in.	Push	19,230	481	21
6 in.	Push	15,770	394	18
8 in.	Push	15,140	379	17
9 in.	Push	14,590	365	16
10 in.	Push	12,820	321	14

* This is actuator displacement, which was not the same as the drift imposed on the cripple wall.

Table 3.8 Summary of load/displacement data for Specimen AL-2 interpolated from envelope curve.

Interpolated drift	Loading direction	Peak load (lbs)	Peak unit load (plf)	Cycle peak/ overall peak (%)
0.4% (0.096 in.)	Push	29,610	740	34
	Pull	23,570	589	30
	Average	26,590	665	32
0.6% (0.144 in.)	Push	40,080	1,002	47
	Pull	32,910	823	42
	Average	36,490	912	44
0.8% (0.192 in.)	Push	46,810	1,170	54
	Pull	42,250	1,056	54
	Average	44,530	1,113	54
1.4% (0.336 in.)	Push	62,980	1,575	73
	Pull	60,810	1,520	77
	Average	61,890	1,547	75
2% (0.48 in.)	Push	78,830	1,971	92
	Pull	73,680	1,842	93
	Average	76,260	1,906	93
2.5% (0.60 in.)	Push	85,920	2,148	100
	Pull	78,950	1,974	100
	Average	82,440	2,061	100
3% (0.72 in.)	Push	85,760	2,144	100
	Pull	78,860	1,972	100
	Average	82,310	2,058	100
4% (0.96 in.)	Push	75,680	1,892	88
	Pull	67,360	1,648	85
	Average	71,520	1,788	87
6% (1.44 in.)	Push	75,400	1,885	88
	Pull	72,970	1,824	92
	Average	74,180	1,855	90
8% (1.92 in.)	Push	64,490	1,612	75
	Pull	61,940	1,548	78
	Average	63,210	1,580	77
10% (2.40 in.)	Push	50,730	1,268	59
	Pull	49,340	1,234	62
	Average	50,040	1,251	61
12% (2.88 in.)	Push	33,680	842	39
	Pull	31,600	790	40
	Average	32,640	816	40

Similar to Specimen AL-1, the tension loads in the anchor bolts connecting the specimen to the concrete foundation were measured using washer load cells. Before the start of the test, all the nuts were tightened to a tension load of approximately 100 lbs. While tension loads in Specimen AL-1 stayed below 400 lbs, loads up to approximately 1200 lbs. were recorded in the AL-2 anchor bolts. This is still a fairly modest tension load given the significant level of loading imposed on the specimen. Plots of anchor bolt forces show that the pattern of anchor bolt loads (particularly towards the specimen ends) match the specimen overall load-defection pattern to some degree; see Figure 3.34. Noted: loads in the bolts towards the specimen ends are higher than found in the middle bolts, suggesting that the anchor bolt tension is part of a global overturning pattern.

Documentation of Specimen AL-2 conditions during testing included visual observations and photographs. which occurred at the designated hold points in the loading protocol, as previously described. The observed behaviors included cracking of stucco, separation of the stucco from the foundation and framing, etc., that were documented over a range of drift levels. Observation of the cripple wall retrofit was possible from the crawlspace interior at several points during testing.

To aid in the tracking and photographing of stucco cracks, the cracks were marked on the stucco finish using colored pens. Different colors were used as follows: green to record stucco cracking observed prior to the start of the test (consistent with anticipated stucco shrinkage cracking); black marker was used to chart the crack lines in the first push (towards the west) to each of the drift ratio; and red and blue markers were used for the first pull (to the east) peak and back to zero displacement, respectively. Other noted damage was marked in the same manner.

Except for the cracking of stucco that occurred prior to the start of testing, the great majority of cracking damage occurred primarily over the height of the cripple wall and at the floor level, with little damage extending up into the superstructure walls. This is illustrated in Figure 3.35, photographed towards the end of the test, where it can be seen that little in the way of stucco cracking is marked in the superstructure; therefore, the subsequent discussion below focuses on the cripple wall and floor levels. Detailed documentation of observations at each drift level are provided in Appendix C.

Prior to the start of testing, hairline cracking of the stucco occurred due to a combination of common shrinkage cracking and progressive cracking as the lead weights were set on the structure. These hairline cracks tended to follow a vertical direction and were generally uniformly distributed along the specimen length; see Figure 3.36.

The main progression of damage during testing involved the stucco on the east and west end walls (perpendicular to the direction of loading) cracking, deteriorating, and finally being pushed off of the supporting sheathing and framing. This deterioration was necessary to allow racking of the north and south cripple walls to accommodate the imposed displacements; see Figure 3.37. Cracks widened, stucco wires broke, stucco pieces dislodged and then fell, and finally the end wall stucco was pushed completely free of the sheathing and framing. While the end wall stucco deteriorated, the stucco on the north and south cripple walls remained substantially planar, with the only hairline visible. Little or no imposed displacement was accommodated by in-plane distortion of the stucco itself; see Figure 3.35.

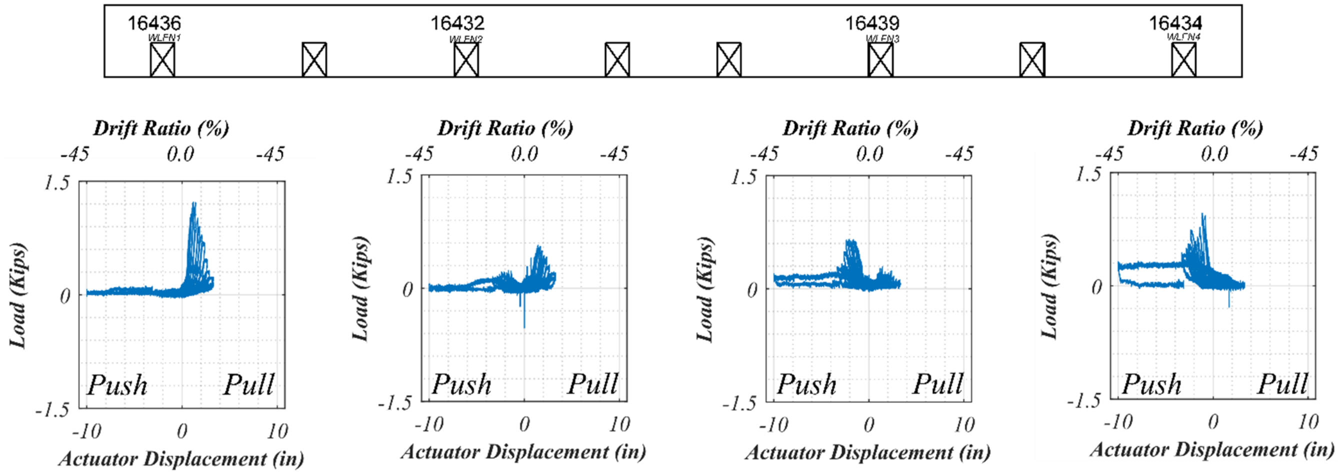

WLFS1 WLFS2 WLFS3 WLFS4

Figure 3.34 Tension developed in the bolts at the south wall.

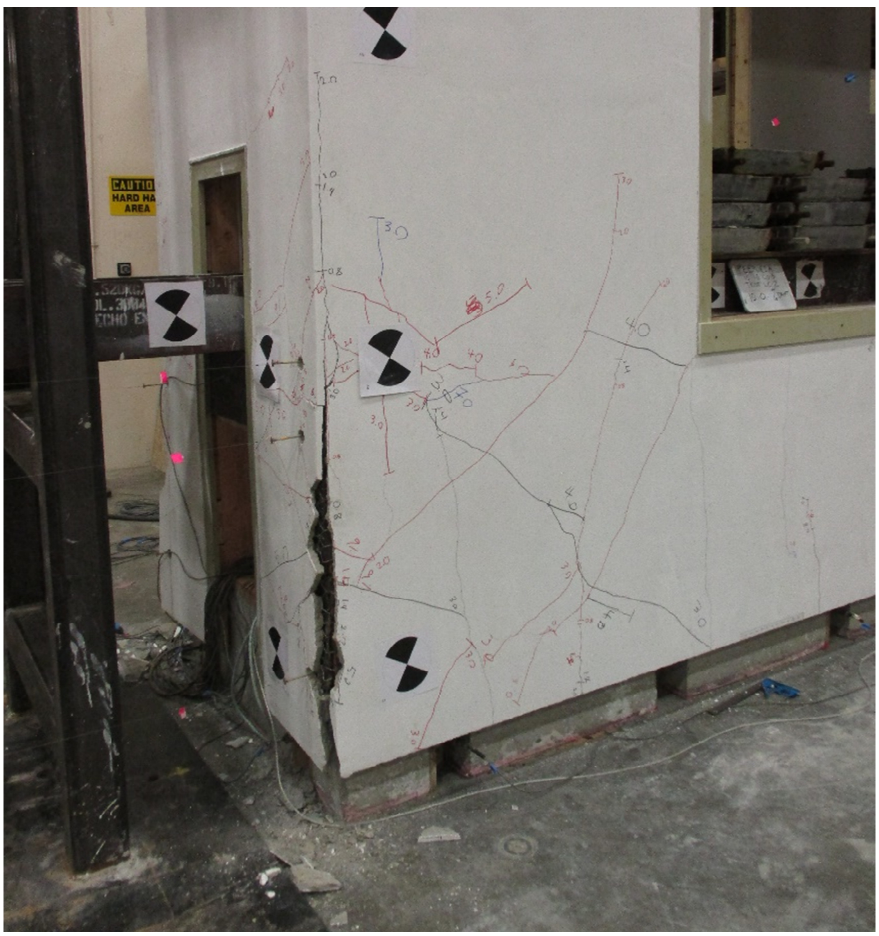

Figure 3.35 Specimen AL-2 near the conclusion of cyclic testing (at zero displacement following cycling to 10% drift). Note that marked stucco cracking is primarily located at the cripple wall and floor levels.

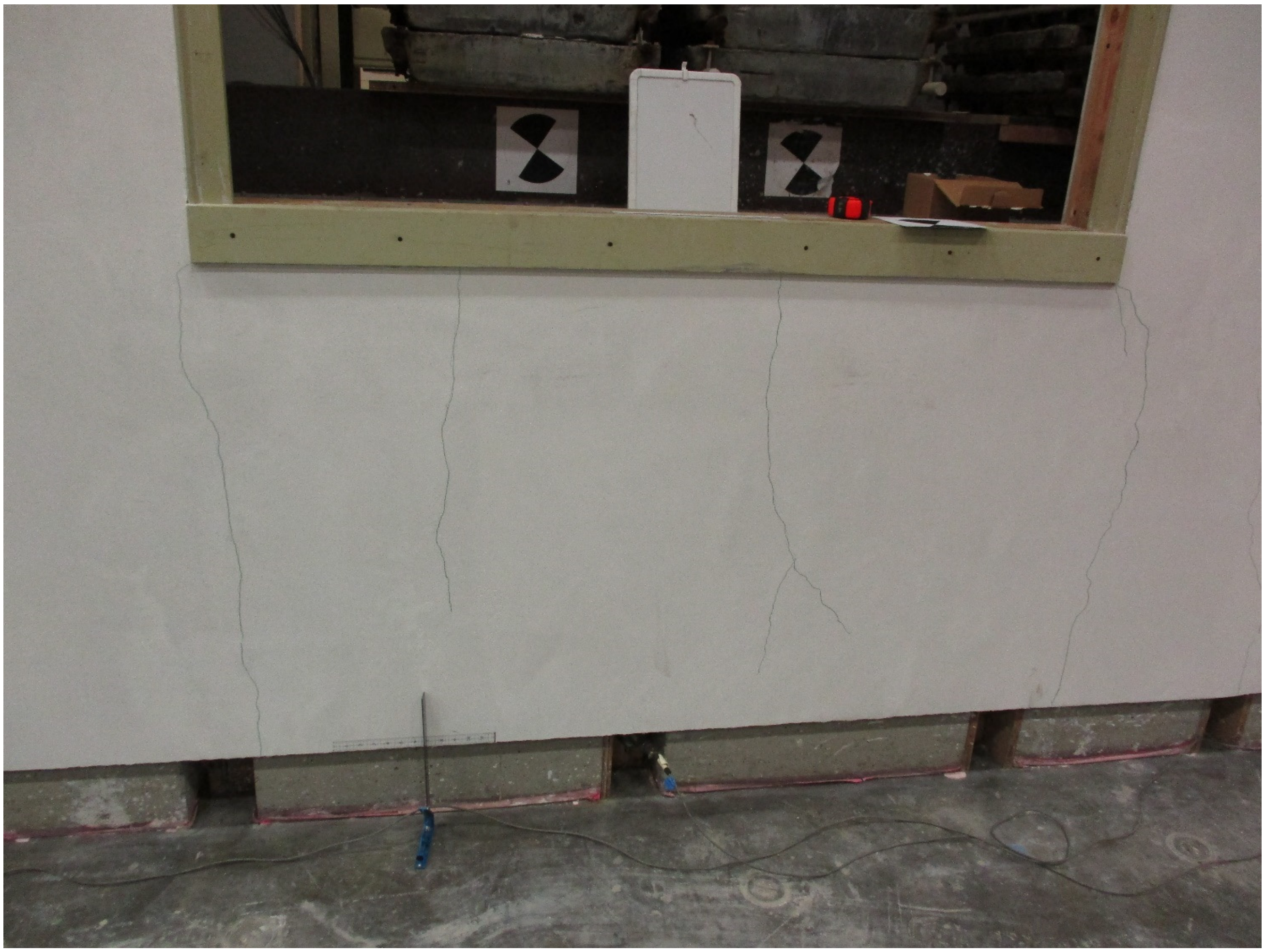

Figure 3.36 Vertical shrinkage and settling cracks before start of loading.

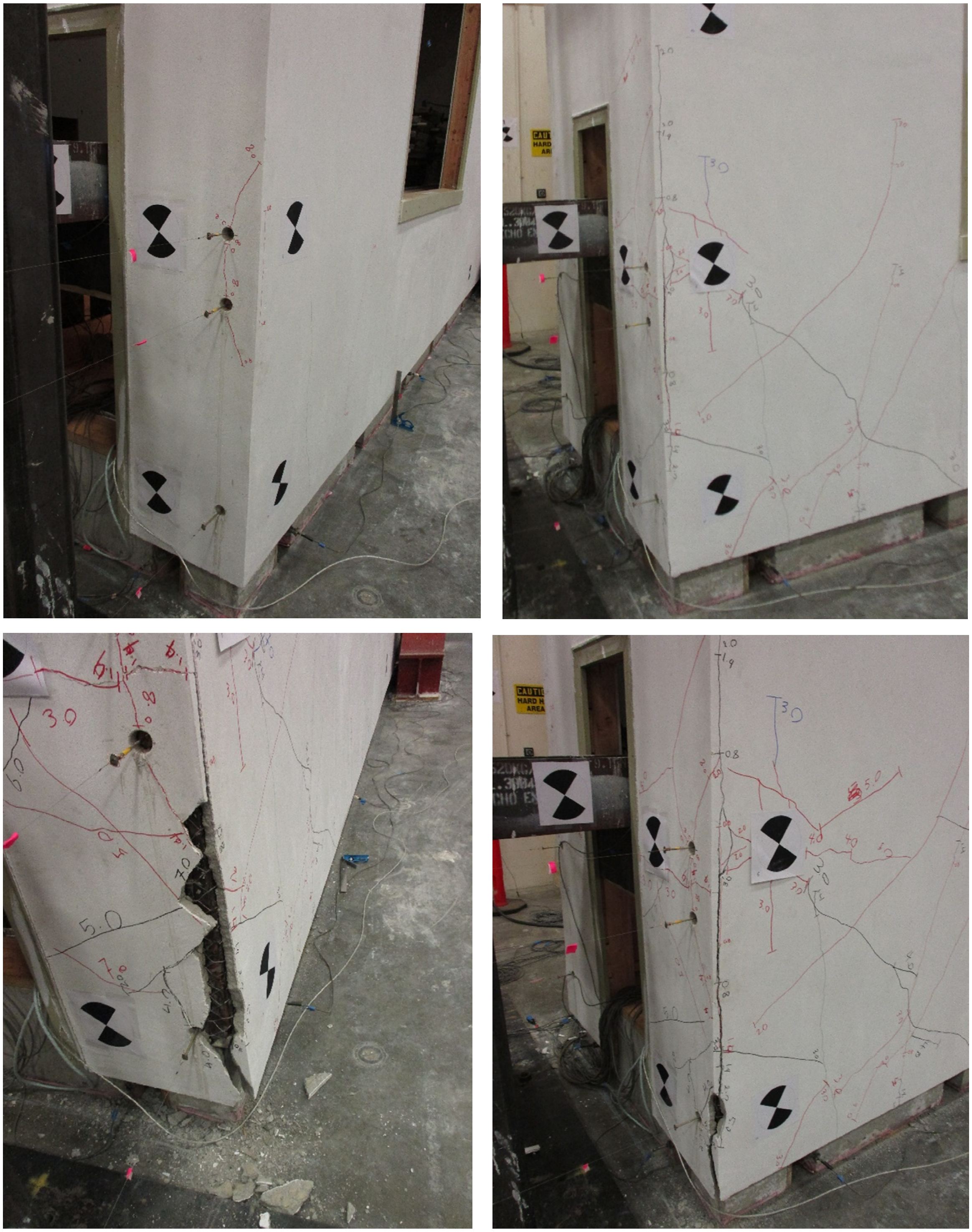

Figure 3.37 Stucco damage observed following drift ratios of 0.8%, 3%, 5% and 9% (clockwise from upper left).

During the progression of the loading, the cripple wall retrofit did not exhibit any visible signs of distress up through a drift ratio of 4%; however, there were indications of sheathing panels rotating and sheathing nails moderately withdrawing as the drift ratio increased up to 9%; see Figure 3.38. At a drift ratio of 11%, the sheathing nailing into the upper top plate had substantially withdrawn, and the sheathing nailing at the bottom plate was partially withdrawn; see Figure 3.39. Note: very little withdrawal of the sheathing nails into the lower top plate was observed due to slip between the upper and lower top plates. In the final monotonic push, the floor diaphragm and upper top plate were pushed off of the lower top plate; see Figure 3.40.

Figure 3.38 Cripple wall retrofit sheathing under imposed drift ratios of 4%, 6%, and 9%.

Figure 3.39 Cripple wall retrofit sheathing under imposed drift ratio of 11%. Nails into upper top plate are substantially withdrawn. Nails into bottom plate have partial withdrawal. Notable is the limited withdrawal of nails into the lower top plate.

Figure 3.40 Floor diaphragm pushed off of cripple walls in final monotonic push.

3.11 POST-TEST FINISH REMOVAL

Following completion of Specimens AL-1 and AL-2 testing, selected portions of the finish materials were removed to allow observation of the underlying materials and any hidden damage. Extensive observations were also made of the interior of the crawlspace. Details of these observations are provided in Appendix D.

3.12 DISCUSSION OF RESULTS

In addition to the general objective of quantifying load-deflection behavior and collecting damage descriptions, two objectives of the testing of Specimens AL-1 and AL-2 were as follows: (1) to compare the pre- and post-retrofit performance of large cripple wall components having realistic boundary conditions to better understand the benefits of retrofit; and (2) to compare the test results of small-components with large-component tests conducted at UCSD. This section provides discussion of results including: general results, the results for Specimen AL-1, the results for Specimen AL-2, and a discussion of the above two objectives.

3.12.1 General Discussion

Prior to testing, the continuity of stucco around the test specimen corners was considered of importance in their design. Based on observations during testing, this continuity had significant effect on the peak shear capacity, the displacement at peak shear capacity, and failure mechanisms. Clearly, the stucco at the corners had to be significantly degraded for cripple wall drift to occur; the inclusion of the stucco wrap around corners modified damage mechanisms, which in turn changed the load and deflection behavior. Up until peak shear capacity at about 3% drift, the stucco primarily remained in place, with a rigid connection to the foundation. Although displacement at the floor pushed on the stucco that pushed the framing relative to the stucco, the bottom of the stucco remained bonded to the foundation; see Figure 3.41(a). After peak shear capacity had been reached, the bottom of the stucco broke free of the foundation, and the stucco at both the superstructure and the cripple wall displaced as a rigid body. The stucco corners at the end walls then broke apart, and the stucco was pushed off and racking of the cripple wall studs occurred; see Figure 3.41(b).

The continuity of the stucco from the cripple wall into the superstructure was also considered to be of importance in the design of the specimen. There was no indication of any significant loading or slip of the furring nails in the superstructure. Racking of wall studs and nail slip seemed largely confined to the floor level and cripple walls without visible interaction with the superstructure framing. Based on the response of the specimens, it is believed that the superstructure played a major role in retaining the stucco's vertical and planar configuration, restraining any global in-plane rotation of the stucco, and helped to restrain in-plane racking of the stucco.

It is assumed that loading from the floor diaphragm was transferred into the stucco walls by a zone or group of stucco nails in the vicinity of the floor diaphragm, just beyond those nails at the cripple wall top plates. This effect of additional transfer of forces into the top of the cripple walls was addressed in the CUREE EDA testing. and the UCSD cripple wall testing with increased the stucco to framing fastening at the top plates, ensuring that load transfer to the cripple walls was not a weak link.

Finally, based on observations during testing, the continuity of the stucco down the face of the foundation was identified to be of importance in the specimen design and had a significant impact on the test results as bond of the stucco to the foundation remained intact up to peak loads. The bond is believed to have contributed to increased peak loads and reduced the displacement at peak loads.

Of these three sources of continuity incorporated into the specimen, the continuity of the stucco around corners and into the superstructure is assumed to be common practice in all dwellings with exterior stucco. Note: the continuity of stucco down the foundation is only applicable to the subset of older dwellings that have not had stucco replaced.

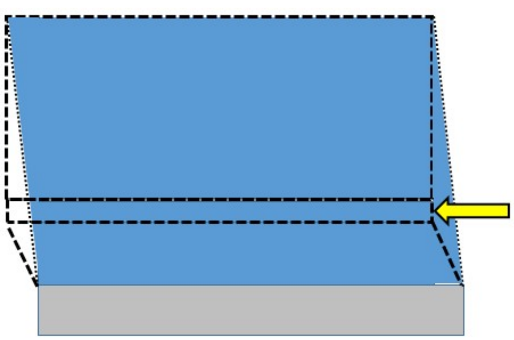

(a)

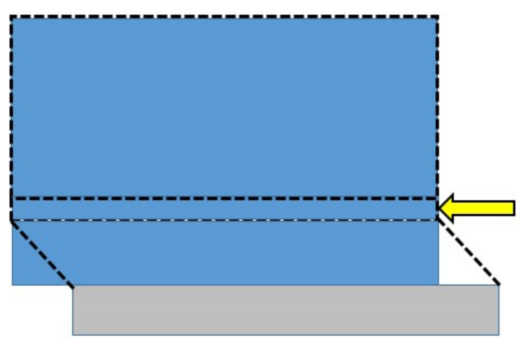

(b

Figure 3.41 Diagram of displacement for Specimens AL-1 and AL-2: (a) at small displacements the stucco remains rigidly bonded to the foundation while the floor framing pushes against the end walls; and (b) at large displacements, the stucco breaks free of the foundation and translates as a rigid body.

3.12.2 Specimen AL-1 Discussion

The displacement of Specimen AL-1 at peak shear capacity of approximately 0.7 in. (see Table 3.3) is reasonably consistent with drifts at peak shear capacity observed in past testing of full story height walls with representative boundary conditions [Arnold et al. 2003] where the peak shear capacity was reached at a displacement of approximately 1 in. This translates to a drift ratio of 2.9% for the Specimen's AL-1 cripple walls, which is notably larger than the 1% per Arnold et al. for full story-height walls. [2003] This pattern of higher drift ratio at peak load in cripple walls is consistent with past cripple wall testing [Chai et al. 2002]. Test of Specimen AL-1 provides an important confirmation for upper-bound test boundary conditions of the drift ratios observed in Chai et al. [2002] for. There appears to be a general trend that cripple walls can sustain higher drift ratios than full story height walls with matching sheathing and finish materials.

Specimen AL-1's peak unit shear capacity of approximately 1300 plf (averaged from Table 3.3 peak values) can be compared to prior testing in which attention was given to the boundary conditions [Arnold et al. 2003] and prior testing where boundary conditions were not considered [Bahmani and van de Lindt, 2016; Pardoen et al. 2003]; see Table 3.9.

The peak unit shear capacities in Table 3.9 can be seen to be wide ranging, with Specimen AL-1's peak capacities falling between the Arnold test results and test results from Pardoen et al [2003], and significantly greater than the Bahmani testing. While Specimen AL-1 and the Arnold et al. [2003] test results also included horizontal lumber sheathing or gypsum wallboard, these are known to contribute only minimal capacity and are not responsible for the differences in peak unit shear capacity. This data makes clear the important influence of boundary conditions on the peak shear capacity. When considering the peak strength of Specimen AL-1, it is important to acknowledge that AL-1 likely represented an upper bound of continuity at boundary conditions. In addition, Specimens AL-1 and AL-2 are recognized as representing an upper bound of condition (lack of deterioration due to decay, etc.) relative to the housing stock.

The Specimen AL-1 peak unit shear capacity of 1300 plf (averaged from Table 3.3) can be compared to the nominal capacities assigned by SDPWS [AWC 2015]. The SDPWS Table 4.3C assigns stucco a nominal capacity of 360 plf for both seismic and wind design. Table 4.3D assigns horizontal lumber sheathing a nominal capacity of 100 plf for seismic and 140 plf for wind design. Summing the stucco nominal capacity of 360 plf with the higher horizontal lumber sheathing capacity (without rules established for reduction when using combined materials) gives a summed nominal capacity of 500 plf, which is approximately 40% of Specimen AL-1's peak shear capacity. Because the strength of these materials is not permitted to be combined in design, the ASD allowable unit shear assigned by SDPWS would be 360/2 or 180 plf, which is 14% of Specimen AL-1's peak shear capacity. The peak of Specimen AL-1's test capacities is significantly higher than SDPWS's nominal and ASD's design capacities.

Specimen AL-1's peak unit shear capacity of 1300 plf can be compared to the capacities used in the numerical studies conducted for *FEMA P-1100*, Vol. 3, Table 4.4; these are summarized in Table 3.10 below.

Table 3.9 Comparison of Specimen AL-1 peak capacities and drifts to prior testing.

Testing	Materials	Boundary conditions considered?	Peak unit shear capacity (plf)	Displacement at peak shear capacity (in.)
Specimen AL-1	Stucco over horizontal lumber sheathing	Yes	1300	0.7
Arnold 1	Stucco exterior, gypboard interior	Yes	1880	1.0
Arnold 2	Stucco exterior, gypboard interior	Yes	1590	1.1
Bahmani	Stucco	No	350	0.75
Freund 1	Stucco	No	650	2
Pardoen 2	Stucco	No	750	3

Table 3.10 Comparison of Specimen AL-1 peak capacities and drifts to *FEMA P-1100* modeling.

Source	Materials	Characterization	Peak unit shear capacity (plf)
Specimen AL-1	Stucco over horizontal lumber sheathing	See discussion	1300
FEMA P-1100	Stucco	Lower bound	347
		Best estimate	695
		Upper bound: top story	1089
		Upper bound: lower story	1570
FEMA P-1100	Horizontal lumber sheathing	Best estimate	190
FEMA P-1100 rule for summing materials	Stucco + horizontal lumber sheathing	Best estimate	885

As noted previously, Specimen AL-1 would be categorized as an upper bound representation of stucco cripple walls. The above table confirms that the peak unit shear capacities are in general alignment with those categorized as upper bound per *FEMA P-1100*. Specimen AL-1's peak shear capacity is noted to be 20% higher than the *FEMA P-1100*'s upper bound top-story value and 20% lower than *FEMA P-1100*'s upper bound lower-story value. Refinement to the *FEMA P-1100* numbers could potentially be made considering this data. When Specimen AL-1 reached its peak shear capacity of 1300 plf, the load transfer occurred via the bond between the stucco and foundation rather than via the nails. Once the bond was broken at a drift ratio of approximately 3%, the residual capacity dropped to about 40% of the peak shear capacity. Based on post-test finish removal (see Appendix D), it is believed that the nails fastening the stucco to the sheathing and framing would have failed (heads pulled out of stucco) immediately after the bond failed. That being said, the peak unit shears for Specimen AL-1 are not tremendously different from the peak unit shears in Table 3.9 as reported in Arnold et al. [2003] (i.e., 1880 and 1590 plf when divided by the length of full-height wall piers and approximately half these values when divided by the full length of the specimen including openings). For this reason, Specimen's AL-1 strength should not be viewed as an unrealistic upper bound.

As shown in Table 3.4, the observed residual capacity out to significant drift ratios is consistent with other tests of horizontal lumber sheathing, which have shown sustained capacity to very large drift ratios. The peak unit loads listed in Table 3.4 are somewhat higher but are reasonably consistent with *FEMA P-1100*'s best estimate of 190 plf peak unit shear for horizontal lumber sheathing. The primary contribution of the horizontal lumber sheathing is further confirmed by the visual observation in later stages of testing where the stucco at the cripple wall level had flared away from the sheathing and framed wall, and, therefore, could not contribute strength.

Regarding P-delta forces: following the final monotonic push, Specimen's AL-1 was brought back to zero displacement, and the actuator turned off so that no load or displacement could be imposed. Several minutes later, the specimen had moved back on its own to a significant portion of the 40% drift (10 in.) imposed in the final monotonic push. In looking at the hysteresis loops, the specimen had a near zero stiffness remaining over a large displacement range, so with a very small P-delta force it moved to a very large displacement. Unlike steel and concrete structures where residual drift is often caused by yielding in large acceleration spikes, residual drift in light-frame structures can be caused by a small P-delta forces and very low residual drift.

3.12.3 Specimen AL-2 Discussion

The Specimen AL-2 peak unit shear capacity was approximately 2100 plf (averaged from Table 3.6), an increase of 60% over the Specimen AL-1 peak unit shear capacity of 1300 plf.; also evident was the increased displacement capacity, particularly at post-peak displacements.

The Specimen AL-2 displacement at peak shear capacity of approximately 0.7 in. (Table 3.6) is reasonably consistent with drifts at peak shear capacity of Specimen AL-1 and with those observed in past testing of full-story height stucco walls with representative boundary conditions [Arnold et al. 2003 where the peak shear capacity was reached at a displacement of approximately 1 in. The drift ratio of 2.8% for Specimen AL-2 cripple walls is again, like Specimen AL-1, notably larger than the 1% reported in Arnold et al.'s study of full-story walls. As seen with Specimen AL-1, this pattern of higher drift ratios at peak load occurring in cripple walls is consistent with past cripple wall testing [Chai et al. 2002], confirming the pattern of higher drift ratios being achieved in cripple walls.

Specimen AL-2's peak unit shear capacity of approximately 2,100 plf can be compared to prior testing where boundary conditions were not considered [Gatto and Uang 2002; Bahmani and van de Lindt 2016; Chai et al. 2002; and Pardoen et al. 2003]. Table 3.11 provides approximate peak unit shear capacities and approximate displacements at peak shear capacity estimated from published hysteresis plots.

The peak unit shear capacities can be seen to be wide ranging, with Specimen AL-2's peak capacities being higher than reported by other researchers. This data makes clear the important influence of boundary conditions on the peak shear capacity.

While Specimen AL-2's boundary conditions might be considered upper bound, the effect of staggering plywood edge nails between the upper and lower top plates was not representative of upper bound conditions and reduced the specimen's peak shear capacity. During testing, only the edge nails on the upper top plate fully participated, suggesting that the full capacity of 3 in. on center plywood edge nailing was not achieved. A study of Figure 3.42 explains why. The figure on the left-hand side shows a complete load path between the floor diaphragm and the upper top plate edge nailing. The figure on the right-hand side shows that the only load path to the lower top plate edge nailing is through 16d@12 nails (shown in red) between the upper and lower top plate; these nails have significantly less capacity than the 8d@6 effective edge nailing at the lower top plate. This needs to be considered when placing the results of Specimen AL-2 in the range between lower and upper bound.

Specimen AL-2's peak unit shear capacity of 2100 plf can be compared to the nominal capacities assigned by SDPWS [AWC 2015]. The SDPWS's Table 4.3A assigns a nominal capacity of 980 plf seismic and 1370 plf wind for the 15/32-rated sheathing nailed with 8d common nails at 3 in. on center. Table 4.3C assigns stucco a nominal capacity of 360 plf for either seismic or wind design. Table 4.3D assigns horizontal lumber sheathing a nominal capacity of 100 plf for seismic and 140 plf for wind. Summing the higher (wind) plywood, the stucco, and the higher (wind) horizontal lumber sheathing nominal capacities (without reduction using combined materials rules) gives a summed nominal capacity of 1870 plf, which is approximately 90% of Specimen AL-2's peak shear capacity. Because the strength of these materials cannot be combined in design, the ASD allowable unit shear assigned by SDPWS for seismic design would be 980/2 or 490 plf, which is 23% of the test peak shear capacity.

Specimen AL-2's peak unit shear capacity of 2100 plf can be compared to the capacities that were used in the numerical studies conducted for the *FEMA P-1100* study; see Vol. 3 and Table 4.4 [FEMA 2019] summarized in Table 3.12 below, further confirming that the peak unit shear capacities are in line with those categorized as upper bound in the *FEMA P-1100* numerical studies in spite of the full capacity of the plywood retrofit likely not being developed. Refinements to the *FEMA P-1100* values could potentially be made considering this data.

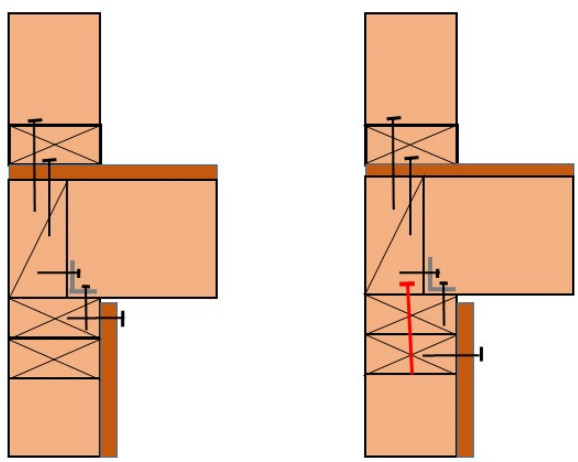

(a) (b)

Figure 3.42 Diagram of load path between diaphragm and cripple wall plywood sheathing for Specimen AL-2: (a) demonstrates complete load path from the diaphragm to the edge nailing on the upper top plates; and (b) has the load path from the diaphragm to the lower top plate limited by the capacity of the 16d nails at 12 in. on center (shown in red).

Table 3.11 Comparison of Specimen AL-2 peak capacities and drifts to prior testing.

Testing	Materials	Boundary conditions considered?	Approximate peak unit shear capacity (plf)	Plywood or OSB sheathing nominal wind capacity (plf)	Approximate displacement at peak shear capacity (in.)
Specimen AL-2	Stucco over horizontal lumber sheathing and 15/32 plywood 8d@3	Yes	2100	1370	0.7
Gatto Tests 17 and 18	Stucco and 15/32 plywood or OSB 8d@4	No	1500	1065	2 to 3
Bahmani	Stucco and 15/32 plywood 8d@4	No	1500	1065	2
Bahmani	Stucco and 15/32 plywood 8d@4 and gypboard	No	1600	1065	2
Pardoen tests 20A and 20B	Stucco and 3/8 OSB 8d@3	No	1700	1150	2
Chai tests 2 and 8	Stucco and 15/32 plywood 8d@4 cripple wall	No	1200 to 1300	1065	1

Table 3.12 Comparison of peak capacities and drift to *FEMA P-1100* modeling.

Source	Materials	Characterization	Peak unit shear capacity (plf)
Specimen AL-2	Stucco over horizontal lumber sheathing with retrofit 15/32 plywood 8d@3	See discussion	2100
FEMA P-1100	Stucco	Lower bound	347
		Best estimate	695
		Upper bound: top story	1089
		Upper bound: lower story	1570
	Horizontal lumber sheathing	Best estimate	190
	15/32 Plywood 8d@3	Best estimate	1364
FEMA P-1100 rule for summing materials	Stucco + horizontal lumber sheathing + Plywood	Best estimate	1806
		Upper bound, lower story stucco, best estimate other	2240

The final failure of the specimen involved the floor diaphragm being pushed off of the cripple walls. The actual separation occurred between the upper and lower top plates of the cripple walls. When failure occurred, the cripple wall plywood edge nailing to the upper top plate had withdrawn completely from the plate, while nailing to the lower top plate was only minimally withdrawn, thus still capable of resisting loads. The load path through the upper top plate nailing [Figure 3.42(a)] was fully effective, while the load path to the lower plate and the diaphragm relied on inter-nailing of the upper and lower top plates [Figure 3.42(b)], making it only partially effective. This is believed to have reduced the capacity provided by the plywood cripple wall sheathing by between 1/2 and 1/3 of full capacity. It is anticipated that with edge nailing fully effective, the peak shear capacity of Specimen AL-2's cripple wall would have been in excess of 2500 plf. The observed failure was reported back to the developers of *FEMA P-1100*, who modified the specified top plate edge nailing prior to publication such that all edge nailing is now required to fall in the upper top plate.

3.12.4 Comparison of Specimens AL-1 and AL-2

Figure 3.43 shows the superimposed hysteresis curves for Specimens AL-1 and AL-2. The superimposed envelope curves are provided in Figure 3.44, and data interpolated from the envelope curves for purpose of comparison is summarized in Table 3.13.

The peak shear capacity of Specimen AL-2 was significantly greater than Specimen AL-1, with a 60% increase in peak shear capacity; see Table 3.13 at 2.5% drift. Although this is a significant increase in capacity, as previously discussed, the peak shear capacity of Specimen AL-2 is believed to have been reduced by the staggering of nails between the upper and lower top plates of the cripple walls. Regardless, the comparison demonstrates that addition of retrofit plywood can achieve a significant increase in peak cripple wall capacity. This clearly demonstrates the benefit of installing cripple wall retrofits.

The comparison of the post-peak drop in capacity of Specimen AL-1 (to approximately 40% of peak shear capacity) and the much more limited drop in Specimen AL-2 clearly exhibits that Specimen AL-2 is more robust, with significant post-peak shear capacity. This significantly increased capacity remains at larger drift levels where Specimen AL-1 drops to below 20% of peak shear capacity at approximately 1-1/2-in. displacement, while Specimen AL-2 remains above 80% of peak shear capacity at this drift. The combination of higher peak shear capacity and retained peak shear capacity out to higher drifts confirms Specimen AL-2 superior performance, demonstrating clearly the benefit of installing cripple wall retrofits.

Figure 3.45 identifies three pairs of points on Specimen AL-1 and Specimen AL-2's hysteresis curves that compares the displacement for a given force level. For Points 2 and 3 for the given force level, the displacement for Specimen AL-1 is notably higher than Specimen AL-2, resulting in more significant damage to Specimen AL-1 compared to Specimen AL-2. The comparison of damage conditions for each pair of points is shown in Figures 3.46, 3.47, and 3.48, implying that for a given earthquake demand level, the damage experienced with a retrofitted structure is anticipated to be less that the damage experienced without performing a retrofit. This further demonstrates the benefit of installing cripple wall retrofits.

Full discussion of the comparison of the small-component test results of Specimen AL-1 versus Specimen Al-2 conducted at UCSD is provided in a separate PEER–CEA Project report.

Table 3.13 **Comparison of interpolated envelope data for Specimen AL-1 and AL-2.**

Interpolated drift	Loading direction	Interpolated load:AL-1 (lbs.)	Interpolated load : AL-2 (lbs)	Interpolated AL-2/ AL-1
0.4% (0.096 in.)	Push	22,510	29,610	1.3
	Pull	20,440	23,570	1.2
	Average	21,480	26,590	1.2
0.6% (0.144 in.)	Push	28,500	40,080	1.4
	Pull	27,720	32,910	1.2
	Average	28,110	36,490	1.3
0.8% (0.192 in.)	Push	34,330	46,810	1.4
	Pull	32,700	42,250	1.3
	Average	33,520	44,530	1.3
1.4% (0.336 in.)	Push	45,070	62,980	1.4
	Pull	43,380	60,810	1.4
	Average	44,220	61,890	1.4
2% (0.48 in.)	Push	50,260	78,830	1.6
	Pull	48,800	73,680	1.5
	Average	49,530	76,260	1.5
2.5% (0.60 in.)	Push	52,660	85,920	1.6
	Pull	49,750	78,950	1.6
	Average	51,200	82,440	1.6
3% (0.72 in.)	Push	51,190	85,760	1.7
	Pull	42,300	78,860	1.9
	Average	46,750	82,310	1.8
4% (0.96 in.)	Push	22,050	75,680	3.4
	Pull	21,740	67,360	3.1
	Average	21,890	71,520	3.3
6% (1.44 in.)	Push	20,730	75,400	3.6
	Pull	19,600	72,970	3.7
	Average	20,170	74,180	3.7
8% (1.92 in.)	Push	7440	64,480	8.7
	Pull	8, 90	61,940	7.4
	Average	7920	63,210	8.0

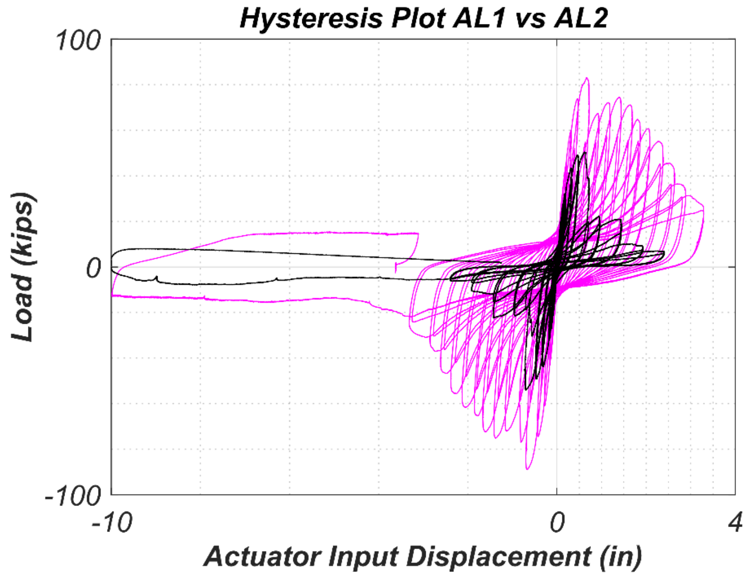

(a)

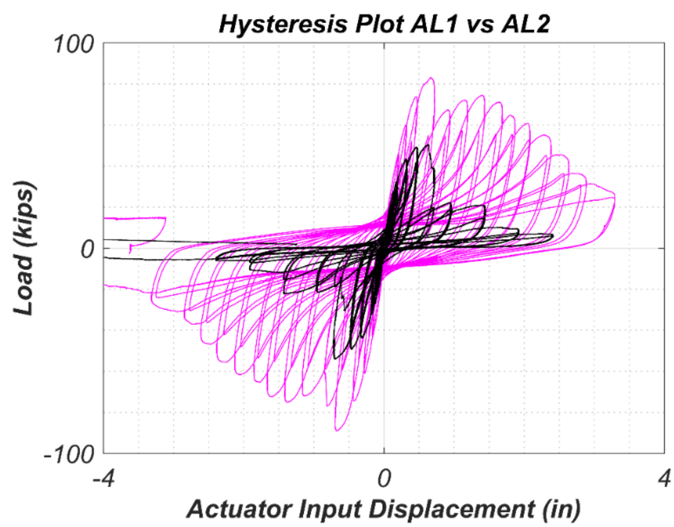

(b)

Figure 3.43 Superimposed hysteresis curves for Specimens AL-1 and AL-2: (a) overall hysteresis curves; and (b) zoomed in hysteresis curves.

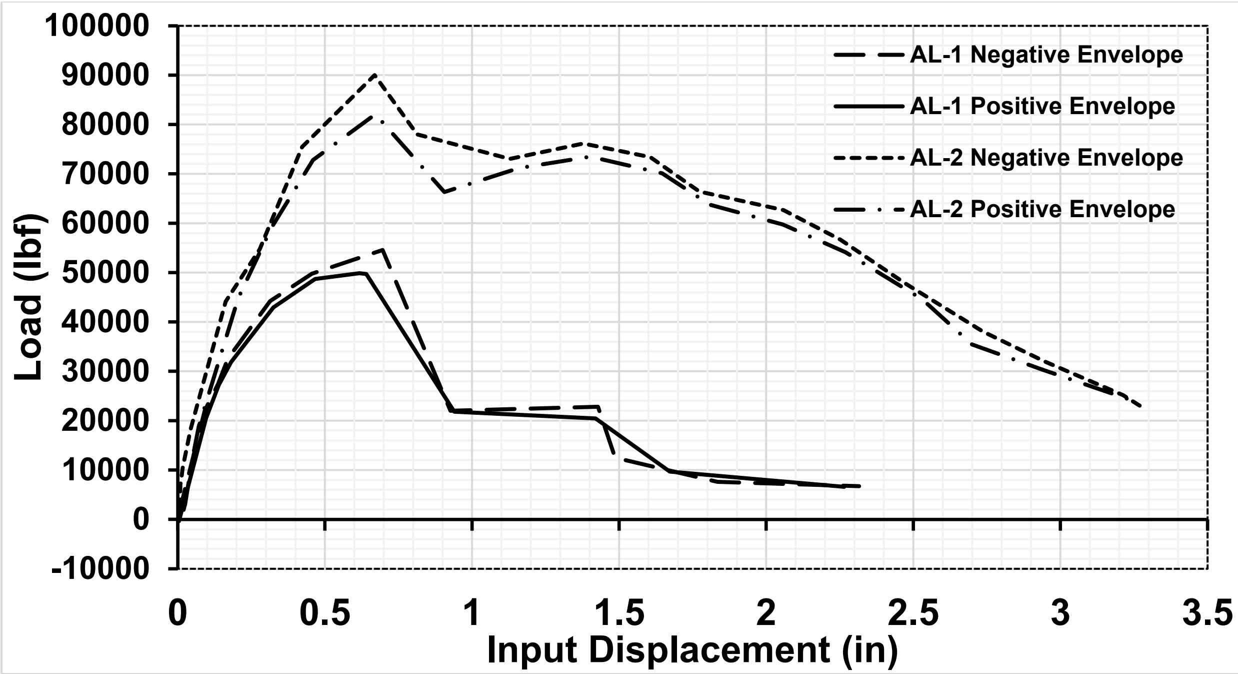

Figure 3.44 Superimposed envelope curves for Specimens AL-1 and AL-2. Specimen weight including lead weight and loading beam is approximately 18 kips. Seismic mass tributary to the specimen is anticipated to be approximately 36 kips.

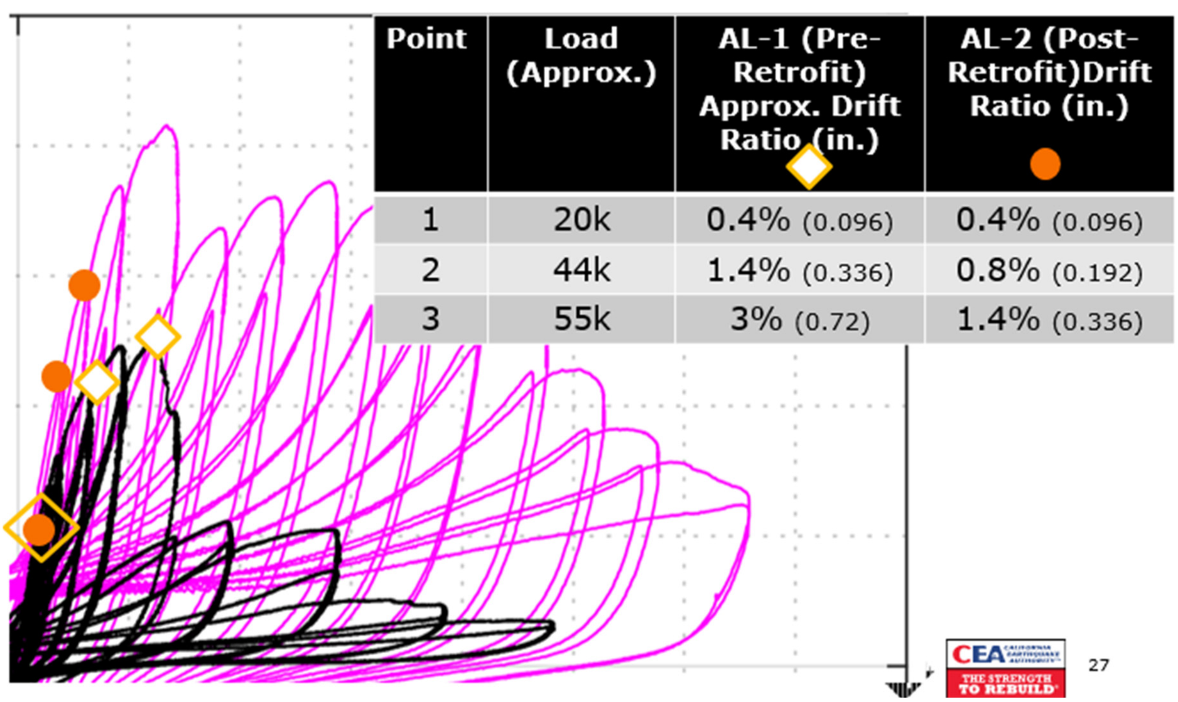

Figure 3.45 Enlarged view of superimposed hysteresis curves for Specimens AL-1 and AL-2.

Point 1: Pre and post @ 0.4% drift

(a) (b)

Figure 3.46 Comparison of damage at 20 kips load for Specimen AL-1 (pre-retrofit) and Specimen AL-2 (post retrofit): (a) pre-retrofit @ 55 kips; and (b) post-retrofit @ 55 kips.

Point 2: pre and post @ 1.4, 0.8% drift

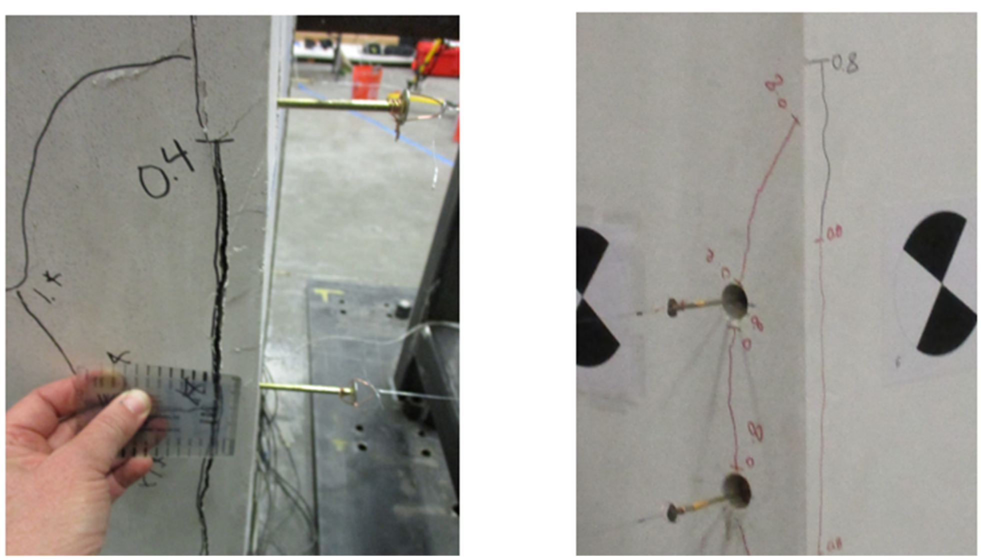

(a) (b)

Figure 3.47 Comparison of damage at 44 kips load for Specimen AL-1 (pre-retrofit) and Specimen AL-2 (post retrofit): (a) pre-retrofit @ 44 kips; and (b) post-retrofit @ 44 kips. Gage in (a) reads greater than 0.10 in.

Point 3: Pre and post @ 3.01, 4% drift

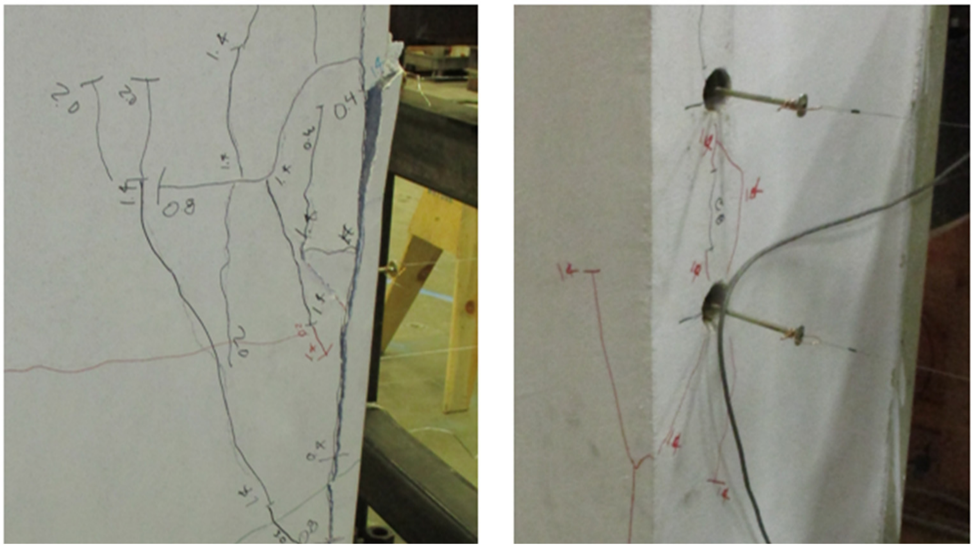

(a) (b)

Figure 3.48 Comparison of damage at 55 kips load for Specimen AL-1 (pre-retrofit) and Specimen AL-2 (post retrofit): (a) pre-retrofit @ 55 kips; and (b) post-retrofit @ 55 kips.

3.13 CONCLUSIONS

Specimens AL-1 and AL-2 investigated the seismic performance of cripple walls with a stucco exterior finish installed over horizontal lumber sheathing. Both tests included a 2-ft-tall cripple wall. Specimen AL-2 included a cripple wall retrofit designed in accordance with *FEMA P-1100* [FEMA 2018a], while Specimen AL-1 was not retrofitted; the specimens were otherwise identical. Earlier tests [Arnold et al. 2003a, b] had identified realistic boundary conditions as significantly affecting both the peak capacity and drift at peak capacity of full-story-height walls with a stucco exterior finish. Therefore, to include the most representative boundary conditions, the test specimens were three dimensional (3D) structures with plan dimensions of 20 ft × 4 ft. Each test specimens was constructed on top of a cast concrete foundation and included a 2-ft-tall cripple wall that extended to reproduce a full structure perimeter, a floor diaphragm, an 8-ft-tall superstructure, and a roof diaphragm; see Figure 3.49. This configuration allowed continuity of the stucco exterior finish around the corners, continuity of the stucco from the cripple wall into the superstructure above, and continuity of the stucco down the face of the foundation (a common detail in older stucco clad houses). Loading was applied parallel to the 20-ft-long walls.

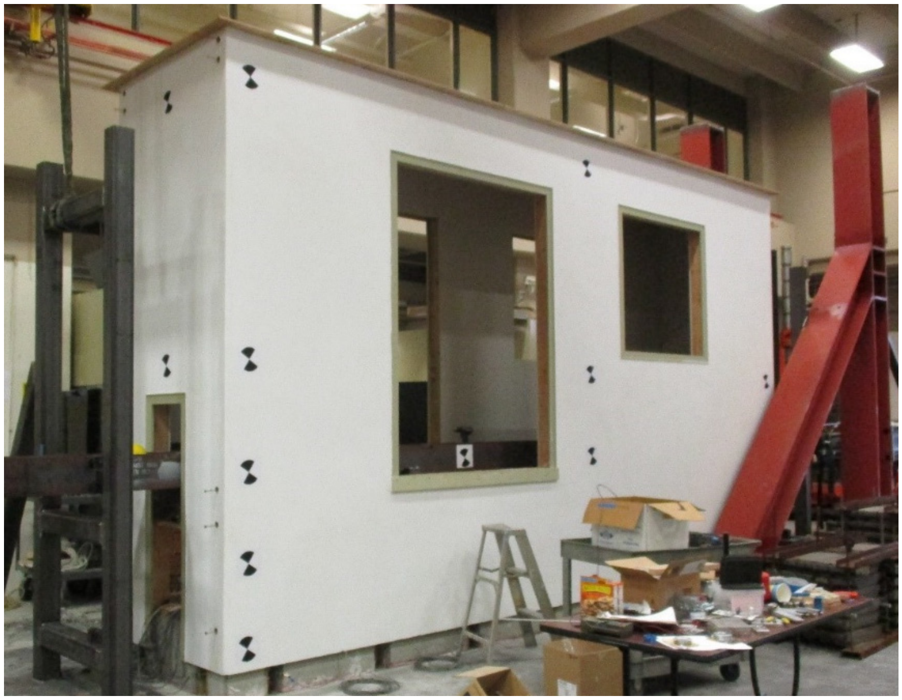

Figure 3.49 Specimen AL-1 prior to start of testing showing the superstructure wall above and cripple wall below.

In addition to the primary objectives noted above, Specimens AL-1 and AL-2 permitted direct comparison of cripple wall performance with and without retrofit, and provided data that could be compared to the PEER–CEA Project small-component tests conducted at UCSD. Comparison with the UCSD small-component tests is discussed in a separate PEER–CEA Project WG4 task.

The following are highlights of the test results for Specimens AL-1 and AL-2, and conclusions based on these results:

- It was demonstrated that the installation of cripple wall retrofits can have a significant beneficial effect, including increasing peak shear capacity, increasing deformation capacity, and reducing damage for a given force level. Also significantly increased was energy absorption, as indicated by increased area under hysteresis curves.
- Specimen AL-1 reached a peak shear capacity (lateral strength) of 51 kips (1300 plf) at a drift ratio of approximately 2.8%;
- Specimen AL-2 reached a peak shear capacity of 82 kips (2100 plf) at a drift ratio of approximately 2.8%;
- These peak capacities approach the capacities in the testing reports by Arnold et al. [2003a, b)], and are significantly higher than other previous tests of stucco wall finishes. The peak capacities are also significantly higher than nominal capacities used to assign allowable shear for design. The capacities achieved are believed to represent an upper bound of strength due to the boundary conditions used;

- The drift ratios at peak capacity of both Specimens AL-1 and AL-2 were significantly greater than observed in previous tests of full-story-height stucco finished walls. This continues a trend first observed in testing by Chai et al. [2002] of drift ratios at peak capacity being higher in cripple walls than in full-story height walls;
- While the capacity of Specimen AL-1 dropped off notably following cycles at peak capacity, in a final monotonic push, it retained 13% of peak capacity to a drift ratio of 38% (a 9-in. drift). Note: prior testing had not extended to drift ratios this large; see Figure 3.50;
- Specimen AL-2 did not experience a drop off in capacity following cycles at peak capacity, but it retained 60% of the peak capacity to a drift ratio of 10% (2.4 in.) and 40% of peak capacity to 12%. In a final monotonic push, it retained 14% residual capacity to a drift ratio of 42% (10 in.). The increase in retained post-peak capacity demonstrates significant benefit from the retrofit; see Figure 3.51;
- The peak capacity of Specimen AL-2 the (retrofitted cripple wall) was significantly greater than Specimen AL-1, with a 60% increase in peak capacity at 2.8% drift; see Figure 3.52. Although this is a significant increase in capacity, the peak capacity of Specimen AL-2 is believed to have been reduced by the staggering of retrofit sheathing nails between the upper and lower top plates of the cripple walls. Regardless, the comparison shows that retrofitting can achieve a significant increase in peak cripple wall capacity, clearly demonstrating the benefit of installing cripple wall retrofits;
- Based on observations during testing, the continuity of the stucco around the test specimen corners had a significant effect on the peak capacity, the displacement at peak capacity, and failure mechanisms. The stucco at the corners had to be significantly degraded for cripple wall drift to occur; the inclusion of the stucco wrap around corners modified damage mechanisms, which in turn changed the load and deflection behavior;
- The continuity of the stucco from the cripple wall into the superstructure was also considered to be important in the design of the specimen. There was no indication of any significant loading or slip of the furring nails in the superstructure. Racking of wall studs and nail slip seemed largely confined to the floor level and cripple walls, without visible interaction with the superstructure framing. Based on the response of the specimens, it is believed that the superstructure played a major role in retaining the stucco's vertical and planar configuration, restraining both global in-plane rotation of the stucco and in-plane racking of the stucco;
- Based on observations during testing, the continuity of the stucco down the face of the foundation was identified to be important in the specimen design and had a significant impact on the test results as the bond between the stucco and the foundation remained intact up to peak capacity. The bond is believed to have

contributed to increased peak loads and reduced the displacement at peak capacity; and

- Detailed descriptions of damage observations at each drift ratio are provided.

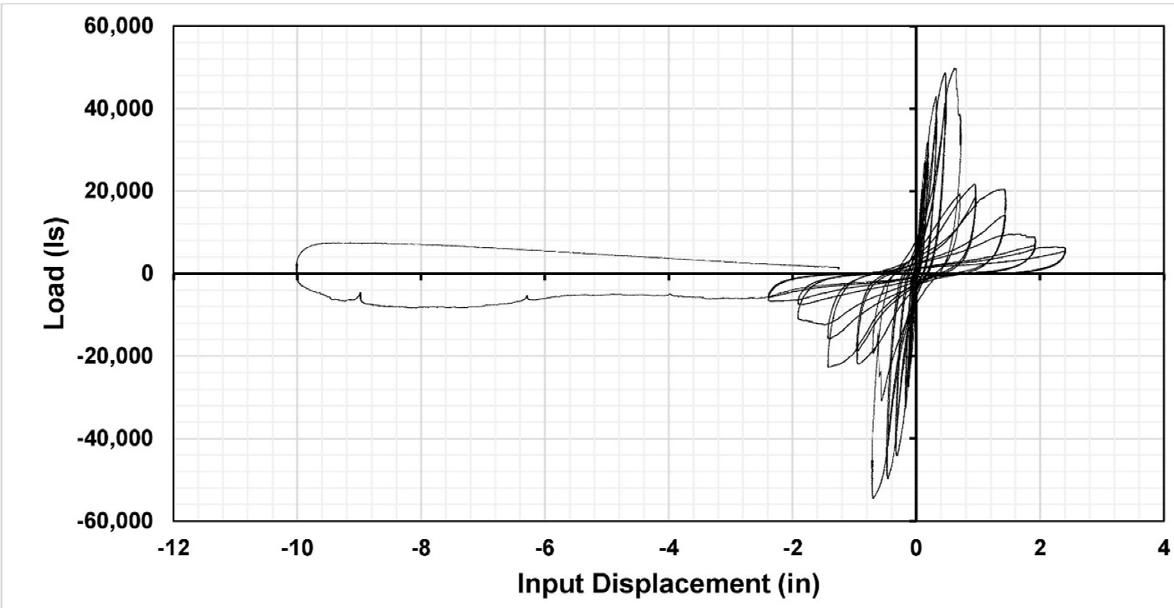

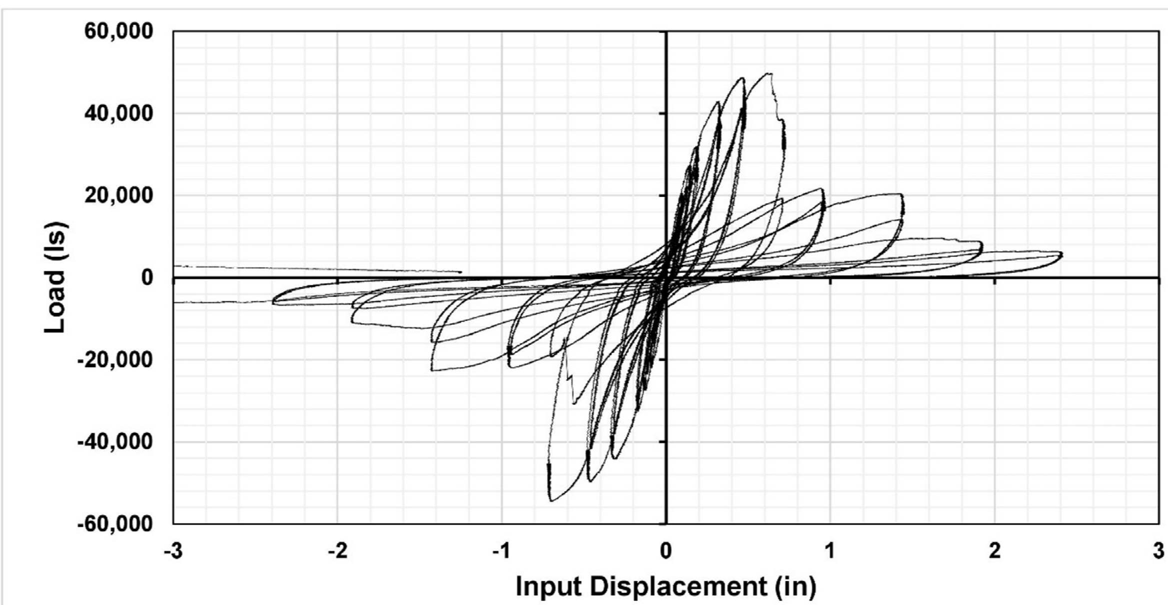

Figure 3.50 Specimen AL-1: lateral load versus lateral displacement for (top) full hysteresis plot including monotonic push at the end; and (bottom) hysteresis plot excluding monotonic push.

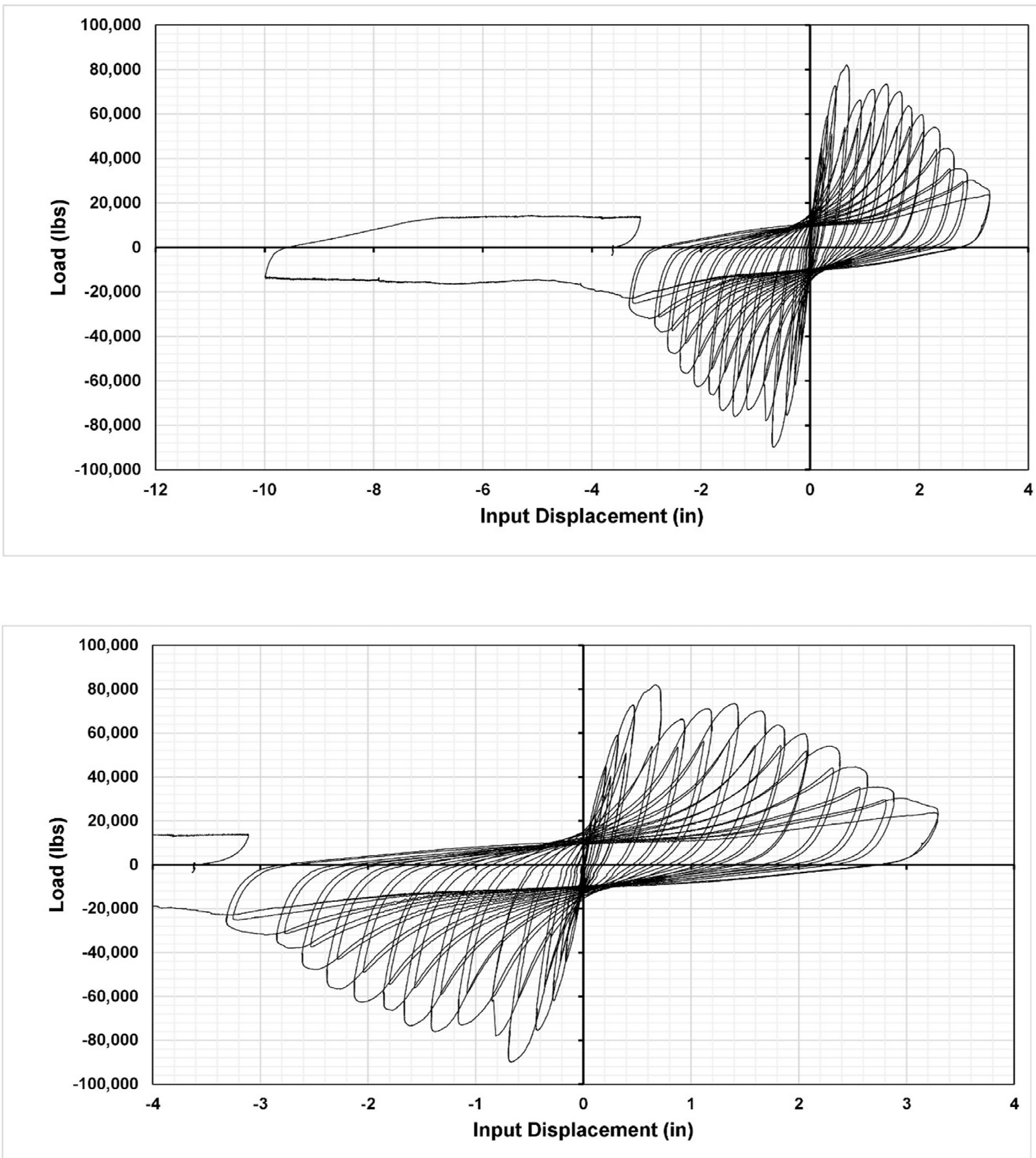

Figure 3.51 Specimen AL-2: lateral load versus lateral displacement of (top) full hysteresis plot including monotonic push at the end; and (bottom) close up of full hysteresis plot.

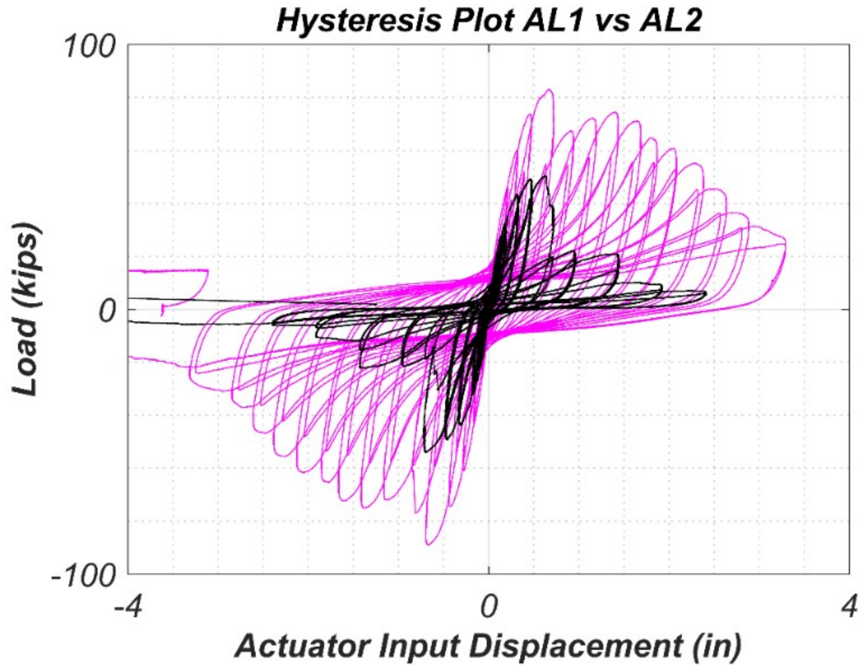

Figure 3.52 **Specimens AL-1 and AL-2: superimposed hysteresis curves. Black lines are Specimen AL-1 (pre-retrofit); magenta lines are Specimen AL-2 (with retrofit).**

4 Group B Load Path Connections

This chapter discusses testing of Specimen B-1. The primary purpose of this testing program was to evaluate the ability of commonly used retrofit load path connectors to develop the strength and displacement capacity of a cripple wall with seismic retrofit sheathing. This information permits comparison to the methods used by *FEMA P-1100* for the design of load path connections and serves to provide data for use by the WG5 numerical studies and WG6 fragility functions. Specimen B-1 load path connectors were selected by the project team as priorities based on the connectors being commonly used in retrofit, but there being little or no published performance information.

The tests were performed on a full-scale, 3D, large component specimen with significant attention given to providing the most representative boundary conditions possible. The large scale and 3D aspects of the specimen provided a small step towards full building testing. The length of the specimen allowed the retrofit plywood to be installed in discreet sections, as would occur in a full dwelling. The end walls, perpendicular to loading, allowed observation of end wall and corner behaviors and damage.

This chapter provides details of construction for Specimen B-1, and presents test results, discussion, and conclusions. Note: the terms “existing” and “unretrofitted” are used interchangeably in this report.

4.1 INTRODUCTION

Test Specimen B-1 was selected to have a horizontal wood (shiplap) siding exterior finish, installed over building paper. Per typical construction practice, no interior finish was installed on the cripple wall. The horizontal wood siding is representative of dwellings originally constructed over a range of years up to the 1940s, and is thought to be representative of a notable portion of the existing dwelling stock in Calfiorina. In addition, damage to horizontal wood siding sheathed cripple walls has been broadly observed in past earthquakes, highlighting the value in retrofitting this construction type. Materials and details of construction were chosen to be consistent with dwellings constructed in the 1930s and 1940s. Further information on details of construction is provided in the following sections.

The configuration of the test specimen was based on a hypothetical single-story model dwelling with a 30- × 40-ft footprint. Like the other large-component tests in the PEER–CEA Project, this test used plan dimensions of 20 ft × 4 ft, reusing the foundation used for prior project tests. The loading of the test specimen was parallel to the 20-ft walls. The test specimen included a 2-ft-high cripple wall at the full specimen perimeter, and a high-load floor diaphragm constructed on top. Specimen B-1 did not incorporate an occupied story above the floor because the project team deemed its presence insignificant based on the horizontal siding, providing little continuity of load path into the story above (especially when compared to stucco) per the observed response from Specimens Al-1 and AL-2. The detailing of the cripple wall framing and relationship to the foundation was selected to be typical of construction up through the 1940s. In particular, it used a foundation sill plate that was wider that the supported studs (Figure 4.1, left hand side), a detail very common for construction in California and other western states.

The specimen design incorporated a retrofit plate type of connector. This connector type is commonly used for anchorage of dwellings to foundations when the crawlspace cripple wall height is 2 ft or less. Instead of requiring vertical drilling for the installation of new anchor bolts into the top of the existing foundation, retrofit plates are installed on the interior face of the foundation stem wall, and bolts are installed horizontally into the existing foundation or stem wall; this provides much better access for drilling and installing the anchors.

Using this connector type for Specimen B-1 required that the cripple wall be constructed inside out, with the horizontal wood siding on the interior of the structure, and the anchorage connectors and retrofit sheathing on the outside; see Figure 4.1, right-hand side. This test configuration provided the additional benefit that there was a high level of access to observe the performance of the retrofit during testing. A section through the specimen is provided in Figure 4.2. Elevations and side views are shown in Figure 4.3. Detailed drawings of Specimen B-1 are provided in Appendix B.

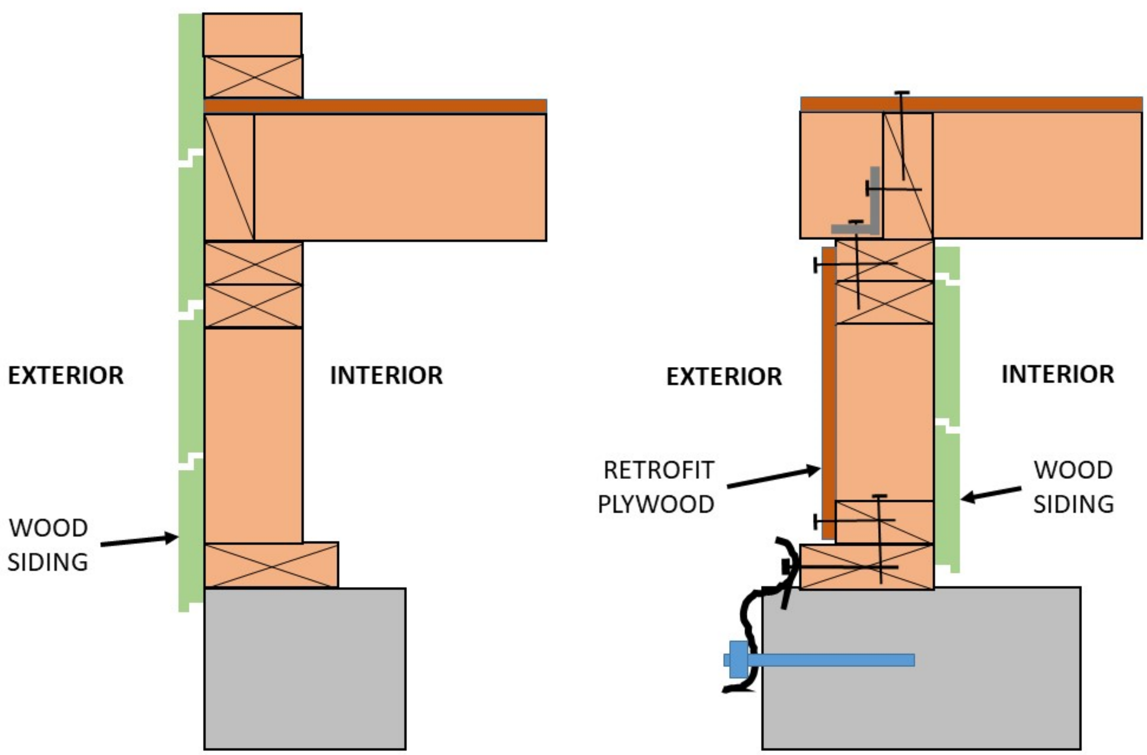

Figure 4.1 **Cripple wall configuration for Specimen B-1; (left) typical existing condition; and (right) with cripple wall constructed inside-out (siding on interior, retrofit on exterior.**

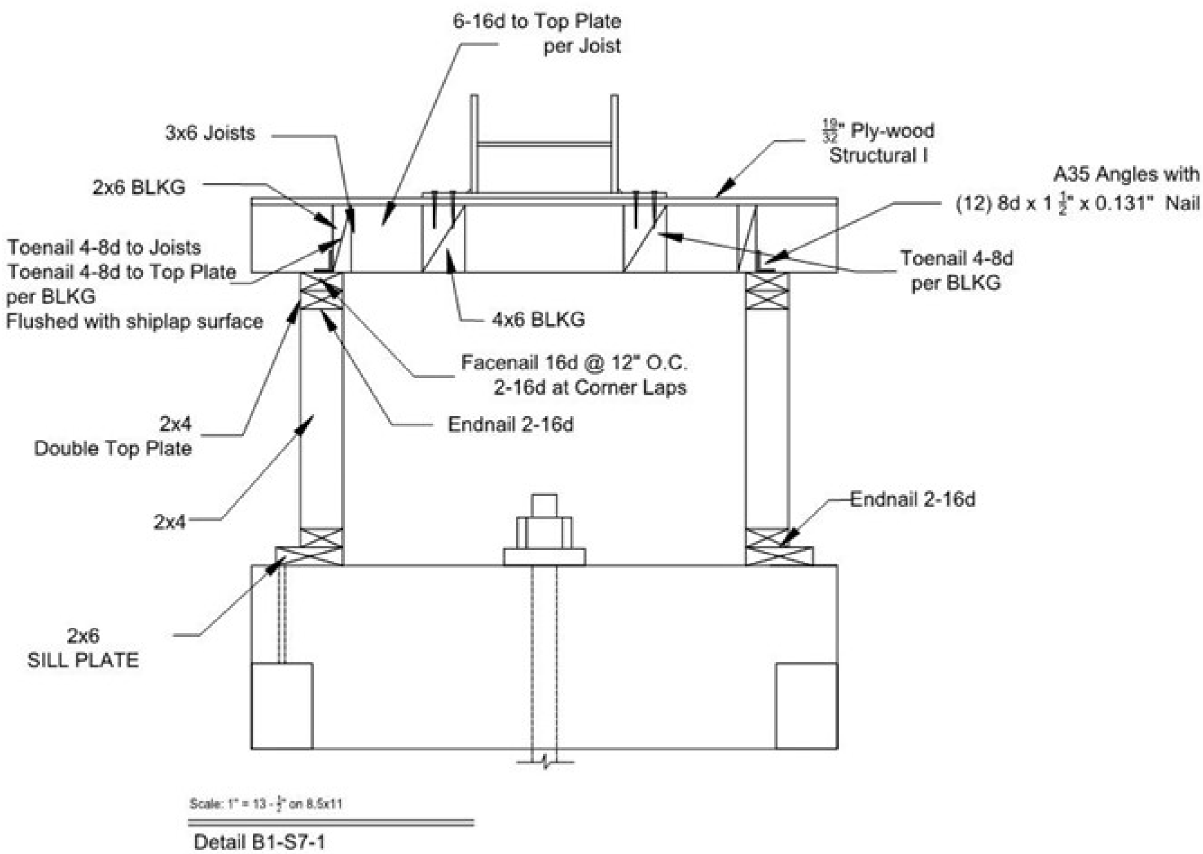

Figure 4.2 Through section view of Specimen B-1.

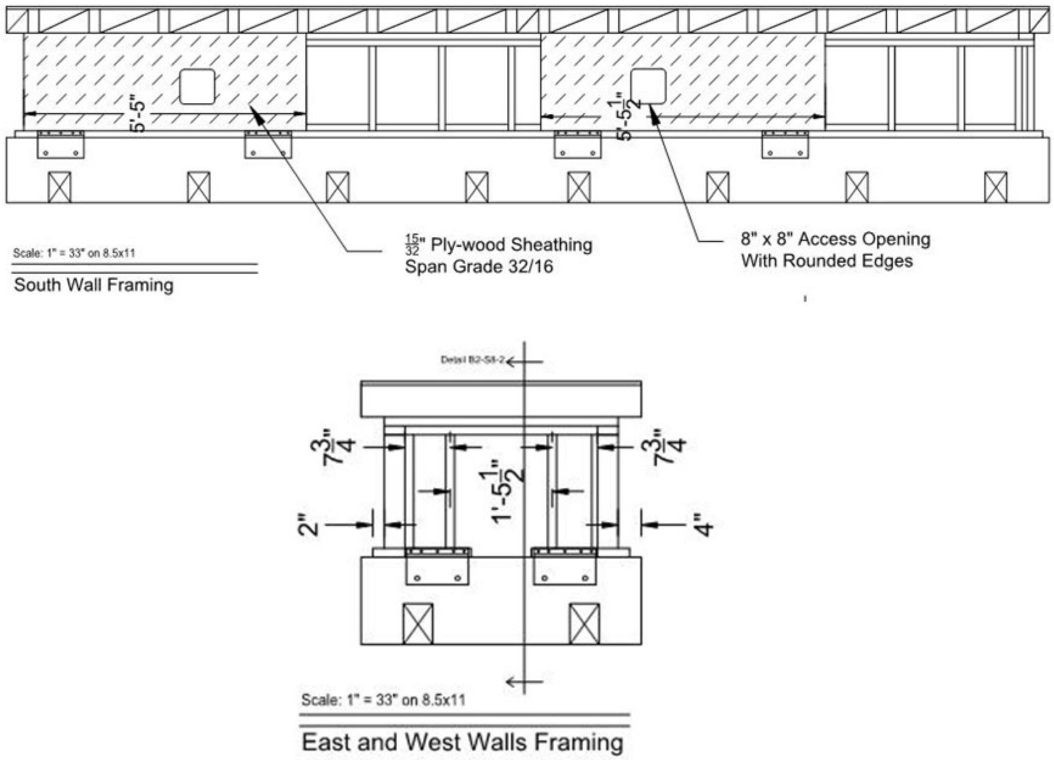

Figure 4.3 (Above) elevations for Specimen B-1, north and south walls and retrofit sheathing, and (below) east and west end walls.

4.2 FRAMING DETAILS

The same foundation used for Specimens AL-1 and AL-2 was used for Specimen B-1, following minor patching of the foundation edge. Unlike Specimens AL-1, AL-2, C-1, and C-2, there were no anchor bolts between the wood framing and the foundation. The anchorage of the cripple walls to the foundation relied entirely on the previously described retrofit plates. These will be discussed in more detail below.

The specimen cripple walls were 2 ft tall, corresponding to the distance between the bottom of the 2 × 6 foundation sill plate and the top of the double top plate (i.e., the clear height of the framed cripple wall). On top of the walls, an approximately 6-in.-tall high-load diaphragm was constructed, consisting of joists at 16 in. on center and 19/32 Structural I plywood sheathing. The diaphragm was designed to be capable of delivering the estimated peak shear capacity of the test specimen.

All framing used Number 2 or better grade Douglas-fir. Minimum fastening tables from era-specific building codes were used for framing fastening, supplemented by more recent code provisions where necessary. The studs were framing members spaced at 16 in. on center. The wall top plates were matching 2 × 4 framing members. The foundation sill plates consisted of 2 × 6 framing members, matching common construction practice as previously discussed. The studs were end-nailed to the foundation sill plate using two 16d common nails. The studs also were end-nailed to the lower top plate using two 16d common end nails. The upper top plate was face-nailed to the lower top plate using 16d common nails at 12 in. on center. At the corner laps, an extra two 16d common face nails were added.

The high-load roof diaphragm was constructed on top of the specimen walls. To accommodate multiple rows of diaphragm edge nailing, as specified for high-load diaphragms by the SDPWS standard [AWC 2015], 4 × 6 and 3 × 6 framing members were used; 4 × 6 nominal Douglas-fir lumber joists were spaced 16 in. on center. Rim joists were selected as 3 × 6 nominal Douglas-fir lumber on all four edges of the diaphragm. Six 8d common nails were used to toe-nail joists to the upper top plate (three at each end of the joist). The blocking on top of the wall top plate was toe-nailed using four 8d common nails (two each end of blocking) to joists and four 8d common nails to the top plate per block. Also, two rows of blocking were provided near the center of the 4-ft- wide diaphragm to provide a substrate for connecting the loading beam to the diaphragm: 19/32-in. Structural I plywood sheathing was used for the diaphragm, with four staggered rows of 10d common nails at 2-1/2 in. on center for each row at the diaphragm interior panel edges and boundaries. Field nailing used one row of 10d common nails spaced at 3 in. on center.

As discussed previously, the main objective of the diaphragm design was to provide enough strength and stiffness so that the diaphragm would adequately transfer loading beam displacements to the specimen walls without acting as a weak link or contributing significant deformation. Figures 4.4 and 4.5 show Specimen B-1 framing. Seen in the lower right in Figure 4.4, the diaphragm framing and sheathing extended approximately 4 in. beyond the face of the cripple wall studs to create an overhang on the exterior of the specimen. This was done to compensate for the inside-out testing configuration (siding on interior and retrofit on exterior). The overhang mimicked floor framing perpendicular to the wall that would be located immediately above the retrofit plywood in a typical retrofit installation. If the plywood were to experience slip upward with respect to the wall framing, the floor joist perpendicular to the wall would restrain this slip in a typical dwelling configuration. Similarly, if the plywood were to experience slip upward with respect to the wall framing in Specimen B-1, the cantilevered joists would serve to restrain the slip. Because retrofit sheathing slip and subsequent bearing on framing was thought to potentially impact the retrofit performance, this detail was incorporated.

Prior to installing exterior shiplap siding for Specimen B-1, building paper (Grade D - 60 Minute) acting primarily as a moisture barrier was installed and directly attached to the wall framing using a standard hammer stapler with 3/8-in.-long leg-collated staples. The building paper covered the interior surface of the north and south walls (under the horizontal wood siding). Three to 5 in. of overlap was provided between adjacent sections of building paper.

Framing and sheathing fasteners were installed with a nail gun. While this created the potential for over-driven nails and subsequent reductions in capacity, little or no overdriving was observed. Therefore, the use of a nail gun is not believed to have affected the testing results. It is noted that finished lumber dimensions have varied over time with “full dimension” (i.e., 2 in. × 4 in.) lumber having been common to the 1920s, an intermediate size (i.e., 1-5/8 in. × 3-5/8 in.) used until the 1960s, and modern sizing (i.e., 1-1/2 in. × 3-1/2 in.) used since. The changing size of framing is not believed to have affected the testing results.

Figure 4.4 (Left top) Specimen B-1 framing overview; (right top) corner; (left bottom) east-end wall; and (right bottom) diaphragm framing overhang.

Figure 4.5 (Left top) Specimen B-1 framing including diaphragm sheathing and nailing; diaphragm framing from interior; (right top) 2-in. extension of 2 × 6 foundation sill plate beyond face of wall studs and blocking; and (right bottom) 2-in. projection of foundation beyond foundation sill plate.

4.3 INSTALLATION OF SPECIMEN B-1 EXTERIOR HORIZONTAL WOOD SIDING (SHIPLAP)

Unlike Specimen C-1 (where Nusko FireBlocker primed finger joint Redwood shiplap siding was selected) it was decided to use shiplap siding available from the local lumber store. This decision reduced ordering lead time and cost and was considered appropriate due to the limited contribution of siding to strength and stiffness. The siding boards used were pine, with dimensions 1 in. × 6 in. × 8 ft. The siding boards were installed with two 8d HDG (Hot Dip Galvanized) common nails at each stud, consistent with applicable building codes. This also matches nailing used for PEER–CEA small-component testing performed at UCSD. Photographs of the shiplap installation are shown in Figure 4.6.

The installed siding length was approximately 18 ft, rather than the full 20-ft length of the specimen. This was in part because the siding was installed on the interior face of the wall, the depth of the east and west wall framing needed to be subtracted out. In addition, the end of the siding boards was held approximately 6 in. back from the corner; see Figure 4.6 (right bottom). This would allow significant racking of the cripple wall without the ends of the siding boards bearing against the east and west end walls. Because this reaction would not occur in typical siding installation (on the dwelling exterior), it was a necessary correction to the siding installation. In addition, the bottom of the siding was held up off of the top of the foundation (Figure 4.6, left bottom) to avoid bearing of the siding on the foundation and possible resulting friction.

Figure 4.6 **(Left top) shiplap exterior siding installation (on interior of specimen due to inside-out construction) overview; (right top) board installation including gaps between boards and nailing; (left bottom) gap between siding and foundation; and (right bottom) ends of siding held back from east and west-end walls.**

4.4 SPECIMEN B-1 RETROFIT

Test Specimen B-1 included a cripple wall seismic retrofit designed in accordance with the *FEMA P-1100* prescriptive design provisions for crawlspace dwellings. Similar to other aspects of the test specimens, the design of the cripple wall retrofit was determined based on a model dwelling, assuming plan dimensions of 30 × 40 ft. For purposes of the retrofit design, the model building was assumed to be one story over a cripple wall. For purposes of retrofit design, the short-period design spectral response acceleration, S_{DS}, as determined in accordance with ASCE 7 [ASCE 2010], was taken to be 1.5. This represents very high seismic hazard areas in accordance with FEMA P-1100.

The model dwelling was assumed to have a horizontal wood siding exterior wall finish, gypsum wallboard interior wall and ceiling finishes, and a composition shingle roof. Using this information, the dwelling weight classification was determined to be light in accordance with FEMA P-1100 (Figure 4.4-1); see Figure 4.7. Next, the required sheathing, retrofit plates, and shear clips were determined from *FEMA P-1100* (Figure 4.4-8), applicable for S_{DS} = 1.5 and one-story dwellings; see Figure 4.8. In this table, the row representing one-story light construction and a total area of 1200 ft^2 was used. The table calls for 10.7 ft of retrofit sheathing to be provided in each of two sections along each of the model dwelling exterior walls. For the test specimen, this was translated to 10.7 ft of sheathing each for the 20-ft length of the north and south walls (21.3 ft total specimen sheathing). This was installed in two sections of 5.4-ft-long sheathing on the north and south walls (four sections at 5.4 ft each total for the specimen). The cripple wall sheathing was of 15/32-in. rated sheathing plywood; 8d common nails were used to fasten the plywood sheathing to the framing, using an edge nail spacing of 4 in. at all panel edges and 12 in. in the field. The sheathing nailing at the top of the plywood was to the upper top plate only, rather than being staggered between the upper and lower top plates, as was done in the Specimen AL-2 retrofit. This was in accordance with revisions to the *FEMA P-1100* details, which were made in response to the test result of Specimen AL-2.

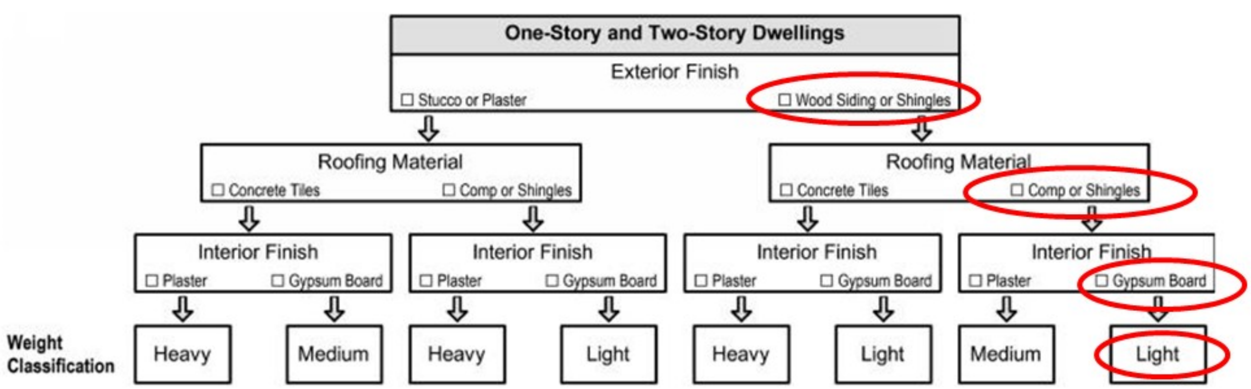

Figure 4.7 Dwelling weight classification from *FEMA P-1100*.

EARTHQUAKE RETROFIT SCHEDULE (S_{DS}= 1.5 Very High Seismic) ONE-STORY

Weight Category	Total Area in Square Feet	☒ Mark row that applies	Length Each of Two Braced Wall Sections Required Along Each Perimeter Wall Line — Wood Structural Panels — Cripple Wall Height									Number of Foundation Connectors or Anchors at Each Perimeter Wall Line Assume Distributed Along Length — Foundation Sill Anchors					Floor to Cripple Wall or Floor to Foundation Sill		
			up to 1'	1'-1" to 2'	2'-1" to 4'-0"		4'-1" to 6'-0"		6'-1" to 7'-0"										
			Without Tie-downs	Without Tie-downs	Without Tie-downs	With Tie-downs	Without Tie-downs	With Tie-downs	Without Tie-downs	With Tie-downs	Panel Edge Nailing	Type "A"	Type "B"	Type "C"	1/2"ø Bolt	5/8"ø Bolt	Type "D"	Type "E" or "F"	Type "G"
1-Story Light Construction	up to 800		8.0'	8.0'	10.7'	8.0'	12.0'	8.0'	13.3'	9.3'	4"	6	10	10	10	7	16	15	20
	801 to 1000		9.3'	9.3'	12.0'	9.3'	13.3'	9.3'	14.7'	10.7'	4"	7	11	12	12	9	19	18	24
	1001 to 1200		10.7'	10.7'	13.3'	10.7'	16.0'	10.7'	16.0'	12.0'	4"	8	13	14	14	10	22	21	28
	1201 to 1500		12.0'	12.0'	14.7'	12.0'	17.3'	12.0'	18.7'	13.3'	4"	10	16	17	17	12	26	25	33
	1501 to 2000		14.7'	14.7'	17.3'	14.7'	21.3'	16.0'	22.7'	16.0'	4"	13	20	22	22	15	34	32	43
	2001 to 2500		18.7'	18.7'	20.0'	18.7'	24.0'	18.7'	25.3'	18.7'	4"	15	24	27	27	18	41	39	52
	2501 to 3000		21.3'	21.3'	22.7'	21.3'	26.7'	21.3'	28.0'	21.3'	4"	18	28	31	31	21	48	46	60
1-Story Medium Construction	up to 800		6.7'	8.0'	10.7'	6.7'	13.3'	9.3'	13.3'	9.3'	3"	7	11	12	12	9	19	18	24
	801 to 1000		8.0'	9.3'	12.0'	8.0'	14.7'	10.7'	16.0'	10.7'	3"	9	13	15	15	10	22	21	28
	1001 to 1200		9.3'	10.7'	13.3'	9.3'	16.0'	12.0'	17.3'	12.0'	3"	10	15	17	17	11	26	25	32
	1201 to 1500		10.7'	12.0'	14.7'	10.7'	17.3'	13.3'	18.7'	14.7'	3"	12	18	20	20	14	30	29	38
	1501 to 2000		13.3'	13.3'	17.3'	13.3'	21.3'	16.0'	22.7'	17.3'	3"	14	23	25	25	17	38	36	48
	2001 to 2500		16.0'	16.0'	20.0'	16.0'	22.7'	17.3'	25.3'	20.0'	3"	17	27	29	29	20	45	43	57
	2501 to 3000		18.7'	18.7'	21.3'	18.7'	25.3'	20.0'	26.7'	21.3'	3"	20	31	34	34	23	53	50	67
1-Story Heavy Construction	up to 800		8.0'	9.3'	12.0'	8.0'	13.3	10.7'	14.7'	10.7'	2"	8	13	14	14	10	22	21	27
	801 to 1000		8.0'	10.7'	13.3'	9.3'	16.0'	12.0'	17.3'	12.0'	2"	10	15	17	17	11	26	25	33
	1001 to 1200		9.3'	12.0'	14.7'	10.7'	17.3'	13.3'	18.7'	13.3'	2"	11	18	19	19	13	30	28	37
	1201 to 1500		10.7'	13.3	16.0'	12.0'	18.7'	14.7'	20.0'	16.0'	2"	13	21	23	23	16	35	34	45
	1501 to 2000		13.3	16.0'	18.7'	14.7'	22.7'	17.3'	24.0'	18.7'	2"	17	26	29	29	20	44	43	56
	2001 to 2500		14.7'	17.3'	21.3'	16.0'	25.3'	20.0'	26.7'	21.3'	2"	20	32	35	34	24	53	51	67
	2501 to 3000		17.3'	20.0'	24.0'	18.7'	28.0'	22.7'	29.3'	24.0'	2"	23	37	40	40	27	62	59	79

Figure 4.8 Retrofit schedule per *FEMA P-1100*.

As shown in Figures 4.8 and 4.9, per the recommendations in *FEMA P-1100* (Figures 4.4-5 and 4.4-8), 22 Type D shear clips were required over the 40-ft length of the model dwelling, with eleven shear clips over the length of each 20-ft wall. Simpson A-35 clips were used. The primary purpose of these clips is to provide a load path from the superstructure (high-load diaphragm and loading beam for Specimen B-1) to the top of the retrofitted shear wall. Proper design of these shear clips is key to achieving the intended benefit of the retrofit.

As shown in Figures 4.8 and 4.10, per *FEMA P-1100* (Figure 4.4-2 and 4.4-8), Type A retrofit plates were selected for the foundation sill plate connection to the foundation over the 40-ft length of the model dwelling, suggesting four retrofit plates over the length of each 20-ft wall. Simpson URFP retrofit plates were used. In addition to the four retrofit plates (each on the north and south walls), two retrofit plates each were provided on the east and west walls, for a total of twelve retrofit plates. The primary purpose of these retrofit plates is to provide a load path from the bottom of the retrofitted wall to the foundation. Proper design of these retrofit plates is key to achieving the intended benefit of the retrofit.

Key detailing for the specimen was taken from *FEMA P-1100* (Figure 4.4-12) and includes installation of blocks on top of the foundation sill plate between studs; see Figure 4.11. This provides framing for the plywood edge nailing to be installed along the bottom edge of the plywood panel. A single piece of 2 × 4 Douglas-fir blocking was used in each stud bay. Four 10d common nails were used to face-nail each piece of blocking to the foundation sill plate. The face nails were staggered with 1-1/2 in. minimum spacing. Note: the 2 × 4 blocking was extended for the full 20-ft length of the north and south walls instead of just being installed where plywood retrofit sheathing occurred. Also used from *FEMA P-1100* (see Figure 4.4-12) were details for the connection of the foundation sill plate to the foundation; see Figure 4.12. Photographs of retrofit installation are shown in Figures 4.13 and 4.14.

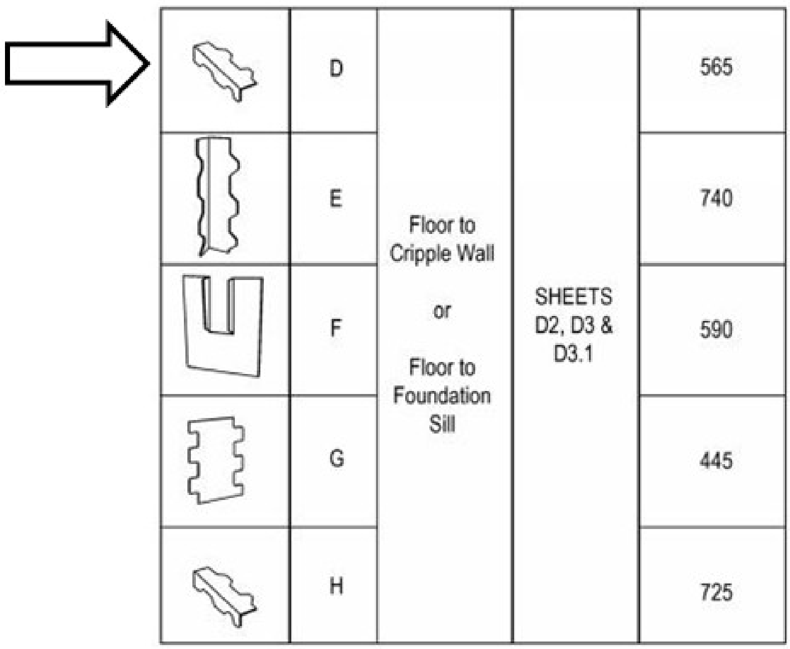

Figure 4.4-5 Floor to cripple wall or foundation sill connectors. Sheet S3.

Figure 4.9 Floor to cripple wall sill connector selection per the recommendations of *FEMA P-1100*.

CONNECTORS				
IMAGE	TYPE		SHEET REF	MIN CAPACITY (lbs) ASD
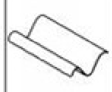	A	Foundation Sill to Foundation	SHEETS D1 & D2	1530
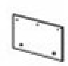	B			960
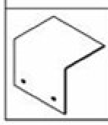	C			875

Figure 4.4-2 Foundation sill anchors. Sheet S3.

Figure 4.10 Retrofit connector types for connection between the foundation sill plate and foundation per *FEMA P-1100*.

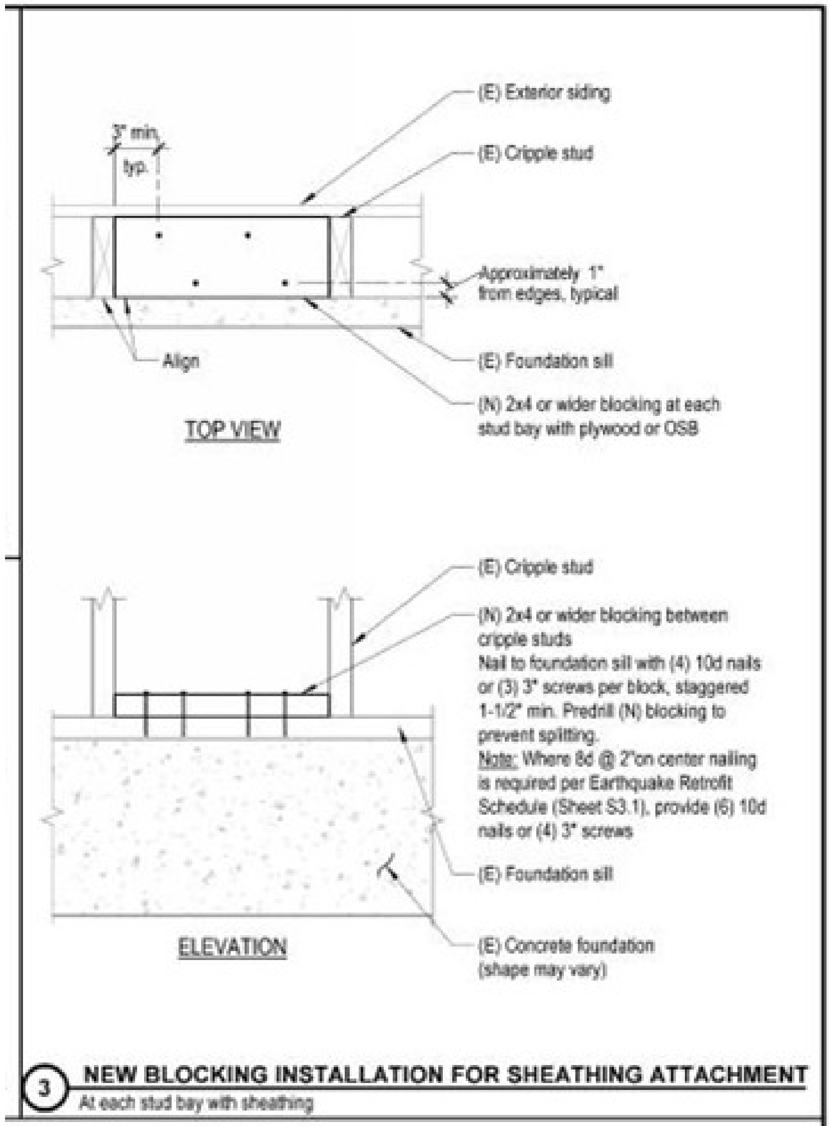

Figure 4.11 New blocks on top of the foundation sill plate, between studs per *FEMA P-1100*.

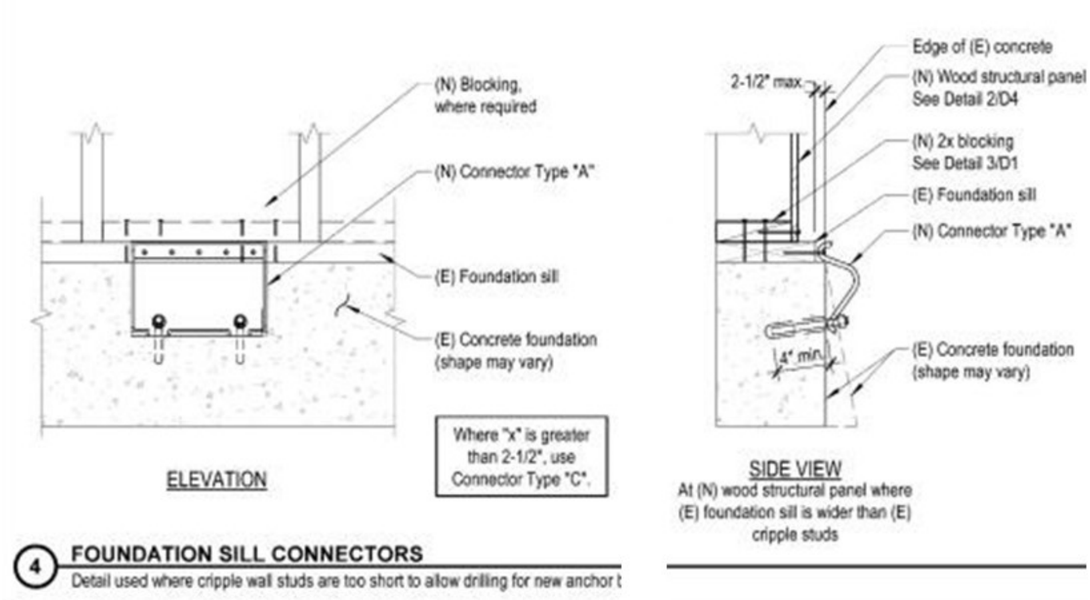

Figure 4.12 Installation of retrofit plates providing load path connection from the foundaiton sill plate to the foundation per *FEMA P-1100*.

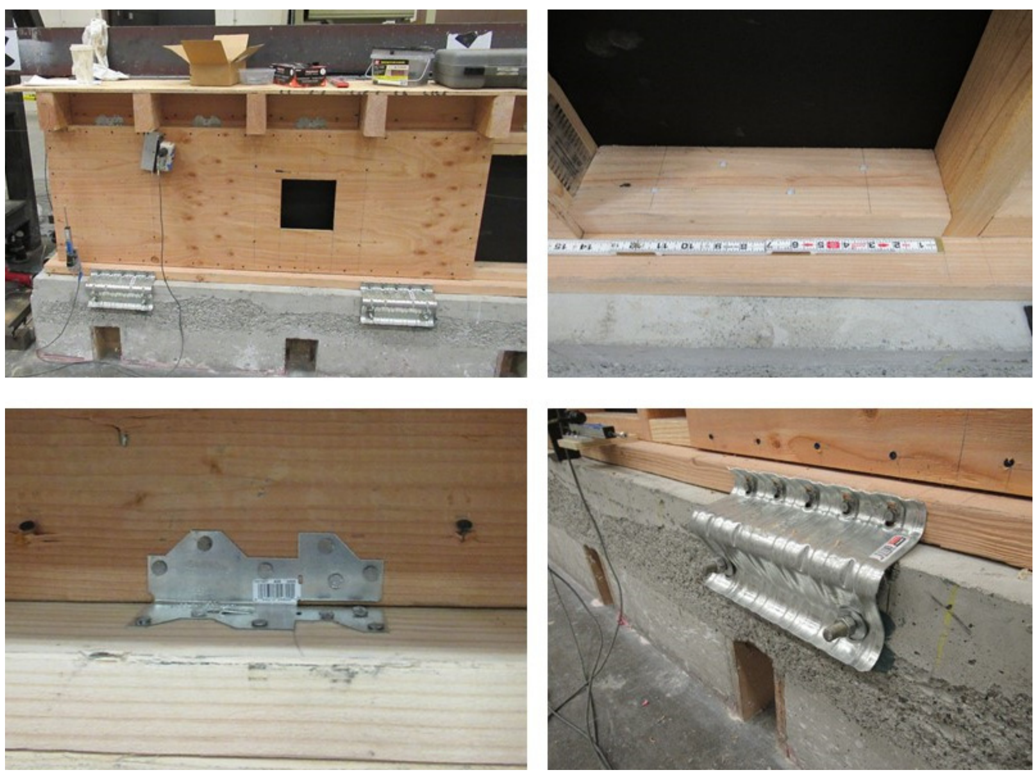

Figure 4.13 (Left top) retrofit details for B-1, overview of retrofit at south–west corner; (right top) blocking installed on top of foundation sill plate with face nails; (left bottom) A35 shear clip connecting dipahragm rim joist to upper top plate;; and (right bottom) URFP retrofit plate connecting foundation sill plate to foundation.

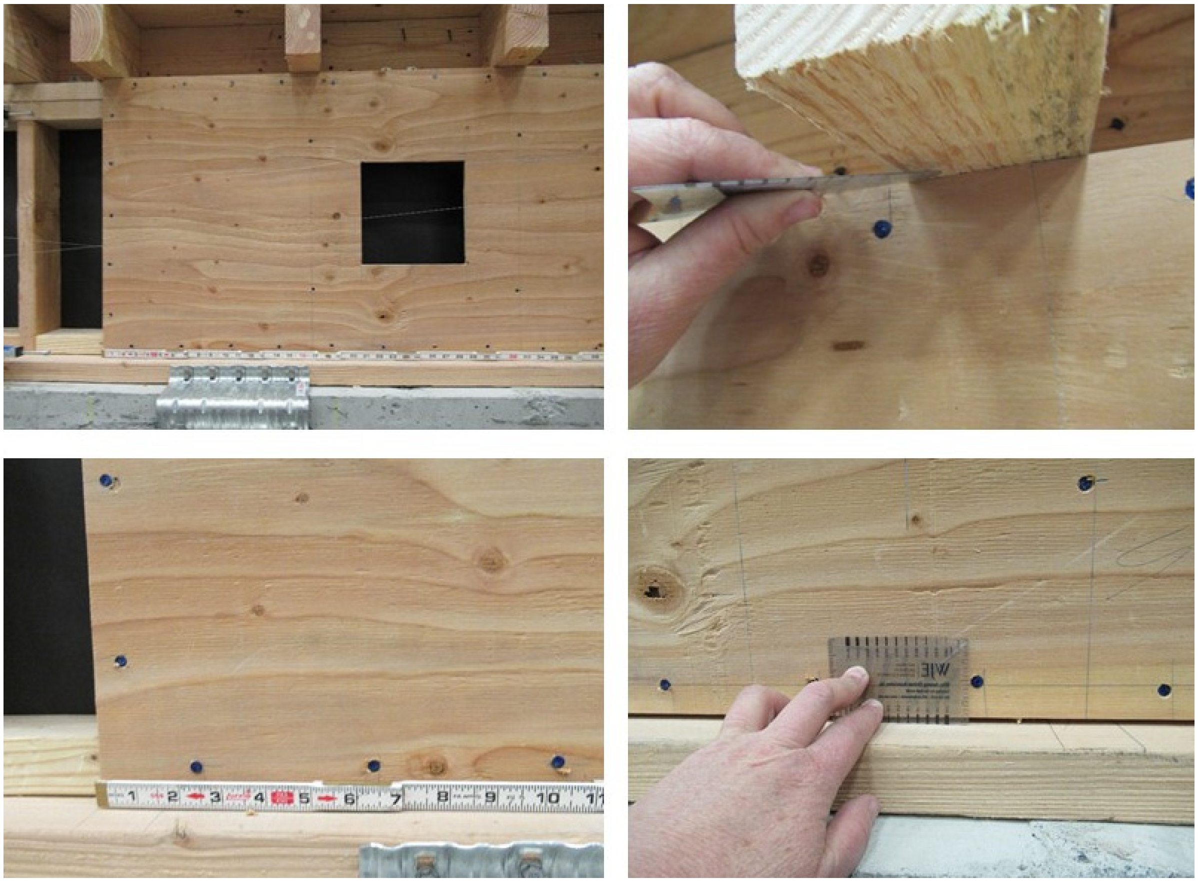

Figure 4.14 (Left top): Retrofit details for Specimen B-1 overall view of sheathing nailing; (left bottom) close up of sheathing nailing; (right top) lack of gap between top of plywood retrofit sheathing and cantilevered diaphragm framing above, and (right bottom) approx. 1/8-in. gap between bottom of plywood retrofit sheathing and foundation sill plate.

4.5 LOADING PROTOCOL

The quasi-static lateral displacement history, as described in Chapter 2, was followed in this testing program. The specimens were first subjected to seven initiation cycles and then subsequent increments that consisted of four, three, and then two cycles as described in Table 4.1. In the Specimen B-1 test, parameter h, was taken as the 24-in. clear height of the walls. A constant loading rate of 0.2 mm/sec (0.0787 in/sec) was used.

For testing Specimen B-1, testing started with pushing to the west to reach the first peak and then the loading was reversed to reach the first pulling peak to the east. These cycles were repeated to the number of cycles designated for each cycle level. Once the peak load occurred, the subsequent drift levels were monitored to see when there was a 40% drop in peak load. This occurred at an 11% drift ratio. After this, each drift cycle was increased by 2% instead of 1%. The cyclic loading continued till the drift level of 15% was achieved (3.6 in. of actuator stroke). After this drift level, the monotonic push was performed to a displacement of 8 in., corresponding to a 33% drift ratio.

Table 4.1 General loading protocol adjusted for Specimen B-1 geometry.

Cycle level	Drift %*	Amplitude (in.)	No. Cycles	Loadin rate (in./sec)	Total time (sec) per cycle level	Inspection type*
1	0.2	0.048	7	0.0787	17	Normal inspection
2	0.4	0.096	4	0.0787	19	Normal inspection
3	0.6	0.144	4	0.0787	29	Normal inspection
4	0.8	0.192	3	0.0787	29	Normal inspection
5	1.4	0.336	3	0.0787	51	Normal inspection
6	2	0.48	3	0.0787	73	Normal inspection
7	3	0.72	2	0.0787	73	Normal inspection
8	4	0.96	2	0.0787	97	Normal inspection
9	5	1.20	2	0.0787	121	Normal inspection
10	6	1.44	2	0.0787	146	Normal inspection
11	7	1.68	2	0.0787	170	Normal inspection
12	8	1.92	2	0.0787	195	Normal inspection
13	9	2.16	2	0.0787	219	Normal inspection
14	10	2.40	2	0.0787	243	Normal inspection
15	11	2.64	2	0.0787	268	Normal inspection
16	13	3.12	2	0.0787	317	Reduced inspection
17	15	3.60	2	0.0787		Reduced inspection
18	Monotonic push	8	1	Manually	N.A.	End inspection

* Normal Inspection: Test was paused to make detailed observations following the first push, first pull, zero displacement at the end of each cycle; Reduced Inspection: First push, zero displacement at the end of each cycle.

4.6 INSTRUMENTATION

Specimen B-1 was extensively instrumented, with instrumentation similar to that used for Specimens AL-1 and AL-2. These instruments recorded the applied lateral loads, global and local displacements, and boundary displacements (loading beam to test specimen and test specimen to foundation).

The overall response of the specimen was characterized using the lateral force measured by the embedded load cell in the actuator, and the lateral displacement measured by a transducer that was referenced to the loading beam. Over the specimen height, several string pots were connected from a stationary frame to the test specimen at different heights to capture absolute displacement of the building at each height. Local deformations of the walls were instrumented with diagonal pairs of string pots. The string pots were mounted on the framing members to measure the overall distortion of the cripple wall framing over the length of the building and the distortion in the middle of the wall length. Several transducers were used to monitor the potential slip and uplift between the specimen and loading beam and between the specimen and foundation.

Even though the slip between the foundation and the strong floor was not expected, the potential slip was monitored using one LVDT at one end of the foundation. In addition, a string pot was connected to the upper corner of the building to monitor potential out-of-plane divergence of the building. Because the loading beam was not restrained to withstand rotation in vertical plane, rotation of the horizontal loading beam was monitored using two LVDTs mounted in the loading beam end closer to the loading actuator and the other end to monitor rotation.

Figure 4.15 illustrates the instrumentation on the south wall of Specimen B-1. Additional details of the instrumentation can be found included with the specimen design drawings in Appendix B.

Several video and still cameras were used both outside and within the specimens to track response. Some of the cameras recorded photos through the entire duration of the test, while others were stopped during the test for various reasons. Hand-held cameras were used to obtain photographs of the specimen through the course of the test and provide a detailed record of the behavior of specimens; see Section 2.3 for further details.

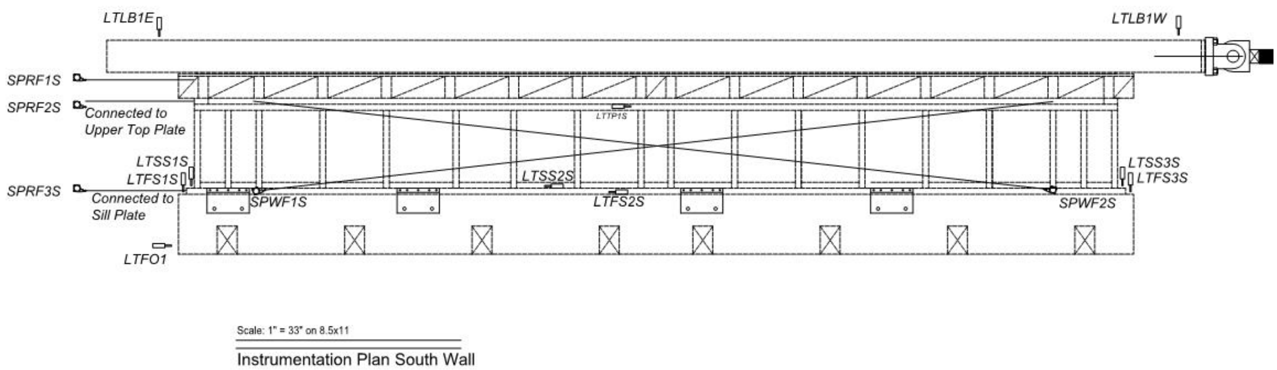

Figure 4.15 Instrumentation layout for south wall of specimen B-1.

4.7 GRAVITY LOADING

The configurations for the test specimens were determined based on a model dwelling, assuming plan dimensions of 30 × 40 ft, which was used to determine the supplemental gravity load to be applied during component testing. Consistent with the retrofit design described in Section 4.4, a one-story model dwelling was used to determine the gravity load. The model dwelling had a horizontal wood siding exterior wall finish, gypsum wallboard interior, wall, and ceiling finishes, and a composition shingle roof. The roof, floor, exterior wall, and interior wall unit weights were assigned as 13, 12, 7, and 7 psf, respectively. Using these weights, a superstructure weight of 44 kips was calculated, corresponding to an average weight of 36 pounds psf of floor area. Both the unit weights and average weight were checked against data from the *FEMA P-1100* project and found to correlate well. Of the 44 kips total superstructure weight, eleven kips was assigned to the test specimen based on the 20-ft length being half of the 40-ft dwelling length, and the assumption that 50% of the weight would be supported on interior walls, and the other 50% on the two exterior walls represented by the specimen. The summed self-weight of the test specimen and loading beam were determined to be approximately one kip. The remaining ten kips was added using lead blocks placed on top of the floor diaphragm.

Note: the weight of 10 kips divided by the 40-ft length of the two cripple walls corresponds to 250 lbs. This is consistent with the light unit vertical load applied in most of the UCSD small-component tests, providing reasonably uniform weight between small and large-component testing programs.

4.8 SPECIMEN B-1 TEST RESULTS

A large volume of data was collected over the course of the test, including visual observations, photo documentation of the interior and exterior at points designated in the loading protocol, and the continuous recording instrumentation via different devices. Key test results for Specimen B-1 are described in this section.

The lateral force versus lateral displacement of Specimen B-1 was recorded over the course of testing using instrumentation in the actuator to measure load and displacement. The overall load-displacement response obtained from the actuator instrumentation is shown in Figure 4.16, with the final monotonic push included. Figure 4.17 is concerned with the cyclic portion of the test, and the data for the cyclic portion of the loading is summarized in Table 4.2. The actual drift achieved, as shown in Table 4.2, varied slightly from the targeted drifts shown in Table 4.1 due to the practical limitations of actuator control. The peak unit loads listed in Table 4.2 are the peak loads divided by a total length of retrofit sheathing of 21.33 ft (10.67 ft each on the north and south walls).

The Specimen B-1 peak shear capacity (33,200 lbs) was seen to occur in the first push direction displacement to approximately 7% drift (shown in the negative quadrant, which was also the direction first loaded). This was larger than the peak shear capacity in the prior pull direction to approximately 6% drift (30,790 lbs). Based on the total length of plywood retrofit sheathing of 21.33 ft, this resulted in peak unit shears of 1560 and 1440 lbs plf for an average of 1500 plf.

The difference in peak shear capacity between the push direction loading and the pull direction is believed to be mainly due to damaged inflicted in the push direction, thus affecting the subsequent lateral strength. Figure 4.18 shows the envelope curves from the positive and negative quadrants superimposed. There is an approximately 8% drop in peak shear capacity from the negative quadrant push direction to the positive quadrant pull direction. This difference is seen to start at about 0.8% drift and remain over most of the drift range. Eight percent is a moderate difference compared to other similar tests, and the character of the envelope curves is similar across the full displacement range.

Following the cycles at peak shear capacity, about three more displacement increments followed with modest reductions in peak shear capacity with each cycle. Once displacement cycles went above 2 in. (8% drift), a more significant drop in peak load occurred, with peak cycle loads between 40 and 60% of peak shear capacity. Following the drop, peak loads largely leveled out, but with residual capacities between 40 and 50% of peak shear capacity still being retained at 16% drift.

Specimen B-1 was tested to higher drift levels than attempted in previous test programs. Providing data in this displacement range is important for the development of numerical models for documenting structural behavior up to and including collapse.

Load deflection information from the final monotonic push is summarized in Table 4.3. This data shows a modest retention of post-peak capacities to very high drift ratios without collapse. Note: collapse did not occur during the final monotonic push, which extended out to the practical displacement limits of the test setup.

As previously noted, the recorded drifts for Specimen B-1 (Table 4.2) differ somewhat from the drifts targeted by the loading protocol due to the practical limits of actuator control. To establish an averaged envelope and to allow direct comparison between specimens, Specimen B-1 loads at the targeted drift levels have been interpolated from the envelope curves and are summarized in Table 4.4.

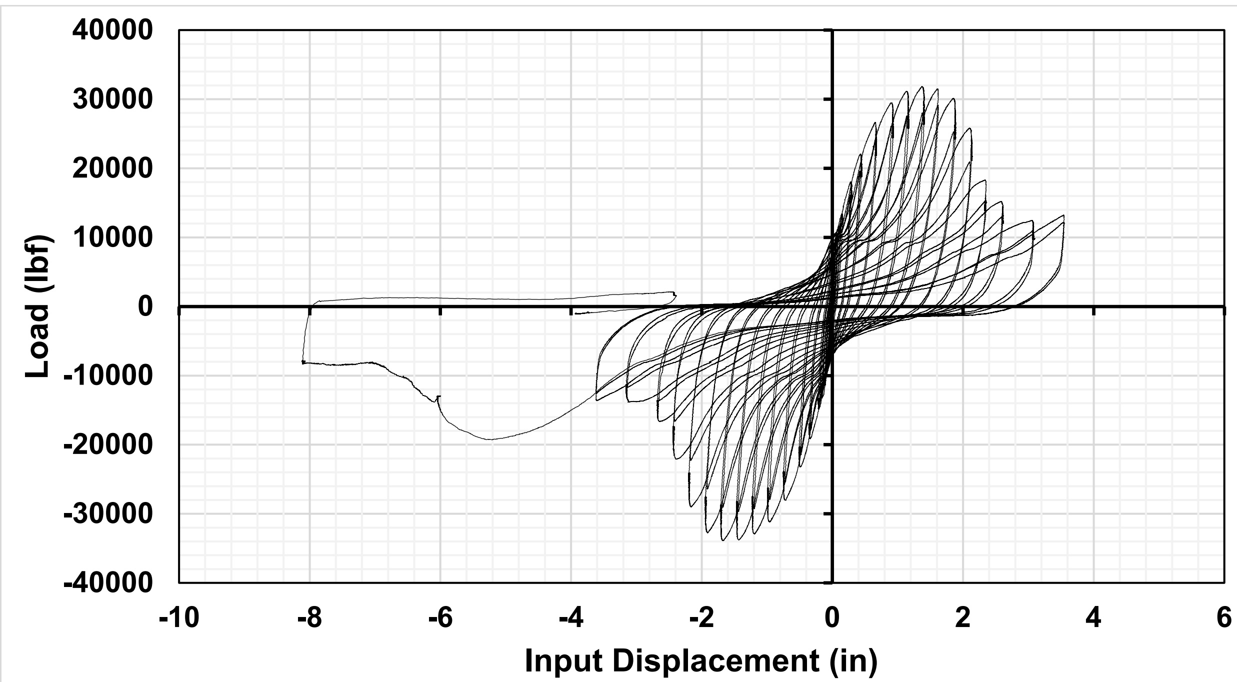

Figure 4.16 **Lateral load versus lateral actuator input displacement of Specimen B-1 with final monotonic push.**

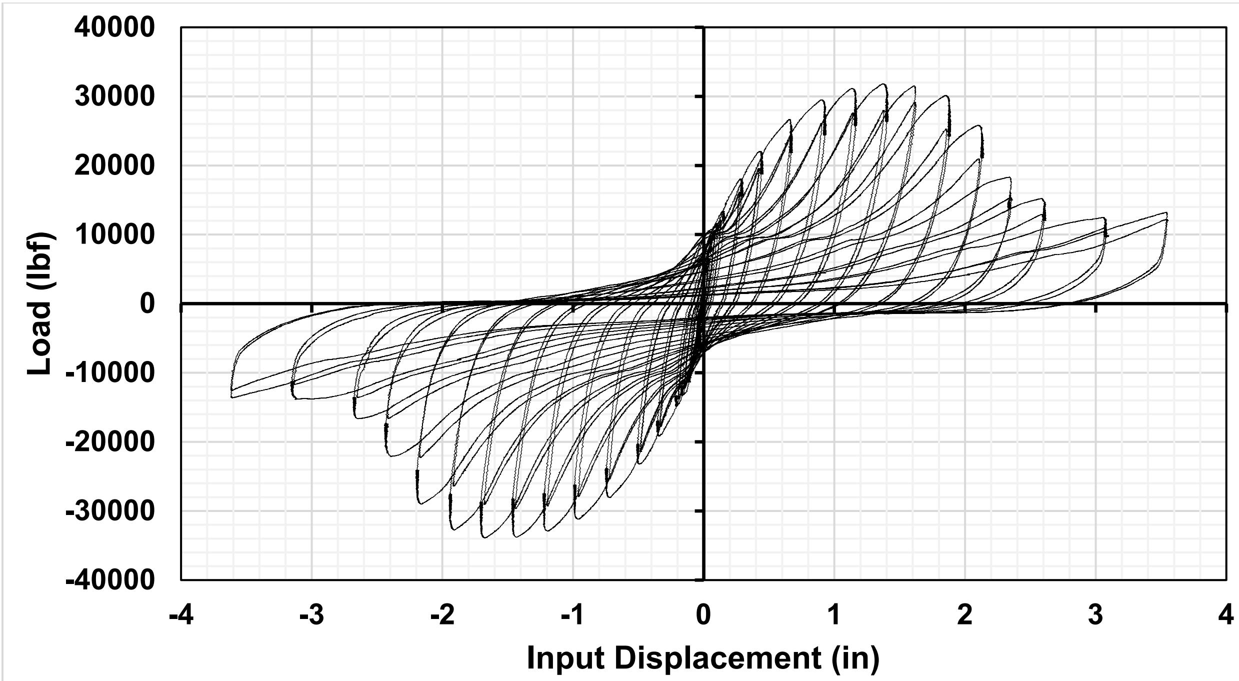

Figure 4.17 Lateral load versus lateral actuator input displacement of Specimen B-1 without monotonic push.

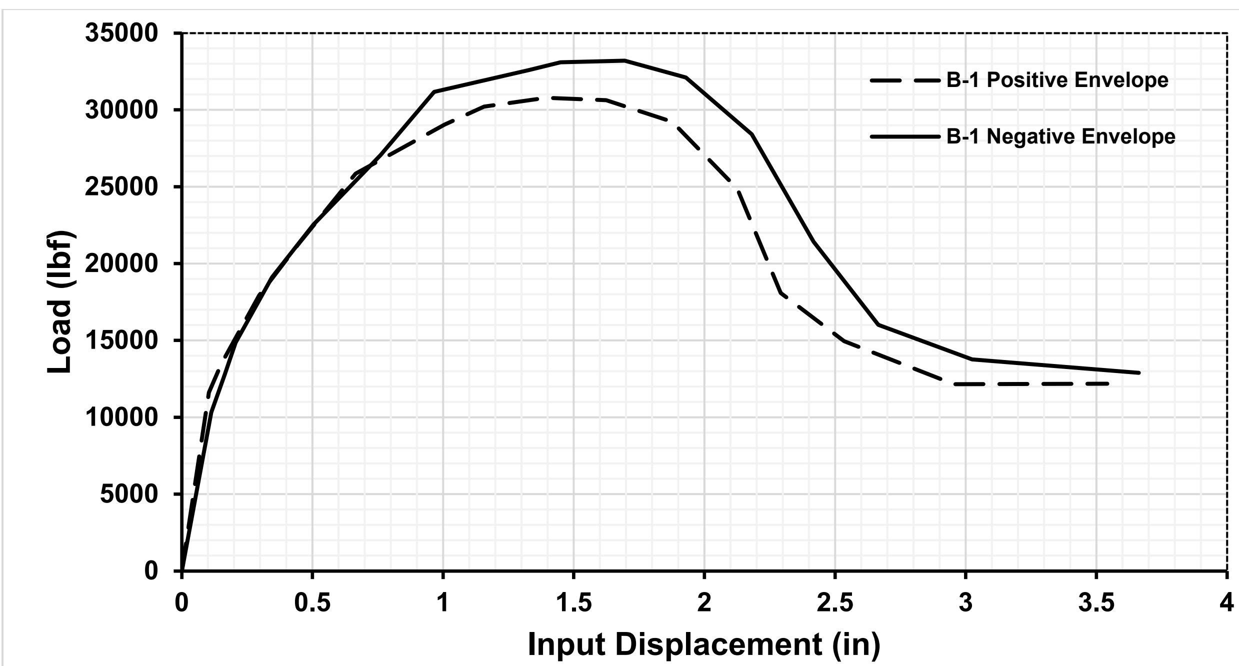

Figure 4.18 Specimen B-1 envelope curves for positive and negative quadrants superimposed.

Table 4.2 Summary of test data for Specimen B-1.

Loading direction	Displacement (in.)	Drift ratio (%)	Peak load (lbs)	Peak unit load (plf)	Cycle peak/ overall peak (%)
First loading direction: push to west (negative quadrant)	0.1131	0.47	10,820	484	31
	0.1648	0.69	12,780	599	38
	0.2060	0.86	14,860	697	45
	0.3460	1.44	19,120	896	58
	0.5037	2.10	22,530	1,056	68
	0.7608	3.17	27,060	1,269	81
	0.9662	4.03	31,170	1,461	94
	1.3304	5.54	32,600	1,528	98
	1.4496	6.04	33,100	1,552	100
	1.6952	7.06	33,210	1,557	100
	1.9292	8.04	32,110	1,505	97
	2.1814	9.09	28,410	1,332	86
	2.4176	10.1	21,430	1,005	65
	2.6653	11.1	16,010	751	48
	3.0240	12.6	13,770	646	41
	3.6618	15.3	12,890	604	39
Second loading direction: pull to east (positive quadrant)	0.1038	0.43	11,610	544	38
	0.1516	0.63	13,480	632	44
	0.2960	1.23	17,930	841	58
	0.4460	1.86	21,260	997	69
	0.6652	2.77	25,850	1,212	84
	1.0052	4.19	29,040	1,361	94
	1.1568	4.82	30,210	1,461	98
	1.3947	5.81	30,790	1,444	100
	1.6243	6.77	30,630	1,436	99
	1.8770	7.82	29,220	1,370	95
	2,1264	8.86	24,860	1,165	81
	2.2918	9.55	18,090	848	59
	2.5346	10.6	14,950	701	49
	2.9543	12.3	12,150	570	39
	3.5415	14.8	12,180	571	40

Table 4.3 Summary of test data for Specimen B-1 monotonic push.

Drift	Drift ratio (%)	Loading direction	Peak load (lbs)	Peak unit load (plf)	Cycle peak/ overall peak (%)
4 in.	17	Push	15,400	722	46
5 in.	21	Push	19,100	895	58
6 in.	25	Push	14,540	682	44
7 in.	29	Push	8,190	384	25
8 in.	33	Push	7,900	370	24

Table 4.4 Summary of load/displacement data for Specimen B-1 interpolated from the envelope curve.

Interpolated drift	Loading direction	Interpolated load (lbs)	Interpolated unit load (plf)	Interpolated load/ interpolated peak (%)
0.6% (0.144 in.)	Push	11,790	553	36
	Pull	13,180	618	43
	Average	12,480	585	39
0.8% (0.192 in.)	Push	14,150	663	43
	Pull	14,730	691	48
	Average	14,440	677	45
1.4% (0.336 in.)	Push	18,820	882	57
	Pull	18,820	882	61
	Average	18,820	882	59
2% (0.48 in.)	Push	22,020	1,032	66
	Pull	21,970	1,030	71
	Average	22,000	1,031	69
3% (0.72 in.)	Push	26,340	1,234	79
	Pull	26,360	1,236	86
	Average	26,350	1,235	83
4% (0.96 in.)	Push	31,050	1,456	93
	Pull	28,260	1,325	92
	Average	29,660	1,390	93
5% (1.20 in.)	Push	32,090	1,504	97
	Pull	30,320	1,421	99
	Average	31,210	1,468	98
6% (1.44 in.)	Push	33,060	1,550	100
	Pull	30,760	1,442	100
	Average	31,910	1,496	100
7 (1.68 in.)	Push	33,200	1,556	100
	Pull	30,320	1,421	99
	Average	31,760	1,489	99
8 (1.92 in.)	Push	32,150	1,507	97
	Pull	28,470	1,335	93
	Average	30,310	1,421	95
9 (2.16 in.)	Push	28,720	1,346	87
	Pull	23,490	1,101	76
	Average	26,110	1,224	82
10 (2.40 in.)	Push	21,950	1,029	66
	Pull	16,690	782	54
	Average	19,320	906	61
11 (2.64 in.)	Push	16,560	776	50
	Pull	14,250	668	46
	Average	14,410	676	45
13 (3.12 in.)	Push	10,980	515	33
	Pull	12,160	570	40
	Average	11,570	522	36

Documentation of the specimen condition during testing included visual observations and photographs. These observations occurred at the designated hold points in the loading protocol described previously. To aid in the tracking and photographing of damage, when practical, the damage was marked on the specimen during testing using colored pens. Different colors were used as follows: the damage occurring in the first push (towards the west) to each drift ratio was marked with a black marker. Red and blue markers were used for the first pull (to the east) peak and back to zero displacement, respectively.

The following provides highlights of test observations. Detailed documentation of observations at each drift level are provided in Appendix C.

The building was thoroughly inspected before the start of testing. No cracking or other signs of damage was observed. The lack of observable damage or other conditions to report continued up through cycling to 0.8% drift. Starting at 0.8 drift, horizontal slip at a number of locations became visible. Three locations were monitored on the south wall using visual indicators of slip (see Figure 4.19):

- Between the top of the retrofit plywood sheathing and the cripple wall top plate,
- Between the bottom of the retrofit plywood sheathing and the foundation sill plate, and
- Between the foundation sill plate and the foundation.

Slip on the order of 1/16 in. was noted at 1.4% drift at both the bottom of the plywood to foundation sill plate and foundation sill plate to foundation. The slip at all three locations increased during testing, with a slip of approximately 1/8 in. at all three locations at a 3% drift ratio, 3/8 in. at all three locations at a 6% drift ratio, and 5/8 in. top and bottom of plywood and 1/4 in. at the foundation at a 7% drift ratio. At this point, because the slip between the plywood and framing increased dramatically due to deterioration of the sheathing nailing, it was found to be no longer practical to track the slip using this method.

The slip at the south wall between the foundation sill plate and the retrofit plate connector was similarly monitored with visual indicators through the course of the testing. No measurable slip at this interface was noted.

Uplift at the base of the cripple walls also occurred over a wide range of drift levels. Starting at 3% drift, the foundation sill plates at the west end of the north and south walls were seen to uplift on the order of 1/4 in. at the west end, with the gap reducing to near zero about 1 ft to the east. While the foundation sill plate on the north and south walls uplifted, the west end wall foundation sill plate did not. At 4% drift, similar uplift was seen at the east end wall, with some uplift occurring between the foundation and the foundation sill plate, and some rocking occurred at the base of the studs. Uplift was seen to increase moderately at the west end of the Specimen B-1 during testing (see Figure 4.20), with the maximum gap reaching about 3/4 in. At the west end, this uplift did not affect the strength of the specimen, and conditions characteristic of damage were not observed. At the east end, splitting of the east-end wall foundation sill plate was seen at 8% drift due to uplift and stud rocking; see Figure 4.21. By 10% drift, the sill had split into two pieces; see Figure 4.22. This condition might have had a significant impact on capacity if bi-directional loading were to occur.

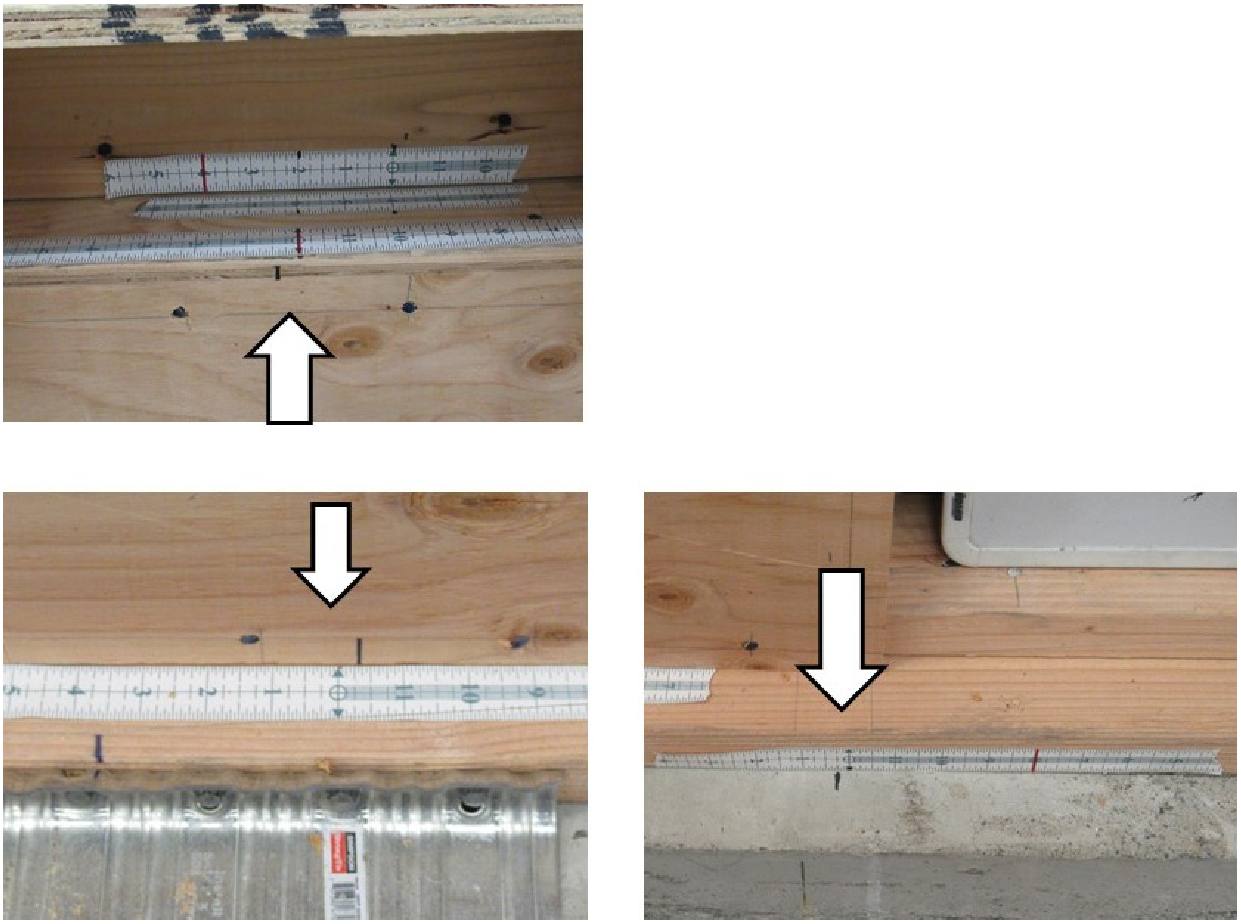

Figure 4.19 **Horizontal slip measured during testing to a drift ratio of 6%: (left top) top of retrofit plywood to cripple wall top plate, (left bottom) bottom of retrofit plywood to foundation sill plate, (right bottom) and foundation sill plate to foundation.**

Working of the plywood sheathing nailing was first noted at a drift ratio of 6% (1.5 in.) but included only modest slip of the sheathing and working of the nail heads; see Figure 4.23. This drift ratio corresponded to the peak shear capacity of the specimen. This behavior progressed at higher drifts with further working and withdrawal of the nails, accompanied by ever increasing gaps developing between the sheathing and the wall framing. At each load cycle, the sheathing kept walking further away from the framing. For each panel, this walking away occurred either at the top or the bottom of the panel, with more significant nail withdrawal at the walking edge and limited nail withdrawal at the other edge. At 9% drift, just prior to the dramatic drop in capacity, the working of the nails and gaps formed can be seen to be quite dramatic; see Figure 4.24. At a drift ratio of 10% and up, portions of the sheathing nails were observed to be completely withdrawn from the wall framing, and either stayed in place due to penetration in the plywood or fell off; see Figure 4.25. Residual capacity at this point is provided by limited sheathing nailing still intact at the plywood panel perimeter and the horizontal wood siding.

Through the course of the testing, the wood siding was observed to remain in generally good condition without damage indicating safety concerns. Slight pull through of the siding nail heads, slight withdrawal of the nail heads, and limited hairline cracks from nail heads and moving along the length of the siding boards were noticed and documented.

Through the course of the testing, there was no visible deterioration or damage to the load path connections (shear clips and retrofit plates). There was also little or no indication of deformation or slip in the connectors or their fasteners. The connectors were demonstrated to be fully capable of supporting the strength and deformation demands of the retrofitted shear wall.

During testing the primary audible indicator of damage was the loud creaking or screeching noise as the sheathing nails withdrew from the framing. This noise began right after the peak shear capacity was reached. Some loud pops also occurred during the testing but were far less pervasive than the nail withdrawal screeching.

Figure 4.20 Foundation sill plate uplift at a 3% drift ratio. South-wall foundation sill plate (right) has a noticeable uplift. West wall foundation will plate (left) had a much smaller uplift, but studs were pulled up off of the foundation sill plate.

Figure 4.21 Fracture of east-wall foundation sill plate and rocking of studs at an 8% drift ratio.

Figure 4.22 East-end wall foundation sill plate fully split at a 10% drift ratio

Figure 4.23 **Modest slip of the plywood retrofit sheathing and sheathing nails at a 6% drift ratio.**

Figure 4.24 **Significant working of sheathing nails and gapping between plywood retrofit sheathing and cripple wall framing at a 9% drift.**

Figure 4.25 Sheathing nails substantially withdraw at a drift ratio of 10%.

4.9 POST-TEST FINISH REMOVAL

Following completion of Specimen B-1 testing, selected portions of the finish materials were removed to allow observation of the underlying materials and any hidden damage. Details of these observations are provided in Appendix D.

4.10 DISCUSSION OF RESULTS

A primary purpose of the Specimen B-1 testing was to determine whether load path connectors selected in accordance with *FEMA P-1100*'s prescriptive retrofit provisions would be capable of supporting the peak shear capacity and deformation requirements of the retrofitted cripple wall. The load path connectors included shear clips connecting the diaphragm rim joist to the top plates of the shear wall, and retrofit plates connecting the cripple wall foundation sill plate to the foundation; see Figures 4.12 and 4.13). The load path connections were observed to more than adequately develop the capacity of the retrofit cripple wall. There was no observed damage and virtually no observed deformation during testing. Similarly, there was no observed damage to the blocking installed on top of the foundation sill plate between studs.

The retrofit plywood was observed to have good strength and very high ductility and displacement capacity. The capacity of the retrofit plywood sheathing and nailing appeared to be the most significant determiner of the capacity of the cripple wall. The damage to the retrofit sheathing occurred in the common modes of sheathing slip and sheathing nail withdrawal. No edge tear out of the sheathing nails was observed; this might be attributed to installing the sheathing nails in the center of the studs, top plates, and bottom of wall blocking, such that an edge distance of 3/4 in. was generally achieved. As plywood panel nail withdrawal progressed, each of the panels experience high withdrawal at either the top or bottom edge, but not both. At the end of the testing, the panels tended to have some fastening at either the top or the bottom of the panel but were completely detached otherwise. At higher drifts, significant gapping occurred between the plywood sheathing and the cripple wall framing in response to nail withdrawal; the vertical bounding of the plywood retrofit sheathing by the floor framing above and the foundation sill plate below appeared to have contributed to the "walking" of the plywood by giving the plywood surfaces to bear on and wedge against.

Of significant is that Specimen B-1 reached peak shear capacity at a drift ratio of approximately 6% and retained 25% of peak shear capacity at a drift ratio of 33%. This is similar to behavior seen in Test Specimens AL-1 and AL-2, altering previous expectations of deformation capacity and post-peak residual strength.

Table 4.5 compares Specimen B-1's peak unit shear capacity of approximately 1500 plf (averaged from Table 4.3 peak values) and displacement at peak shear capacity with previous wood structural panel cripple wall testing [Chai et al., 2002] and prior wood structural panel shear wall testing for full story height walls [Bahmani and van de Lindt 2016; Gatto and Uang 2002].

Table 4.5 shows that the peak unit shears, displacements at peak shear capacity, and drift ratios at peak shear capacity vary widely. The peak unit shear capacity is the highest for Specimen B-1. This is likely due in part to the capacity of the siding, which was not present in the other tests. Other possible items affecting this capacity include the 3/4 in.-edge distance on the sheathing nailing, and the constraint provided to the sheathing by floor framing above and the foundation sill plate below, restricting sheathing slip in the horizontal direction. The drift and drift ratio at peak shear capacity of 2.5% reported by Bahmani and van de Lindt [2016] is typical of that reported in similar testing of full story height walls. Compared to this, the 6% drift ratio for Specimen B-1 and 4% for Chai reflect a pattern of larger drift ratios for cripple walls relative to full story height walls. The higher drift and drift ratio reported by Gatto and Uang [2002] appear to be an anomaly in light of the results documented herein but deserve further evaluation.

Specimen B-1's peak unit shear capacity of 1500 plf (averaged from Table 4.3) can be compared to the nominal capacities assigned by SDPWS [AWC 2015]. The SDPWS Table 4.3D assigns horizontal lumber sheathing a nominal capacity of 100 plf for seismic and 140 plf for wind design. Table 4.3A assigns a nominal capacity for 15/32 in.-rated sheathing with 8d nails at 4 in. on center of 760 plf for seismic and 1065 plf for wind design. Summing the nominal wind capacities of 140 and 1065 plf (without including rules established for reduction when using combined materials) gives a summed nominal capacity of 1205 plf, which is approximately 80% of the Specimen B-1 peak shear capacity of 1500 plf. Because the strengths of these materials are not permitted to be combined in design, the ASD allowable unit shear assigned by SDPWS would be 760/2 or 380 plf, which is approximately 25% of Specimen B-1's peak shear capacity.

Specimen B-1's peak unit shear capacity of 1500 plf can be compared to the capacities that were used in the numerical studies conducted for *FEMA P-1100*, Volume 3, Table 4.4 and are summarized in Table 4.6 below, which shows Specimen B-1's peak unit shear capacity to be 71% of the *FEMA P-1100* analysis values based on best estimate values. Specimen B-1's drift at peak shear capacity is notably different than found in the *FEMA P-1100* document. Consideration should be given to adjusting the drift in future numerical studies.

Table 4.5 Comparison of Specimen B-1 peak capacities and drifts to prior testing.

Testing	Materials	Peak unit shear capacity (plf)	Displacement at peak shear capacity (in.)	Drift ratio at peak shear capacity (%)
PEER–CEA Specimen B-1	Horizontal wood siding exterior, 15/32 plywood retrofit rated sheathing 8d@4	1500	1.4	6
Chai Specimen 1	15/32 OSB 8d@4	840	1	4
Bahmani W-01	8 ft ×8 ft wall 15/32 plywood rated sheathing 8d@4	900	2.5	2.5
Gatto Test 6	8 ft ×8 ft wall 15/32 plywood STR I 8d box @4	1300	5	5

Table 4.6 Comparison of Specimen B-1 peak capacities and drifts to *FEMA P-1100* modeling.

Source	Materials	Characterization	Peak unit shear capacity (plf)	Drift ratio at peak shear capacity (%)
Specimen B-1	Horizontal wood siding exterior, retrofit plywood sheathing with 8d@4	See discussion	1500	6
FEMA P-1100	Horizontal wood siding	Best Estimate	190	4.0
	Wood structural panel 8d@4, intermediate anchorage, aspect ratio > 0.67	Best Estimate	976	2.1
	Wood structural panel 8d@4, intermediate anchorage, aspect ratio $\leq$ 0.67	Best Estimate	976	3.15
FEMA P-1100 Rule for Summing Materials	Horizontal Lumber Sheathing + Plywood	Best Estimate	1071	NA

During the course of loading of the north and south walls, the east and west walls were required to accommodate the same floor diaphragm drift. A significant benefit to the use of a 3D structure for Specimen B-1 was the opportunity to observe the response of the east and west walls, including their participation in resisting of uplift due to overturning, and the deformations imposed as the diaphragm displacement pushed the top of the wall out with respect to the wall bottom; see Figure 4.22. This was found to cause uplift and gapping in the west wall without necessarily causing damage that impacted the capacity of the specimen. The east wall experienced splitting of the foundation sill plate that did not impact the capacity for longitudinal loading but would have an impact for transverse or bi-axial loading. Further study of this type of full-scale building effect is needed.

4.11 CONCLUSIONS

Specimen B-1 investigated the seismic performance of load path connectors commonly used in cripple wall retrofits. A cripple wall retrofit designed in accordance with *FEMA P-1100* was installed on 2-ft-tall cripple walls with an exterior finish of horizontal wood siding. Like the other large-component tests, this test used plan dimensions of 20 ft × 4 ft. The test specimen included cripple walls at the full specimen perimeter and a high-load floor diaphragm constructed on top; see Figure 4.26. Specimen B-1 did not incorporate a superstructure story above the floor because the Project Team deemed its presence insignificant to the results.

The detailing of the cripple wall framing and relationship to the foundation was selected to be typical of construction up through the 1940s. In particular, it used a foundation sill plate that was wider that the supported studs, a detail very common in older houses in California and other western states; see Figure 4.27. The retrofit included plywood sheathing on the face of the cripple wall, shear clips (Simpson A35s) from the cripple wall top plate to the floor framing above the cripple wall, and plates (Simpson URFPs) from the 2-in.- × 6-in.- foundation sill plate to the foundation. The use of plates is common in cripple walls that are 2 ft or less in height because of the difficulty of retrofitting a house by installing anchor bolts.

In addition to the primary objectives noted above, Specimen B-1 evaluated the ability of commonly used load path connectors to improve the strength and displacement capacity of a cripple wall with seismic sheathing. The intent of the *FEMA P-1100* provisions was to ensure that the load path connectors selected using either the prescriptive or engineered design methods of retrofit be capable of developing the combined capacity of the finish materials and sheathing retrofit. Specimen B-1 served as one data point to confirm that this is achievable.

Figure 4.26 Specimen B-1 prior to start of testing.

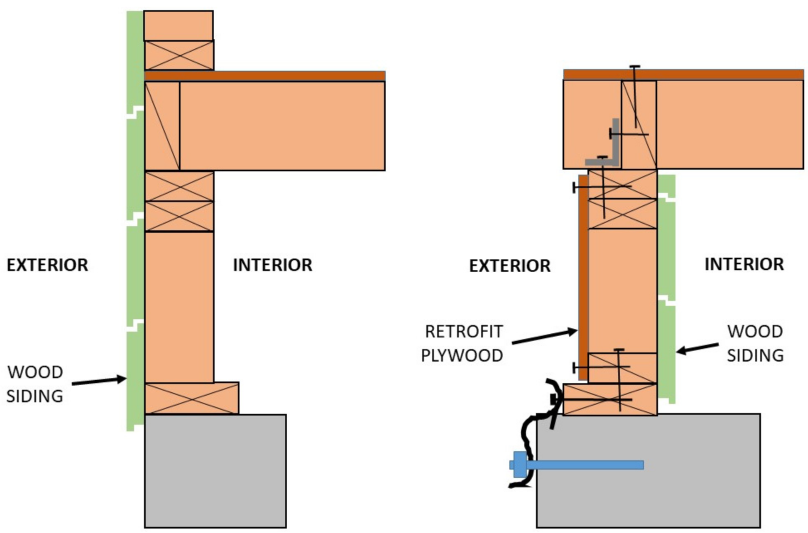

Figure 4.27 Specimen B-1 cripple wall configuration: (left) typical existing condition; and (right) with cripple wall constructed inside-out (siding on interior, retrofit on exterior).

The following are highlights of Specimen B-1 testing results and conclusions:

- Specimen B-1 reached a peak capacity (lateral strength) of 32 kips (1500 pounds per foot of plywood sheathing) at a drift ratio of approximately 6%; and
- Specimen B-1 did not experience a drop off in capacity following cycles at peak capacity, retaining 60% of the peak capacity to a drift ratio of 10% (2.4 in.) and 36% of peak capacity to 13% (3.12 in.). In a final monotonic push, it retained 24% residual capacity to a drift ratio of 33% (8 in.). The retained post-peak capacity—similar to Specimen AL-2—demonstrates significant benefit from the retrofit; see Figure 4.28.

- The peak capacity reached in testing is 1.25 times the sum of the tabulated nominal (wind) capacities for the horizontal wood siding and the plywood sheathing retrofit. This, coupled with observations during testing, confirm that the cripple wall was able to reach its full peak and post-peak strengths without the load path connectors (shear clips and retrofit plates) serving as weak links.
- The plywood retrofit was observed to have good strength and very high ductility and displacement capacity. The capacity of the plywood sheathing retrofit and nailing appeared to be the most significant determiner of the capacity of the cripple wall. The damage to the sheathing occurred in the common modes of sheathing slip and sheathing nail withdrawal. This confirms that the full benefit of the plywood retrofit, including both the strength and ductility, were able to be utilized.
- The load path connections designed in accordance with *FEMA P-1100* were observed to more than adequately develop the capacity of the retrofitted cripple wall. There was no observed damage and virtually no observed deformation to the connectors during testing. Similarly, there was no observed damage to the blocking installed on top of the foundation sill plate between studs. This serves as one datapoint confirming the adequacy of load path connector design in accordance with *FEMA P-1100*; and
- Detailed descriptions of damage observations at each drift ratio are provided.

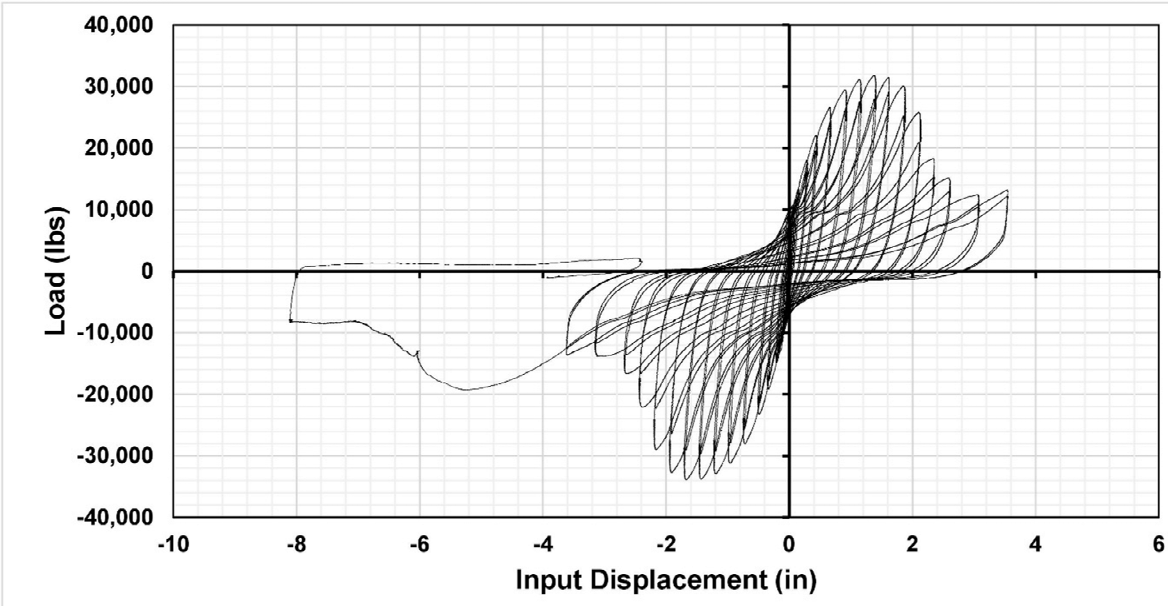

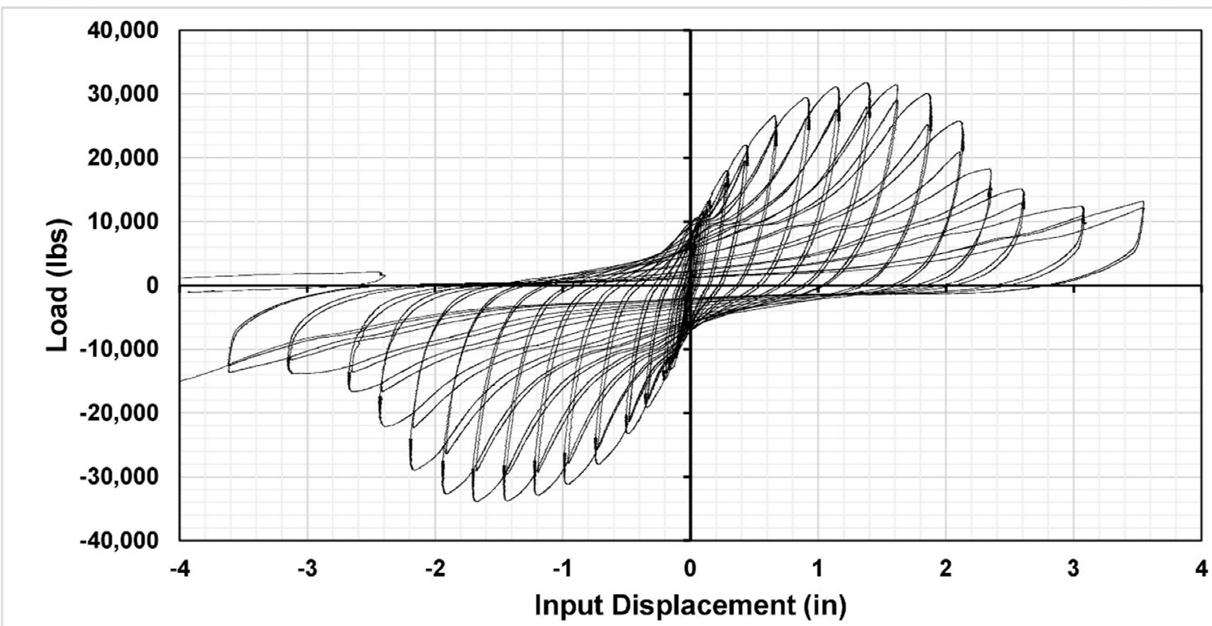

Figure 4.28 (Top) Lateral load versus lateral actuator input displacement of Specimen B-1 with final monotonic push; and (bottom) lateral load versus lateral actuator input displacement of Specimen B-1 without monotonic push.

5 Group C Combined Materials in Occupied Stories Testing

This chapter discusses Test Specimens C-1 and C-2. The primary purpose of this testing was to evaluate wall finish and sheathing materials commonly found in occupied stories of California dwellings, with the information being used to inform WG5 selection of parameters for numerical studies and WG6 fragility functions. Specimens C-1 and C-2 finish materials were selected by the project team as priorities to supplement the minimal amount of currently available data for occupied stories of dwellings.

The tests were performed on full-scale specimens with significant attention given to providing the most representative boundary conditions possible. Earlier tests [CUREE 2003] had identified realistic boundary conditions that significantly affect both the peak shear capacity and drift at peak shear capacity of full-story-height walls with a stucco exterior finish. Representative boundary conditions are thought to have varying degrees of influence across a range of finish materials. The inherent continuity of interior plaster means that the influence of boundary conditions could affect results the same way.

This chapter provides details of construction for Specimens C-1 and C-2, and presents test results, discussion, and conclusions. Note: the terms “existing” and “unretrofitted” are used interchangeably in this report.

5.1 INTRODUCTION

Test Specimen C-1 was selected to have a horizontal wood (shiplap) siding exterior finish, installed over building paper, and plaster on wood lath interior finish. While this combination could be representative of dwellings originally constructed over a range of years, the design was targeted to be representative of construction in the 1930s and 1940s. This is from the later years of this type of construction and is thought to be representative of a notable portion of the existing dwelling stock in California from that era. Test Specimen C-2 was selected to have a plywood panel (T1-11) siding exterior finish, installed over building paper, and a gypsum wallboard interior finish. The design for Specimen C-2 used materials and construction details that were representative of construction practices of 1960s and 1970s for standard housing. Further information on details of construction is provided in the following sections.

The installation chosen for the Specimen C-2 plywood panel (T1-11) siding specifically included a miss-installation that is commonly found in the existing building stock. In this miss-installation, edge nailing of the plywood siding is only provided at one of the two abutting siding panels at vertical joints. One of the panels is edge nailed, and the other is simply clamped in place by the edge nailed panel; see Figure 5.1. At that time this may have been considered adequate for a siding installation. Now it is thought to adversely impact the seismic bracing capacity of the siding. This miss-installation was included because it is so common in the housing stock, that knowing the impact of the installation error could be significant.

The configurations of the test specimens were based on a hypothetical single-story model dwelling with a 30- × 40-ft footprint. The test specimens include 8-ft-tall walls seated on the concrete foundation covered by a roof structure. Each of these walls was chosen to have one door (sliding glass or French door) and one window, with the layout of each wall a mirror image of the other. These wall configurations are the same as those used in Specimens AL-1 and AL-2. The loading of the test specimen was parallel to the 20-ft walls.

The configuration at the base of Specimens C-1 and C-2 was chosen to represent a dwelling in which the occupied story walls are supported on a wood-framed floor that is in turn supported on a stem wall; see Figure 5.2. This base of wall configuration was reasonably common in the eras of interest and is still commonly used for new dwellings on hillsides; it is shown on the left-hand side of Figure 5.2. The adaptation of this detail for testing is found on the right-hand side of Figure 5.2. The nailing of the wall bottom plates to the 4 × 6 nailers is intended to represent a lower bound but realistic condition for fastening of the wall base.

Elevations and side views of the test specimen are shown in Figure 5.3. Detailed drawings of Specimens C-1 and C-2 are provided in Appendix B. A summary of the key characteristics of the two test specimens is provided in Table 5.1. Details of construction follow.

Table 5.1 Test matrix for Specimens C-1 and C-2.

	Exterior finish	Interior finish	Super-structure height (ft)
C-1	Horizontal wood siding (shiplap)	Plaster on wood lath	8
C-2	Plywood panel siding (T1-11) with a typical non-shear wall installation	1/2-in. gypsum wallboard installed per conventional construction	8

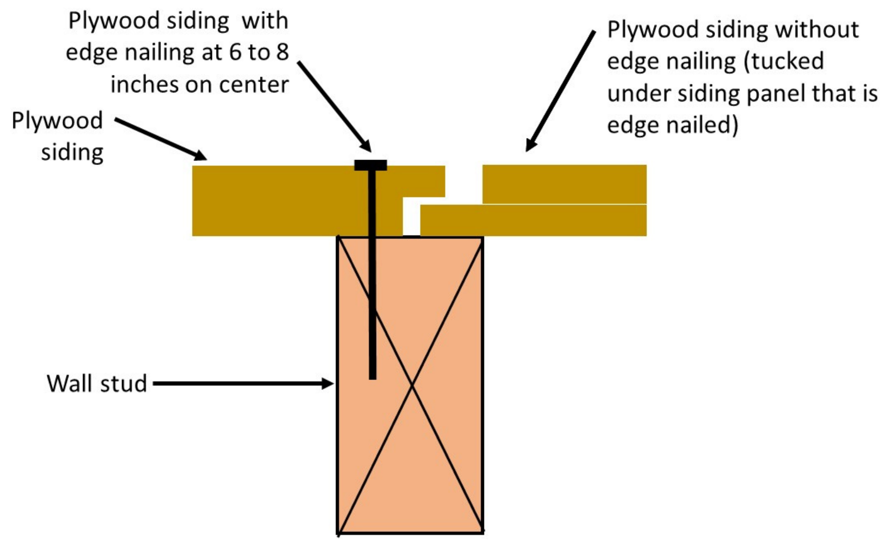

Figure 5.1 **Section through stud and vertical siding joint at abutting panel edges. The miss-installation shown only includes edge nailing on one of the two abutting panels. This miss-installation was specifically included in construction of Specimen C-2.**

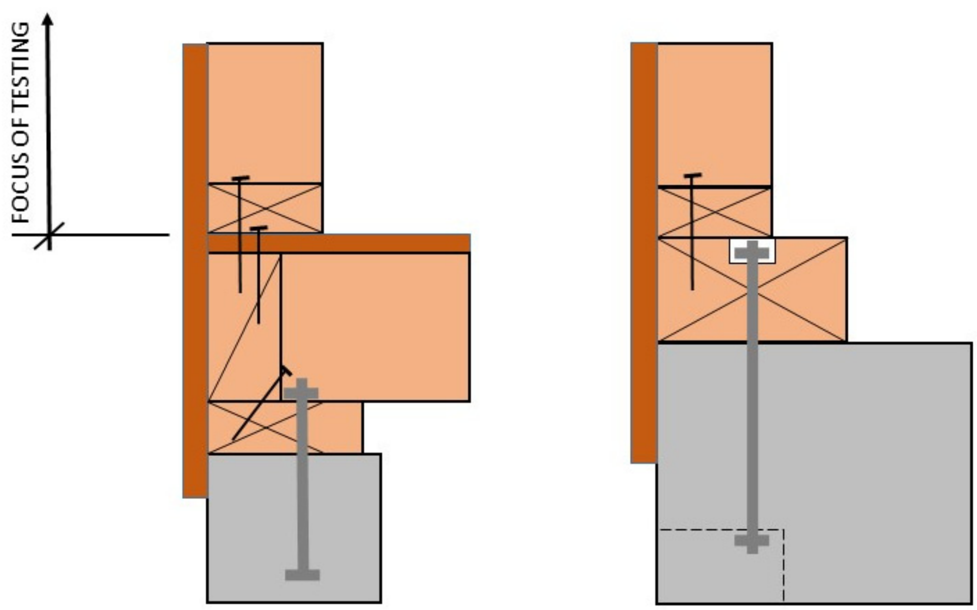

Figure 5.2 **(Left) Base condition for Specimens C-1 and C-2 including the typical construction detail being represented and (right) the configuration used in the specimens.**

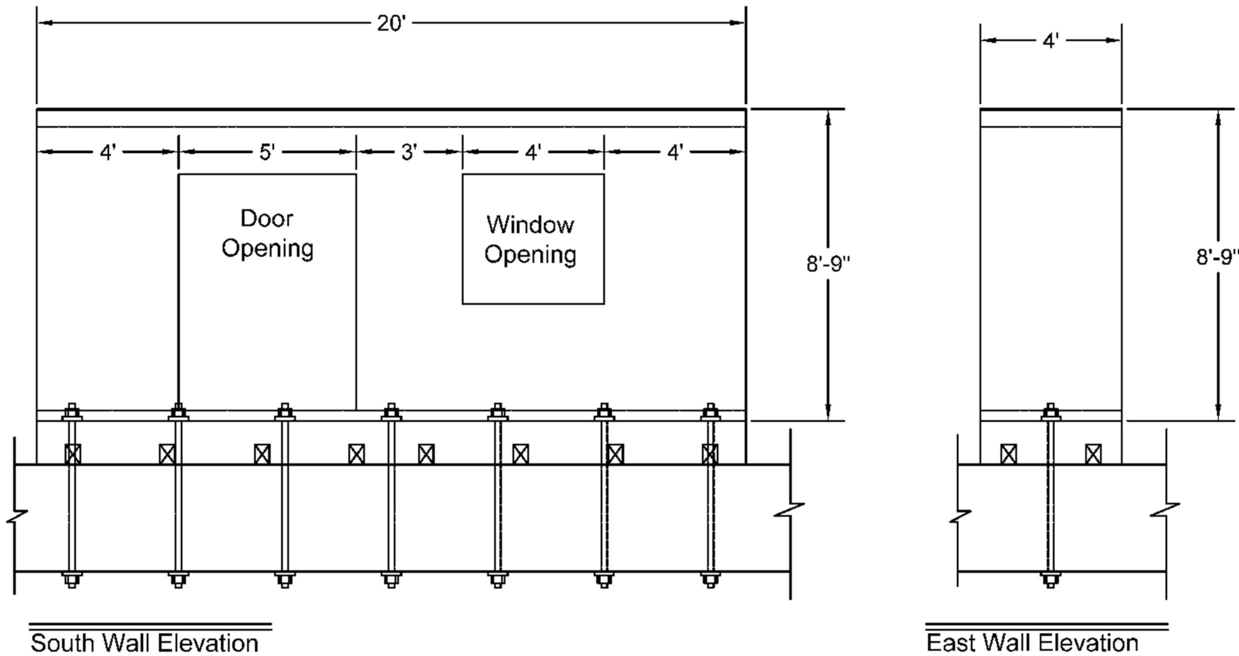

Figure 5.3 Elevation and section figures of test specimens.

5.2 FRAMING DETAILS

The foundation was for Specimens AL-1 and AL-2 was re-used for Specimens C-1 and C-2, following minor patching of the foundation edge. For the base of wall condition, the wall bottom (sole) plates were nailed to a 4 × 6 wood nailer; see Section 5.1. The 4 × 6 nailers were bolted to the foundation perimeter using 1/2-in. all-thread rods distributed along the long and short sides of the building; see Figure 5.4. Four bolts were used on each of the 20-ft-long sides and two bolts on each of the 4-ft-long sides. As was the case for Specimens AL-1 and AL-2, all-thread bolts inserted into an existing sleeve were used to allow reuse of anchorage for multiple test specimens. Special attention was paid to ensure a tight fit between the anchor rod and the conduit, to minimize the slip between the 4 × 6 nailer and the foundation. Special attention was also paid to the countersinking of the anchor rods and their nuts into the 4 × 6 nailers so that the top of the nailer would be smooth and not interfere with movement of the wall bottom plate. Similar to previous tests, load cells were used to measure the tensile force in some of the anchor bolts during testing.

The specimen walls were 8 ft tall, corresponding to the distance between the top of the foundation 4 × 6 nailer and top of the double top plate (i.e., the clear height of the framed wall). On top of the walls, an approximately 6-in.-tall high-load diaphragm was installed, consisting of joists at 16 in. on center and 19/32 STR I plywood sheathing. The diaphragm was designed to be capable of delivering the estimated peak shear capacity of the test specimens.

All framing was Number 2 or better grade Douglas-fir. Minimum fastening tables from era-specific building codes were used for framing fastening, supplemented by more recent code provisions where necessary. The studs were 2 × 4 framing members spaced at 16 in. on center. The wall top and bottom plates were matching 2 × 4 framing members. The studs were end-nailed to the sill plate using two 16d common nails. The studs also were end-nailed to the lower top plate using two 16d common end nails. The upper top plate was face-nailed to lower top plate using 16d common nails at 12 in. on center. At the corner laps, an extra two 16d common face nails were added.

The wall 2 × 4 bottom plates were nailed to the 4 × 6 nailers with two rows of 16-penny sinker nails spaced 6 in. on center in each row. Although this is more nailing than typical conventional regarding bottom (sole) plate nailing, it was estimated to have a shear capacity in balance with the design shear capacities assigned to the wall-bracing materials. This nailing was used with the intent of avoiding the premature failure anticipated if typical bottom plate nailing was used.

The high-load diaphragm was constructed on top of the specimen walls. To accommodate multiple rows of diaphragm edge nailing—as specified for high-load diaphragms by the SDPWS Standard [AWC 2015]—4 × 6 and 3 × 6 framing members were used; 4 × 6 nominal Douglas-fir lumber joists were spaced 16 in. on center. Rim joists were selected as 3 × 6 nominal Douglas-fir lumber on all four edges of the diaphragm. Six 8d common nails were used to toe-nail joists to the upper top plate (three at each end of the joist). The blocking on top of the wall top plate was toe-nailed using four 8d common nails (two each end of blocking) to joists and four 8d common nails to the top plate per block. Also, two rows of blocking were provided near the center of the 4-ft diaphragm width to provide a substrate for connecting the loading beam to the diaphragm; 19/32-inch Structural I-plywood sheathing was used for the diaphragm, with four staggered rows of 10d common nails at 2-1/2 in. on center each row at the diaphragm interior panel edges and boundaries. Field nailing used one row of 10d common nails spaced at 3 in. on center. As discussed previously, the main objective of the diaphragm design was to provide enough strength and stiffness so that the diaphragm would adequately transfer loading beam displacements to the specimen walls without acting as a weak link or contributing significant deformation.

Twenty-eight pairs of A35 shear clips were used to add extra connection capacity between the upper top plate and the high-load diaphragm rim joist. Twelve 8d common nails were used for each shear clip (6 nails on each leg); see Figure 5.5. The same framing details were used for both specimens, while interior and exterior finishes differed. Wall-framing elevations are shown in Figure 5.6, and Figure 5.7 shows details of the framing of a typical section. Figure 5.8 shows a diaphragm framing plan on the right-hand side of the figure, and on the left-hand side, a plan locating the A35 shear clips connecting the diaphragm rim joists to the wall top plates is depicted.

Framing and sheathing fasteners were installed with a nail gun. While this created the potential for over-driven nails and subsequent reductions in capacity, little or no overdriving was observed. Therefore, the use of a nail gun is not believed to have affected the testing results. It is noted that finished lumber dimensions have varied over time with “full dimension” (i.e., 2 in. × 4 in.) lumber having been common to the 1920s, an intermediate size (i.e., 1-5/8 in. × 3-5/8 in.) used until the 1960s, and modern sizing (i.e., 1-1/2 in. × 3-1/2 in.) used since. The changing size of framing is not believed to have affected the testing results.

(a) (b)

Figure 5.4 **Platform block under the superstructure wall: (1) anchor rods flush cut with top of 4 × 6; and (b) wall bottom plate on 4 × 6 nailer.**

Figure 5.5 **A35 bracket installed between the high-load diaphragm and upper top plate.**

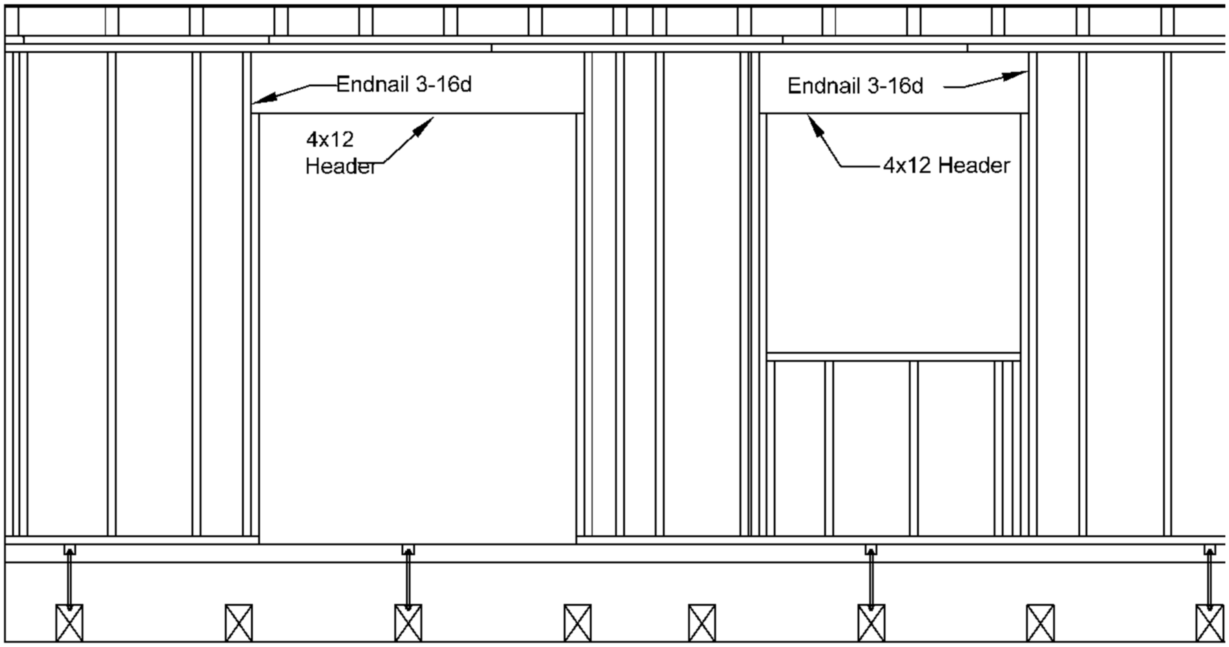

(a)

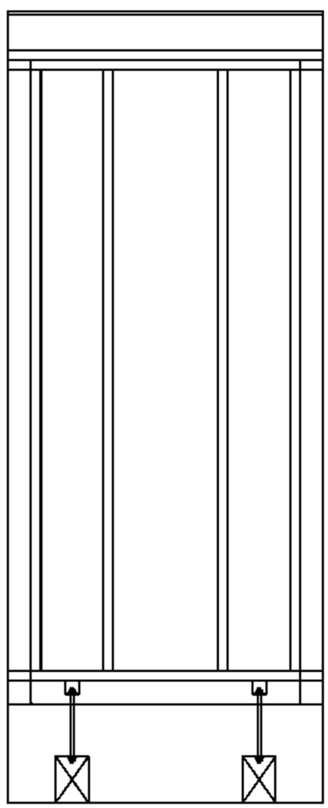

(b)

Figure 5.6 Wall framing elevations: (a) south wall framing; and (b) east and west wall framing.

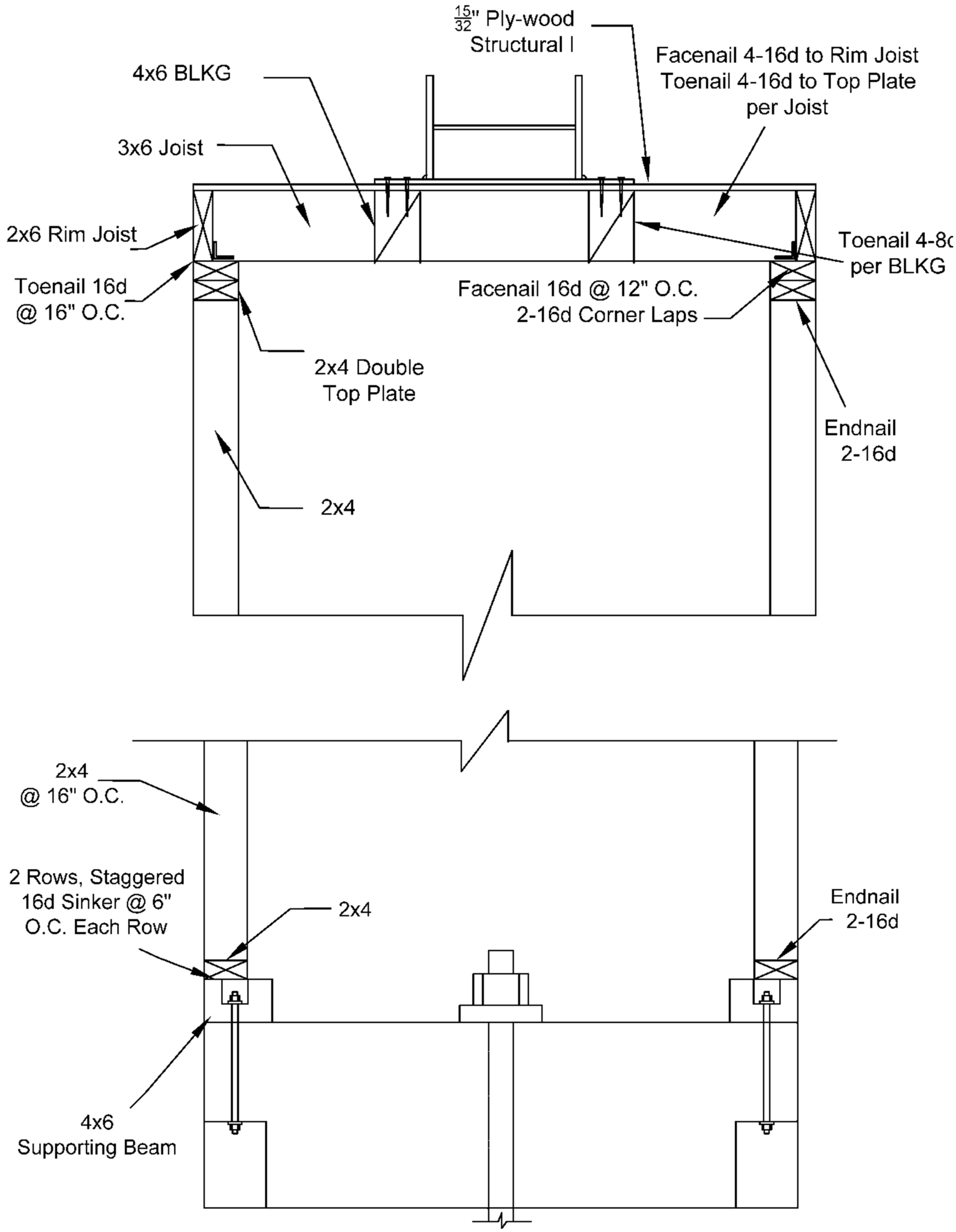

Figure 5.7 Section illustrating test-specimen framing.

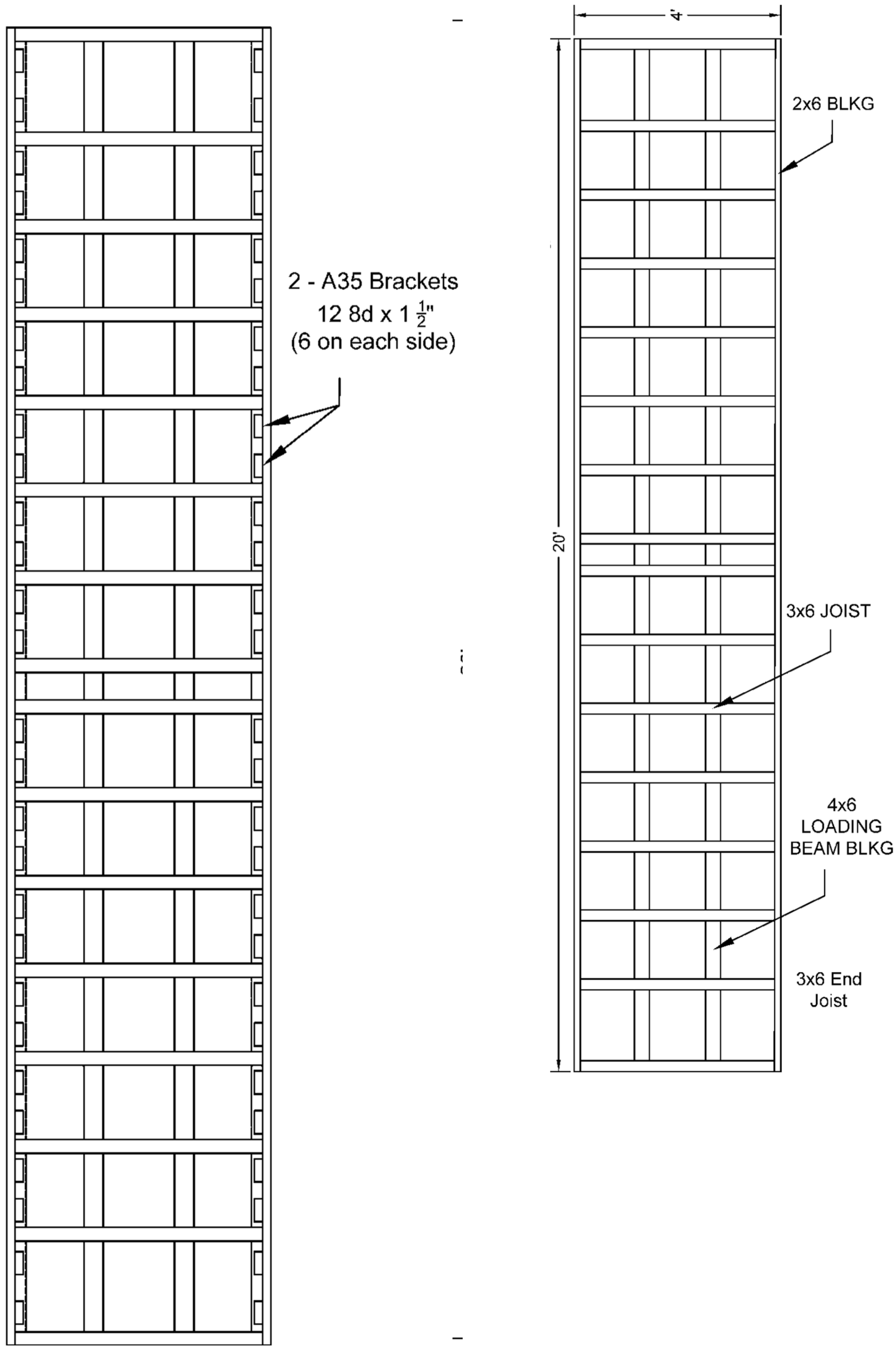

(a) (b)

Figure 5.8 (a) Diaphragm framing plan and (b) locations of A35 shear clips (left).

(a) (b) (c) (d) (e) (f)

Figure 5.9 Framing details (photos are for Specimen C-1 but similar for C-2): (a) framing detail at lower southwest corner; (b) staggered nailing of sill plate; (c) opening headers; (d) southwest frame view; (e) wall to roof configuration; and (f) high-load diaphragm from inside.

Prior to installing exterior shiplap for Specimen C-1 or exterior T1-11 plywood siding for Specimen C-2, building paper (Grade D-60 Minute), which acted primarily as a moisture barrier, was installed and directly attached to the wall framing using a standard hammer stapler with 3/8-in.-long leg-collated staples. The building paper covered the entire outer surface of the walls. Three to five inches of overlap was provided between adjacent sections of building paper. Details of building paper installation are shown in Figure 5.10.

(a) (b)

Figure 5.10 **Installation of building paper installation. These photographs are for Specimen C-1, application for Specimen C-2 were similar: (a) application of building paper; and (b) overlap of building paper.**

5.3 INSTALLATION OF SPECIMEN C-1 EXTERIOR HORIZONTAL WOOD SIDING (SHIPLAP)

Consistent with common dwelling construction in the 1930s and 1940s, redwood shiplap siding was used for exterior side of Specimen C-1. After considering several available siding choices, it was decided by the project team that use of a redwood species for the siding was most representative of the building stock at that time, and that the properties of the siding might impact the test results. Nusko FireBlocker Primed Finger Joint Redwood shiplap siding (Pattern #793) was selected. Each siding board had dimensions of 1 in. × 6 in. × 20 ft, with finger-jointed construction. The siding boards were installed with two 8d HDG (Hot Dip Galvanized) common nails at each stud, consistent with applicable building codes. This also matches nailing used for PEER–CEA Project's small-component testing performed at UCSD. Photographic documentation of application of the siding board is shown in Figures 5.11 and 5.12.

(a) (b)

(c)

Figure 5.11 Shiplap exterior siding installation showing fascia board and corner trim: (a) back side of shiplap; (b) nailing pattern in west end of south wall; and (c) south wall shiplap view.

Figure 5.12 Shiplap exterior siding installation showing fascia board and corner trim.

5.4 INSTALLATION OF SPECIMEN C-1 INTERIOR GYPSUM PLASTER OVER WOOD LATH

Gypsum interior plaster materials and installation for Specimen C-1 were provided by general contractor Saarman Construction and their sub-contractor GreenWall Tech. First, wood lath was installed and followed by two-coats of gypsum plaster. Primary references for the gypsum plaster and lath installation were the 1935 edition of the UBC [1935].

The first step was to install the wood lath. Number 1-grade redwood lath that was reasonably clear, evenly manufactured, and free from detrimental defects was installed. Per the UBC 1935 recommendations, wood lath with the dimensions of 5/16-in. × 1-1/2-in. redwood was used. The lath was installed horizontally, extending the full length of the walls. At least eight hours before nailing the lath in place, the lath was thoroughly soaked. Following installation of the lath on the wall framing, the lath was kept moist using water sprayed with a bottle until the plaster was applied. Each lath board was nailed to the supporting studs with 3d fine blued nails. The nails were provided at each stud crossing at approximately 16 in. on center and at each end of each lath board. The vertical gap of 3/8-in. between the lath boards was used per building code minimum requirements. Nails were driven in full length. Because the lath was prone to splitting during nailing when nails were installed at the very ends of the lath boards, the ends of the boards were pre-drilling for the 3d nails but not at other nail locations. A 3/4-in.-square, continuous wood plaster stop was installed at the door and window openings to give the plaster installers a surface to strike the plaster off to. The plaster stops were installed with 6d finish nails spaced at 12 to 16 in. on center.

After the installation of the wood lath, the gypsum plaster was installed in two coats, including a base coat and a finish coat. The second (finish) coat was thinner and installed on top of the base coat, whose primary function was to provide a workable surface for painting or installation of other finishes.

A 5/16-in.-thick base coat—measured from the exterior face of the wood lath—was installed directly on top of wood lath. This plaster coat was attached to the wood lath by pushing the plaster through the gap between the wood lath boards such that keys were created on the back side of the lath. The base coat consisted of a mixture of two-parts by volume of clean graded kiln-dried Monterey plaster sand, and one part of Redtop Gypsum Plaster mixed with water using a rotary mixer. The finish coat was applied a few days following the application of the base coat. First, the surface of the base coat was sprayed with a water to moisten the surface moist. The finish coat materials consisted of one part ready-to-mix USG Diamond Veneer finish gypsum, mixed with enough water to obtain a workable mixture. A hand-held, powered rotary mixer was used to mix the material. The surface of the finish coat was applied so that the surface was smooth and ready for painting, although no painting was provided for the test specimen. Application steps and details of installing the gypsum plaster over wood lath are shown in Figures 5.13 through 5.16.

Figure 5.13 Lath installation details: (a) soaking lath before installation; (b) redwood lath; (c) 3/8 in.-lath spacing; (d) lath and plaster stop at opening corners; (e) top corner lath installation; and (f) bottom corner lath installation.

(a)

(b)

(c)

(d)

Figure 5.14 Application of gypsum plaster: (a) mixing ingredients using a rotary mixer; (b) application of first coat on lath; (c) base coat at opening, see plaster stop; and (d) sample cube from base and finish coats for material testing.

(a) (b)

(c)

Figure 5.15 Application of gypsum plaster: (e) plaster application; (f) base coat vs. finish coat; and (g) lock formed in the back of lath and plaster droppings accumulated within the wall.

(a)

(b)

Figure 5.16 Gypsum plaster finished texture: (a) finish coat finished texture; and (b) base coat finished texture before covering by finish coat.

5.5 INSTALLATION OF SPECIMEN C-2 EXTERIOR PLYWOOD SIDING (T1-11)

For Specimen C-2, the exterior plywood panel (T1-11) siding was installed first, followed by the installation of the gypsum wallboard interior wall and ceiling finishes. Prior to installation of the plywood siding, building paper was installed and directly attached to the wall framing, as previously discussed. For siding, 19/32-in.-thick 4-ft × 9-ft plywood siding panels with vertical grooves spaced at 8 in. on center were used; this is the pattern used for plywood siding T1-11. The 8-ft edges of the siding had ship-lapped joints, and 8d HDG (Hot Dip Galvanized) common nails were spaced at 6 in. for edge nailing and 12 in. for field nailing. Photographic documentation of the installation of the T1-11 siding; see Figures 5.17 and 5.18.

As previously discussed in Section 5.1, it was decided to include a common miss-installation in which siding panel edge nailing is provided on only one of the two panels abutting at vertical panel joints; see Figure 5.2.

(a)

(b)

(c)

Figure 5.17 Installation of T1-11 plywood siding: (a) top of wall detail; (b) end walls; and (c) T1-11 siding south wall.

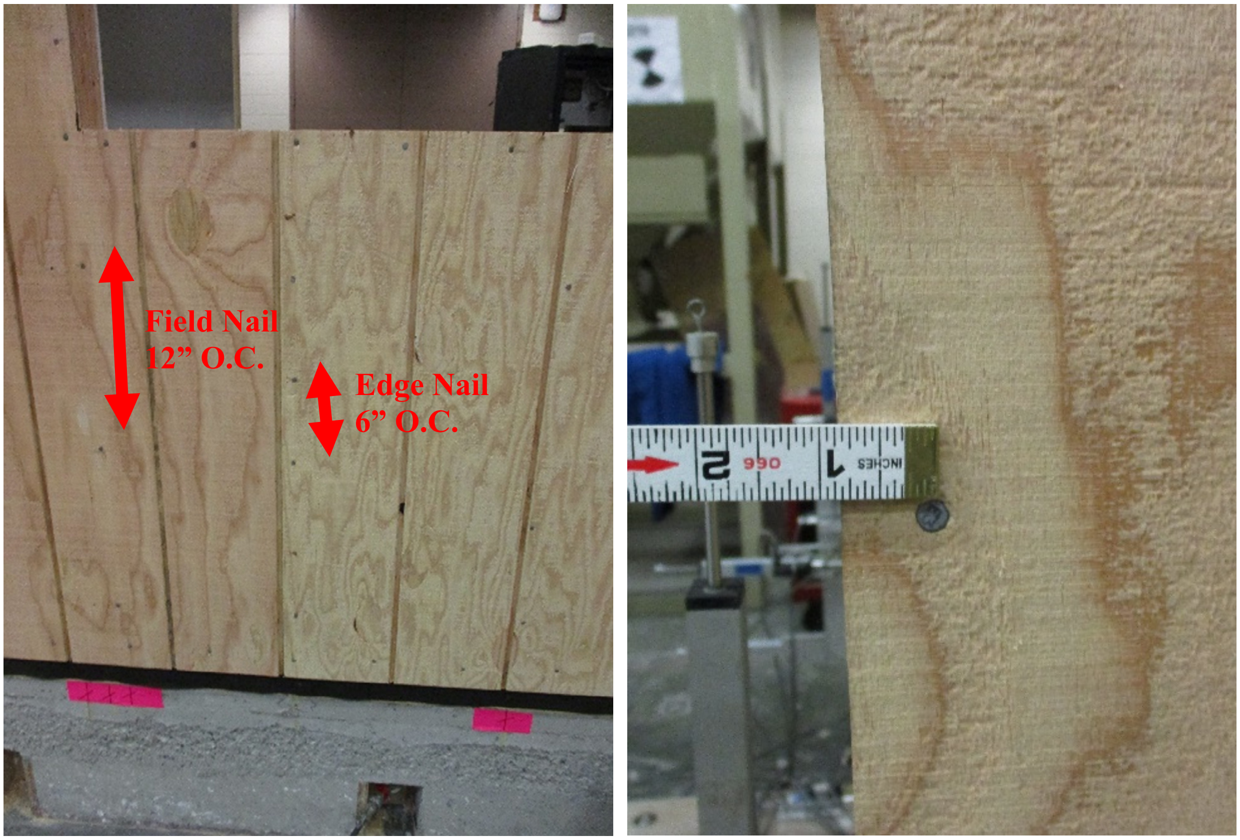

(a) (b)

Figure 5.18 Installation of T1-11 plywood siding; (a) nailing at joint at window opening; and (b) nail spacing from edge of T1-11 boards.

5.6 INSTALLATION OF SPECIMEN C-2 INTERIOR GYPSUM WALLBOARD

The interior finish for Specimen C-2 walls was composed of 1/2-in.-thick gypsum wallboard, and installed in 4 × 8-ft boards, oriented vertically. The board was fastened using 0.086-in. × 1-5/8-in. drywall nails (which is roughly equivalent to code specified 5d cooler nails), spaced 7 in. on center over the full height of each typical stud (spaced at 16 in. on center) at studs at edges of door and window openings, and at corners. The boards were installed to fully cover the walls and ceiling. At the wall to ceiling interface, “floating corner” details were used in which the first fastener in ceiling gypsum board was installed 12 in. away from the wall. At the bottom of the gypsum board sheets, a 1/8-in. vertical gap was provided between the bottom of the gypsum wallboard and the 4 × 6 nailer; this is consistent with common installation procedure where the gypsum wall board is kicked up snug to the ceiling prior to nailing.

To provide finishing for wallboard joints as well as to cover nail heads, fiberglass paper tape was set in DAP DryDex lightweight low-dust joint compound. The joint compound surface was flushed with the surface of the gypsum boards; see photographic documentation in Figure 5.19.

(a)

(b)

(c)

(d)

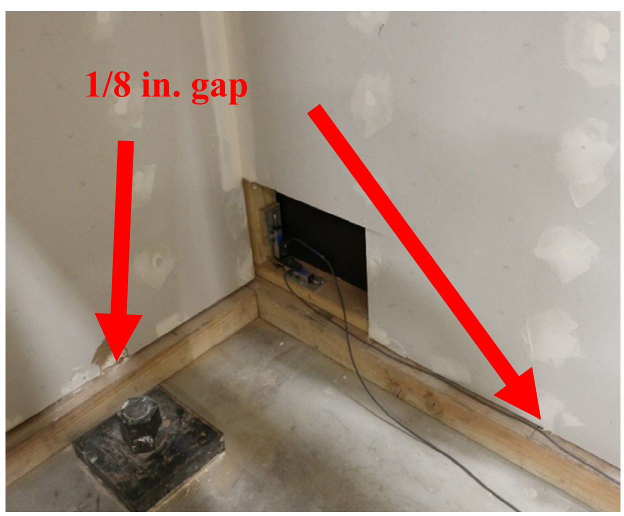

(e)

Figure 5.19 **Installation of gypsum wallboard: (a) cupped head drywall nails; (b) DryDex joint compound; (c) fiberglass joint tape; (d) joint compound to cover joints and nail heads; and (e) 1/8-in. gap at the gypsum board bottom end.**

5.7 LOADING PROTOCOL

The quasi-static lateral displacement history described in Chapter 2 was followed in this testing program. The specimens were first subjected to seven initiation cycles and then subsequent increments that consisted of four, three, and then two cycles; see Table 5.2 for Specimen C-1 and Table 5.3 for Specimen C-2. In Specimen C-1 and C-2 tests, the parameter "h," was taken as the 96 in. clear height of the walls. A constant loading rate of 0.4 mm/sec (0.1574 in./sec) was used for both specimens; see Section 2.2. While a higher loading rate was used compared to other UCB testing, this still falls within applicable recommendations; see Section 2.2.

For Specimen C-1, testing started with pushing to the west to reach the first peak, and then the loading was reversed to reach the first pulling peak to the east. These cycles were repeated to the number of cycles designated for each cycle level. Once the peak load occurred, the subsequent drift levels were monitored to chart when a 40% drop in peak load, which occurred a drift ratio of 7%. After this point, each drift cycle was increased by 2% instead of 1%. The cyclic loading continued till the drift level of 15% was achieved (14.4 in. of actuator stroke). Since the actuator stroke was limited to 17 in., after this drift level the monotonic push was performed to the system limitation. For safety reasons, the monotonic push of the specimen was directed eastward by pulling of the specimen. The displacement history for Specimen C-1 is shown in Table 5.2.

The loading protocol for Specimen C-2 followed a similar pattern as Specimen C-1. Testing started with pushing to the west to reach the first peak, and then the loading was reversed to reach the first pulling peak to the east. These cycles were repeated to the number of cycles designated for each cycle level. After reaching the peak load at 3%, nails between the sill plate and platform block started to pull out, and the specimen began to show signs of reduced stability. To better record the behavior, the specimen was tested all the way to a 6% drift ratio in 1% increments. For safety reasons, the test was stopped at this point and the monotonic push was deemed unfeasible. The displacement history as performed for Specimen C-2 is shown in Table 5.3.

Table 5.2 General loading protocol adjusted for Specimen C-1 geometry.

Cycle level	Drift %*	Amplitude (in.)	No. Cycles	Loading rate (in./sec)	Total time (sec) per cycles level	Inspection type*
1	0.2	0.192	7	0.1575	34.16	Normal inspection
2	0.4	0.384	4	0.1575	39	Normal inspection
3	0.6	0.576	4	0.1575	58.52	Normal inspection
4	0.8	0.768	3	0.1575	58.5	Normal inspection
5	1.4	1.344	3	0.1575	102.39	Normal inspection
6	2	1.92	3	0.1575	146.28	Normal inspection
7	3	2.88	2	0.1575	146.28	Normal inspection
8	4	3.84	2	0.1575	195.04	Normal inspection
9	5	4.8	2	0.1575	243.8	Normal inspection
10	6	5.76	2	0.1575	292.58	Normal Inspection
11	7	6.72	2	0.1575	341.34	Normal inspection
12	9	8.64	2	0.1575	438.86	Normal inspection
13	11	10.56	2	0.1575	536.38	Normal inspection
14	13	12.48	2	0.1575	633.9	Normal inspection
15	15	14.4	2	0.157	731.42	Normal inspection
15	Monotonic push	15.5	1	N.A	End inspection	N.A

* Normal Inspection: first pull, first push, zero displacement at the end of each cycle.

Table 5.3 General loading protocol adjusted for Specimen C-2 geometry.

Cycle level	Drift %*	Amplitude (in.)	No. Cycles	Loading rate (in./sec)	Total time (sec) per cycles level	Inspection type*
1	0.2	0.192	7	0.1575	34.16	Normal inspection
2	0.4	0.384	4	0.1575	39	Normal inspection
3	0.6	0.576	4	0.1575	58.52	Normal inspection
4	0.8	0.768	3	0.1575	58.5	Normal inspection
5	1.4	1.344	3	0.1575	102.39	Normal inspection
6	2	1.92	3	0.1575	146.28	Normal inspection
7	3	2.88	2	0.1575	146.28	Normal inspection
8	4	3.84	2	0.1575	195.04	Normal inspection
9	5	4.8	2	0.1575	243.8	Normal inspection
10	6	5.76	2	0.1575	292.58	Normal inspection

* Normal Inspection: first pull, first push, zero displacement at the end of each cycle.

5.8 INSTRUMENTATION

Specimens C-1 and C-2 were extensively instrumented. Specimens C-1 and C-2 instrumentation protocol were similar to that used for Specimens AL-1 and AL-2. These instruments were grouped as recording: the overall specimen response, local deformations, and control measurements. These instruments recorded the following data parameters: applied lateral loads, anchor bolt forces, global and local displacements, and boundary displacements. In addition, several videos and still cameras were located both outside and within the specimens to track the behavior of interest. The instrumentation plans for both specimens were identical, so the following description of the details is applicable to both Specimens C-1 and C-2.

The overall response of the specimen was characterized using the lateral force measured by the embedded load cell in the actuator, and the lateral displacement measured by a transducer that was referenced to the loading beam. Over the specimen height, several string pots were connected from a stationary frame to the test specimen at different heights to capture absolute displacement of the building at each height.

Local deformations of the specimen's walls were extensively instrumented. Several diagonal pairs of string pots were used to measure the deformation of the walls. A number of transducers were used to monitor the potential slip and uplift between the specimen and loading beam, and between the specimen and 4 × 6 nailers.

Even though the slip between the foundation and the strong floor was not expected, the potential slip was monitored using one LVDT at one end of the foundation. In addition, a string pot was connected to the upper corner of the building to monitor potential out-of-plane divergence of the building. Because the loading beam was not restrained to withstand rotation in vertical plane, rotation of the horizontal loading beam was monitored using two LVDTs mounted in the loading beam end closer to the loading actuator and the other end to monitor the rotation.

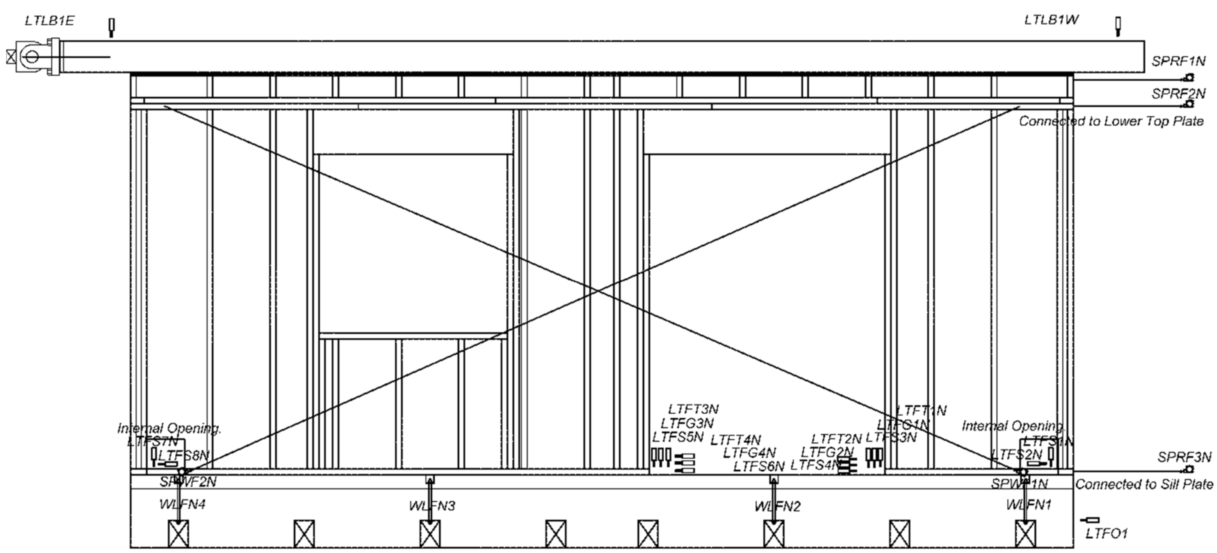

Figure 5.20 Instrumentation layout for north wall Specimens C-1 and C-2.

Several video and still cameras were used both outside and within the specimens to track the behavior of interest. Some of the cameras recorded photographs through the entire duration of the test, while others were stopped during the test for various reasons. Hand-held cameras were used to obtain photographs of the specimen through the course of the test and provide a detailed record of the behavior of specimens; see Section 2.3 for further information.

The tension in the anchor bolts connecting the platform block to the concrete foundation was recorded using eight washer loads cells. These washer load cells were placed into the access openings that were cast into the concrete foundation. The anchor bolts were hand tightened to a snug fit, and then turned with a wrench enough to have a preload in the general range of 500 pounds per bolt show up in the load cell. There was no intent to specifically pre-load the bolts but only ensure that increases in tension would be captured by the load cell. The mapping of the washer load cell alongside with the data tag for each is provided in Figure 5.21.

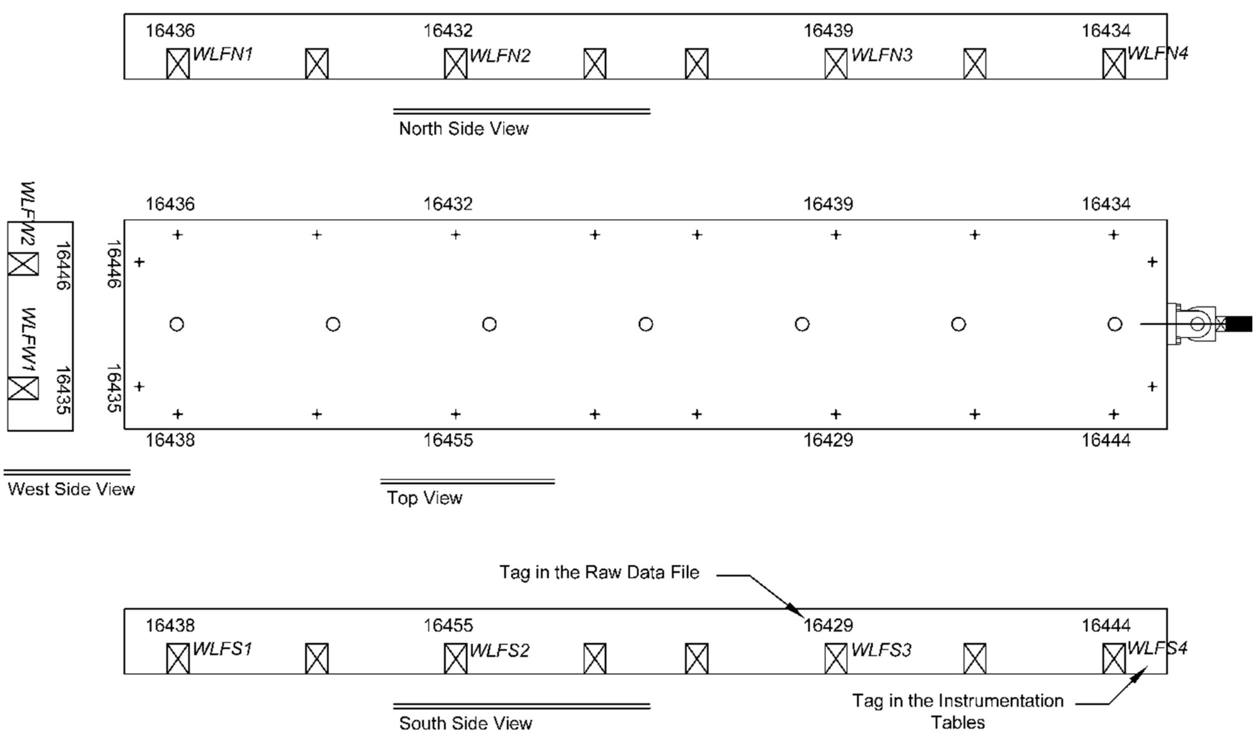

Figure 5.21 Location and mapping of the washer loads to measure the tension in the bolts for Specimens C-1 and C-2.

5.9 GRAVITY LOADING

The configurations for the test specimens were determined based on a model dwelling assuming plan dimensions of 30 ft × 40 ft. This model dwelling was used to determine the supplemental gravity load to be applied during component testing. Models with both one story and two stories were studied in testing of Specimens C-1 and C-2.

For Specimen C-1, the model dwelling has a horizontal wood siding exterior wall finish, a plaster on wood later interior wall and ceiling finish, and a composition shingle roof. The roof, exterior wall and interior wall unit weights were assigned as 185, 13, and 18 lbs psf, respectively. Using these weights, a total structural weight of 47 kips (including the roof and the full height of the walls) was calculated, corresponding to an average weight of 40 lbs per square foot of floor area. Both the unit weights and average weight were checked against data from the *FEMA P-1100* project and found to correlate well. The model dwelling weight was then recalculated to include the weight of the roof and the upper half of the walls, resulting in a total weight of 36 kips or 30 psf over the floor plan. This was done based on the idea that the weight of the upper half of the walls can reasonably be mobilized to resist story overturning, while the weight at the bottom half will act locally at the wall location.

Of the 36 kips total upper structure weight, 9 kips was assigned to the test specimen based on the 20 ft-length being half of the 40-ft dwelling length, and assuming that 50% of the weight would be supported on interior walls and the other 50% on the walls represented by the specimen. The summed self-weight of the specimen and loading beam were determined to be approximately 2.8 kips. The balance of approximately six kips was added using lead blocks at the roof level.

Specimen C-2 had a plywood panel siding exterior wall finish, a gypsum wallboard interior wall and ceiling finish, and a composition shingle roof. The roof, exterior wall, and interior wall unit weights were assigned as 13, 7, and 7 lbs psf, respectively. Similar to Specimen C-1, the house weight was calculated using the roof and upper half of the walls. An upper structure weight of 23.4 kips was calculated, corresponding to an average weight of 20 lbs per square foot of floor area. Of the 23.4 kips total superstructure weight, 5.9 kips was assigned to the test specimen based on the 20 ft-length being half of the 40-ft dwelling length, and assuming that 50% of the weight would be supported on interior walls and the other 50% on the walls represented by the specimen. The summed self-weight of the specimen and loading beam were determined to be approximately 1.5 kips. This left a difference of 4.4 kips; an additional five kips were added at the roof level using lead blocks.

5.10 SPECIMEN C-1 TEST RESULTS

A large volume of data was collected over the course of Specimen C-1 testing, including crack mapping, visual observations, photo documentation of the interior and exterior finish materials at the points designated in the loading protocol, and the continuous recording of the response. Key test results for Specimen C-1 are described in this section.

The lateral force versus lateral displacement of Specimen C-1 was recorded over the course of testing using instrumentation in the actuator to measure load and displacement. The overall load-displacement response obtained from the actuator instrumentation is shown in Figure 5.22 and summarized in Table 5.4. As shown in Table 5.4, the actual drift achieved varied slightly from the targeted drifts shown in Table 5.2 due to the practical limitations of actuator control. The peak unit loads listed in Table 5.4 are the peak loads divided by a total length of full-height wall of 22 ft (11 ft each on the north and south walls).

The Specimen C-1 peak shear capacity (11,390 lbs) occurred in the first push direction displacement to approximately 1.1% drift (shown in the negative quadrant). This was larger than the peak shear capacity in the subsequent pull direction to approximately 1.1% drift (9500 lbs). Based on the total length of full-height wall of 22 ft, this resulted in peak unit shears of 518 and 432 pounds plf, with an average of 470 plf. Spalling of the interior plaster was observed starting at a drift ratio of approximately 0.2% and had become widespread at the 1.1% drift ratio, corresponding to peak shear capacity.

The drop in load between the first cycle push direction loading and the subsequent pull direction is believed to be mainly due to damaged inflicted in the push direction, which affected the subsequent lateral strength. Figure 5.23 shows the envelope curves in the positive and negative quadrants superimposed. There was an approximately 20% drop in peak shear capacity from the negative quadrant push direction to the positive quadrant pull direction. Up to 2% drift, the load recorded for the push and pull directions have significant differences. At 2% drift and above, the envelope curves mirror each other well, with no significant differences.

In the displacement cycle immediately following the cycles at peak shear capacity, a significant drop to approximately 60% of peak shear capacity occurred. This drop was seen in both the push and pull displacement directions. The post-peak load of approximately 60% of peak was maintained out to drifts of 15% to 16%, with very limited additional drop in load. In this latter portion of the envelope curves, the strength is believed to be primarily contributed by the exterior wood siding, with the wood lath and retained plaster keys still providing some contribution.

Specimen C-1 was tested to higher drift levels compared to previous test programs. Providing data in this displacement range is important for development of numerical models intended to describe structure behavior up to and including collapse.

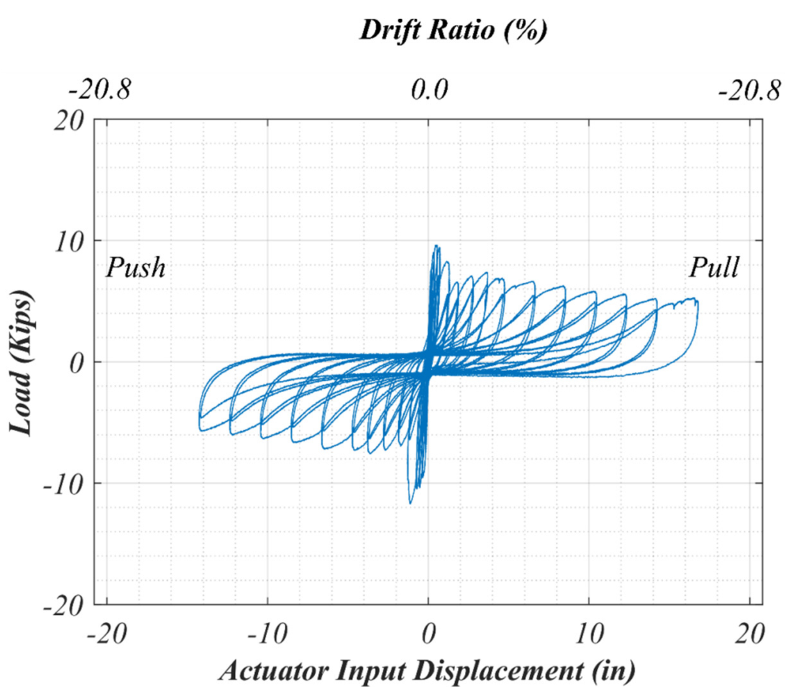

Figure 5.22 **Lateral load versus lateral actuator input displacement of Specimen C-1. Specimen weight including lead weight and loading beam is approximately 9 kips. Seismic mass tributary to the specimen is anticipated to be approximately 18 kips.**

Table 5.4 Summary of test data for Specimen C-1.

Loading direction	Displacement (in.)	Drift ratio (%)	Peak load (lbs)	Peak unit load (plf)	Cycle peak/ overall peak (%)
First loading direction: push to west	0.1631	0.17	7,040	320	62
	0.3521	0.37	9.470	430	83
	0.5498	0.57	10,100	459	89
	0.7245	0.75	10,150	461	89
	0.8254	0.86	10,300	468	90
	1.0313	1.1	11,390	518	100
	1.7933	1.9	6,510	296	57
	2.7623	2.9	6,860	312	60
	3.7421	3.9	7,200	327	63
	4.7131	4.9	6,910	314	61
	6.2778	6.6	6,940	315	61
	8.2929	8.6	6,430	292	56
	10.2100	10.6	6,050	275	53
	12.1137	12.6	5,730	260	50
	14.0511	14.6	5,500	250	48
Second loading direction: pull to east	0.1681	0.20	7,100	322	75
	0.3378	0.35	9,010	410	95
	0.5455	0.57	9,500	432	100
	0.7146	0.74	9,060	412	95
	1.0253	1.1	8,250	375	87
	1.8458	1.9	6,350	289	67
	2.5238	2.6	7,070	321	74
	3.5135	3.7	7,400	336	78
	4.4814	4.7	6,890	313	73
	6.4213	6.7	6,740	306	71
	8.3651	8.7	6,370	290	67
	10.2456	10.7	5,960	271	63
	12.2162	12.7	5,650	257	59
	14.1808	14.8	5,320	242	56

Testing included a final monotonic displacement following cyclic loading. Due to the limits of the test setup and the available actuator displacement range, the monotonic displacement was in the pull direction (toward the east) up to 16% drift, which is only modestly larger than the highest cyclic loading drift. This monotonic displacement shows up as the last cycle in the positive quadrant is shown in Figure 5.22. This last displacement cycle can be seen to have been completed, with the actuator pulling the specimen back to zero displacement. The peak load for this monotonic push is approximately 5000 lbs. (230 plf). This is still about half of the peak specimen capacity.

At stop of testing, there was no particular indication that similar capacity could not continue for larger drift ratios should additional actuator capacity have been available.

As previously noted, the recorded drifts for Specimen C-1 differ somewhat from the drifts that were targeted by the loading protocol due to the practical limits of actuator control; see Table 5.4). Specimen C-1 loads at the targeted drift levels have been interpolated from the envelope curves and are summarized in Table 5.5.

Documentation of the specimen's condition during testing included visual observations and photographs. These occurred at the designated hold points in the loading protocol. The observed behaviors included plaster cracking, spalling and separation from the wood lath, siding nail partial pull through and partial withdrawal, and many other details that were documented over a range of drift levels.

To aid in the tracking and photographing of damage, the damage was marked on the specimen during testing using colored pens. For marking of cracking, a line was drawn alongside the length of the crack and a tick mark was drawn at the observable crack end, along with a numerical indication of the drift ratio at which the crack was first noted. Other damage was marked in a similar manner. Different colors were used as follows: the damage occurring in the first push (towards the west) to each of the drift ratio was marked with a black marker. Red and blue markers were used for the first pull (to the east) peak and back to zero displacement, respectively.

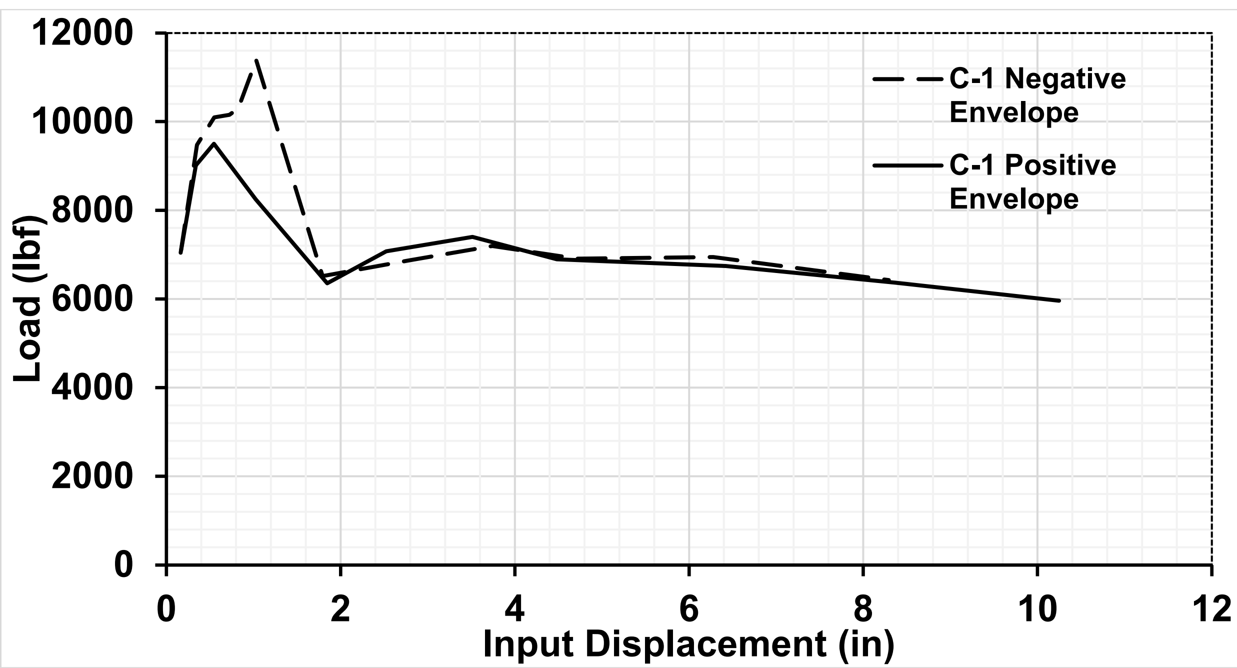

Figure 5.23 **Specimen C-1 envelope curves for positive and negative quadrants superimposed. Specimen weight including lead weight and loading beam is approximately 9 kips. Seismic mass tributary to the specimen is anticipated to be approximately 18 kips.**

Table 5.5 Summary of load/displacement data for Specimen C-1 interpolated from envelope curve.

Interpolated drift	Loading direction	Interpolated load (lbs)	Interpolated unit load (plf)	Interpolated load/ interpolated peak (%)
0.2% (0.192 in.)	Push	7,410	337	75
	Pull	7,370	335	78
	Average	7,390	336	76
0.4% (0.384 in.)	Push	9,570	435	94
	Pull	9,120	415	97
	Average	9,350	425	96
0.6% (0.576 in.)	Push	10,110	460	99
	Pull	9,420	428	100
	Average	9,770	444	100
0.8% (0.768 in.)	Push	10,220	465	100
	Pull	8,920	405	95
	Average	9,570	435	98
1.4% (1.344 in.)	Push	9,390	427	92
	Pull	7,510	341	80
	Average	8,450	384	86
2% (1.92 in.)	Push	6,560	298	64
	Pull	6,430	292	68
	Average	6,500	295	67
3% (2.88 in.)	Push	6,900	314	68
	Pull	7,190	327	76
	Average	7,050	320	72
4% (3.84 in.)	Push	7,170	326	70
	Pull	7,230	329	77
	Average	7,200	327	74
6% (5.76 in.)	Push	6,930	315	68
	Pull	6,790	309	72
	Average	6,860	312	70
8% (7.68 in.)	Push	6,590	300	64
	Pull	6,500	295	69
	Average	6,550	298	67
10% (9.6 in.)	Push	6,170	280	60
	Pull	6,100	277	65
	Average	6,140	279	63
12% (11.52 in.)	Push	5,830	265	57
	Pull	5,760	262	61
	Average	5,800	264	59
`14% (13.44 in.)	Push	5,570	253	55
	Pull	5,450	248	58
	Average	5,510	250	56

The following provides highlights of these observations. Detailed documentation of observations at each drift level is provided in Appendix C.

The building was thoroughly inspected before the start of testing. No cracking or other signs of damage was observed. Damage was first observed to occur on the very first push direction displacement to 0.2% drift. This included a popping sound, which signaled (a) the initiation of plaster cracks in tension zones at door and window corners, and (b) the initiation of small puckers indicating plaster finish coat buckling in compression zones; see Figure 5.24. The same behavior occurred in the subsequent pull displacement to 0.2% drift. It had not been anticipated that damage would be occur at such a low drift ratio. The peak load levels at 0.2% drift were 7040 and 7100 lb., between 60 and 70 % of the peak specimen capacity.

The plaster finish coat started spalling during displacement cycles to 0.4% drift; spalling of the full-thickness (multi-coat) plaster started during displacement cycles to 0.6% drift; see Figures 5.25 and 5.26). During displacement to 0.6% drift, plaster keys started breaking off of the back side of the plaster and falling down into the wall cavity between studs, and the plaster started pulling away from the wood lath, particularly around the windows and doors; see Figure 5.27. By the end of displacement cycles to 1.4% drift, approximately half of the plaster had fallen, or was loose and appeared to be about to fall. During the 1.4% drift displacement cycles, marking of plaster cracks became impractical and was discontinued; see Figure 5.28.

Plaster on the 20 ft-long north and south walls had substantially fallen off by the end of displacement to 4% drift, with plaster remaining on the end walls and in patches towards the top and bottom of the north and south walls. After the plaster had fallen off, plaster keys often remained wedged between the wood lath boards, and then incrementally fell out in later cycles. The plaster keys appeared to have provided enough connection between the wood lath boards that the lath boards and their nails continued to contribute to the specimen capacity; see Figure 5.29. Eventually most keys fell out, and in local areas buckling of the wood lath could be observed. There was no degradation observed to the wood lath or its nailed connection to the studs during testing.

During testing, there were a number of audible indicators of damage. These included the previously mentioned popping sounds associated with initial plaster cracking at 0.2% drift. In addition, a rainfall sound was heard, which was associated with the plaster keys breaking off and falling down the stud cavity to the wall bottom plate. The rainfall sounds from falling keys was noticed starting at 0.8% drift and continued through the balance of the testing.

Through the course of the testing the wood siding was observed to remain in generally good condition without visible damage that would be of safety concern. Slight pull through of the siding nail heads, slight withdrawal of the nail heads, and limited hairline cracks from nail heads and moving along the length of the siding boards were noticed and marked starting at approximately 1.4% drift.; see Figure 5.30. At 4% drift, gapping started to be noticed between the back face of the siding boards and the studs; see Figure 5.31. This was initially noticed to be about 1/16-in. and never increased to significantly more than this. During testing, the siding boards were never seen to bear against each other along their length. In some cases, the gaps between boards got close to closing at the compression end of the specimen but became wider at the uplift end and were not bearing or transferring shear through friction along their length.

During testing there were some indicators of global overturning behavior, including signs of limited downward movement at the compression end of the specimen and uplift at the tension end. It is believed that this global overturning behavior led to damage seen at the bottom of the end wall plaster starting at 0.4% drift; see Figure 5.32. Starting at 7% drift, gaps were noticed opening up at the floor level between the studs and the wall bottom plate and the door trimmers. Cracking of the siding at base of the end walls was first noticed at the east end wall at 9% drift, and later also occurred at the west end wall; see Figure 5.33.

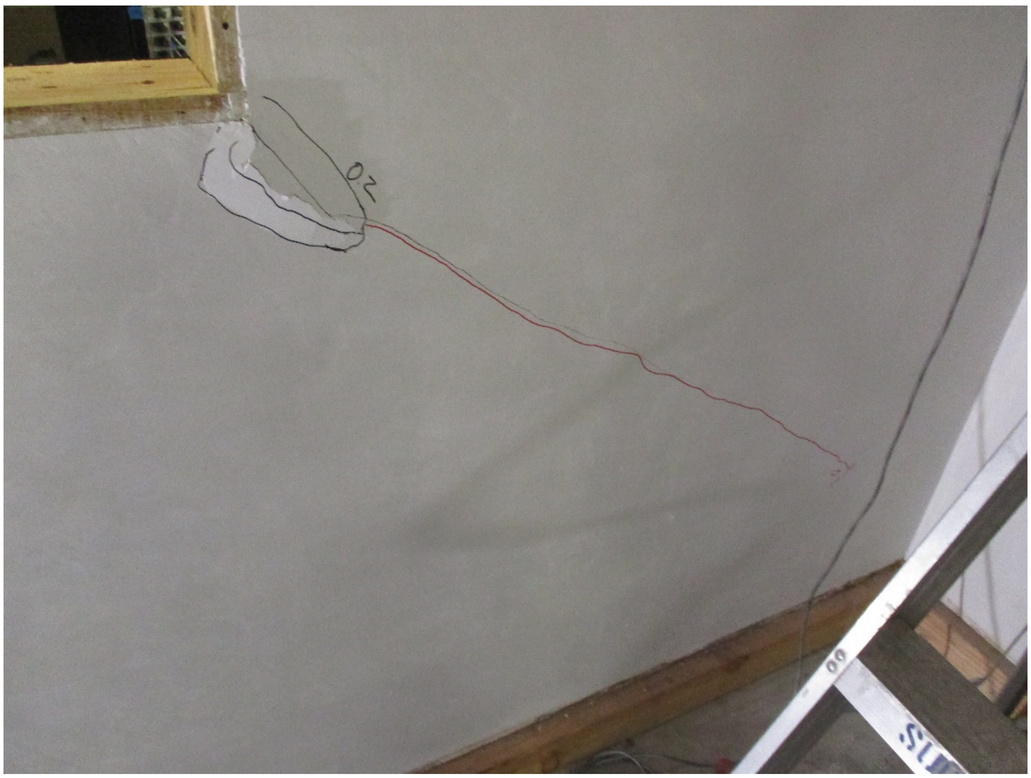

Figure 5.24 Plaster cracking and finish coat buckling at 0.2% drift.

Figure 5.25 Plaster finish coat spalling at 0.4% drift.

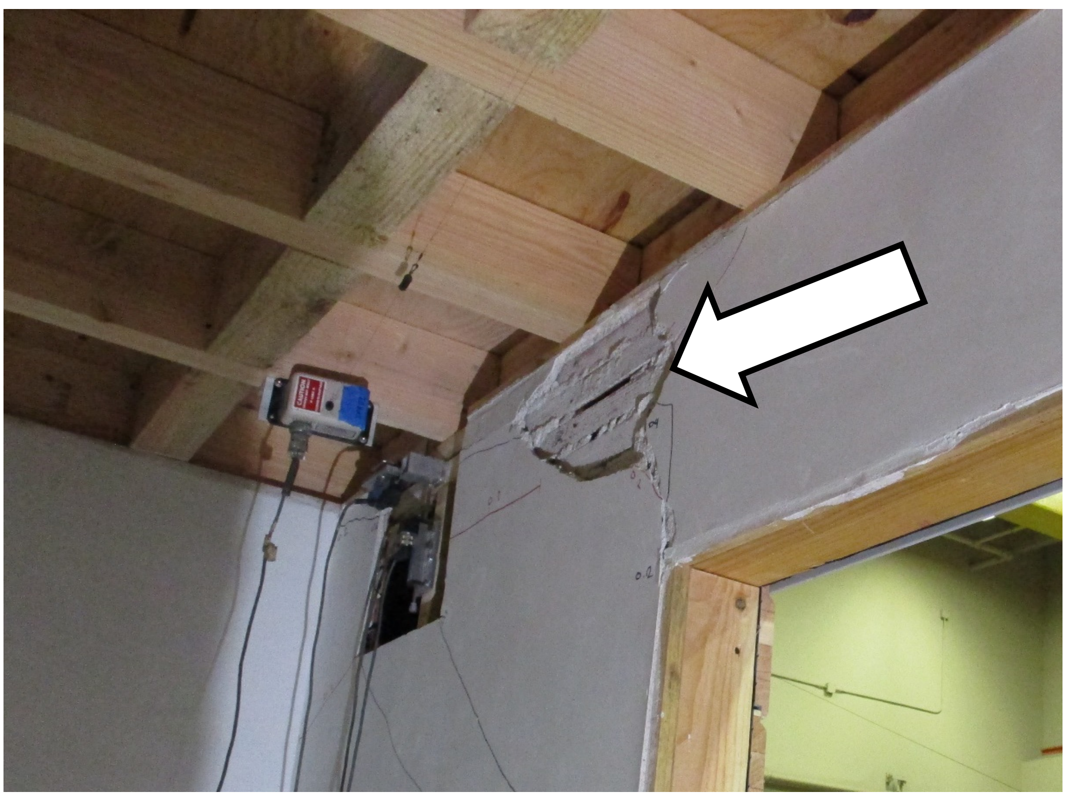

Figure 5.26 Spalling of plaster at 0.6% drift.

Figure 5.27 **Plaster damage at 0.6% drift ratio. Face of plaster originally installed flush with and struck off to trim board now has approximately 5/8-in. out-of-plane offset by window. This indicates that the plaster is no longer attached to the wood lath.**

Figure 5.28 **Extensive spalling of plaster at 1.4% drift.**

Figure 5.29 **Plaster keys still in place between wood lath boards at 4% drift.**

Figure 5.30 **Hairline splitting of siding and partial nail head pull through observed between 1.4% and 3% drift.**

Figure 5.31 Slight gapping between siding boards and studs at 4% drift.

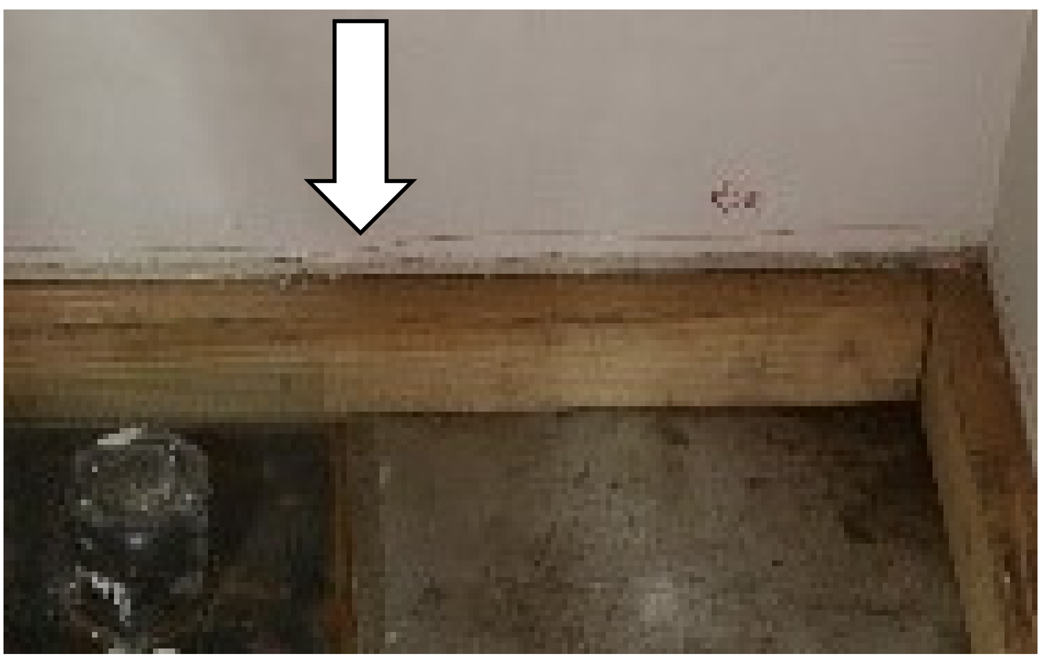

Figure 5.32 Damage to base of end wall plaster starting at 0.4% drift, believed to be due to global uplift.

Figure 5.33 Cracking of siding boards at the east-end wall.

5.11 SPECIMEN C-2 TEST RESULTS

Similar to Specimen C-1, the lateral force versus lateral displacement of Specimen C-2 was recorded using embedded instrumentation in the actuator to measure input displacement. This data is shown in Figure 5.34 and summarized in Table 5.6. The peak lateral load in the push direction was 90,000 lbs and in the pull direction was 82,100 lbs. Both occurred at a drift of between 2-1/2 and 2-3/4 in. (2.7% to 2.9% drift).

The overall character of the envelope curves in the push and pull directions was very similar up to approximately 2-1/2% drift, as seen in the superimposed positive and negative quadrant envelope curves in Figure 3.35. Beyond this, the envelope curve for the negative quadrant is somewhat lower than the positive quadrant.

There was a drop in peak load in both the positive and negative quadrants in the displacement cycles following the peak shear capacity cycles. Specimen C-2 loads dropped to approximately 60% of peak shear capacity (a capacity reduction of approximately 40%) at a drift ratio between 4% and 5%. Beyond this, the load continued to drop, reducing to approximately 30% of peak shear capacity at approximately 6% drift. This behavior was significantly different than Specimen C-1, which maintained a significant portion of peak shear capacity to much higher drift ratios.

Similar to Specimen C-1, the recorded drifts for Specimen C-2 (Table 5.6) differ somewhat from the drifts that were targeted by the loading protocol due to the practical limits of actuator control. Specimen C-2 loads at the targeted drift levels have been interpolated from the envelope curves and are summarized in Table 5.7.

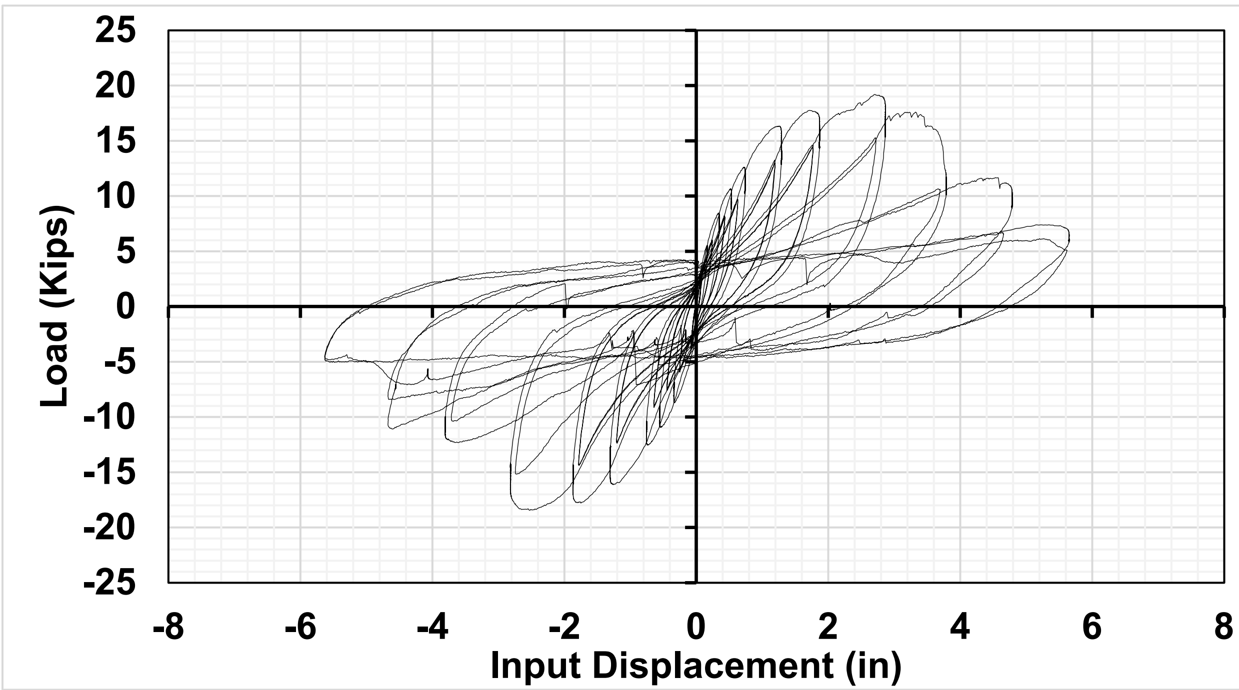

Figure 5.34 Lateral load versus lateral actuator input displacement of Specimen C-2.

Table 5.6 Summary of test data for Specimen C-2.

Loading direction	Displacement (in.)	Drift ratio[1] (%)	Peak load (lbs)	Peak unit load (plf)	Cycle peak/ overall peak (%)
First loading direction: push to west	0.0917	0.10	3,990	181	22
	0.3208	0.33	8,370	380	46
	0.5482	0.57	10,660	485	58
	0.7454	0.78	12,450	566	68
	1.3936	1.5	15,630	710	85
	1.7188	1.8	17,710	805	97
	2.5805	2.7	18,350	834	100
	3.8017	4.0	11,620	528	63
	4.5202	4.7	10.860	494	59
	5.6244	5.9	4,540	206	25
Second loading direction: pull to east	0.1691	0.18	4,910	223	26
	0.3570	0.37	8,590	390	45
	0.5191	0.54	10,090	459	53
	0.7322	0.76	11,920	542	62
	1.2750	1.3	16,260	739	85
	1.6919	1.8	17,710	805	93
	2.7446	2.9	19,100	868	100
	3.4011	3.5	17,380	790	91
	4.5019	4.7	11,600	527	61
	5.6220	5.9	6,470	294	34

1. The noted drift ratio is the imposed actuator displacement divided by the wall clear height of 96 inches. For drift ratios above 2% the actuator displacement is anticipated to include a combination of slip of the wall bottom plate and the drift imposed on the wall.

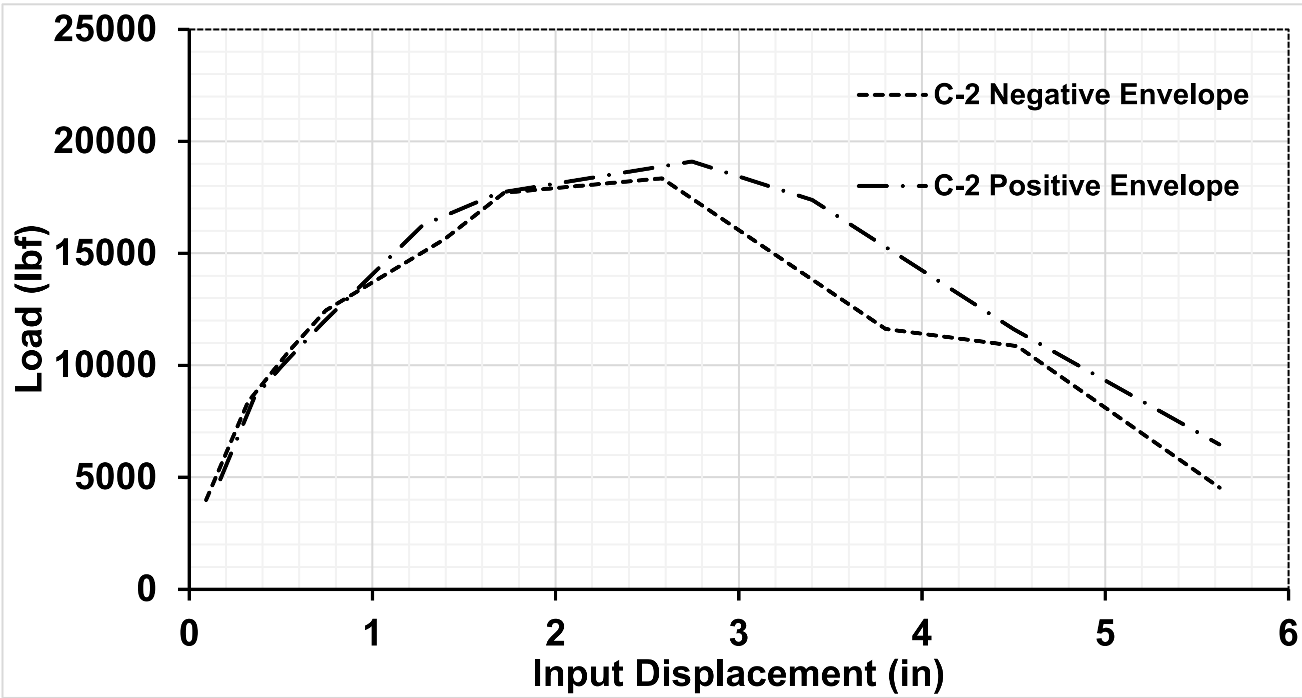

Figure 5.35 Specimen C-2 positive and negative quadrant envelope curves superimposed. Specimen weight including lead weight and loading beam is approximately 5.9 kips. Seismic mass tributary to the specimen is anticipated to be approximately 11.8 kips.

Table 5.7 **Summary of load/displacement data for Specimen C-2 interpolated from envelope curve.**

Interpolated drift[1] % (in.)	Loading direction	Peak load (lbs)	Peak unit load (plf)	Cycle peak/ overall peak (%)
0.2% (0.192)	Push	5,910	269	33
	Pull	5,360	244	29
	Average	5,640	256	31
0.4% (0.348)	Push	9,010	410	50
	Pull	8,840	402	47
	Average	8,930	406	50
0.6% (0.576)	Push	10,920	496	61
	Pull	10,580	481	56
	Average	10,750	489	60
0.8% (0.768)	Push	12,560	571	70
	Pull	12,200	554	65
	Average	12,380	563	69
1.4% (1.344)	Push	15,310	696	86
	Pull	16,500	750	88
	Average	15,910	723	89
2.0% (1.92)	Push	17,860	812	100
	Pull	18,010	819	96
	Average	17,940	815	100
3% (2.88)	Push	16,700	759	93
	Pull	18,740	851	100
	Average	17,720	805	99
4% (3.84)	Push	11,580	526	65
	Pull	15,080	685	80
	Average	13,330	606	74
6% (5.76)	Push	9,260	421	52
	Pull	10,240	465	52
	Average	9,750	443	54

1. The noted drift ratio is an interpolation of the imposed actuator displacement divided by the wall clear height of 96 inches. For drift ratios above 2% the actuator displacement is anticipated to include a combination of slip of the wall bottom plate and the drift imposed on the wall.

As occurred with Specimen C-1, documentation of Specimen C-2 conditions during testing included visual observations and photographic documentation. These occurred at the designated hold points in the loading protocol. The observed behaviors included damage to taped gypsum wallboard joints, rotation of plywood siding panels, and many other details, documented over a range of drift levels.

To aid in the tracking and photographing of damage, the damage was marked on the specimen using colored pens as follows: damage in the first push to each of the drift ratios was marked with a black marker, and the red and blue markers were used for the first pull peak and back to zero displacement, respectively.

The following provides highlights of these observations. Detailed documentation of observations at each drift level is provided in Appendix C.

Prior to the start of testing, no damage was evident in the plywood siding or the gypsum wallboard interior. Damage was initially occurred with hairline cracking of the joint compound and limited puckering at joint tape in the gypsum wallboard starting at 0.4% drift. This damage at the gypsum wallboard joints increased in severity and extent at 0.6% drift; see Figure 5.36. At 0.8% drift, indications of nails pops were noted as hairline cracking around nail heads began; see Figure 5.37. Over the balance of the testing, the disruption seen at the gypsum wallboard panel joints continued to increase, with the panel joints eventually rotating fairly independent of each other; see Figure 5.38.

As the specimen started to experience global overturning behavior, the gypsum wallboard nails at the end-wall bottom plates experienced edge tear out to the bottom of the panel, gouging out the gypsum core and leaving a pile of debris below; see Figure 5.39. This behavior was also observed on the north and south walls as uplift in those walls increased. At the side of the windows and doors, the gypsum wallboard was observed to separate from the wall framing, and slots were observed to be gouged in the back face of the gypsum wallboard; see Figure 5.40. Beyond this and limited local breakage, the gypsum wallboard panel remained in reasonably good condition throughout the testing, such that it might be possible to repair the gypsum wallboard with limited re-nailing and re-taping rather than complete removal and replacement.

Signs of rotation of the plywood siding were first noted at 1.4% drift due to the relative slip of abutting panels at vertical joints; see Figure 5.41. This can be described as “working” of the siding rather than damage. This rotation continued, with very minor sliding of the siding at the windowsill seen at 2% drift. At 3% drift, a tearing fracture occurred in one section of siding that had been cut for a window opening; see Figure 5.42]. This was the only tear noted during testing, which extended for less than 1 ft. At 3% drift, notable slip was observed at the vertical siding joints at the door and window headers, with some pull through of the sheathing nail heads noted; see Figure 5.43. This behavior was generally limited to the areas above the doors and above and below the windows, without extending into the full-height wall piers. The reader is reminded that at these vertical joints, in an intended miss-installation was used, resulting in only one of the two abutting panels being edge nailed, which accentuated vertical slip at these joints. Another significant behavior observed was at the end walls where the siding was pulled up and slid longitudinally during loading in one direction, and then the wall sat back down on the bottom of the siding panel in reverse loading, fracturing the bottom of the siding; see Figure 5.44. This behavior increased in severity over the course of the testing.

At the end of testing, the majority of the plywood siding still appeared to be functioning as a seismic bracing element as intended and is not thought to have degraded significantly. This is because the fastening of the wall to the foundation was the weak link, limiting the load transmitted to the plywood siding. The nailing of the siding, with only one of the two panels edge nailed at abutting vertical joints, was observed to result in locally higher slip at panel joints, and local distortion of window sills and top plates, but was not seen to inhibit to any degree the ability of the siding at provide in-plane bracing for seismic loads.

The performance of Specimen C-2 was largely driven by the performance of the nailed connection between the 2 × 4 wall bottom plates and the 4 × 6 nailers below. The use of this detail had been selected with the understanding that it would represent a lower bound condition for the load path at the base of the wall. This lower bound condition was confirmed and quantified by the testing. Starting at displacements of 1.4% drift, uplift of the bottom plate off of the 4 × 6 nailer was observed; see Figure 5.45. At this drift, a gap of 3/8 to 1/2-in. between the bottom plate and 4 × 6 nailer was observed. The extent and severity of the uplift gap progressed throughout the testing. In addition, longitudinal sliding of the specimen was noted at a drift of 2%. By the time the drift reached 4%, the bottom plates at the doors were simultaneously experiencing approximately 1 in. of uplift and several inches of slip in both the longitudinal and transverse directions; Figures 5.46–5.48.

In addition, uplift occurred at the end walls and extended several feet along the length of the north and south walls; see Figures 5.49 and 5.50. As this occurred, a substantial number of nails between the bottom plate and 4 × 6 were withdraw under uplift displacements. As the wall sat back down under load reversals, some bottom plate nails were pushed up with heads withdrawing from the bottom plate, while others were crushed under the bottom plate and bent. Because much of the bottom plate lifted up during the lateral loading, partially withdrawn nails were required to simultaneously carry both lateral loads and withdrawal loads; see Figure 5.51. Eventually, a substantial number of the nails were fully withdrawn and no longer able to transmit load between the wall bottom plate and the foundation. At the end of the testing, the specimen was being pushed approximately 4 in. in each direction of the top of the foundation and 4 × 6 nailers; see Figure 5.52.

Twice during testing, restraining straps were added to avoid premature failure of the test specimen. The first restraint was added to the center wall piers during the course of cycles to 4% drift; see Figure 5.53. A second restraint was added at the west wall piers before the start of cycles to 6% drift; see Figure 5.54. The behavior of concern that caused the restraints to be added can be seen in Figures 5.46 to 5.48. At the door openings, the wall bottom plates had out-of-plane offsets of several inches. It was feared that under reverse loading, the base of the wall might be pushed outward and off of the edge of the foundation, possibly resulting in local collapse. The testing results up through the first push and pull cycles to 4% drift were completed prior to installation of the restraints and can be considered fully valid. Starting with the balance of the cycles to 4% drift, the results of the testing need to be clarified as having occurred with the restraints in place. Had the restraints not been installed, it is possible that the test specimen would not have achieved 5% drift.

Figure 5.36 Specimen C-2 gypsum wallboard joint cracking and disruption at 0.6% drift.

Figure 5.37 Specimen C-2 gypsum wallboard nail pops at 0.8% drift.

Figure 5.38 Specimen C-2 gypsum wallboard panels with significant joint deterioration.

Figure 5.39 Piles of gypsum debris from Specimen C-2 where bottom plate nails have pulled out of gypsum wallboard.

Figure 5.40 Specimen C-2 gypsum wallboard at side of door. The gypsum wallboard has separated from wall framing, and nail has cut a vertical gouge in the gypsum wallboard. The red line shows the length of the gouge, estimated at 1 in.

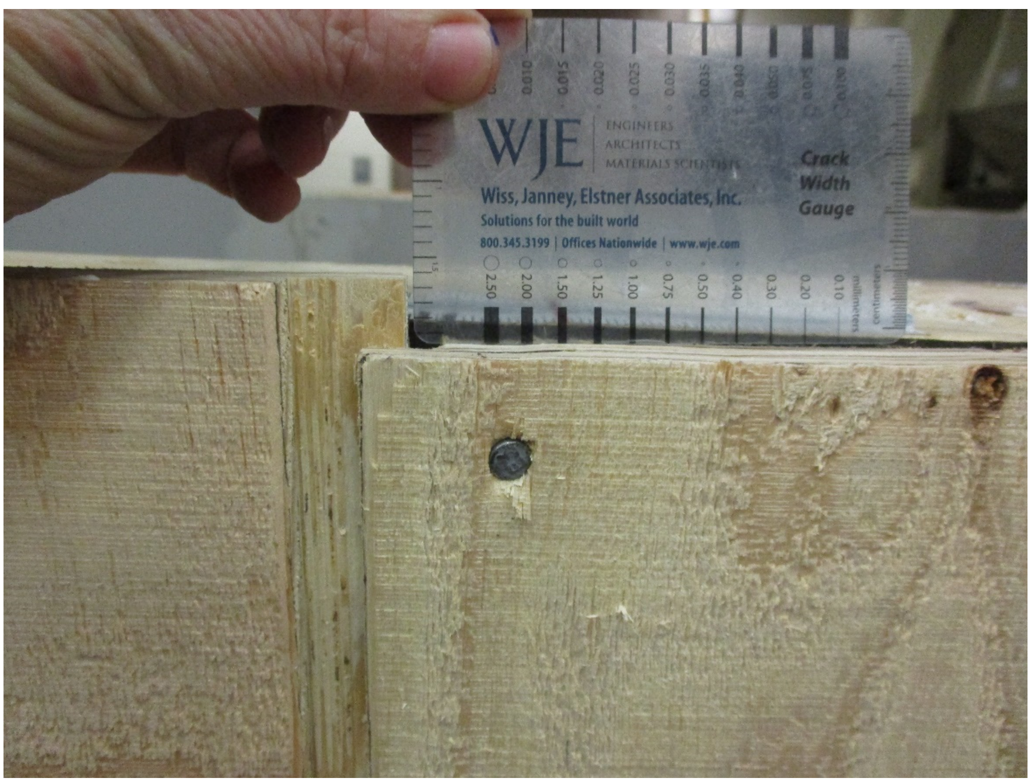

Figure 5.41 Specimen C-2 vertical slip of plywood siding at vertical joint under the window. Panel on right-hand side is edge nailed along the vertical joint. Panel on left-hand side is not edge nailed.

Figure 5.42 Specimen C-2 plywood siding fracture starting from window corner.

Figure 5.43 Specimen C-2 plywood siding vertical joint has slipped with some pull through of the nail heads.

Figure 5.44 Specimen C-2 east end wall has sat back down on top of panel siding, causing fracture. The bottom of the plywood siding became tucked under the wall bottom plate.

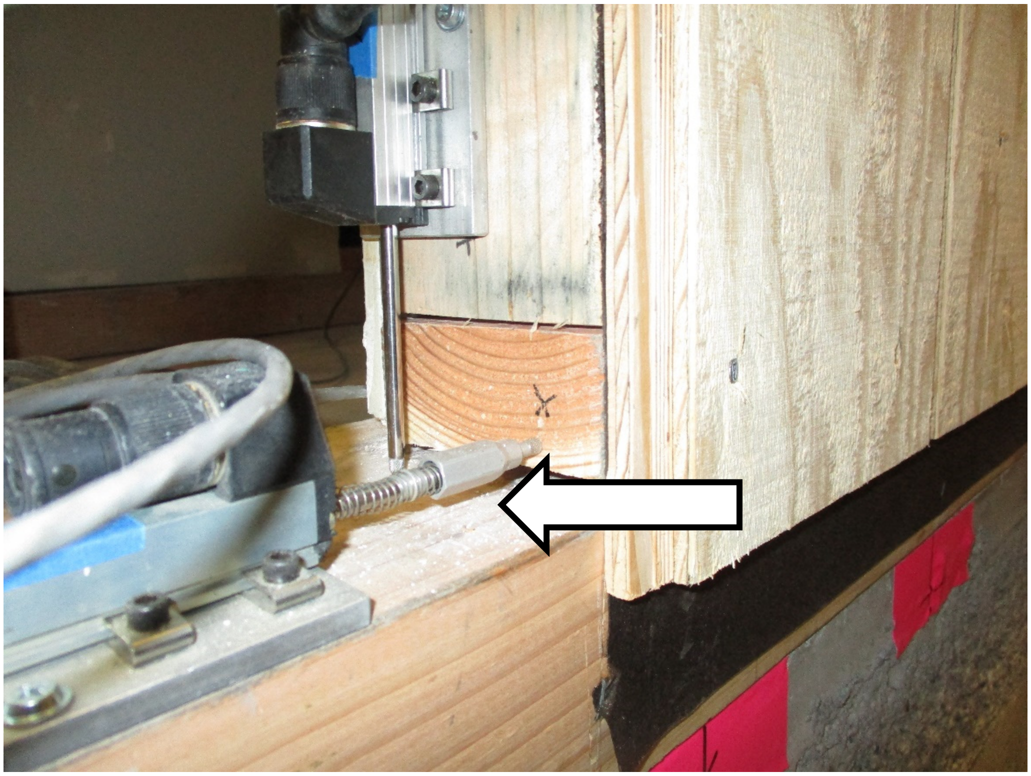

Figure 5.45 Specimen C-2 wall at door opening has uplifted between 3/8 and 1/2 in.

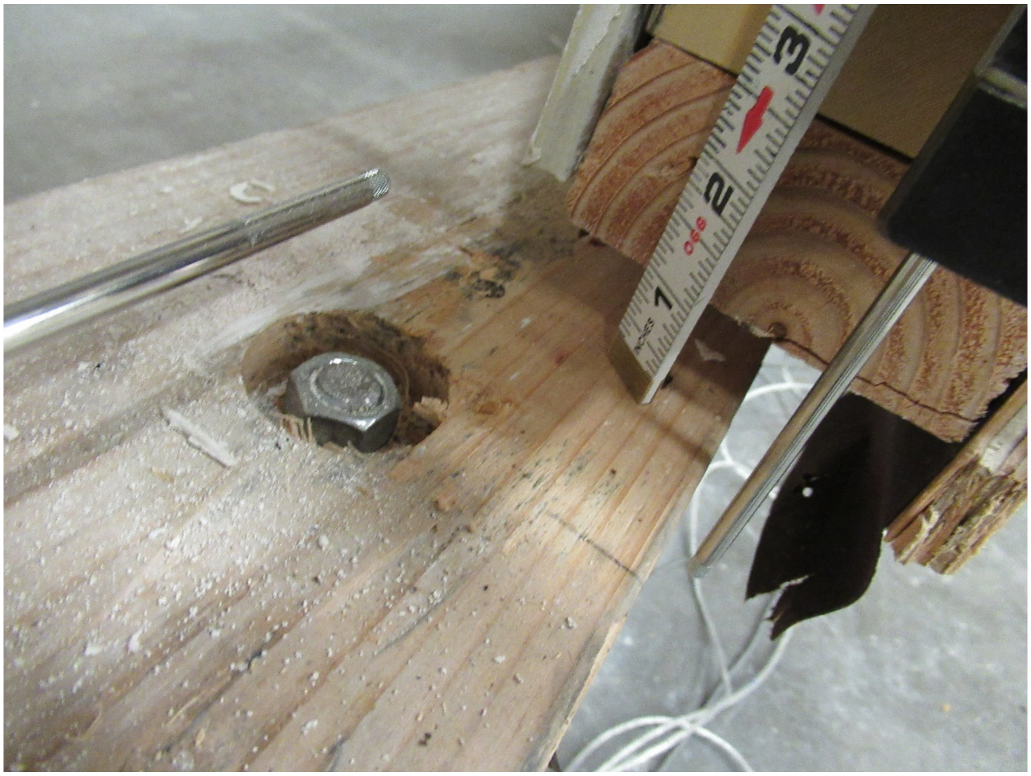

Figure 5.46 **Specimen C-2 wall bottom plate uplift of approximately 1 in. at door opening.**

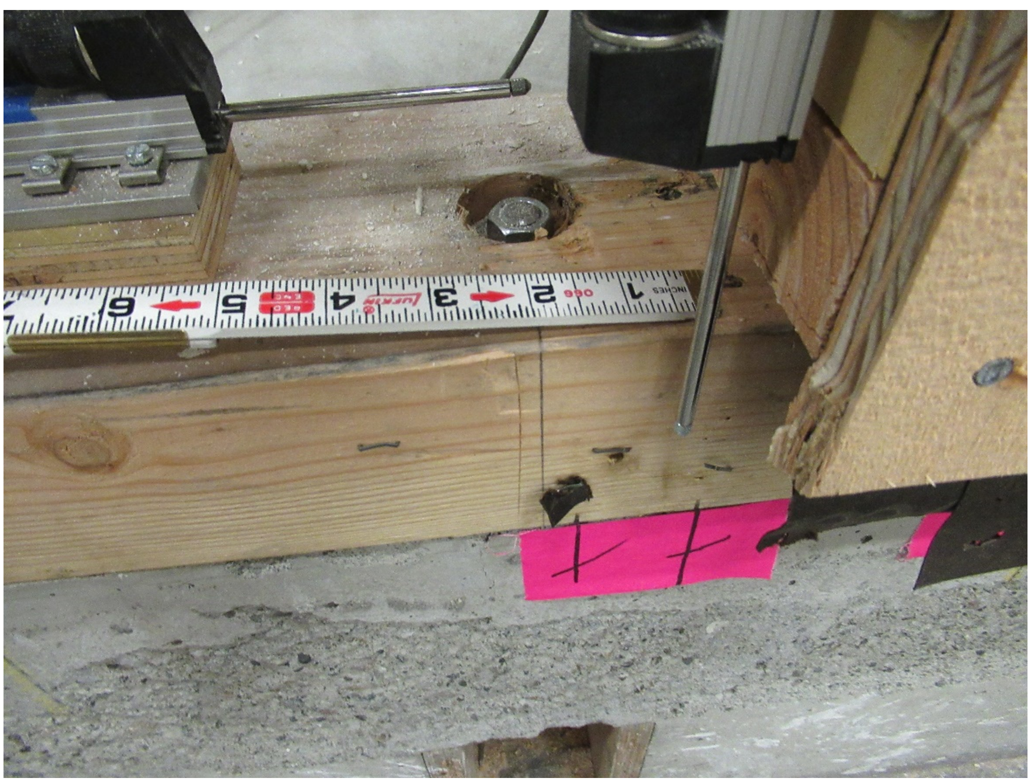

Figure 5.47 **Specimen C-2 wall bottom plate longitudinal slip of approximately 2 in. at door opening.**

Figure 5.48 Specimen C-2 wall bottom plate transverse slip of approximately 1-1/2 in. at door opening.

Figure 5.49 Specimen C-2 wall uplift in north wall extending over a distance of several feet.

Figure 5.50 Specimen C-2 close up of north wall bottom plate uplift from 4 × 6 nailer near wall end. Bottom plate nails can be seen to be withdrawing from the 4 × 6 nailer.

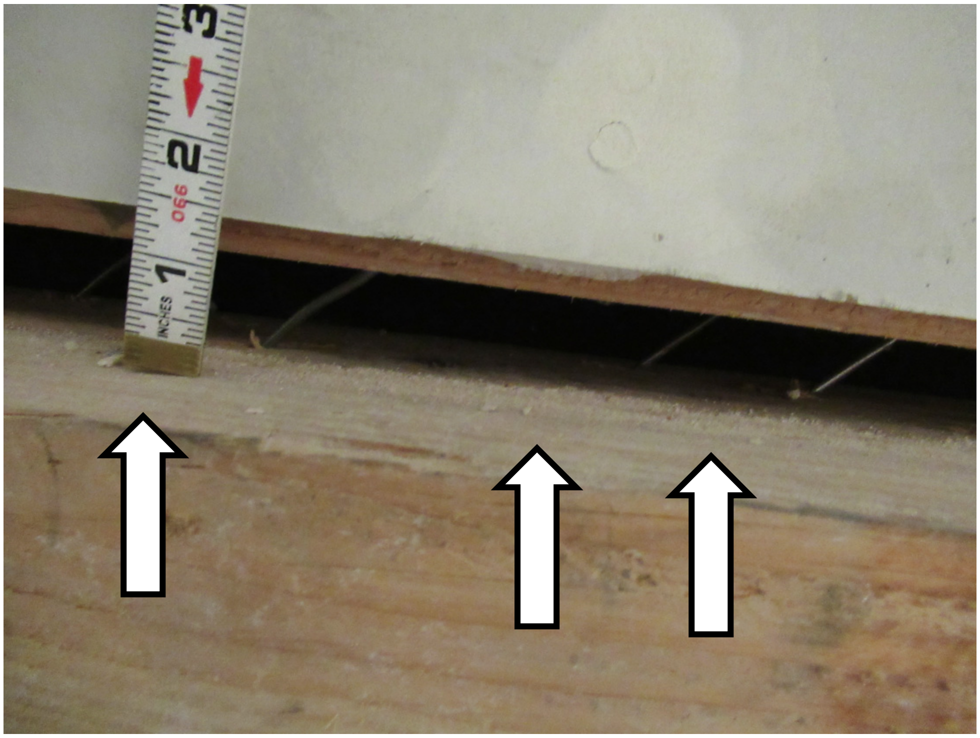

Figure 5.51 Specimen C-2 wall bottom plate is displaced vertically and longitudinally. The bottom plate nails being pointed to are withdrawn from the 4 × 6 and racked to approximately 45°.

Figure 5.52 The base of the wall of Specimen C-2 has slid approximately 4 in. longitudinally along the 4 × 6 nailer.

Figure 5.53 Strap restraint is added to Specimen C-2 following initial cycles to 4% drift but before the balance of cycles. The strap served to keep the base of the center wall piers from further slip in the transverse direction that might have resulted in the wall piers moving off of the foundation.

Figure 5.54 Specimen C-2 with a second strap restraint added at the west wall piers prior to start of cycles to 6% drift.

5.12 POST-TEST FINISH REMOVAL

Following completion of Specimen C-1 and C-2 testing, selected portions of the finish materials were removed to allow observation of the underlying materials and any hidden damage. Details of these observations are provided in Appendix D.

5.13 DISCUSSION OF RESULTS

This section provides discussion of results for Specimen C-1, followed by results for Specimen C-2, and discussion comparing the performance of Specimen C-1 versus C-2.

Specimen C-1 was observed to have a reached a high percentage of the peak shear capacity in the very first displacement cycle to 0.2% drift. Later comparisons to other available test results indicate that this high initial stiffness is not unusual. More unexpected were the significant popping noises and cracking and spalling of the plaster occurring in the very first displacement cycles. This suggests that the plaster was damaged, possibly requiring the initiation of repair at much lower drift levels than the materials testing in other PEER–CEA Project specimens.

As previously discussed, the peak capacities in the push and pull directions were noticeably different; see Figure 5.23. This appears to be consistent with the observed brittle behavior up to peak shear capacity. The difference in capacities is a logical outcome of damage occurring in the first push peak displacement affecting the capacity in the subsequent pull displacement.

Following the peak shear capacity, the post-peak capacities remained remarkably level at about 300 plf to 16% drift. Although similar behavior had been seen in the past for horizontal lumber sheathing, Specimen C-1 appeared to gain additional capacity from the remaining plaster keys and their interaction with the nailed wood lath. This is based on an anticipated peak shear capacity of approximately 200 plf for the siding acting alone [FEMA 2012]. The retention of capacity out to 16% drift is significantly different from assumptions generally made in numerical studies and from the behavior seen in wood structural panel braced walls. This will be discussed in more detail below.

Specimen C-1's peak unit shear capacity of approximately 470 plf (averaged from Table 5.4 peak values) and displacement at peak shear capacity can be compared to prior testing of stucco finishes with attention given to boundary conditions [Arnold et al. 2003] and prior plaster on wood lath testing where boundary conditions were not considered [FPL 1956; Schmid 1984; and Carroll 2006]; see Table 5.8. While the peak capacities seen in Table 5.8 are widely varying, it is notable that the displacement at peak shear capacity is very uniform, whether or not attention was given to boundary conditions. Envelope curves from available testing considered in development of numerical modeling for *FEMA P-807* [FEMA 2012] and *FEMA P-1100* [FEMA 2019] are shown in Figure 5.55, with the envelope curve for Specimen C-1 superimposed. Note that the data plotted in Figure 5.54 is a combination of plaster on wood lath only [FPL 1956; Schmid 1984] and plaster on wood lath in combination with horizontal wood siding (PEER–CEA) and [Carroll 2006].

This figure suggests that the peak shear capacity for plaster on wood lath is highly variable, and that Specimen C-1 falls at the lower end of the range of observed strengths. There are several aspects that could have resulted in the strength for Specimen C-1 falling towards the bottom end of available data, even though constructed in controlled laboratory conditions. Two primary aspects that bear consideration are the materials and workmanship and the age of the plaster at testing. Plaster on wood lath is an archaic construction type that is rarely used today. Although utmost care was taken to use representative materials and installation techniques, and work was performed by contractors that are regularly involved in installing similar systems, the materials or workmanship could have varied from that used in the 1930s and 1940s in a way that affected performance. These tests are being compared to testing by FPL [1956] and Schmid [1984] that was conducted on wall assemblies constructed circa 1930, and test results from Carroll [2006] using plaster constructed in the laboratory with very non-typical materials and techniques.

Another aspect of Specimen C-1 that bears consideration is the age of the plaster at testing. Specimen C-1 was tested approximately one month after installation of the plaster finish coat. Although this was decided to be a reasonable age to allow curing to near target strength, it is possible that due to age the physical properties of the plaster varied from plaster in place since the 1930s. This is a recognized and unavoidable limitation of laboratory testing.

Worth pointing out in Figure 5.55 is that Specimen C-1 retains post-peak shear capacity to significant drift ratios while none of the other specimens do. This retention of capacity is more consistent with available test data for horizontal wood sheathing and siding tested alone. Regardless, the retained capacity to 16% drift far exceeds published test information for any of these materials.

Table 5.8 Comparison of Specimen C-1 peak capacities and drifts to prior testing.

Testing	Materials	Boundary conditions considered?	Peak unit shear capacity (plf)	Displacement at peak shear capacity (in.)
	Plaster on wood lath, horizontal wood siding	Yes	470	1.1
	Stucco exterior, gypboard interior	Yes	1880	1.0
	Stucco exterior, gypboard interior	Yes	1590	1.1
	Plaster on wood lath	No	1040	1
	Plaster on wood lath	No	470	1
	Plaster on wood lath, horizontal wood siding	No	655	1

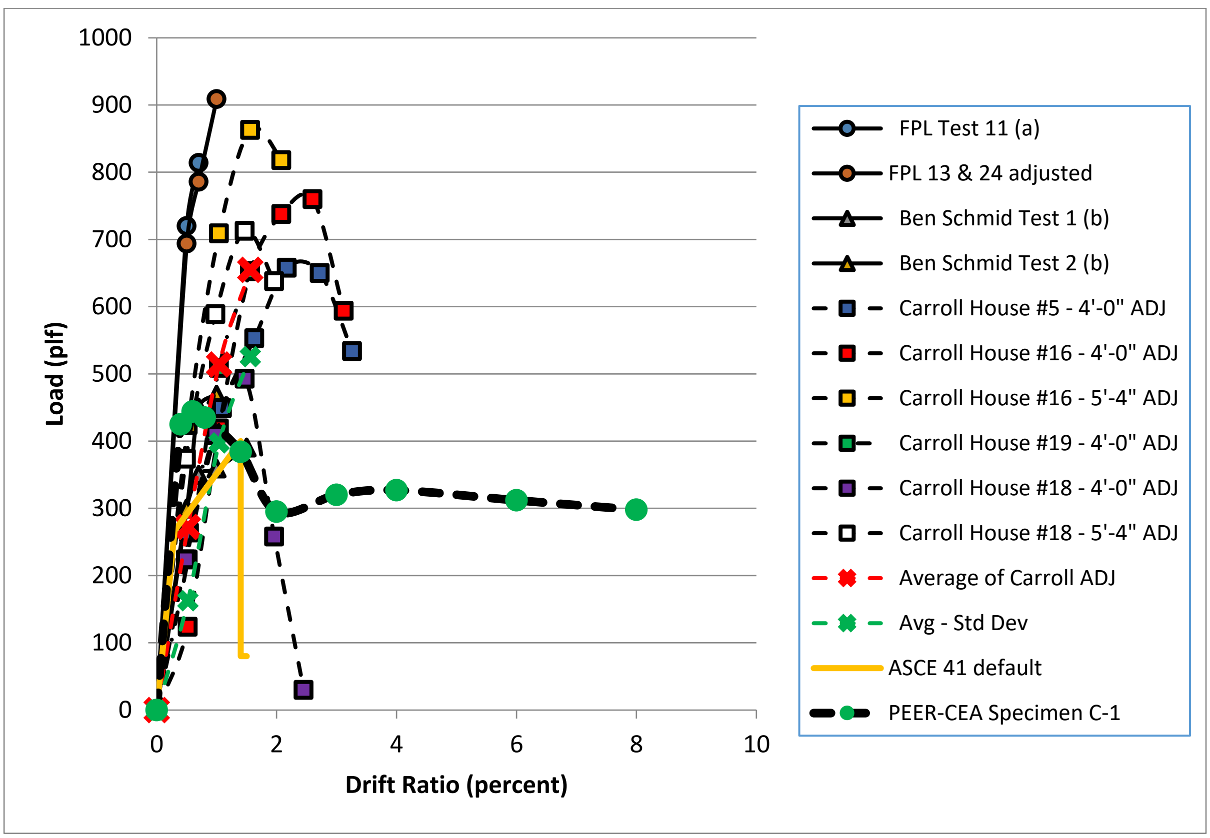

Figure 5.55 Envelope curves for plaster on wood lath bracing walls, with and without horizontal wood siding, and with and without having consideration given to boundary conditions based on FEMA [2012c].

Specimen C-1's peak unit shear capacity of 470 plf (averaged from Table 5.4) can be compared to the nominal capacities assigned by SDPWS [AWC 2015]. Table 4.3D of SDPWS assigns horizontal lumber sheathing a nominal capacity of 100 plf for seismic and 140 plf for wind design. As the closest comparable tabulated system, Table 4.3C assigns a plaster on gypsum lath nominal capacity of 200 plf for both seismic and wind design. Summing the plaster on gypsum lath nominal capacity with the higher of the horizontal lumber sheathing capacities (without rules established for reduction when using combined materials) gives a summed nominal capacity of 340 plf, which is approximately 70% of Specimen C-1's peak shear capacity of 470 plf. Because the strength of these materials is not permitted to be combined in design, the ASD allowable unit shear assigned by SDPWS would be 200/2 or 100 plf, which is approximately 20% of Specimen C-1's peak shear capacity. As another point of comparison, ASCE 41 [ASCE 2017] provides a tabulated expected (peak) strength for plaster on wood lath of 400 plf, and horizontal lumber siding of 80 plf. If summed, these values would agree very well with the peak shear capacity of Specimen C-1. Because ASCE 41 does not permit these to be summed, a user would be limited to an expected strength of 400 plf for the plaster, which is approximately 85% of the test peak load of 470 plf. This suggests that the ASCE 41 expected strengths are generally in alignment with Specimen C-1.

Similar to the continuity of stucco in Specimens AL-1 and AL-2, the continuity of the plaster on wood lath in Specimen C-1 was an important design consideration. Although there are other potential aspects affecting peak strength, as noted previously, the information in Table 5.8 suggests that neither the inherent continuity of the plaster nor the larger size of the test component dramatically changed the displacement at peak shear capacity; in fact, the displacements at peak shear capacity are surprisingly uniform across the group. Further, the peak shear capacity of Specimen C-1 is at the lower bounds of available testing. This suggests that the effects of boundary conditions and test component size are not nearly as significant for plaster on wood lath as observed for stucco. Like Specimens AL-1 and AL-2, damage to Specimen C-1 tended to initiate at the door and window openings rather than the specimen boundaries. It is recommended that detailed comparisons of damage mechanisms between Specimen C-1 and other tested plaster on wood lath components would be of value to determine if mechanisms are similar across the range of testing.

There was still considerable benefit to the use of a 3D large-component specimen. Benefits included observation of a wider range of behaviors and damage mechanisms, particularly at corners and end walls.

One of the most notable aspects of Specimen C-2's hysteresis plot (Figure 5.34) is that it is remarkably similar to the hysteresis curves commonly observed in testing of plywood (wood structural panel) shear walls. Figure 5.56 provides one point of comparison from Gatto and Uang [2002]. Note: even with Specimen C-2 having no tie-downs to resist overturning uplift and having been purposely constructed with miss-nailing of the plywood siding, the overall load-deflection behavior is still very similar to other shear wall tests. Important aspects include the specimen reaching peak shear capacity at drift ratios of between 2% and 4%, with no appreciable residual capacity at a drift ratio of 6%. The reader is cautioned that Specimen C-2's behavior mechanisms and damage modes (including the withdrawal of nails at the bottom plate being the weak link) were considerably different than commonly observed in plywood shear-wall testing.

Specimen C-2's peak unit shear capacity of approximately 850 plf (averaged from Table 5.6). Two groups of testing from the CUREE-Caltech Woodframe Project [Gatto and Uang 2002; Pardoen et al. 2003] are included in Table 5.9 to provide points of comparison.

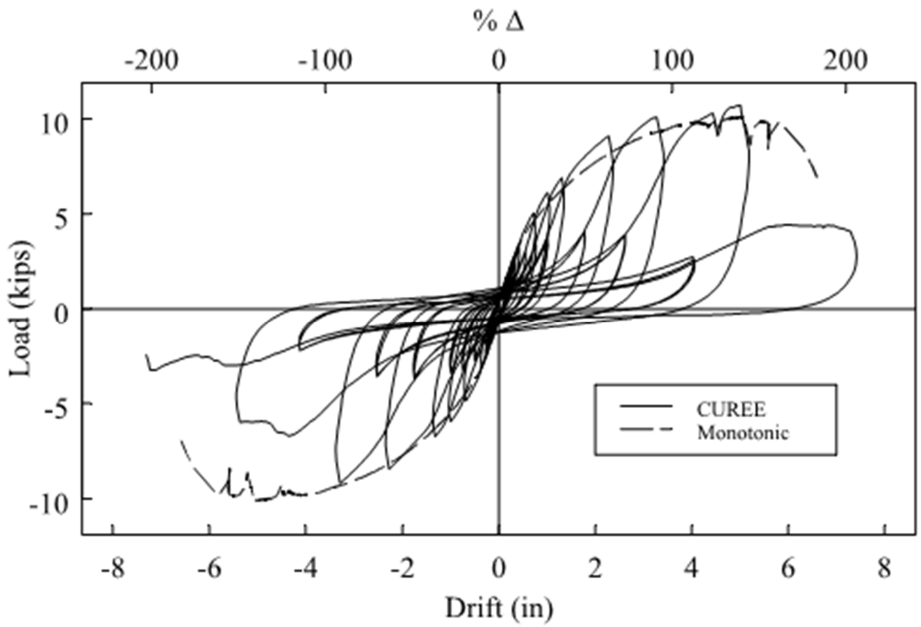

Figure 5.56 Hysteresis plot for an 8 ft × 8 ft plywood shear wall tested using the CUREE protocol (Figure 5.28b from Gatto and Uang [2002]).

Table 5.9 Comparison of Specimen C-2 peak capacities and displacements to prior testing.

Testing	Materials	Approximate peak unit shear capacity (plf)	Approximate displacement at peak shear capacity (in.)
Specimen C-2	Plywood siding exterior, 8d@6, gypboard interior	850	2.8
Gatto Test 6	15/32 STR I plywood 8 ft × 8 ft 8d box@4	1,300	5
Gatto Test 14	15/32 STR I plywood 8 ft × 8 ft 8d box@4, gypboard back side	1,400	5
Freund 4A	Plywood 8 ft × 16 ft fully sheated 8d@6	722	3
Freund 4B	Plywood 8 ft × 16 ft fully sheated 8d@6	762	1.5
Freund 5A	Plywood 8 ft × 16 ft with pedetrian door 8d@6	974	2
Freund 5B	Plywood 8 ft × 16 ft with pedestrian door 8d@6	805	2

Peak unit shears from Specimen C-2 are comparable to the test results from Freund et al. [2003], but notably less than either Gatto and Uang's value [2002]. Note: by the time Specimen C-2 reached peak shear capacity, slip was observed between the wall bottom plates and the 4 × 6 nailers. Because of this, the drift imposed on the wall may not have progressed much beyond 2 in. If this is true, the peak shear capacity of the plywood siding and gypsum wallboard might not have been reached due to the bottom plate slippage acting as a controlling mechanism. This is consistent with the lack of significant damage to the plywood siding on the wall piers.

There was minimal adverse effect on Specimen C-2 performance due to the intentionally included miss-installation of the siding. During testing, some very local additional slip and bending of sill framing and top plates occurred. These behaviors were largely overshadowed by the effect of the base of wall fastening and resulting uplift behavior. When considering the effect of the miss-installation, it should be noted that because one sheet of plywood covered most wall piers, the number of vertical joints that might have been adversely affected was small; additional effects from the missing nailing might have occurred if more substantial connections of the bottom plates had been provided, thus avoiding overturning as the primary failure mode.

Specimen C-2's peak unit shear capacity of 850 plf can be compared to the nominal capacities assigned by SDPWS [AWC 2015]. Table 4.3A the SDPWS assigns a nominal capacity of 320 plf seismic and 450 plf wind for 3/8-in. plywood siding nailed with 8d common nails at 6 in. on center. Table 4.3C assigns a gypsum wallboard nominal capacity of 200 plf for both seismic and wind design. Summing the higher (wind) plywood siding value and the gypsum wallboard (without reduction using combined materials rules), gives a summed nominal capacity of 650 plf, which is approximately 75% of Specimen C-2's peak shear capacity. Because the strength of these materials cannot be combined in design, the ASD allowable unit shear assigned by SDPWS for seismic design would be 320/2 or 160 plf, which is 19% of the test peak shear capacity. Note: the SDPWS' nominal capacities for plywood siding are intended to be applied to siding panels installed with uniform edge nailing at all panel edges. This testing was conducted with a common miss-installation, without edge nailing on one of the two edges at vertical abutting panel joints. There is no method available to determine a design capacity for this miss-installation, but a reduction in peak shear capacity to less than that for properly nailed sheathing should be anticipated.

The final failure mechanism of the specimen involved the withdrawal of practically all the nails fastening the wall bottom plates to the 4 × 6 nailers at the base of the structure. The combined withdrawal and shear created significant demands on the nails. As uplift of the specimen increased, the nails had to resist the combined withdrawal and shear loads, while also experiencing partial withdrawal reducing its capacity. Most of the nails eventually withdrew completely from the 4 × 6 nailers. Many were bent flat between the bottom plates and the nailers during load reversals. Eventually the wall structure could be fairly easily pushed back and forth across the 4 × 6 nailers and foundation. Restraints were added during testing to 4% drift, with a second restraint strap added during loading to 6% drift. Without the restraints, it is anticipated that the base of the wall piers at the doors would have spread and fallen off of the foundation. Although there was no clearly observed brittle failure, the failure mechanisms observed were severe and should be avoided as residents in these structures could be injured or killed. These mechanisms started to be observed at or just beyond the peak shear capacity. Unlike engineered plywood shear walls, for which post-peak loading is thought to be acceptable in a maximum considered earthquake, it is suggested that it would not be acceptable for the construction used in Specimen C-2.

While creating the most realistic boundaries conditions drove the choice to use a large, 3D test component for the stucco and plaster testing, the choice to use the similar component geometry for Specimen C-2 came more from the convenience of reusing the foundation and the laboratory test setup. Additionally, there were significant benefits to using this component type and size, including the ability to observe the impact of siding installed around door and window openings and judging the global behavior associated with the higher level of continuity that proved to be close to that of a full dwelling.

Specimens C-1 and C-2 provided two examples of dwelling superstructure construction representative of two different eras of dwelling construction, both prevalent in California's dwelling stock. While the tests were not developed for the purposes of direct comparison, it is worthwhile to discuss a few aspects of the specimens and testing results. Figure 5.57 shows the superimposed positive and negative quadrant envelope curves for Specimens C-1 and C-2.

The combinations of interior and exterior finish materials tested in Specimens C-1 and C-2 are commonly found in California's housing stock. Most dwellings having these materials would not have had any engineered design for wind or seismic loads. For this reason, they represent a lower bound for the strength and seismic performance of dwellings.

The base detail with a 2 × 4 bottom plate nailed to a 4 × 6 nailer was the same for both tests. Although this did not prove to be a weak link for Specimen C-1, it did act as a weak link for Specimen C-2. This could be a function of both the lower capacity of Specimen C-1 and changes in mechanics of uplift and overturning between the two different specimens.

The peak shear capacity of Specimen C-2 was nearly double that of Specimen C-1, suggesting significantly better seismic performance; however, by the time it reached peak shear capacity significant damage was observed in the next displacement cycle, restraints were added to the specimen to avoid premature failure. Compare this performance to Specimen C-1, which had a lower peak shear capacity but maintained nearly 50% of the peak shear capacity out to a drift ratio of 16%. When put in terms used to classify vertical elements of seismic force-resisting systems, Specimen C-2 would be categorized as non-ductile in that catastrophic damage could occur just past peak shear capacity, while Specimen C-1 could be categorized as highly-ductile, while having moderate capacity in the event of a severe event. Figure 5.56 captures this difference in response. This pattern is counter-intuitive, which would normally classify Specimen C-2 as ductile based on the performance of wood structural panel shear walls and categorize Specimen's C-1 configuration with plaster on wood lath as non-ductile.

In terms of level of damage and repair costs for ground motions lower than design or maximum considered earthquake, Specimen C-1 exhibited widespread damage to the plaster by a drift level of about 1.1%; the damage to the gypsum wallboard remained moderate up to peak shear capacity. This suggests that repair costs for Specimen C-1 might be anticipated to be higher following a moderate earthquake.

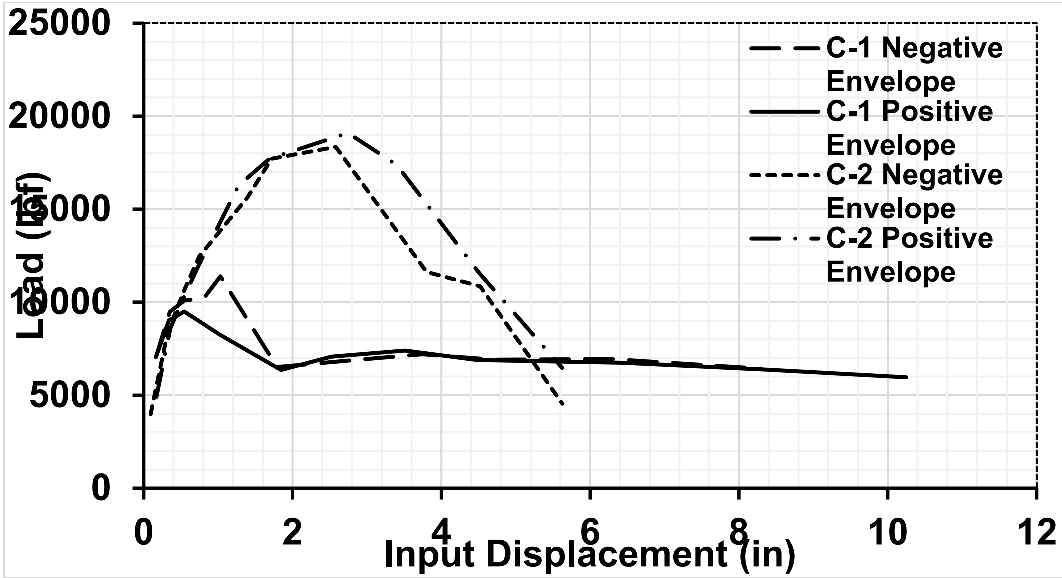

Figure 5.57 **Superimposed envelope curves for Specimens C-1 and C-2. Note that Specimen C-1 response is truncated at 10% drift while the testing continued to 16%.**

5.14 CONCLUSIONS

Tests of Specimens C-1 and C-2 investigated the seismic performance of wall finishes and sheathing material combinations commonly found in occupied stories of California dwellings. Test Specimen C-1 was constructed with a horizontal wood (shiplap) siding exterior finish, installed over building paper, and plaster on wood lath interior finish; see Figure 5.58. The construction was targeted to be representative of construction practices of the 1930s and 1940s. Test Specimen C-2 was constructed with a plywood panel (T1-11) siding exterior finish, installed over building paper, and a gypsum wallboard interior finish (Figure 5.59); the installation of the plywood siding included a mis-installation that is prevalent in the housing stock; see Figure 5.60. Specimen C-2 used materials and construction details that were representative of housing construction practices of 1960s and 1970s. The Specimens C-1 and C-2 finish materials were specifically selected by the Project Team to supplement the limited amount of currently available data for occupied stories of dwellings. Regarding the most representative boundary conditions, the test specimens were three 3D structures with plan dimensions of 20 ft × 4 ft. The test specimens included 8-ft-tall walls seated on the concrete foundation and a roof structure. Each of these 20-ft-long walls was constructed with one door (i.e., a sliding glass or French door) and one window, with the layout of each wall a mirror image of the other.

The configuration at the base of Specimens C-1 and C-2 was chosen to represent a dwelling in which the occupied story walls are supported on a wood-framed floor that is, in turn, supported on a stem wall. This base of wall configuration was reasonably common in the eras of interest and is still commonly used for new dwellings on hillsides. The adaptation of this detail for testing used a 4 × 6 nailer bolted down to the foundation, and the framed wall bottom plate nailed to the 4 × 6 nailer; see Figure 5.61. This base condition is intended to represent a lower bound but realistic condition for fastening of the wall base.

Figure 5.58 Specimen C-1 prior to start of testing.

Figure 5.59 Specimen C-2 prior to start of testing.

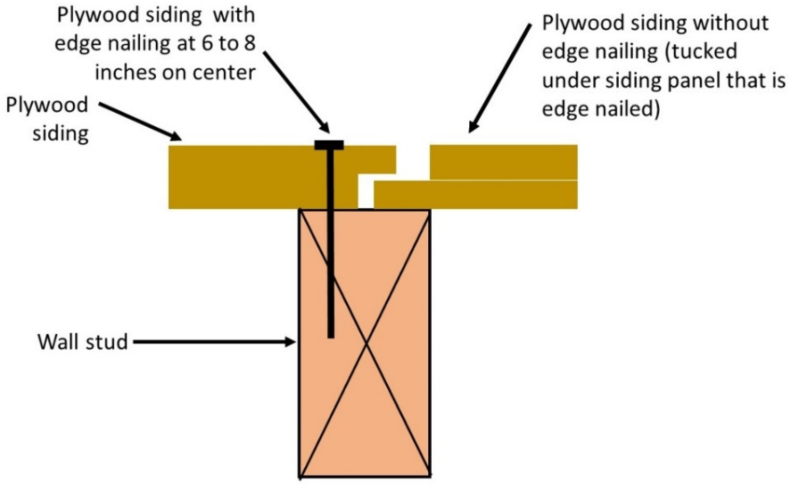

Figure 5.60 Section through stud and vertical siding joint at abutting panel edges. The mis-installation shown only includes edge nailing on one of the two abutting panels. This mis-installation was specifically included in construction of Specimen C-2.

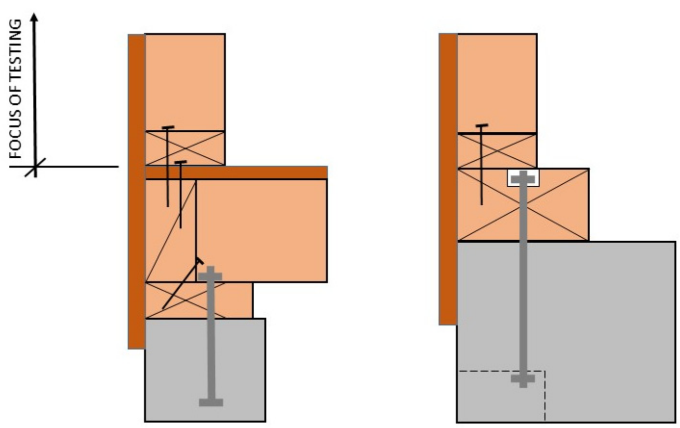

Figure 5.61 (Left) Base condition for Specimens C-1 and C-2 including the typical construction detail being represented and (right) the configuration used in the specimens.

The following are highlights of the test results for Specimen C-1:

- Specimen C-1 reached a peak capacity (lateral strength) of 11.4 kips (520 plf) at a drift ratio of approximately 1.1% in the negative quadrant (first displacement direction) and a peak lateral strength of 9.5 kips (430 plf) in the positive quadrant at a drift ratio of approximately 0.6%;
- Although the capacity of Specimen C-1 dropped off notably following cycles at peak capacity, the retained capacity stabilized at a drift ratio of 2% (1.9 in.) with a residual capacity of 6.5 kips (two-thirds of peak capacity), and substantially maintained this capacity out to at drift ratio of 14% (13.4 in.). The

testing was stopped when the test setup displacement range had been exhausted; at the conclusion of testing, there was no indication that the test specimen would not be able to continue retaining capacity to higher drift ratios. This retention of capacity is more consistent with available test data for horizontal wood sheathing and siding tested alone. Regardless, the retained capacity to 14% drift far exceeds published test information for any of these materials; see Figure 5.62;

- Specimen C-1 was observed to have a reached a high percentage of the peak capacity in the very first displacement cycle to 0.2% drift, accompanied by significant popping noises and cracking and spalling of the plaster occurring in the very first displacement cycles. This suggests that the plaster would require repair at much lower drift levels than the materials tested in other PEER–CEA Project specimens;

- Available data from previous tests show significant variation in peak capacity of specimens with plaster on wood lath. The peak unit shear capacity of Specimen C-1 falls at the lower end of the range of observed strengths. There are several aspects that could have contributed to the strength for Specimen C-1 falling towards the bottom end of available data, even though constructed in controlled laboratory conditions. Two primary aspects that bear consideration are the materials and workmanship, and the age of the plaster at testing. Plaster on wood lath is an archaic construction type that is rarely used today. Although utmost care was taken to use representative materials and installation techniques, and work was performed by contractors that are regularly involved in installing similar systems, the materials or workmanship could have varied from that used in the 1930s and 1940s in a way that affected performance. These tests are being compared to tests conducted on wall assemblies constructed circa 1930, and test results using plaster constructed in the laboratory with very non-typical materials and techniques. Another aspect that bears consideration is that Specimen C-1 was tested approximately one month after installation of the plaster finish coat. Although this was decided to be a reasonable age to allow curing to near target strength, it is possible that due to age, the physical properties of the plaster varied from plaster in place since the 1930s. This is a recognized and unavoidable limitation of laboratory testing;

- Specimen C-1 displacement at peak capacity can be compared to prior testing results of stucco finishes with attention given to boundary conditions and prior plaster on wood lath testing where boundary conditions were not considered. While the peak capacities varied widely, it is notable that the displacement at peak capacity is very uniform, with a range of 1.0 to 1.1 in.;

- It is notable that there was no evidence of any significant uplift behavior involving separation of the 2 × 4 bottom plate from the 4 × 6 nailer bolted to the foundation. This is in significant contrast to the response of Specimen C-2; and

- Detailed descriptions of damage observations at each drift ratio are provided.

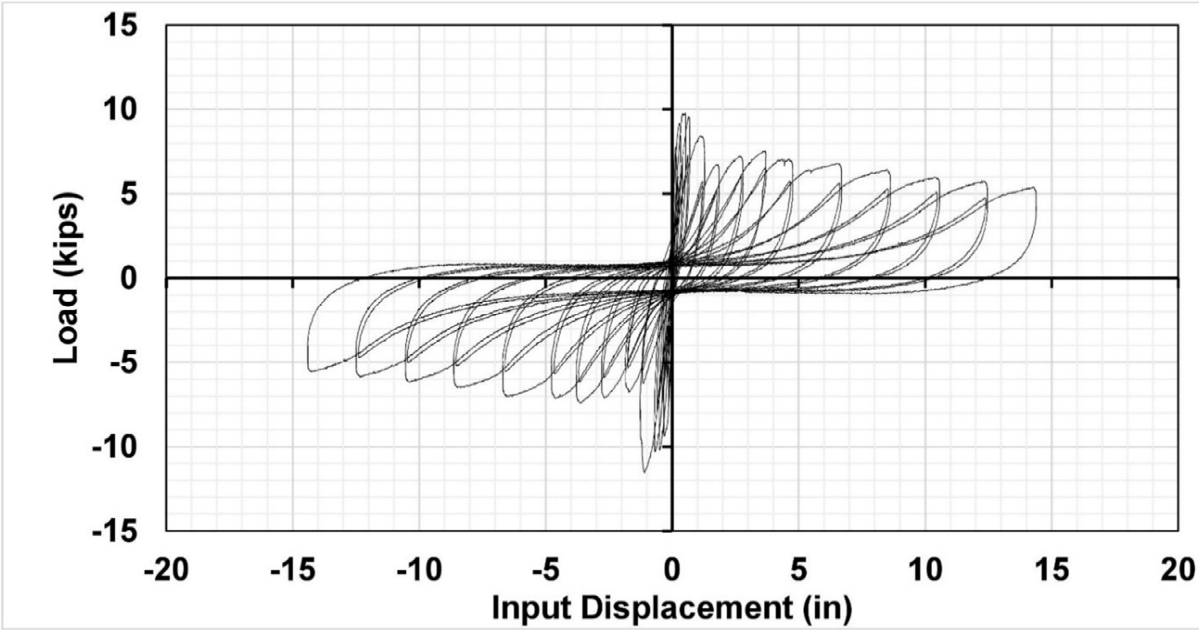

Figure 5.62 Specimen C-1: lateral load versus lateral actuator input displacement.

The following are highlights of test results for Specimen C-2:

- Specimen C-2 reached a peak capacity (lateral strength) of 18.4 kips (830 plf) at a drift ratio of approximately 2.7% in the negative quadrant (first displacement direction) and a peak lateral strength of 19.1 kips (870 plf) in the positive quadrant at a drift ratio of approximately 2.9%;
- Specimen C-2 was only able to be tested to drift ratios of approximately 6% due to significant deterioration and concerns regarding stability. At stop of testing, Specimen C-2 retained approximately 30%; of peak capacity, as shown in Figure 5.63; and
- The final failure mechanism of Specimen C-2 involved the withdrawal of practically all the nails fastening the wall bottom plates to the 4 × 6 nailers at the base of the structure. The combined withdrawal and shear created significant demands on the nails. As uplift of the specimen increased, the nails had to resist the combined withdrawal and shear loads, while also experiencing partial withdrawal reducing their capacity. Most of the nails eventually withdrew completely from the 4 × 6 nailers. Many were bent flat between the bottom plates and the nailers during load reversals. Eventually, the wall structure could be pushed back and forth across the 4 × 6 nailers and foundation fairly easily. Restraints were added during testing to 4% drift, with a second restraint strap added during loading to 6% drift. Without the restraints, it is anticipated that the base of the wall piers at the doors would have spread and fallen off the foundation. Although there was no clearly observed brittle failure, the failure mechanisms observed were severe and should be avoided. These mechanisms started to be observed at or just beyond peak capacity. Unlike

engineered plywood shear walls, for which post-peak loading is thought to be acceptable in a maximum considered earthquake, it is suggested that it would not be acceptable for the construction details used in Specimen C-2.

- Specimens C-1 and C-2 provide two examples of dwelling superstructure construction representative of two different eras of construction, both prevalent in California's housing stock. While the tests were not developed for the purpose of direct comparison, it is worthwhile to discuss a few aspects of the specimens and testing results. The base detail with a 2 × 4 bottom plate nailed to a 4 × 6 nailer was the same for both tests. Although this did not prove to be a weak link for Specimen C-1, it did act as a weak link for Specimen C-2. This could be a function of both the lower capacity of Specimen C-1 and changes in mechanics of uplift and overturning between the two different specimens;
- The peak capacity of Specimen C-2 was nearly double that of Specimen C-1, suggesting significantly better seismic performance; however, by the time it reached peak capacity, significant damage was observed and in the next displacement cycle, restraints were added to the specimen to avoid premature failure. Compare this performance to Specimen C-1, which had a lower peak capacity but maintained nearly 50% of the peak capacity out to a drift ratio of 16%. When put in terms used to classify vertical elements of seismic force-resisting systems, Specimen C-2 would be categorized as non-ductile in that catastrophic damage could occur just past peak capacity, while Specimen C-1 could be categorized as highly-ductile, while having moderate capacity. Figure 5.64 captures this difference in response. This pattern is counter-intuitive in that it would be common to categorize Specimen C-2 as ductile based on the performance of wood structural panel shear walls and categorize Specimen's C-1 configuration with plaster on wood lath as non-ductile; however observed behavior suggests the opposite; and
- Detailed descriptions of damage observations at each drift ratio are provided.

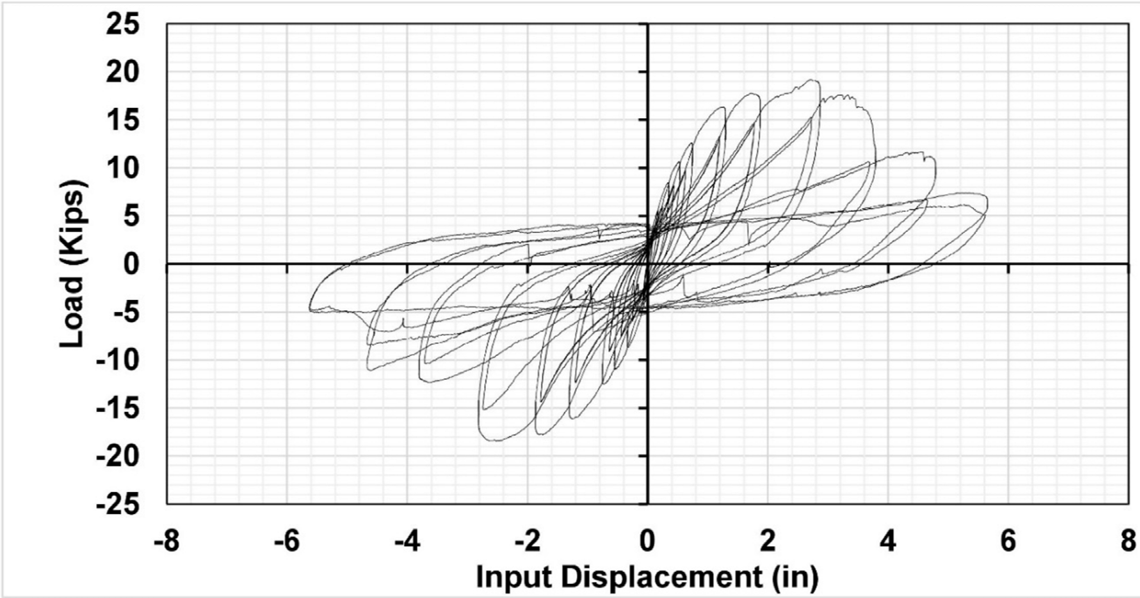

Figure 5.63 Specimen C-2: lateral load versus lateral actuator input displacement.

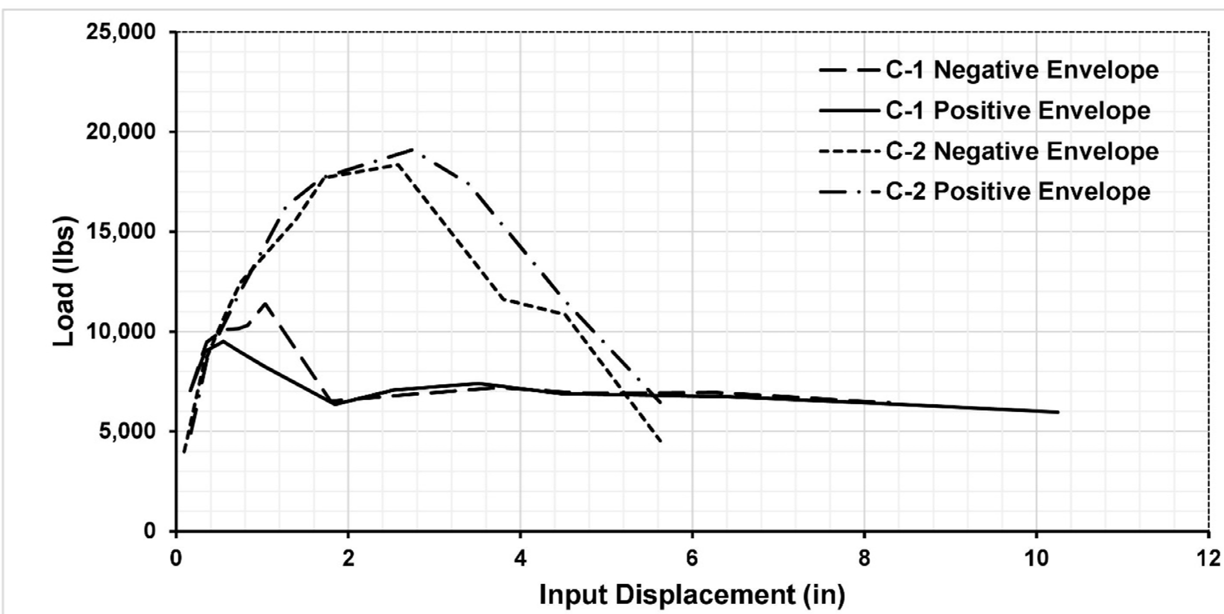

Figure 5.64 Specimens C-1 and C-2: superimposed envelope curves. Note that Specimen C-1's response is truncated at 10% drift while the testing continued to 16%.

REFERENCES

Arnold A.E., Uang C., Filiatrault A. (2003a). Cyclic behavior and repair of stucco and gypsum woodframe walls: Phase I, *CUREE -Caltech Woodframe Project Publication No. EDA-03*, Department of Structural Engineering, University of California, San Diego, CA.

Arnold A.E., Uang C., Filiatrault A. (2003b). Cyclic behavior and repair of stucco and gypsum woodframe walls: Phase II, *CUREE -Caltech Woodframe Project Publication No. EDA-07*, Department of Structural Engineering, University of California, San Diego, CA.

ASCE (2010). *Minimum Design Loads and Associated Criteria for Buildings and Other Structures*, *ASCE 7-10*, American Society of Civil Engineers, Reston, VA.

ASCE (2017). *Seismic Evaluation and Retrofit of Existing Buildings, ASCE 41-17*, American Society of Civil Engineers, Reston, VA.

AWC (2015). *Special Design Provisions for Wind and Seismic*, American Wood Council, Leesburg, VA.

Bahmani P., van de Lindt J. (2016). Experimental and numerical assessment of woodframe sheathing layer combinations for use in strength-based and performance-based design, ASCE, *J. Struct. Eng*., 142(4).

Carroll C. (2006) *Wood Materials and Shearwalls of Older Light-Frame Residential Structures*, Master of Science thesis, Department of Civil Engineering, Oregon State University, Corvallis, OR.

Chai Y.H., Hutchinson T.C., Vukazich S.M. (2002). Seismic behavior of level and stepped cripple walls, *CUREE -Caltech Woodframe Project Publication No. W-17*, Division of Civil and Environmental Engineering, University of California, Davis, CA.

Christovasilis I., Filiatrault A., Wanitkorkul A. (2009). Seismic testing of a full-scale two-story light-frame wood building: NEESWood benchmark test, *Technical Report MCEER-09-0005*, University at Buffalo, State University of New York, Buffalo, NY.

CUREE (2007, updated 2010). General guidelines for the assessment and repair of earthquake damage in residential woodframe buildings. *CUREE -Caltech Woodframe Project Publication No. EDA-02*, Consortium of Universities for Research in Earthquake Engineering, Richmond, CA.

FEMA (2012a). *Simplified Seismic Assessment Guidelines for Detached, Single-Family Wood-Frame Dwellings, FEMA P-50*, Federal Emergency Management Agency, Washington, DC.

FEMA (2012b). *Seismic Retrofit Guidelines for Detached, Single-Family, Wood-Frame Dwellings, FEMA P-50-1*, Federal Emergency Management Agency, Washington, DC.

FEMA (2012c). *Seismic Evaluation and Retrofit of Multi-Unit Wood-frame Buildings with Weak First Stories, FEMA P-807*, Federal Emergency Management Agency, Washington, DC.

FEMA (2015). *Performance of Buildings and Nonstructural Components in the 2014 South Napa Earthquake, FEMA P-1024*, prepared by the Applied Technology Council for the Federal Emergency Management Agency, Washington, D.C.

FEMA (2018). *Vulnerability-Based Seismic Assessment and Retrofit of One- and Two-Family Dwellings, FEMA P-1100,* Vol. 1, Prestandard, Federal Emergency Management Agency, Washington, DC.

FEMA (2019). *Vulnerability-Based Seismic Assessment and Retrofit of One- and Two-Family Dwellings, FEMA P-1100-3,* Vol. 3, Background Documentation, Federal Emergency Management Agency, Washington, DC.

Fennel W.A., Moore K., Mochizuki G. (2009). *Structural Engineers Association of Northern California 2008-2009 Special Projects Initiative Report on Laboratory Testing of Anchor Bolts Connecting Wood Sill Plates to Concrete with Minimum Edge Distance*, Structural Engineers Association of Northern California, San Francisco, CA.

Ficcadenti S., Freund E., Pardoen G., Kazanjy R. (2004). Cyclic response of shear transfer connections between shearwalls and diaphragms in woodframe construction, *CUREE Publication No. W-28*, CUREE, Richmond, CA.

Fischer D., Filiatrault A., Folz B., Uang C.-M., Seible F. (2001). Shake table tests of a two-story woodframe house *CUREE Publication No. W-06*, CUREE, Richmond, CA.

Forest Products Laboratory (1951). *Results of Racking Tests of a Few Types of House-Wall Constructions*, U.S. Department of Agriculture, Forest Service, Forest Products Laboratory, MI.

Forest Products Laboratory (1956). *The Rigidity and Strength of Frame Walls, Information Reviewed and Reaffirmed*, U.S. Department of Agriculture, (No. 896), Forest Service, Forest Products Laboratory, Madison, WI.

Forest Products Laboratory (1958). *Adequacy of Light Frame-Wall Construction*, U.S. Department of Agriculture, (No. 2137), Forest Service, Forest Products Laboratory, Madison, WI.

Gatto K., Uang C.-M. (2002). Cyclic response of woodframe shearwalls: loading protocol and rate of loading effects *CUREE Publication No. W-13*, Consortium of Universities for Research in Earthquake Engineering, Richmond, CA.

ISO (1998). Timber structures-joints made with mechanical fasteners-quasi static reversed cyclic test method, *ISO/TC 165 WD 16670*, International Organization for Standardization, Secretariat, Standards Council of Canada, Ottawa, Canada.

Krawinkler H, Parisi F., Ibarra L., Ayoub A., Medina R. (2001). Development of a testing protocol for woodframe structures, *CUREE Publication No. W-02*, Consortium of Universities for Research in Earthquake Engineering, Richmond, CA.

Mahaney J., Kehoe B. (2002). Anchorage of woodframe buildings: laboratory testing report, *CUREE Publication No. W-14*, CUREE, Richmond, CA.

McMullin K., Merrick D. (2002). Seismic performance of gypsum walls: experimental test program, *CUREE Publication No. W-15*, Consortium of Universities for Research in Earthquake Engineering, Richmond, CA.

Mosalam K., Machado C., Giliniorz K.-U., Naito C., Kunkel E., Mahin S.A. (2002). Seismic evaluation of an asymmetric three-story woodframe building, *CUREE Publication No. W-19*, Consortium of Universities for Research in Earthquake Engineering, Richmond, CA.

Mosalam K., Hashemi A., Elkhoraibi T., Takhirov S. (2008). Seismic evaluation of wood house over garage, *Proceedings, 14th World Conference on Earthquake Engineering*, Beijing, China.

Ni C., Karacabeyli E. (2007). Performance of shear wall with diagonal or transverse lumber sheathing, ASCE, *J. Struct. Eng*., 133(12).

Pacific Coast Building Officials (1937). *Uniform Building Code*, Pacific Coast Building Officials' Conference, Los Angeles, CA.

Pacific Coast Building Officials (1943). *Uniform Building Code*, Pacific Coast Building Officials' Conference, Los Angeles, CA.

Pardoen G.C., Waltman A., Kazanjy R., Freund E., Hamilton C.H. (2003). Testing and analysis of one-story and two-story shear walls under cyclic loading, *CUREE Publication No. W-18*, Consortium of Universities for Research in Earthquake Engineering, Richmond, CA.

Schmid B. (1984). *Shear Test of Existing Wood Lath and Plaster Walls Relative to Division 88*, Ben L. Schmid, Consulting Engineer, Pasadena, CA.

Shepherd R., Delos-Santos E.O. (1991). An experimental investigation of retrofitted cripple walls, *Bull. Seismol. Soc. Am*., 81(5): 2111–2126.

The Pacifi c Earthquake Engineering Research Center (PEER) is a multi-institutional research and education center with headquarters at the University of California, Berkeley. Investigators from over 20 universities, several consulting companies, and researchers at various state and federal government agencies contribute to research programs focused on performance-based earthquake engineering.

These research programs aim to identify and reduce the risks from major earthquakes to life safety and to the economy by including research in a wide variety of disciplines including structural and geotechnical engineering, geology/seismology, lifelines, transportation, architecture, economics, risk management, and public policy.

PEER is supported by federal, state, local, and regional agencies, together with industry partners.

PEER Core Institutions

University of California, Berkeley (Lead Institution)
California Institute of Technology
Oregon State University
Stanford University
University of California, Davis
University of California, Irvine
University of California, Los Angeles
University of California, San Diego
University of Nevada, Reno
University of Southern California
University of Washington

PEER reports can be ordered at https://peer.berkeley.edu/peer-reports or by contacting

Pacific Earthquake Engineering Research Center
University of California, Berkeley
325 Davis Hall, Mail Code 1792
Berkeley, CA 94720-1792
Tel: 510-642-3437
Email: peer_center@berkeley.edu

ISSN 2770-8314
https://doi.org/10.55461/HXYX5257